Ultrasonically assisted synthesis and degradation of poly(dimethylsiloxane)

Brown, David

Award date:
1999

Awarding institution:
University of Bath

ULTRASONICALLY ASSISTED SYNTHESIS AND DEGRADATION OF POLY(DIMETHYLSILOXANE)

submitted by David Brown

for the degree of PhD

of the University of Bath

1999

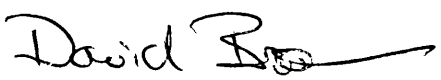

ProQuest LLC
789 East Eisenhower Parkway
P.O. Box 1346
Ann Arbor, MI 48106-1346

Dedicated to my wife, Karen,
whose love gives each day it's meaning.

ACKNOWLEDGEMENTS

Firstly, to Gareth, for giving me the opportunity to conduct research in such an interesting area of chemistry. For all your time, help, patience and for making sure I completed on time.

To Richard Taylor, Avril Surgenor and Claire Thompson at Dow Corning, for their support of this project, their ideas, the copious quantities of D_4 and for the Pub lunches!

To Dave Snell, Phil Drake, Simon Crook, Roger Jardine and Simon Hickling for making sure there was never a dull moment in the lab, and for ensuring the coffee was always on!

To my Mum, Mike, and the rest of my family. For your love and encouragement.

Finally, to Karen, for all your love and support. I could not have done this without you.

SUMMARY

This thesis describes the research conducted for a PhD at the University of Bath, supported by Dow Corning through an EPSRC 'CASE' Award. The research is concerned with the use of ultrasound in the synthesis and modification of poly(dimethylsiloxane), PDMS.

The research can be conveniently divided into three distinct phases. The initial phase of the research investigated using ultrasound as a means to control the molecular weight and polydispersity of a commercially available, high viscosity PDMS. High intensity, low frequency ultrasound can cause non-random cleavage of polymer chains in solution, and a number of workers have developed kinetic schemes in an attempt to model this 'ultrasonic degradation' of polymers. The research described in this thesis shows that the maximum rates of degradation of PDMS are obtained with high ultrasonic intensities, low solution temperatures and low solution concentrations. The experimental data has been analysed using two of the available degradation models, with both models fitting the data well. The models are shown to be a useful means of comparing degradations conducted under different conditions. Further work in this area attempted to determine the nature of the chain-ends formed when the PDMS chains are cleaved by ultrasound, using radical and ionic traps. Unlike polymers with a C-C backbone, which cleave homolytically to generate radicals, the results suggest that the siloxane is cleaved heterolytically.

The second phase investigated the effect of ultrasound on the polymerisation of the cyclic monomer, octamethylcyclotetrasiloxane (D_4). Both acid and base catalysed polymerisations were studied, under ultrasonic and 'silent' conditions, and in both cases polymerisations under ultrasound were observed to be faster than the silent equivalent.

The third phase of the research investigated routes to copolymers of PDMS with organic polymers, such as polystyrene. Initial, unsuccessful studies attempted to produce these copolymers via sonication of PDMS in the presence of monomers. However, the new technique of Atom Transfer Radical Polymerisation (ATRP) was successfully employed to synthesise copolymers of PDMS with polystyrene and poly(methyl methacrylate).

CONTENTS

Chapter 1

Introduction

1 INTRODUCTION

1.1 Aims and Objectives

The use of ultrasound in chemistry began in the 1930's and since then ultrasound has been successfully applied to a diverse range of chemical reactions and processes. In polymer chemistry, ultrasound has been found to not only enhance polymerisation reactions but also break the polymer chains in a non-random process. This 'degradation' of polymers in an ultrasonic field offers a degree of control over the final structure of the polymer. The fundamental aim of this project is to apply ultrasonic techniques to the synthesis of poly(dimethylsiloxane), (PDMS); to see how ultrasound affects the polymerisation and how it can be used to control the structure of the final polymer.

The program of work can be divided into three areas. The first part of the project was directed towards understanding how changing the experimental conditions, such as temperature, concentration and ultrasonic intensity, influences the degradation of the polymer, so that these effects may be used to control the molecular weight and the molecular weight distributions, during synthesis and as a stand alone process. The second phase of the work studied the kinetics of polymerisation of the cyclic siloxane, octamethylcyclotetrasiloxane (D_4), under ultrasound, using acid and base initiators, and comparing these to the classic 'silent' polymerisation. These studies should enable the mechanism of the sonochemical enhancement of the polymerisation reaction and polymer modification to be elucidated.

The final phase investigated possible routes to synthesising copolymers of poly(dimethylsiloxane) and common organic polymers. In particular, the new technique of Atom Transfer Radical Polymerisation (ATRP) was studied as a potential method for effectively producing block copolymers.

1.2 What is a Polymer?

A polymer is a very large molecule (macromolecule) constructed from numerous smaller, repeating chemical units. These repeating units are derived from small molecules known as monomers. The repeat unit of a polymer is usually equivalent, or nearly equivalent, to the monomer and the number of repeat units in a polymer chain is usually referred to as the degree of polymerisation (DP). For example, poly(vinyl chloride), or PVC, is a polymer produced from the polymerisation of the monomer vinyl chloride.

Polymer:

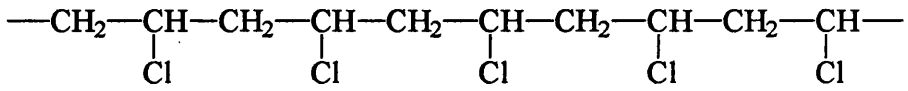

repeat unit ('mer'):

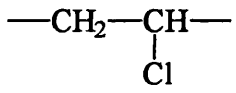

monomer:

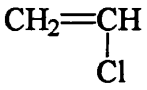

In most cases, monomers polymerise to form long linear chains. However, in some case the chains can be branched, or even interconnected to form three-dimensional networks.

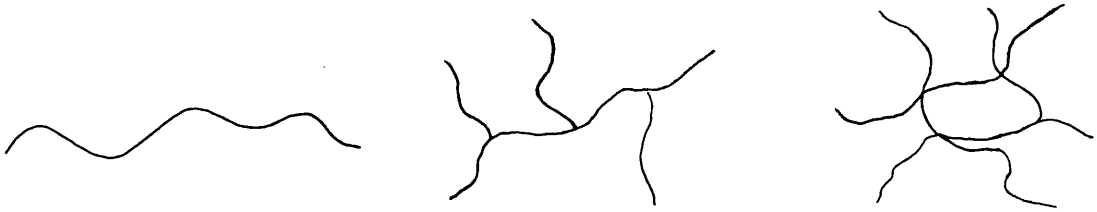

Linear Branched Network

Polymers can be natural substances, such as cellulose and natural rubber, man-made substances, which include the majority of the common, everyday polymers, and even biological substances such as proteins and DNA.

1.2.1 Copolymers

A polymer made of only one type of monomer, as in the case of poly(vinyl chloride), is known as a 'homopolymer'. A polymer that is formed from two different monomers is known as a 'copolymer'. A 'terpolymer' results if three different

monomers are incorporated into one polymer. Copolymers are important materials as they can exhibit the better qualities of the parent homopolymers and not the undesirable properties. Thus, an application may require properties that cannot be met by one homopolymer, but a copolymer derived from two different polymers may display all the properties necessary for the task. Industrially important copolymers include those containing styrene and butadiene (styrene-butadiene rubber, or SBR) and the terpolymers of acrylonitrile, butadiene and styrene (ABS). A large range of ABS materials can be made by simply varying the ratios of the three monomers.

The sequence of monomer units in a copolymer can vary, and the variation in structure can manifest itself dramatically in the physical properties of the final copolymer:

Random copolymers have a random arrangement of monomer units in the chain.

i.e. -A-A-B-A-A-B-B-B-B-A-B-A-A-A-B-B-A-B-

(where A and B represent the monomer units)

Alternating copolymers as their name suggests, have an alternating sequence of monomer units.

i.e. -A-B-A-B-A-B-A-B-A-B-A-B-A-B-A-B-A-B-

Block copolymers consist of a block of one type of monomer unit connected a block of the other.

i.e. A-A-A-A-A-A-A-A-A-A-B-B-B-B-B-B-B-B-B - diblock

i.e. A-A-A-A-A-A-A-B-B-B-B-B-B-A-A-A-A-A-A - triblock

Graft copolymers consist of a main homopolymer chain with branches of another type of homopolymer.

i.e.

```
-A-A-A-A-A-A-A-A-A-A-A-A-A-A-A-A-A-A-A-A-
   |                       |
   B                       B
   |                       |
   B                       B
   |                       |
   B                       B
```

1.3 Polymer Molecular Weights

1.3.1 Definition of Molecular Weights

Molecular weight is probably the most important feature distinguishing polymers from low molecular weight, simple molecules. Not only are polymer molecular weights many times larger than those for small molecules but, perhaps more importantly, it is impossible to assign an exact molecular weight to a polymer.

Due to their statistical nature, polymerisation reactions do not give polymer chains which have the same length. The length of a chain is determined by random events and thus the final product consists of a mixture of chains of differing lengths, i.e. there is a distribution of molecular weights (figure 1.1). It is therefore impossible to assign a unique molecular weight to a polymer in the same way as is possible with small molecules. Only an average molecular weight can be quoted.

The desirable properties and versatility of polymers is a direct result of the large molecular weight of the chains, and the exact properties of a particular polymer sample are dependent on the molecular weight of that sample. It is therefore important to know the molecular weight of a polymer. Average molecular weights can be defined in a number of ways and it has been found that the different averages correlate to the various properties of polymers.

Number average molecular weight (M_n)

This value depends on the number of chains with each molecular weight and is defined as:

$$M_n = \frac{\sum n_i M_i}{\sum n_i} \qquad (1)$$

where n_i is the number of chains with molecular weight of M_i

This value determines the colligative properties of the polymer solution, such as osmotic pressure, and also properties of the solid polymer, such as brittleness and tensile strength.

In a 'typical' polymer, this value lies near the peak of the molecular weight distribution curve.

Weight average molecular weight (M_w)

This depends on the weight of polymer molecules with each molecular weight, and is defined as:

$$M_w = \frac{\sum w_i M_i}{\sum w_i} = \frac{\sum n_i M_i^2}{\sum n_i M_i} \qquad (2)$$

where w_i is the weight of polymer with molecular weight M_i.

This value determines properties such as the hardness of the solid polymer.

It is found that M_w is greatly influenced by high molecular weight chains and hence, M_w is always greater than M_n.

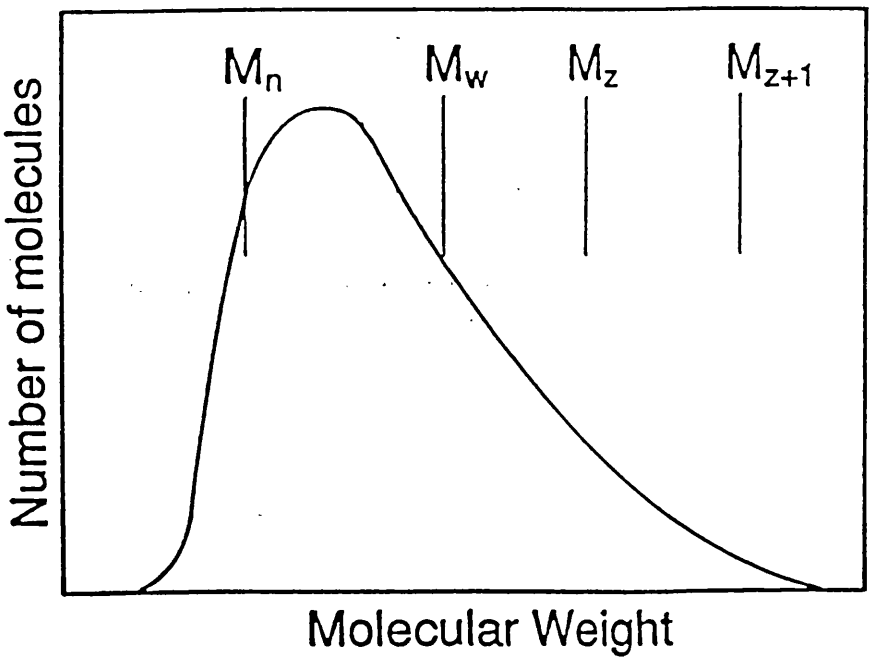

Figure 1.1 - Molecular weight distribution curve

'Z' and 'Z+1' averages (M_Z and M_{z+1})

These are higher order averages, however they are not commonly used. They correlate properties such as sedimentation and diffusion.

Of the four different averages, number-average, and weight-average molecular weights are the most widely used.

1.3.2 Polydispersity

The molecular weight does not completely characterise a polymer. Different polymer samples can have the same average molecular weight value, but have different distributions of chain lengths (figure 1.2).

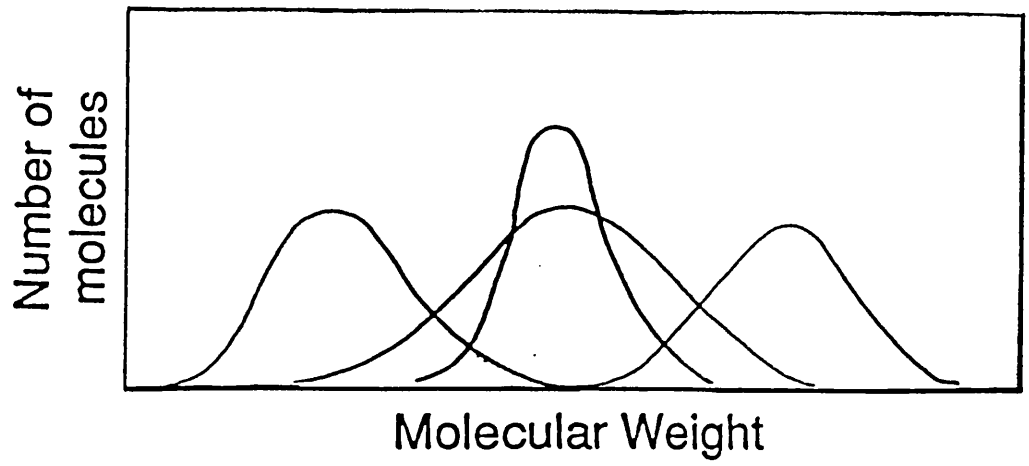

Figure 1.2 - Different distributions of polymer molecular weights

To overcome this, a polydispersity, γ , is defined.

$$\gamma = \frac{M_w}{M_n} \qquad (3)$$

The polydispersity gives an indication of the broadness of the molecular weight distribution curve. When $\gamma = 1$, all the molecular weight averages are equal (all the chains are the same length) and the polymer is said to be monodisperse. As the distribution of molecular weights gets wider γ increases and for commercially produced polymers, γ is approximately 2.

1.4 Polymerisation [1,2,3]

The reaction of many monomer molecules to form a polymer is known as a polymerisation reaction and there are two main types: step-growth polymerisation and chain-growth polymerisation. The subsequent separation of polymers into step-growth and chain-growth is a useful means of classifying polymers.

These two methods are used for the production of the majority of the commercially available polymers, however, there are other types. Living polymerisation, coordination polymerisation and ring-opening polymerisation are also possible, although these processes are used on a much smaller scale for the production of more speciality polymers. Also, their mechanisms are usually extensions of the chain-growth polymerisation.

1.4.1 Step-Growth Polymerisation

Step-growth polymerisation usually proceeds via the condensation of two or more molecules with the subsequent elimination of a small molecule, such as H_2O, HCl or CH_3OH. Examples of polymers produced by this process include nylon (polyamides), polyesters, polycarbonates and polysiloxanes. For example, the polyester 'terylene' is produced by the reaction of ethylene glycol and teraphthalic acid. An exception to this occurs with polyurethanes, which are step-growth polymers but whose polymerisation proceeds without the loss of a small molecule.

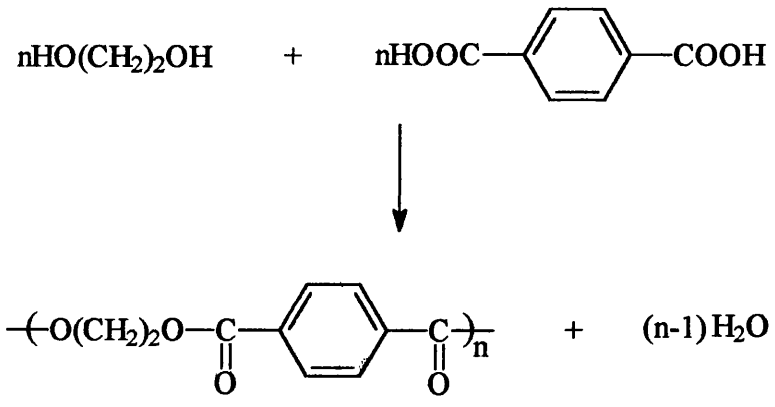

The production of terylene

All step-growth polymerisations show the same general characteristics, these include:

- The initiation of the polymerisation, the propagation (i.e. the 'growth' of the chains) and the termination reactions are essentially identical in mechanism and rate.
- Any two molecular species can react, i.e. a monomer molecule can react with another monomer molecule as easily as with a polymer molecule. Hence, slow random growth occurs.
- The monomer disappears early in the polymerisation and at an average DP of 10 repeat units, less than 1% of the monomer remains.
- The molecular weight increases steadily throughout the reaction and a high conversion of monomer to polymer is needed for high molecular weights.
- At any point in the polymerisation, all molecular species are present in a calculable distribution.

Step-growth polymerisation can be further subdivided into two groups. In the first group, two different monomers polymerise but each monomer contains only one functional group:

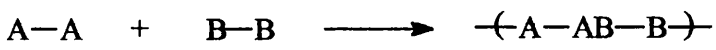

In the second group, the monomer contains more than one functional group:

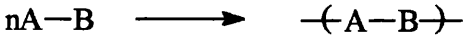

In order to obtain high molecular weight polymers, bifunctional monomers are generally used. However, monofunctional and trifunctional monomers can be incorporated into the chains. Monofunctional molecules allow a degree of control over the molecular weight, while trifunctional monomers allow the formation of branched and cross-linked structures.

1.4.2 Chain-Growth Polymerisation

Whereas step-growth polymerisation requires the use of difunctional monomers, chain-growth polymerisation involves the reaction of unsaturated monomers (i.e. those containing a C=C double bond) to form the polymer. The most

important polymers produced by this method are those derived from unsaturated vinyl monomers, for example, poly(methyl methacrylate) is derived from methyl methacrylate.

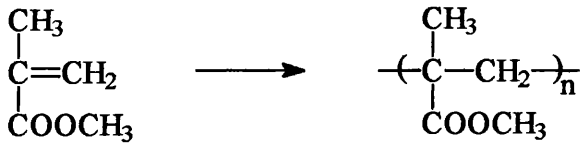

Other industrially important polymers include poly(vinyl chloride), polythene (poly(ethene)), polystyrene and poly(isobutylene).

An initiating species is used to open the double bond of a monomer molecule creating an 'active centre', usually a free radical, on the molecule. This active centre can then react with the double bond of another monomer molecule, bonding the two molecules and regenerating the active centre at the end of the new, longer molecule. Hence, chain growth is achieved by the sequential addition of monomer to the active centre at the end of a growing polymer chain. This illustrates a fundamental difference between step-growth and chain-growth polymerisations. In step-growth, the propagation reaction can occur between any two species present; monomer and monomer, monomer and polymer, or polymer and polymer. In chain-growth, propagation only occurs by addition of monomer to polymer. Another important aspect of chain-growth is that no atoms of monomer are lost as a result of the polymerisation.

Unlike step-growth polymerisation, where the initiation, propagation and termination reactions are essentially identical, in chain-growth, these stages are distinct and differ in both rate and mechanism.

- Initiation is the creation of the active centre. This is usually achieved by the use of a free radical initiator (I-I), such as azobisisobutyronitrile (AIBN).

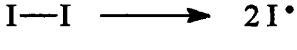

- Propagation involves the repeated addition of monomer to the growing chain.

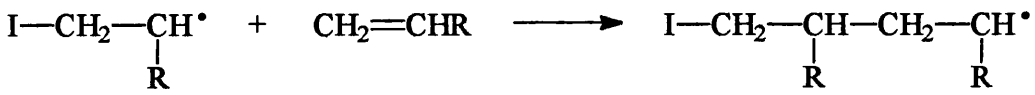

- Termination occurs when chain-growth is stopped by the extinction of the active centre. For free radicals, this can occur by combination (when two radicals react to form a single bond), or by disproportionation (where a radical abstracts a proton from another chain leaving it with a double bond).

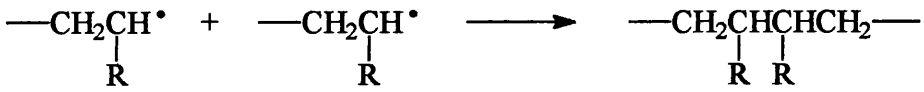

Combination

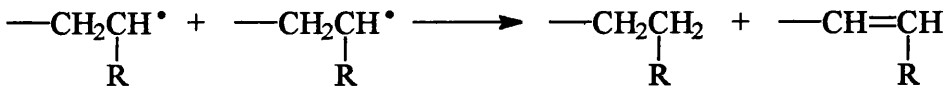

Disproportionation

- High molecular weight material is formed almost immediately and the molecular weight then hardly changes throughout the rest of the reaction.
- The concentration of monomer decreases steadily throughout the polymerisation.
- At any time, the reaction mixture contains only monomer, high molecular weight polymer and approximately 10^{-8} parts of growing chains.

With some exceptions polymers made by chain-growth polymerisation contain only carbon atoms in the main chain of the polymer, whereas step-growth polymers may have heteroatoms, such as oxygen and nitrogen (originating from the monomer functional groups) as part of the main chain.

Although the most common mechanism for chain-growth polymerisation involves radical intermediates, other mechanisms are possible. These include ionic polymerisation, coordination polymerisation and ring-opening polymerisation.

1.4.3 Ionic Polymerisation

Ionic chain-growth polymerisation occurs when the active centre is either anionic (a carbanion, C^-) or cationic (a carbocation, C^+) in nature. Obviously, the polymerisation is initiated by anionic or cationic initiators.

Given the reactive nature of free radicals, radical initiated chain-growth is generally non-specific, i.e. the nature of the 'R' group in the vinyl monomer CH_2=CHR, does not affect the polymerisation. However, this is not the case for ionic polymerisations since the formation and stabilisation of a carbanion or cabocation will be dictated by 'R'.

Anionic chain-growth occurs when R is an electron-withdrawing group, such as -COOH and -CH=CH_2. These groups help to stabilise the negative charge of the carbanion. Monomers that undergo anionic chain-growth include butadiene, methyl methacrylate and styrene. Typical initiators include alkyl metals, in particular butyl lithium, and Grignard reagents.

Cationic chain-growth will occur when R is an electron-donating group, for example, an alkyl chain. These will stabilise the positive charge of the carbocation. Examples of monomers that undergo cationic polymerisation include ethylene, isobutylene and styrene. The most important initiators are Lewis acids, such as $AlCl_3$ and BF_3, in conjunction with a co-catalyst, usually a Lewis base, such as water.

Ionic polymerisations are usually conducted at temperatures much lower than those for free radical polymerisations, typically below 0°C, and at such low temperatures high rates of polymerisation are observed.

Mechanistically, ionic chain-growth polymerisation is much more complex than free radical chain-growth and is often difficult to define. However, both anionic and cationic polymerisations are analogous to free radical polymerisations in that they consist of the same three general steps: generation of the active centre via the initiator, addition of monomer to the active centre of a growing chain and termination of the active centre to halt polymerisation.

In contrast to free radical polymerisation, termination of ionic polymerisation never involves the reaction between two chains because of the electrostatic repulsion that occurs between two positive or two negative charges. In cationic polymerisation a hydrogen abstraction from the growing chain by the counter-ion occurs to leave the chain terminally unsaturated, while regenerating the original initiating species.

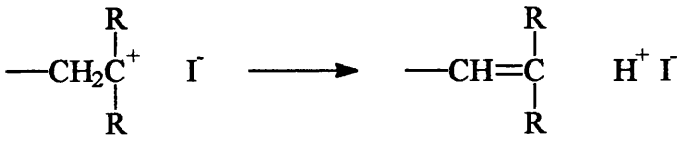

Anionic polymerisation cannot terminate by proton transfer to initiator as it would involve the formation of the hydride ion (H^-). Instead proton transfer has to occur to an impurity capable of forming a stable product. Water, methanol, ethanol carbon dioxide and oxygen are effective terminating agents.

The termination of free radical polymerisation can occur in a number of ways and given their highly reactive nature, can occur easily at any time during the polymerisation. Hence, at the end of the polymerisation the chains are all different lengths. In contrast, as the only way anionic polymerisation can terminate is between the chain and an impurity, if the monomer has been rigorously purified and there are no impurities present, termination of the chains cannot occur. All the chains will therefore grow at the same rate, to the same length and the polymerisation will continue until all the monomer has been consumed. However, the reactive ionic active centre will remain intact and if further monomer is added, the polymerisation will start again until the added monomer has been used up. Because of this property, these polymerisations where the active centre is not destroyed have been termed 'living polymerisation'. Living polymerisation will be discussed further in section 1.4.6.

1.4.4 Co-ordination Polymerisation

Co-ordination polymerisation involves the use of 'Ziegler-Natta' catalysts, named after Karl Ziegler[4] and Giulio Natta[5] who independently discovered the catalysts in the 1950's. These catalysts are complexes formed between main-group metal alkyls, such as $(CH_3CH_2)_3Al$, and transition metal salts, such as $TiCl_4$, the growing polymer chain being co-ordinated to the catalyst while chain-growth occurs. This method has the advantage that gases such as ethylene, which require high temperatures and pressures for conventional free-radical polymerisation, can be polymerised under more ambient conditions. However, the biggest advantage is that because of the spatial requirements of the catalyst, the polymers produced by this method are stereoregular and highly crystalline. For example, polyethylene produced via coordination polymerisation is linear and highly crystalline - the so called High

Density Polyethylene (HDPE). Polyethylene produced in a high temperature, radical process is extensively branched and has little crystallinity - Low Density Polyethylene (LDPE). Industrially coordination polymerisation is used in the production of polypropylene as well as polyethylene.

The most important catalysts are solids, i.e. the polymerisation system is heterogeneous. Soluble catalysts are known, however they require non-polar monomers and stereoselectivity is poor. Hence, work in this area has concentrated on the heterogeneous systems. Unfortunately, because the catalyst is insoluble, the mechanism and kinetics of the polymerisation are difficult to establish and the choice of catalyst for a particular system is very much trial and error. Essentially the polymerisation occurs via chain-growth, with propagation taking place at a carbon-transition metal bond and the active centre being anionic in nature.

1.4.5 Ring-Opening Polymerisation

Ring-opening polymerisation occurs when a heteroatom-containing ring is transformed into a linear chain. An ionic initiator is used to open the ring, generating a linear molecule with an ionic active centre at the end. The active centre then causes the ring-opening of another molecule, leading eventually to a linear polymer. For example, poly(ethylene oxide) is produced by the ring-opening polymerisation of ethylene oxide.

The tendency to ring-open depends on the ring size. In small rings the driving force is the release of ring strain.

Industrially this method is used for the production of poly(ethylene oxide), polyesters (from lactones), polyamides (from lactams) and polysiloxanes. The ring-opening polymerisation of siloxanes is discussed in greater detail in section 1.9.

1.4.6 Living Polymerisation

As explained in section 1.4.3, if a monomer undergoing anionic polymerisation has been vigorously purified and is free from impurities, the lack of terminating reactions mean that the active centre is not destroyed when the monomer is used up.

The polymerisation is said to be 'living', a phrase first coined by Szwarc[6] . Living polymerisation is a powerful synthetic tool as the living-nature allows fine control over the molecular weight and the synthesis of tailor-made copolymers.

In conventional free radical or ionic chain-growth polymerisations, although each chain grows at the same rate, termination can occur at any time and the chains will be different lengths at the end of the polymerisation. In step-growth polymerisation, the fact that polymer molecules can react as easily with each other as with a monomer molecule also means that the chains grow to different lengths. In both step and chain-growth, a distribution of molecular weights exists and a typical polydispersity of approximately 2 is obtained. However, in living polymerisation there are no termination reactions and all the chains grow at the same rate to the same length. The molecular weight is then determined by the ratio of monomer to initiator, and the polymer will essentially be monodisperse with a polydispersity approaching 1. A plot of molecular weight against conversion easily distinguishes between the three mechanisms (figure 1.3).

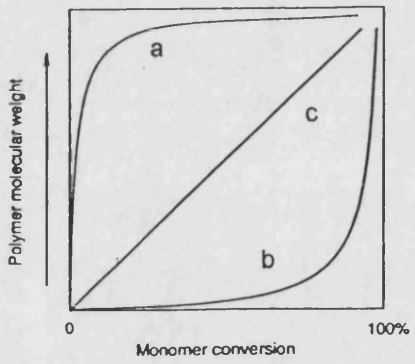

Figure 1.3 - Plot of molecular weight against conversion for different polymerisation mechanisms

In free radical and non-living ionic polymerisation, high molecular weight polymer is formed early in the reaction (a), while in step-growth polymerisation, high molecular weights are only present towards the end of the reaction (b). In contrast, for living polymerisations the molecular weight is directly proportional to the conversion (c).

As well as molecular weight control, living polymerisation also allows structural control of the polymer, and copolymers can be easily produced. A living

polymerisation is initiated and once the monomer has been consumed a second, different, monomer is added. The living chain-ends will initiate the polymerisation of the second monomer resulting in the formation of an AB-type block copolymer. The lengths of the blocks is then dependent on the amount of each monomer used. It is therefore possible to synthesise many different copolymers by this method of sequentially adding different monomers to a living polymerisation. Functionally-terminated polymers can also be prepared by the reaction of the living ends with an appropriate reagent.

Only in a small number of monomers is living polymerisation nearly perfect, although many more fit the theory close enough to be useful in synthesis. Styrene and ethylene oxide are examples of monomers that give rise to truly living polymerisations, and they require only monomer and initiator. For a large number of monomers more complex systems are required to inhibit chain-termination. An initiator is obviously required and is attached to the non growing chain-end. A catalyst is necessary for initiation and propagation, but is not consumed, while a chain-end stabiliser decreases the polymerisation rate. In all living polymerisations the initiation must be faster than the propagation if monodisperse polymers are to be produced. If initiation is slower, the first chain formed will be longer than the last and a polydisperse polymer will be produced[7].

Living polymerisation can be either anionic and cationic, although cationic living polymerisation is more complex than anionic. Until recently, it was believed that free radical living polymerisation would not be possible, however, it has been discovered that living polymerisation conditions can be achieved which have a free radical mechanism.

1.5 Atom Transfer Radical Polymerisation (ATRP)

1.5.1 Free Radical Living Polymerisation

In ionic living polymerisation, electrostatic repulsions stop the chain ends from reacting with one another and the polymerisations are only terminated by impurities or added terminating species. In contrast, free radicals will easily react with each other and, until recently, living free radical polymerisation was deemed to be impossible. However, recent developments have shown that by careful control of the reaction conditions it is possible to prepare well-defined polymers by a radical mechanism.

Termination cannot be completely excluded, however, and the mechanisms have been termed "living" [8].

Initial attempts at producing a "living" radical polymerisation employed sulphur-centred radicals. The sulphur-centred radicals reacted reversibly with the growing polymer chain ends, controlling the radical concentration. However, they also initiated the formation of new polymer chains, resulting in uncontrolled chain growth. The final polymers were found to have polydispersities similar to traditional free radical polymerisations[9,10].

To overcome this, a free radical polymerisation having "living" characteristics was developed in which the polymerisation was mediated by a nitroxide. Low polydispersity polystyrene was prepared using a mixture of benzoyl peroxide and 2,2,6,6-tetramethylpiperidinyloxy (TEMPO) as an initiating system[11] . Subsequent work confirmed the "living" nature of the system and the approach has since been used to prepare star and graft polymers, as well as low polydispersity copolymers. A variety of TEMPO derivatives have also been shown to give "living" polymerisation of styrene[12].

The success of this approach can be related to the ability of the stable nitroxide free radicals, such as TEMPO, to react at or near diffusion controlled rates with the carbon-centred free radical of the growing polymer chain end, in a thermally reversible process. This dramatically lowers the concentration of free radicals in the polymerisation. This, coupled with the inability of the nitroxide radicals to initiate polymerisation, leads to the controlled polymerisation[12].

However, although the use of TEMPO and other stable, related nitroxide free radicals, is relatively successful for the "living" polymerisation of styrene, and substituted styrenes, it is not as good for acrylics and methacrylics[13].

1.5.2 ATRP

Atom transfer radical addition has been widely used in organic synthesis as an efficient method of C-C bond formation. An extension of the technique has been applied to the polymerisation of vinyl monomers and has emerged as an effective method of achieving "living" radical polymerisation. It was first demonstrated by Sawamoto and Matyjaszewski.

Sawamoto[14] polymerised methyl methacrylate with an initiating system consisting of CCl_4, $RuCl_2(PPh_3)_3$ and methylaluminium bis(2,6-di-*tert*-butylphenoxide). The polymers produced had polydispersities in the range 1.3 - 1.4.

Matyjaszewski[15] used 1-phenylethyl chloride as an initiator for the polymerisation of styrene, with CuCl complexed by 2,2'-bipyridine (bpy) as a promoter for the chlorine atom transfer. Polydispersities less than 1.5 were obtained and Matyjaszewski coined the term 'Atom Transfer Radical Polymerisation' (ATRP) to describe this method of radical "living" polymerisation.

The principle of ATRP is that a copper (I) complex activates reversibly the dormant polymer chains via a halogen atom transfer reaction, and it is this dynamic equilibrium which is responsible for the controlled behaviour of the polymerisation[16]. The proposed mechanism for the polymerisation being[16,17]:

Initiation

$$R{-}X + 2\,bpy\,/\,CuX \underset{k_b}{\overset{k_a}{\rightleftharpoons}} R^{\bullet} + 2\,bpy\,/CuX_2$$

(X = Cl/Br) $\qquad k_a << k_b$

$$R^{\bullet} + monomer \longrightarrow P_1^{\bullet}$$

Propagation

$$P_n{-}X + 2\,bpy\,/\,CuX \underset{k_d}{\overset{k_c}{\rightleftharpoons}} P_n^{\bullet} + 2\,bpy\,/CuX_2$$

$k_c << k_d$

$$P_n^{\bullet} + monomer \longrightarrow P_{n+1}^{\bullet}$$

Termination

$$P_n^{\bullet} + P_m^{\bullet} \longrightarrow P_{n+m} \,/\, P_n^{=} + P_m^{H}$$

note: P_{n+m} and $P_n^{=} + P_m^{H}$ represent termination by combination and disproportionation respectively.

Thermodynamically, the equilibrium must lie toward the side of the dormant chain ends to maintain a sufficiently low steady state concentration of radicals so that termination is minimised. Kinetically, the exchange between dormant and active chain ends must be fast, otherwise not all of the chains will grow at the same rate and the polydispersity will increase.

Typically, ATRP shows three dominant features[17,18]:

- The first order rate plot is linear, indicating that the concentration of active species is constant throughout the polymerisation.
- The molecular weight (M_n) increases linearly with conversion.
- The polydispersity should be below 1.5.

As well as styrene, acrylates, methacrylates and acrylonitrile have all been polymerised using ATRP[19]. Also, the initiator and catalyst are not just restricted to 1-phenylethyl chloride and CuCl. Many alkyl halides, R-X, in conjunction with $Cu^{I}X$, where X is Br or Cl, can be used as efficient initiating systems[20,21].

A drawback of the CuX/bpy complex in these polymerisations is that they are only slightly soluble in the reaction medium, i.e. the ATRP is heterogeneous. In order to increase the solubility of the complex, Matyjaszewski added solubilising side chains at the 4,4'-positions of the 2,2'-bipyridine. This homogeneous ATRP yielded well defined polymers with polydispersities less than 1.10, while the optimum ratio of ligand-to-copper (I) halide was found to be 2:1[16].

Further work has been done to extend the ATRP method by using multidentate amine ligands, in place of 2,2'-bipyridine and its derivatives. Tetramethylethylenediamine, pentamethyldiethylenetriamine and hexamethyl-triethylenetetramine were all successfully employed in styrene, methyl acrylate and methyl methacrylate ATRP. The reactions showed the characteristic linear increase of M_n with conversion, and low polydispersity. In particular the tridentate and tetradentate ligands resulted in faster polymerisation compared to 2,2'-bipyridine[22].

The use of chiral ligands in the ATRP of methyl methacrylate has also been investigated as a possible way of controlling the stereochemistry of the polymer backbone. However, while ATRP was effectively performed, the enantiomerically pure chiral ligands used had no effect on the stereochemistry of the resulting polymers[13].

ATRP typically requires temperatures in excess of 80°C so as to obtain satisfactory rates of polymerisation. However, the ATRP of methyl methacrylate has also been performed effectively at temperatures down to 15°C, while still having control of the molecular weights and obtaining low polydispersities. The ATRP was even shown to proceed at -15°C, although control over the molecular weight was not as effective[18]. At these lower temperatures, the addition of 4-methoxyphenol (methyl hydroquinone, MeHQ) to the reaction was found to accelerate the rate of polymerisation. This was attributed to the MeHQ acting as a coordinating ligand for the copper catalyst, displacing one of the diimine ligands used in the polymerisation. This creates a coordination site on the copper which may then facilitate propagation. A similar effect was observed when benzoic acid was added to the polymerisation.

The preparation of block copolymers using ATRP has also been demonstrated. A homopolymer containing a halide-terminated chain end is used as an initiator for the ATRP of a second, different, monomer. If the initiator is only functionalised at one chain end, an AB-type block copolymer results. If it is functionalised at both ends, an ABA-type block copolymer will be produced. This technique has been used to create copolymers of polyTHF with styrene, methyl acrylate and methyl methacrylate[23].

1.6 Characterisation of Polymers

1.6.1 Determination of Molecular Weight [1,2]

Given that the molecular weight and polydispersity are such important properties of a polymer, a number of techniques have developed to determine these parameters. All the techniques involve the use of polymer solutions, so the polymer must be soluble in a solvent for the molecular weight to be determined. In principle, all of them, apart from viscosity measurement and Gel Permeation Chromatography (GPC), can be used to obtain absolute values of the molecular weight. Methods using viscosity or GPC require calibration with samples of known molecular weight.

End group analysis can be useful if the polymer has end-groups suitable for analysis by physical or chemical means, e.g. a carboxylic acid, which can be used in a titration. By knowing how many end groups there are, the number of polymer chains and therefore the molecular weight, can be determined. This method gives a value for the number average molecular weight and can also give information on the degree of

branching in a polymer, if the molecular weight has already been determined by another method. However, this method is limited to relatively low molecular mass products. As the molecular weight increases, the percentage of the end groups becomes smaller and the degree of uncertainty increases.

Osmometry involves the measurement of the osmotic pressure between the polymer solution and the solvent, separated by a semi-permeable membrane. Osmotic pressure is a colligative property, i.e. it is dependent on the number of polymer molecules in the solution. This method therefore determines the number average molecular weight for the sample. The chief drawback of osmometry is the passage of low molecular weight polymers through the membrane. It is therefore only suitable for polymers with molecular weights greater than ~10 000.

Ebulliometry and cryoscopy are also techniques that involve the colligative properties of the polymer solution. Ebulliometry relies on the fact that the presence of the polymer will cause the boiling point of the solvent, in which it is dissolved, to increase. While cryoscopy measures the decrease in the freezing point of the solvent. Both methods will give accurate molecular weights up to 30 000, however, they are not widely used.

Light scattering relies on the fact that light passing through a solution will be scattered. The intensity of the scattered light is dependent on several factors, including the concentration of the solution and the size (i.e. molecular weight) of the polymer molecules. Thus, for solutions of known concentration, the molecular weight can be determined. This technique gives a value for the weight average molecular weight, however, it is quite difficult and time consuming. Despite this, it is effective and can be used for polymers with molecular weights ranging from 10 000 to 10 million.

Ultracentrifugation is based on the principle that molecules under the influence of a strong centrifugal force (i.e. when the solution is rotated) will distribute themselves according to their size, perpendicular to the axis of rotation. This method gives the M_z average and information on the molecular weight distribution can be obtained from concentration gradient measurements. However, it is most effective with monodisperse systems and only approximate values are obtained with polydisperse polymer samples. It also requires the most intricate and expensive instrument.

Solution viscometry involves the measurement of the viscosity of dilute solutions. Until the development of gel permeation chromatography, it was the simplest and most widely used technique for routine measurement of molecular weight. It is based on the fact that the viscosity of a polymer solution increases as the molecular weight increases. One drawback of this method is that the so-called 'Mark-Houwink' constants must be known for the polymer in the solvent. It therefore requires calibration with polymers of known molecular weight (or a reliance on the values determined in the literature). Also, the molecular weight obtained is the viscosity average molecular weight, not the more useful number or weight average molecular weights.

Gel Permeation Chromatography (GPC) is a form of HPLC and has become the most widely used method for molecular weight determination. It fast and accurate and was the method used in this work for the determination of all the molecular weight data.

1.6.2 Gel Permeation Chromatography (GPC)

Gel permeation chromatography separates macromolecules according to their size. A schematic diagram of the components in a typical GPC system is shown in figure 1.4.

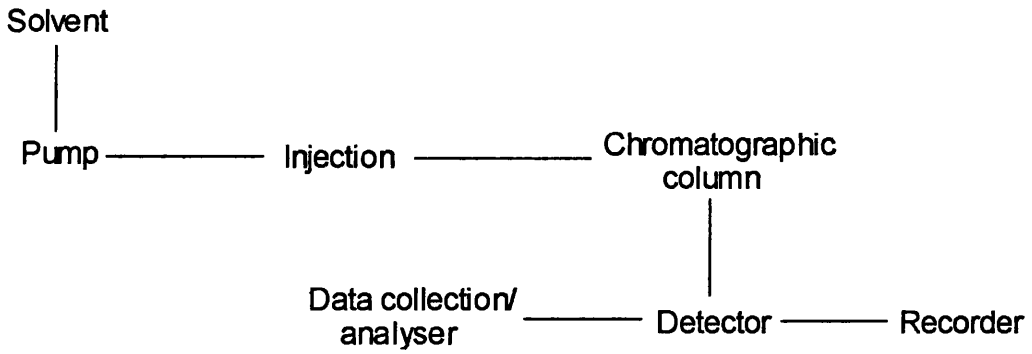

Figure 1.4 - The components of a GPC system

The chromatographic column is packed with porous beads which have a range of pore sizes. Typical column packings are silica or styrene-divinyl benzene copolymers[24]. If a mixture of different sized polymer molecules is eluted through the column, the smaller molecules can enter the pores and their flow through the column

will be retarded. Large molecules will be excluded from the pores and will flow through the column relatively unhindered. Hence, the polymer molecules are separated according to their size with the largest molecules emerging from the column first and the smallest emerging last. The concentration of each species emerging from the column is then measured by a detector. The two most common detectors are a differential refractometer, which compares the refractive index of the column effluent to a reference of pure solvent, and a UV/visible spectrophotometer for polymers with a significant absorbance. The resulting chromatogram is therefore a concentration-time profile, an example of which is shown in figure 1.5.

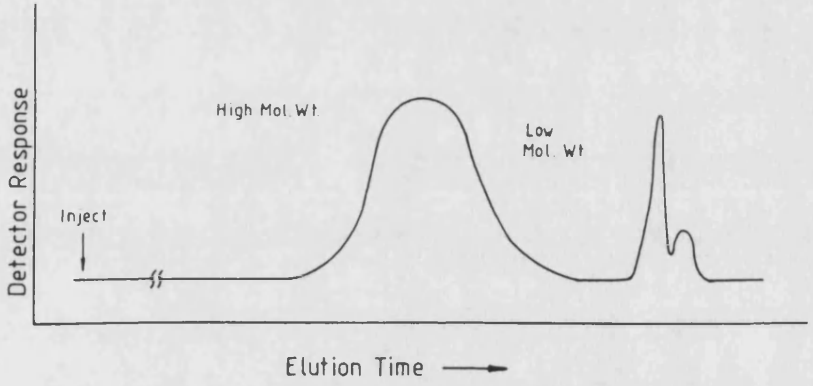

Figure 1.5 - GPC chromatogram

The retention time of each polymer species is directly related to the molecular weight, so to determine the molecular weight of the sample, the relationship between the molecular weight and the retention time needs to be known. The particular GPC set-up therefore needs to be calibrated by running narrow distribution polymer samples of known molecular weight through the GPC under identical conditions (eluent, flow rate and concentration). By knowing the relationship between the molecular weight and the retention time (figure 1.6), the chromatograms of the unknown samples can be transformed into a concentration-molecular weight profile and the various molecular weight averages and the polydispersity can be calculated using the formulae given previously.

Calibration standards are available for a number of polymers, such as polystyrene and poly(methyl methacrylate), however, there are many polymers for which standards are not available. In this case, the molecular weight of an unknown sample can be determined in two ways:

1) Calibrate the GPC with standards of a polymer that is available, for example, polystyrene. The molecular weight obtained for the unknown can then be quoted as a 'polystyrene equivalent' molecular weight.

2) Use a 'universal calibration'.

Universal calibration is based on the fact that a plot of hydrodynamic volume against retention time gives the same relationship for a large number of polymers[25]. Hydrodynamic volume, h.v., is related to molecular weight, M, by,

$$h.v. = M[\eta] \qquad (4)$$

where, $[\eta]$ is the intrinsic viscosity. Since $[\eta]$ is given by the Mark-Houwink equation ($[\eta] = KM^a$), if a calibration is performed using standards of polymer x, then as long as the Mark-Houwink constants, K and a, are known for the unknown polymer, y, its molecular weight can be determined from,

$$K_x M_x^{(1+ax)} = K_y M_y^{(1+ay)} \qquad (5)$$

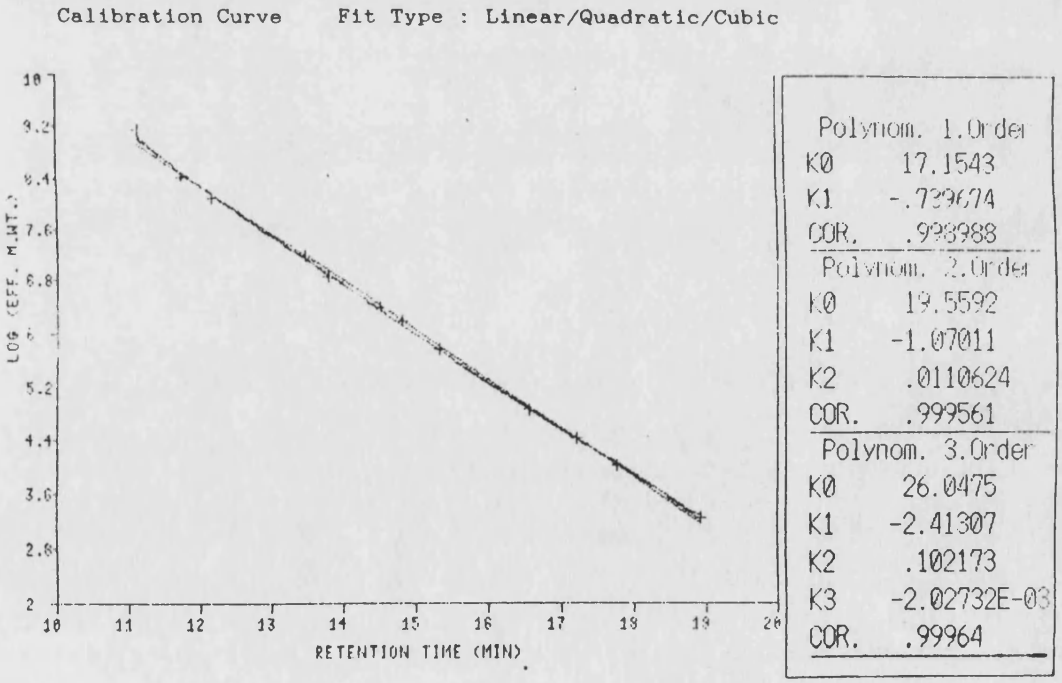

Figure 1.6 - Plot of log (molecular weight) against retention time

1.6.3 Spectroscopy

Although the molecular weight and polydispersity are probably the most commonly measured parameters of a polymer, knowledge of the chemical composition and sometimes the stereochemistry are also useful. For this information, spectroscopic methods, in particular, infrared and NMR, are invaluable.

As the IR and NMR spectra depend on the chemical structure of the sample under study, they provide a quick method of identifying polymers. Also, as a polymer will give a different spectrum to the monomer from which it is derived, they can be used to follow polymerisations as they occur.

Both ^{1}H and ^{13}C NMR can yield useful information about a polymer, however, of even more importance for polysiloxanes is the use of ^{29}Si NMR. For polysiloxanes, ^{29}Si NMR is significantly more useful than ^{1}H or ^{13}C NMR and it is a powerful technique for investigating the nature of the end groups.

The stereochemistry, or tacticity, of a polymer can also be investigated using spectroscopy. The IR spectra of highly stereoregular polymers are distinguishable from their less regular counterparts, although NMR has been found to yield more reliable information regarding polymer tacticity than IR.

1.6.4 Thermal Analysis

Stereoregular polymers will show partial crystallinity, i.e. there will be crystalline and amorphous regions. The crystalline regions are formed from the stereoregular components in the molecule. However, the absence of any stereoregularity in parts of the chain, branching and copolymerisation will all inhibit crystallisation and result in amorphous regions.

At sufficiently low temperature, both crystalline and amorphous polymers will be solid. When they are heated, two possibilities exist. Solid amorphous polymers are brittle and glassy in character. If they are heated, they will eventually become less rigid and more rubbery. The temperature at which the polymer passes from the hard, glassy to the soft, rubbery state is well defined and is referred to as the glass transition temperature, Tg. If it is heated still further, the rubbery polymer will eventually become a viscous liquid.

When crystalline polymers are heated, there will be a point where the solid polymer will melt and become a viscous liquid. However, because they are only

partially crystalline, the melting point is not well defined and will be dictated by the extent of crystallinity in the polymer. Also, the fact there are amorphous regions means the polymer usually exhibit a Tg as well.

Being able to measure the Tg (and melting point, if applicable) is important as it is the point where significant changes in the physical properties of the polymer, such as the heat capacity and refractive index, occur. The Tg is influenced by the molecular mobility of the polymer chains and so molecular features which either increase or decrease this mobility will cause differences in the value of Tg. Effects which can alter the Tg of a polymer include: hydrogen bonding, cross-linking, pendant groups attached to the polymer backbone and the presence of an inherently rigid structure, such as a phenylene group, in the backbone. Thus, seeing how the Tg has changed for a polymer will also provide information regarding the interactions between the chains in the polymer.

The usual way of measuring the Tg is to use Differential Scanning Calorimetry (DSC). DSC works by measuring the amount of energy required to heat the sample at the same rate as a control sample (usually just an empty sample holder). If the sample suddenly absorbs heat due to a transition, whether it's due to the Tg or melting, the energy required to keep heating it at the same rate as the control will increase. Measuring the energy required to heat the sample and control is usually achieved by measuring the electric current. As electric current can be easily monitored with great accuracy, this technique offers a sensitive way of measuring the Tg. An example of a DSC trace for poly(dimethylsiloxane) is shown in figure 1.7.

In this trace, the Tg is visible at approximately -120°C. The polymer chains then become sufficiently mobile near -80°C to align and partially crystallise. The melting peak can then be seen at approximately -40°C.

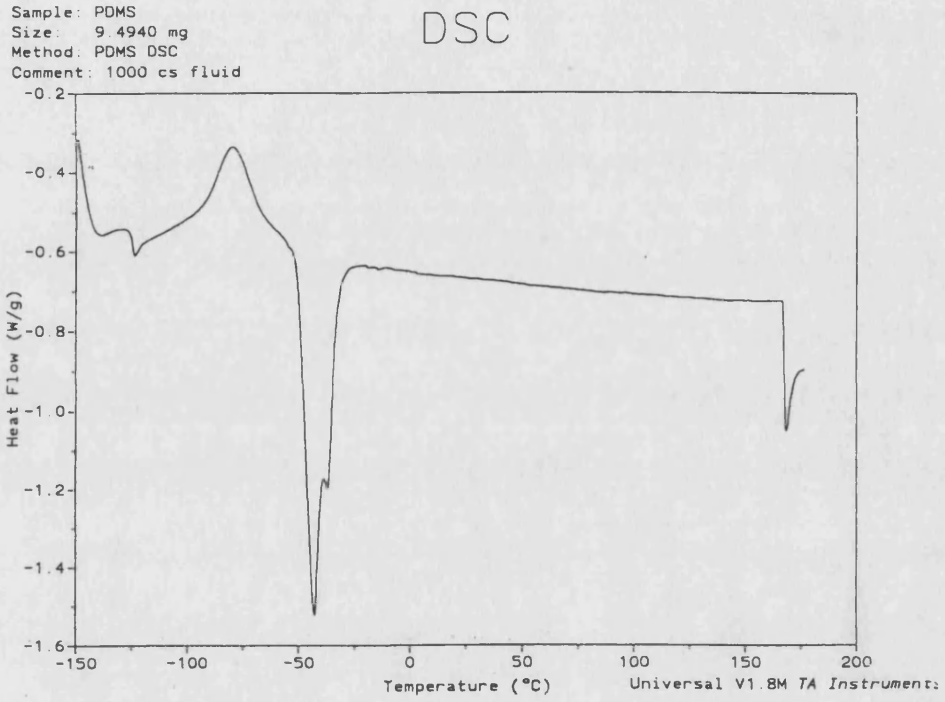

Figure 1.7 - DSC trace of poly(dimethylsiloxane)

1.7 Polysiloxanes

Polysiloxanes ('silicones') are the most common and probably the most important of the inorganic polymers. They are synthetic polymers of the general formula $R(SiR_2O)_nSiR_3$ and have found widespread use in medical and industrial processes due to their chemical inertness and superior physical properties.

Organosilicon compounds have been known since the 1860's when Friedel and Crafts[26] synthesised tetraethylsilane from tetrachlorosilane and diethyl zinc. However, it was Kipping who, from the turn of the century, conducted much of the early systematic investigations into the chemistry of the organosilicon compounds using the Grignard process. Hydrolysis of the materials he synthesised were found to give rise to compounds containing Si-O bonds and Kipping spent some time trying to synthesise compounds containing a silicon-oxygen double bond, i.e. the silicon analogue of a ketone. He called these compounds 'silicones', however, contrary to expectation, his products displayed properties quite different from ketones and they did not undergo the classical reactions of ketones[27]. Kipping also found that, unlike organic chlorides, chlorosilanes hydrolysed to poorly defined oily and glue-like products containing alternating silicon and oxygen atoms[28], although he persisted in calling them silicones and the term remains in use today. Kipping did not consider these polysiloxanes to be very significant, but by the 1940's several groups were actively engaged in the synthesis and characterisation of polysiloxanes. It was discovered that the thermal and oxidative stability of the polymers was much greater than most of the usual organic polymers. They also displayed chemical inertness, resistance to weathering and a relatively weak dependence of physical properties on temperature[27].

The 'direct process' for the manufacture of chlorosilanes was discovered by Rochow[29] and it provided a feasible procedure for the industrial manufacture of the organochlorosilanes, the precursors to polysiloxanes, and manufacture then began in the 1940's.

Military uses dominated early product development, with such uses as fluids for damping aircraft instruments and rubber for insulation. After World War II, civilian uses followed these patterns, but the use of polysiloxanes was expanded to include applications such as water repellents, lubricants and furniture polishes. Pharmaceutical applications began in the 1950's, and in the 1960's novel silicone

elastomers were introduced and sold as sealants and adhesives that cured without heat (room temperature vulcanising (RTV) rubbers)[33]. In 1969, Neil Armstrong became the first man on the moon, wearing a boot made of a silicone rubber[30].

The use of polysiloxanes continues to grow and today they are to be found in a myriad of functions, their unique properties finding application in fields as diverse as DIY and cosmetic surgery.

1.7.1 Structure

Polysiloxanes are polymers containing a backbone of Si-O bonds. The silicon atoms in the chain are also substituted with two side groups. These can be varied, changing the properties of the polymer.

The major classes of polysiloxanes discussed in this report are:

Cyclic siloxanes.

As their name suggests, these are cyclic molecules, although they are not polymers. They have the general structure:

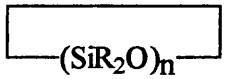

Two cyclic siloxanes have been used in the work:

Hexamethylcyclotrisiloxane - $(SiMe_2O)_3$

Octamethylcyclotetrasiloxane - $(SiMe_2O)_4$

Linear polysiloxanes.

Linear chain polysiloxanes have the general structure

$$R_3Si\text{-}O\text{-}(\text{-}SiR_2\text{-}O\text{-})_n\text{-}SiR_3$$

of which poly(dimethylsiloxane), or PDMS, (where R=Me) is probably the most widely used and is the polymer used in this work.

Other important classes of siloxanes are the silanols and siloxanediols:

$R_3Si\text{-}OH$	- silanols
$HO(SiR_2O)_nSiR_2OH$	- siloxanediols

Ring-opening polymerisation of the cyclic siloxanes and condensation reactions of the siloxanediols are the two ways in which polysiloxanes can be produced.

1.7.2 Nomenclature

The terminology for naming a polysiloxane consists of specifying the side groups and then the backbone. For example, the polymer with the repeat unit ($SiMe_2O$) is called 'poly(dimethylsiloxane)'. However, there is a 'shorthand' notation in which the letters M, D, T and Q are used to indicate the functionality of the siloxane[31-33]. Thus,

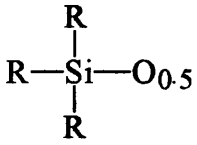

is designated **M** (monfunctional unit),

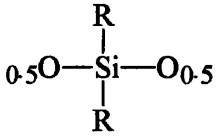

is designated **D** (difunctional unit),

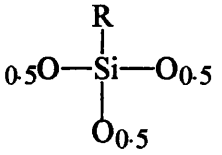

is designated **T** (trifunctional unit),

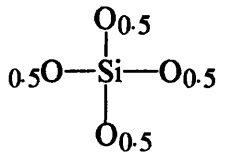

is designated **Q** (quadrifunctional).

Unprimed R groups imply methyl groups, since these are the most common and most important. Primed R groups are used for other substituents, of which phenyl is probably the most important[34].

An M unit usually ends a polymer chain, while D units continues the chain. Hence,

MM is $Me_3SiOSiMe_3$

$MD_{10}M$ is $Me_3SiO[SiMe_2O]_{10}SiMe_3$

and D_4 is the cyclic tetramer $[SiMe_2O]_4$

The structure of linear polysiloxanes can generally be described by MD_xM. Polysiloxanes containing significant quantities of T and Q units are more branched and give rise to the silicone resins[32].

1.7.3 Structural Features

Like carbon, silicon has 2 outer *s*-electrons and 2 outer *p*-electrons, thus allowing 4 bonds. However, unlike carbon, silicon has available, vacant *3d*-orbitals. The early view of the bonding in the Si-O bond considered that some of the unusual properties of siloxanes were due to the lone pairs of electrons on the oxygen interacting with the vacant *d*-orbitals, with the resulting $d\pi$-$p\pi$ interactions imparting partial double bond character to the Si-O bond[33] . As a result, the Si-O bonds are unexpectedly strong and the Si-O-Si bond angle is much larger than expected. However, reanalysis of the siloxane bond using ab initio methods[144,145] has challenged this view.

Comparison of the bond angles about oxygen along the series, dimethyl ether (C-O-C = 112°), methoxy silane (Si-O-C = 121°) and disiloxane (Si-O-Si =144°) shows the bond angle widening as the methyl groups are replaced by silyl groups. The large bond angle about the oxygen contributes to the unusual properties of polysiloxanes, and as well as $d\pi$-$p\pi$ interactions, enhanced steric and electrostatic effects have also been proposed to account for this effect. However, ab initio

calculations and analysis of the HOMO's of disiloxane, have shown that the bonding is better described in terms of the interaction between the oxygen *2p*-orbital and the σ^* LUMO of SiH_3.

In disiloxane, the key interactions are between the π and σ-type lone pair orbitals on oxygen and the degenerate $\pi(SiH_3)$ group orbitals. The HOMO for disiloxane is generated from combination of the n_π with the $\pi(SiH_3)$ orbitals, while the combination of n_σ with $\pi(SiH_3)$ generates the HOMO-1. A plot of these orbitals show that they are primarily localised on the hydrogens. The contributions on oxygen are very small and there is no clear evidence for the involvement of the *d*-orbitals on silicon. For comparison, the corresponding HOMO and HOMO-1 in dimethyl ether reveals hybridisation at oxygen with noticeable bulging in the lone pair directions. The bending in dimethyl ether and disiloxane is then promoted by mixing of the oxygen *2p*-orbital (HOMO) with the $\sigma^*(SiH_3)$ LUMO. However, compared to dimethyl ether, the HOMO of disiloxane has significantly less *2p* character on oxygen and consequently the *2p*(O) - $\sigma^*(SiH_3)$ overlap on bending is significantly lower for the disiloxane. Hence the bending is not as favourable and the bond angle about oxygen is greater. It is therefore the *2p*(O) - $\sigma^*(SiR_3)$ interaction, and not the $d\pi$-$p\pi$ interactions between the lone pairs and vacant 3d-orbitals, that account for the unusual properties of the siloxane bond.

The siloxane backbone is one of the most flexible of all polymers. The Si-O bond length is 0.164 nm, which is considerably longer than the C-C bond length of 0.153 nm of most organic polymers[34] . Also, the oxygen atoms in the chain have no side groups. The result of these two factors is that, compared to similar organic polymers, the steric interactions between the side groups on the siloxane chain are much lower. The comparatively long Si-C bonds (0.188 nm) also helps to relieve steric clashes.

The Si-O-Si bond angle (180 - θa) of 143° is much larger than usual (as described above) and torsional rotations about the chain can occur without incurring serious energy penalty. The tetrahedral bonding around the Si atoms (180 - θb) is more usual at 110°. As a result of these bond angles, the planar 'trans' conformation (as shown) closes upon itself in the course of about 11 units[35] (note that adherence to planarity over the span of such a number of units will be very rare, given the flexibility

of the chain and the many number of conformations available to it).

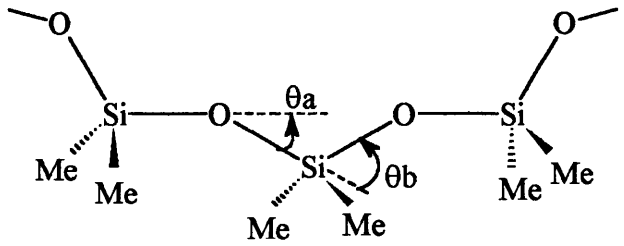

The combined effect of the large bond lengths and bond angles, with the diminished steric interactions between side groups, results in the siloxane chain being very flexible[34]. It is this flexibility which gives rise to some of the properties which make polysiloxanes suited to so many applications.

1.7.4 Properties

Polysiloxanes have some unusual properties which have made them useful for a wide variety of industrial and medical applications. The main properties are[27,32-34,36]:

- Thermal and oxidative stability at high temperatures (300°C and higher).
- They retain flexibility and elasticity at very low temperatures (-60°C and lower). i.e. they have a very low Tg.
- They are relatively indifferent to changes in temperature. Silicone oils change less in viscosity with change in temperature than organic oils.
- They are inert. They resist sunlight, weathering, many chemicals and they are not corrosive to metals. Hence their use for medical purposes.
- The chains have a very low surface energy and surface tension, polysiloxanes consequently exhibit unusual surface properties. For example, they are water repellent but have a high permeability to gases. They are good anti-foaming agents (i.e. they can break down foams) and can prevent surfaces from sticking to each other (a property known as 'release' or 'abhesiveness').
- They can show thermotropic behaviour, i.e. they can have liquid crystalline properties

1.7.5 Applications

The unique properties of silicones have found them being employed for a wide range of uses. Some examples of medical[34,37] and non-medical[32,36,38] applications are:

Medical applications

Prostheses, artificial organs, facial reconstruction, tubing and catheters, all take advantage of the inertness, stability and pliability of polysiloxanes. Artificial skin, contact lenses and drug delivery systems, also utilise their high gas permeability.

Polysiloxanes are also used in cosmetic products, such as the base for lipsticks.

Non-medical applications

Typically include; silicone oils and greases, adhesives, sealants, waterproofing, anti-foams, mold-release agents, electrical insulators, protective coatings, heat transfer fluids, polishes, inks and gas chromatography substrates, among many others. A recent application has been the use of polysiloxanes in micro-lithography.

1.8 Synthesis of Polysiloxanes

The process for making polysiloxanes involves a number of steps, beginning with the reduction of silica to silicon. The silicon is then converted to a chlorosilane, which is then subsequently hydrolysed to produce the monomers from which the polysiloxanes are obtained.

1.8.1 Silica to Silanes

The silicon in polysiloxanes is obtained from the mineral silica, which is the natural source of silicon. Silica is reduced to silicon metal in an electric furnace[33,34].

$$SiO_2 + 2C \longrightarrow Si + 2CO$$

The first industrial process then converted the silicon to tetrachlorosilane.

$$Si + 2Cl_2 \longrightarrow SiCl_4$$

This was then reacted with a Grignard reagent;

$$SiCl_4 + 2RMgX \longrightarrow R_2SiCl_2 + 2MgClX$$

This method is, however, operationally difficult and costly. It was replaced by the 'Direct Process' (or 'Rochow Process')[34,39] which consists of an organic halide reacting directly with elemental silicon.

$$Si + 2RCl \longrightarrow R_2SiCl_2 \text{ (using a catalyst)}$$

where RCl is usually methyl chloride. A metallic catalyst, principally copper and copper compounds, at a temperature of 250 - 350°C is also used. The process also yields $RSiCl_3$ and R_3SiCl, however, these can be removed by distillation.

1.8.2 Hydrolysis of the Silanes

Hydrolysis of the diorganchlorosilanes produces diorganosilanediols, which contain the $-SiR_2O-$ units required in polysiloxanes.

$$Me_2SiCl_2 + 2H_2O \longrightarrow Me_2Si(OH)_2 + 2HCl$$

Dimethyl silanediol is not very stable and readily condenses. The condensation gives rise to a mixture of cyclic and linear structures[33,38].

$$nMe_2Si(OH)_2 \longrightarrow HO(Me_2SiO)_n H \quad \text{linear siloxanediols}$$

$$nMe_2Si(OH)_2 \longrightarrow [Me_2SiO]_n \quad \text{cyclic siloxanes}$$

The relative proportions of the products obtained depends on the reaction conditions used. For example, when an excess of water is used in the hydrolysis, about half the material occurs as linear polysiloxanediols[27]. The other half consists of a mixture of cyclic species, mainly the tetramer (D_4). Only a small amount of the trimer (D_3) is produced. Decreasing amounts of the higher numbered cyclics (upto n=10) can

be separated and identified[33]. Rapid removal of the hydrochloric acid by neutralisation leads almost exclusively to short chain siloxanediols. However, if there is prolonged contact with HCl, upto two-thirds of the product will be cyclic siloxanes[32].

Pure cyclic siloxanes can be produced by cyclisation. This is performed by heating the hydrolysis mixture with potassium hydroxide. Potassium hydroxide catalyses an equilibrium reaction in which the Si-O-Si bonds are continually cleaved and reformed. During the reaction, the lower boiling cyclics (D_4 and D_5) are continuously distilled from the reaction mixture. The cyclic siloxanes are thus constantly reformed to maintain the equilibrium until the siloxane mixture is nearly all converted to the desired cyclic siloxanes[32].

The ratio of cyclic to linear dimethylsiloxanes and the chain length of the linear oligomers can be varied over a relatively wide range by means of the hydrolysis conditions. Control of the hydrolysis reaction to give predominantly cyclic or linear oligomeric dimethylsiloxanes is important because high molecular mass PDMS can be produced both by ring-opening polymerisation of the cyclic siloxanes and by polycondensation of the linear siloxanediols.

Hydrolysis of higher alkyl homologues, e.g. diethyldichlorosilane, give higher yields of the smaller cyclic compounds under comparable conditions. However, aryldichlorosilanes give high yields of diols when hydrolysed[33].

Hydrolysis of a mixture of dimethyldichlorosilane and trimethylchlorosilane gives a series of trimethylsiloxy chain-terminated products, along with hexamethyldisiloxane and cyclics, i.e.

$$MM \qquad D_n \qquad MD_xM$$

Again, the particular distribution of the three types depends on the reaction conditions. The chain length of the linear oligomers is dependent on the M:D ratio. Trimethylsiloxy-terminated dimethylsiloxanes (MM and MD_xM) are used to control the molecular weight during polymerisation (ring-opening or polycondensation).

1.9 Ring-Opening Polymerisation

The polymerisation to form polysiloxanes can be performed in two ways: the ring-opening polymerisation of cyclic siloxanes, and the polycondensation of siloxanediols. Ring-opening polymerisation allows greater control over the molecular weight and is therefore the preferred method for the synthesis of high molecular weight polymer.

$$(SiR_2O)_{3 \text{ or } 4} \longrightarrow (\text{-}SiR_2O\text{-})_n$$

3 = hexamethylcyclotrisiloxane

4 = octamethylcyclotetrasiloxane

n = degree of polymerisation

Ring-opening polymerisation may be achieved using both anionic and cationic catalysts, and may also be classified as thermodynamically or kinetically controlled[40].

1.9.1 Thermodynamically Controlled Polymerisation

Polymerisation is thermodynamically controlled when it is allowed to reach equilibrium, hence this method is often referred to as equilibration. The process involves the continual cleavage and reforming of the Si-O bonds in a mixture of cyclic and linear siloxanes, until the system reaches thermodynamic equilibrium[41] . The preferred monomer is octamethylcyclotetrasiloxane (D_4) and equilibrium can be achieved using acid (cationic) or base (anionic) catalysts[32].

High molecular weight polymers can be produced and molecular weight control is achieved by using the hexaorganodisiloxanes ($R_3SiOSiR_3$) as chain transfer agents[42] . To produce simple, linear PDMS, the R group is methyl. However, the functionality of the end-groups can be changed by changing the nature of the R groups. Thus, if vinyl end groups are required, the following chain transfer agent can be used[39]:

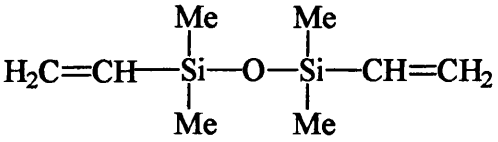

The siloxanes with modified end-groups are produced by the hydrolysis of the appropriate organochlorosilane. For the vinyl group, this would be:

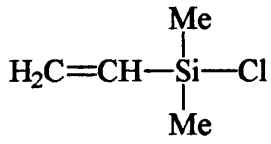

Difunctionally-terminated polysiloxanes play an important part in silicone technology and other important end groups include, -OH, -OMe, -OEt and -NH_2 [41].

The polymerisation is thermodynamically driven by an increase in entropy. The bonds linking the monomer units are similar in energy to those found in the siloxane ring, thus the net energy change during polymerisation is small and insignificant. However, there is an increase in entropy due to the increased internal molecular freedom of the siloxane segments in going from the cyclic to the linear structure. This is the opposite of organic polymerisations which are driven by an enthalpy decrease as the entropy change is negative[34].

Both the acid and base catalysed polymerisations are complex equilibrium polymerisations, comprising a series of competing reactions involving both cyclic and linear species. A simple reaction scheme for the polymerisation of D_4 using an initiator, I, (which can be an acid or a base), hexamethyldisiloxane, M_2, (for molecular weight control), and representing the growing polymer chain as P_n*, is[43]:

Initiation: $I + D_4 \rightleftharpoons P_4^*$

Propagation: $P_n^* + D_4 \rightleftharpoons P_{n+4}^*$

Depropagation: $P_n^* \rightleftharpoons P_{n-x}^* + D_x$

Redistribution: $P_n^* + P_m \rightleftharpoons P_{n+x} + P_{m-x}^*$

Transfer: $P_n^* + M_2 \rightleftharpoons P_n + M^*$

$M^* + D_4 \rightleftharpoons P_4^*$

Redistribution and depropagation are inevitable and in these processes siloxane bonds interchange so as to bring about variation in both molecular weight and the relative amounts of cyclic and linear species (i.e. equilibration is occurring). At equilibrium a Gaussian distribution of molecular weights among the linear molecules exists, while the cyclics show a monotonically decreasing concentration as the ring size increases[27]. A theoretical analysis of systems such as this, where cyclic molecules are in equilibrium with linear molecules, has been developed by Jacobson and Stockmayer[44] and experimental studies on equilibrated polysiloxanes have confirmed the predictions of the theory[27]. The molecular weight of the resulting linear polysiloxanes depends on the amount of end-blocker ('M') used. Obviously, the greater the amount of end-blocker, the lower the resulting molecular weight.

In the polymerisation of D_4, Grubb and Osthoff[45] concluded that the rate of polymerisation of D_4 to PDMS is governed by the competing polymerisation and depolymerisation reactions, i.e.

$$P_n + D_4 \rightleftharpoons P_{n+4}$$

However, the equilibrium involves cyclic species other than D_4 and this was first reported by Scott[46] . Brown and Slusarczuk[47] later confirmed the presence of cyclic species upto D_{25} using GPC and GLC techniques and were able to demonstrate the presence of a continuous population of cyclics upto D_{400} (at equilibrium) using fractionation and high resolution GPC.

At equilibrium, the reaction mixture contains approximately 10 - 15% cyclic species, and although the other cyclics are present, the majority of this is D_4. The equilibrium amount of D_3 is minimal and this is due to the ring strain present in the ring. It has been found that the position of the equilibrium is independent of the type of catalyst (acid or base) used and is determined by the nature of the substituents on the silicon atoms, the temperature and the concentration of the siloxane units in the system (i.e. whether the polymerisation is conducted in the bulk or in solution)[41]. Conducting the polymerisation in solution gives rise to an increase in cyclisation and above a certain dilution no linear species are formed[44].

Before the resulting polymer is used for commercial applications, the lower molecular weight species (mostly cyclics) are removed by distillation. They can then be recycled back into the polymerisation process[32].

1.9.2 Kinetically Controlled Polymerisation

Kinetically controlled polymerisation is based on the enhanced reactivity of the cyclotrisiloxanes as a result of the ring strain present in the molecule (15 $kJmol^{-1}$ for D_3 [41]). In this polymerisation the ring-opening is much faster than the equilibration, so the process essentially consists of two steps:

1 - chain propagation leading to linear polymer

2 - redistribution and cyclic formation until equilibrium is reached

$$\text{monomer} \xrightarrow{k_1} \text{linear polymer} \underset{k_3}{\overset{k_2}{\rightleftharpoons}} \text{cyclics} \qquad k_1 > k_2$$

Hence, if the polymerisation is quenched at a suitable moment, equilibration can be avoided. Using this method allows the production of polysiloxanes with low polydispersity (i.e. a narrow molecular weight distribution), however, control of the process is obviously more difficult than thermodynamically controlled polymerisation.

1.9.3 Anionic Polymerisation

Anionic (i.e. base catalysed) polymerisation is the principal method for the production of high molecular weight and functional polysiloxanes. It can be achieved using strong inorganic alkalis such as metal hydroxides and quaternary ammonimum and phosphonium hydroxides[33]. Organometallic compounds such as *n*-butyl lithium can also be used[27].

Initiation involves nucleophilic attack of the monomer, resulting in ring-opening and the formation of a metal silanolate.

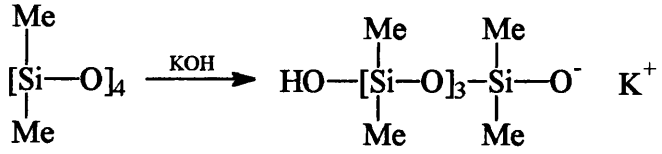

Chain propagation then occurs with the active species being the silanolate anion.

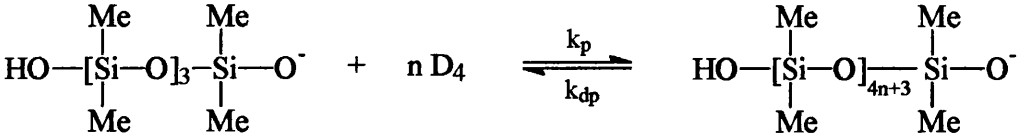

Redistribution and cyclic formation (section 1.9.5) proceed by attack of the active centre on the Si-O bonds within the linear polymer molecule[27].

The production of a metal silanolate, when a metal hydroxide reacts with the cyclic siloxane, was first noted by Hyde[42] in 1949. Grubb and Osthoff[45] confirmed this finding, concluding that the metal silanolate was the catalytic species and that the polymerisation was an addition polymerisation (D_4 units are added to the end of a growing chain).

The reactivity of the silanolate is dependent on the nature of the counter-ion. For metal silanolates, larger metal ions result in more active catalysts. Thus, the order of reactivity is:

$$Cs^+ > Rb^+ > K^+ > Na^+ > Li^+$$

which is also the order in which the degree of ionisation of their metal salts, or silanolate derivatives, decreases[33]. Quaternary ammonium and quaternary phosphonium silanolates have approximately the same order of activity as Cs^+ [43].

The reactivity of the metal silanolates can be enhanced by the addition of 'cocatalysts' or 'promoters', such as crown ethers, dimethyl sulphoxide (DMSO) and dimethyl formamide (DMF). These act by complexing the cation counter ion which weakens the interaction between the silanolate anion and the cation counter ion. This increases the concentration of free anions, which are more reactive to nucleophilic attack at the silicon atoms of the monomer and have faster rates of propagation in the polymerisation reaction[27].

The ring size of the monomer used will also affect the reaction rate. The relative rate is in the order:

$$D_3>D_4>D_5<D_6<D_7\sim D_8\sim D_9$$

This order can be explained by the fact that the energy change when a silanolate anion attacks the silicon atom of a cyclic siloxane is constant (i.e. the energy change for D_3 is the same as that for D_7). However, the entropy change does vary with ring size[33].

In general, the anionic polymerisations show a number of general features:

- the polymerisation exhibits an induction period which is more pronounced at lower temperatures
- the rate of consumption of monomer obeys first order kinetics
- the order in the catalyst is fractional and often 0.5

The rate determining step in the polymerisation is the propagation/depropagation reaction[43],

$$D_4 + P^*_n \underset{k_{dp}}{\overset{k_p}{\rightleftharpoons}} P^*_{n+4}$$

and the reported activation energy is 19.5 kcalmol^{-1} (~82 kJmol^{-1}). For cyclotrisiloxanes, the activation energy is approximately 16.5 kcalmol^{-1} (~69 kJmol^{-1}), the difference closely matching the ring strain in the molecule[39].

Once equilibration is complete, the catalyst must be deactivated. This is usually done through neutralisation (for example, KOH is neutralised by phosphoric acid) or by washing. The catalyst needs to be removed as even traces of the catalyst left behind can cause degradation of the polymer by depolymerisation[32]. Degradation can be avoided by the use of 'transient' catalysts such as tetramethylammonium hydroxide and tetrabutylphosphonium hydroxide. These are effective at polymerisation temperatures, but on heating to a higher temperature for a short time they decompose to give volatile products[48] . They are therefore easily removed from the system at the end of the polymerisation and produce stable polymers with improved resistance to thermal degradation at high temperatures[33].

1.9.4 Cationic Polymerisation

Acid catalysts can also be used in the ring-opening polymerisation of cyclic siloxanes and some of the first commercially available high molecular weight siloxane polymers were prepared in this way[43].

Important catalysts are strong sulphonic acids, such as triflic acid (CF_3SO_3H) and protonic acids such as sulphuric acid (H_2SO_4)[42]. Some commercial processes utilise H_2SO_4 in the form of acidic silicates, diatomaceous earth and sulphonated polystyrene cation exchange resins[27]. However, despite the fact that cationic polymerisation has been known and used commercially for many years, the mechanism for the polymerisation is not fully understood.

Two general mechanisms have been proposed for the polymerisation: addition polymerisation and acidolysis/condensation[42,43].

In addition polymerisation chain growth occurs by the reaction of monomer with some active propagating centre, -SiX, which may be an oxonium ion (R_3O^+), or a discrete silicenium ion (R_3Si^+).

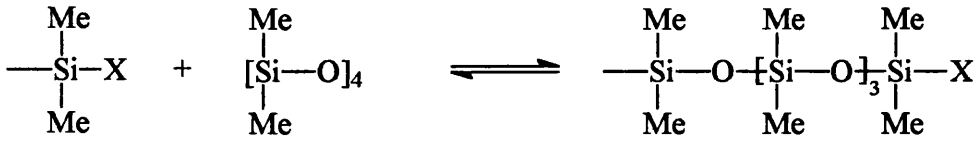

Wilczek et al[49] proposed that a protonated silanol, i.e. a primary oxonium ion, dominates as the reactive intermediate when additional water is absent, although protonated monomer (secondary oxonium ion) may become important at higher water concentration. They considered that tertiary trisilyloxonium ions and silicenium ions were only likely to be formed as transient, very short-lived species. However, Olah et al[146] showed that both D_3 and D_4 could be polymerised by trisilyloxonium ions, prepared *in-situ* via Corey hydride transfer.

Of the mechanisms proposed for cationic polymerisation, most have preferred not to invoke a discrete silicenium ion as the active species[43]. Numerous attempts have been made to form a stable, discrete silicenium ion in the condensed phase, however, the existence of long-lived silicenium ions has been controversial and, at best, only partial silicenium ions have been produced.

Free silicenium ions are positively charged, planer, three-coordinate species with a L-Si-L bond angle of 120°. However, partial cations with varying degrees of silicenium ion character have been produced, whereby the silicon is four coordinate, with partial bonding to the fourth coordination site, and possesses the majority of the positive charge. The fourth coordination site is generally occupied by a solvent molecule (solvent-separated ion pair) or a weakly coordinating anion (intimate ion pair).

Partial silicenium ions in solution and in the solid have been prepared with ever decreasing covalency of the fourth coordination site, including complexes of acetonitrile, ethers, water, sulfolane, aromatics and dichloromethane[147]. However, the most successful has been the solvent-free complexes of carborane anions[147,148] although the complex of $Pr^{i}_{3}Si(Br_5\text{-}CB_9H_5)$, in which the carborane anion $Br_5\text{-}CB_9H_5^-$ is very weakly coordinated via a bromine atom, only has about one third silicenium character.

Thus, if the silicenium ion is involved in the cationic ring-opening polymerisation, its existence is likely to be fleeting and Chojnowski has proposed that if it does form it will be transformed immediately into an oxonium ion[40].

Acidolysis/condensation is thought to occur via electrophilic attack on the siloxane oxygen by a proton, resulting in the formation of silanol (SiOH) and silyl ester (SiA) groups.

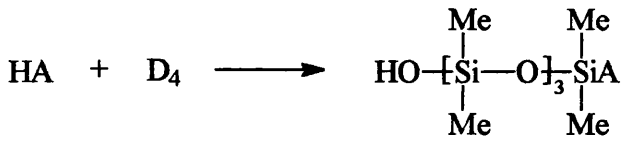

where HA represent the acid.

The products may then undergo polycondensation and hydrolysis reactions to form oligomers and, subsequently, polymers.

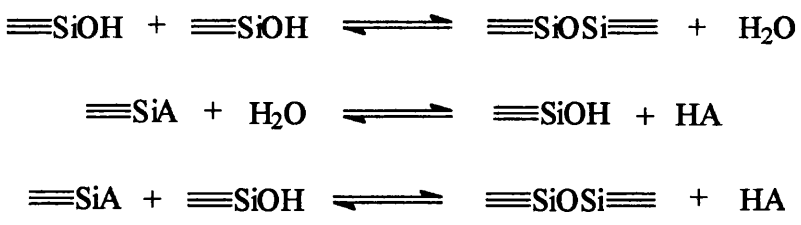

The polymerisation is very sensitive to additives. Ethers are found to decrease the reaction rate, weaker acids can increase the rate, while water can act as both a promoter and an inhibitor[40]. For example, in the polymerisation of D_3 initiated with triflic acid the reaction is slow and shows a negative apparent order in the monomer. On addition of water, the rate increases by a factor of 100, the order in monomer becomes first order and the activation energy increases by 75 $kJmol^{-1}$. In D_4 the activation energy was found to increase from 24 $kJmol^{-1}$ to 72 $kJmol^{-1}$ on addition of water. This effect was explained by considering the equilibria in the acidolysis/condensation mechanism. The introduction of water liberates the acid and consequently increases the rate. Also, the water can form strong complexes with the acid and this complexation can modify the acid reactivity[49].

The cationic polymerisation is a complex process and is not as well understood as the anionic polymerisation. There are many questions surrounding the exact mechanism and although most workers agree that both the addition and acidolysis/condensation mechanisms are likely to occur simultaneously[43], the mechanism varies in detail with the variation of monomer, acid and reaction conditions[40].

1.9.5 Secondary Reactions

In both the anionic and cationic polymerisation of cyclic siloxanes, as well as the propagation reactions that lead to chain growth and high molecular weight polymers, other intra and intermolecular reactions occur. It is these reactions that are responsible for cyclic formation and redistribution. They proceed by attack of the propagating active centre on the Si-O bonds within the linear polymer molecules.

Intramolecular reactions occur when an active centre attacks a siloxane bond within the same molecule. This is often known as 'back-biting' and results in the formation of the cyclic species. Each of the cyclics can re-enter the polymerisation reaction until equilibrium is reached

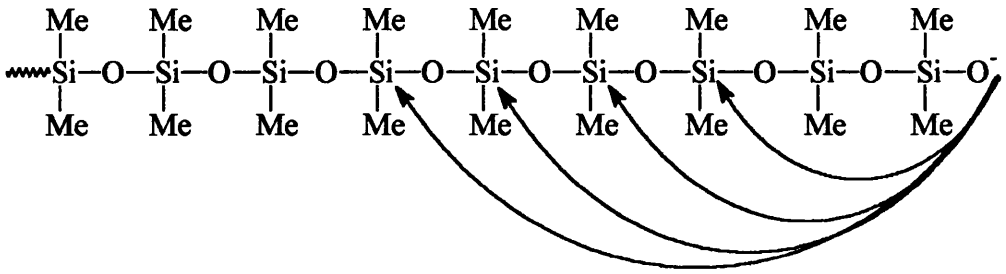

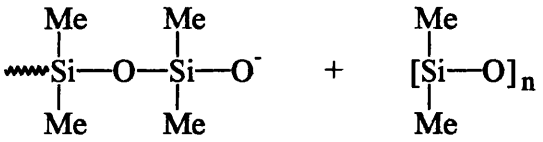

n = 3,4,5,6.....

Intermolecular reactions occur as siloxane exchange processes. These reactions result in a broadening of the polymer molecular weight distribution[27].

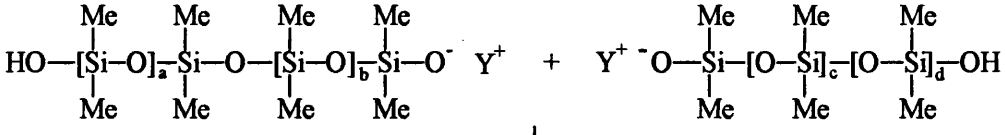

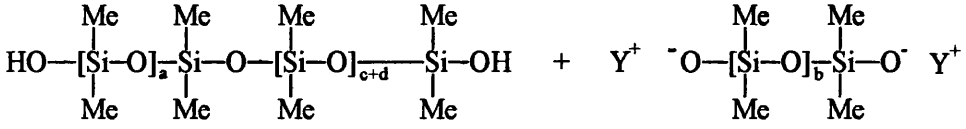

1.10 Polycondensation of Siloxanediols

In addition to the ring-opening polymerisation of cyclic siloxanes polysiloxanes can also be produced by polycondensation of siloxanediols.

Siloxanediols ($HO[Me_2SiO]_nOH$) are produced by the hydrolysis of the dichlorosilanes[33,38]. If high molecular weight linear polymers are required, high purity dichlorosilanes are needed. If any trichlorosilanes or tetrachlorosilanes are present, they will hydrolyse to form the T and Q units resulting in branched structures[38].

As the linear siloxanediol oligomers are thermally stable, for condensation to occur the reaction must be catalysed and this can be achieved using both acids and bases[50].

If no other species are present the final polymer will be OH-terminated. Reactions of the terminal OH groups with another silicon derivative containing the labile -SiX group can be used to functionalise the polymer.

$$\sim\!\!\sim SiOH + R_3SiX \longrightarrow \sim\!\!\sim SiOSiR_3 + HX$$

X is typically OH, OR, Cl and NR_2. This technique can be used for the preparation of block copolymers (if R is another polymer)[27] and is also the basis for cross-linking polysiloxanes to produce silicone elastomers[50].

1.10.1 Acid Catalysed

Many acids will catalyse the polycondensation reaction, including HCl, H_2SO_4, HNO_3, and H_3PO_4, although industrially, polychlorophosphazenes $[(PNCl_2)_x]$ are used.

The mechanism proposed for the condensation consists of two processes[50]:

i. formation of a primary oxonium ion,

$$\equiv SiOH + HX \rightleftharpoons \equiv SiOH_2^+ X^-$$

ii. reaction of a silanol with the oxonium ion.

$$\equiv SiOH + \equiv SiOH_2^+ X^- \rightleftharpoons \equiv SiOSi\equiv + HX + H_2O$$

Thus, the overall reaction is,

$$2\equiv SiOH \rightleftharpoons \equiv SiOSi\equiv + H_2O$$

The water produced in the reaction must be removed and when the desired chain length has been reached, the catalyst is deactivated with ammonia or an amide[32].

Oxonium ions have been postulated as intermediates in both cationic ring-opening and polycondensation. However, unlike silicenium ions, oxonium ions have been prepared and isolated. Relatively stable, long-lived ions have been produced, supplying evidence to suggest that oxonium intermediates are involved in

both acid-catalysed polymerisations.

Olah et al[149] prepared a series of (trimethylsilyl)oxonium ions by protonation of the corresponding silanol, ether or siloxane, in FSO_3H-SbF_5/SO_2 at –78°C, while in their quest for isolation of the silicenium ion, both Kira et al[150] and Reed et al[151] generated silyloxonium ions.

Kira et al attempted to use tetrakis[3,5-bis(trifluormethyl)phenyl]borate (TFPB) as a counter-anion for silicenium ions. However, the reaction of hydrosilanes with trityl-TFPB and NaTFPB in ether at low (-70°C) temperatures, failed to produce silicenium ions, but did generate silyloxonium ions which were stable enough for analysis by NMR.

Reed et al isolated a protonated silanol, $[Bu^t_3Si(OH_2)]^+$, as a crystalline salt that was stable at room temperature and allowed a crystal structure to be obtained. They used the carborane anion $Br_6CB_{11}H_6^-$ as a weakly coordinating anion in the complex $(Pr^i_3Si)(Br_6CB_{11}H_6)$. They treated this partial silicenium ion with wet solvents leading to displacement of the weakly coordinated anion and the formation of $[Bu^t_3Si(OH_2)]^+$. The proton NMR provided strong evidence for the formulation of the cation as the protonated silanol, while ^{11}B NMR of the anion showed it to be that of the free ion. The crystal structure showed weakly associated cations and anions and suggested some hydrogen bonding of the O-H bonds of the cation to the Br atoms of the anion. The most notable features of the oxonium structure were the trigonal flattening of the four-coordinate silicon (with an average C-Si-C bond angle of 116°) and a long Si-O bond (1 – 2 nm longer than typical Si-OH or Si-OR bonds).

1.10.2 Base Catalysed

Polycondensation can be catalysed by adding strong bases, such as KOH, NaOH and LiOH. The reaction consists of two stages[50]:

i. formation of a silanolate,

$$\equiv SiOH + M^+OH^- \rightleftharpoons \equiv SiO^- M^+ + H_2O$$

ii. nucleophilic attack of the silanol by the silanolate.

$$\equiv SiO^- M^+ + \equiv SiOH \rightleftharpoons \equiv SiOSi\equiv + M^+OH^-$$

where MOH represents the base used. Thus, the overall reaction is,

$$2\equiv SiOH \rightleftharpoons \equiv SiOSi\equiv + H_2O$$

1.11 Polysiloxane Copolymers

The unique properties of polysiloxanes (1.7.4) such as thermal and oxidative stability, elasticity and low surface energy fulfil a wide range of needs and they have subsequently found widespread and diverse use. However, despite their outstanding properties, to develop useful mechanical properties very high molecular weights are required. Although, even then they can exhibit cold flow and weak rubbery properties. Therefore, in many commercial applications PDMS is usually cross-linked and then filled (upto 50 % by weight) with finely divided, high surface area silica. This can dramatically improve the mechanical properties of the polymer. The tensile strength of silicone elastomers filled with silica can be as much as 50 times that of the unfilled polymer[32]. However, other problems can be encountered in processing filled and cross-linked polymers.

The synthesis of siloxane copolymers offers an alternative method of improving the mechanical strength of polysiloxanes. The soft, rubbery polysiloxanes can be linked to a hard, glassy or crystalline polymer to produce a copolymer. The properties of the copolymer will depend on the particular polymer used, the block lengths and the composition. These systems usually show two phase morphologies, where the hard segment domains serve as physical cross-links and/or reinforcing filler for the continuous rubbery phase[41].

One of the first examples of siloxane-organic block and graft copolymers were those of polysiloxane and poly(ethylene oxide). These materials can be produced in two ways. Reaction between SiX-terminated siloxane and OH-terminated poly(ethylene oxide), where X is H, Cl, OR or NR_2,

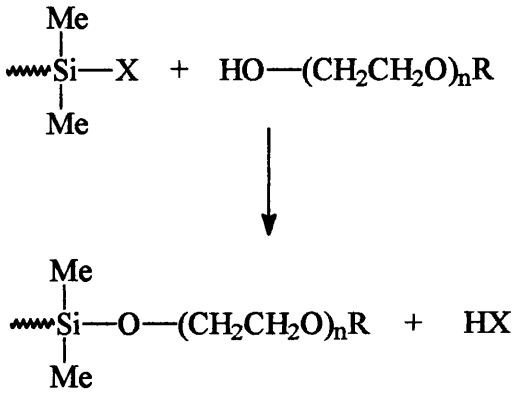

and hydrosilylation between a hydride terminated siloxane and a vinyl terminated poly(ethylene oxide) using a platinum catalyst (e.g. chloroplatinic acid).

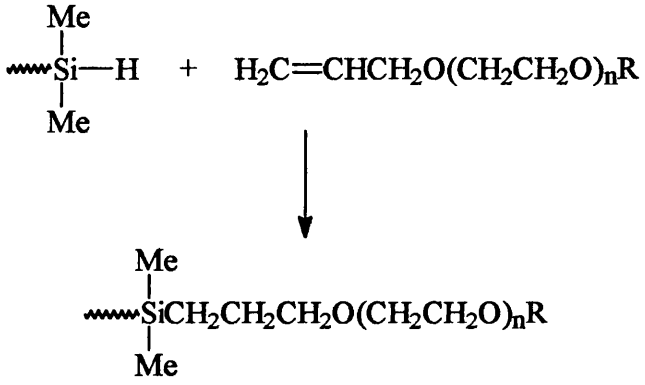

The copolymers produced have surfactant properties, the siloxane component strongly influencing the surface tension, and are widely used as foam stabilisers for the production of polyurethane foams[32].

These two methods of condensation and hydrosilylation have also been used to produce many other copolymers.

Condensation reactions can be utilised for the synthesis of a wide range of copolymers and this is due to the wide variety of functionally terminated siloxane oligomers that can be produced. These have the general form,

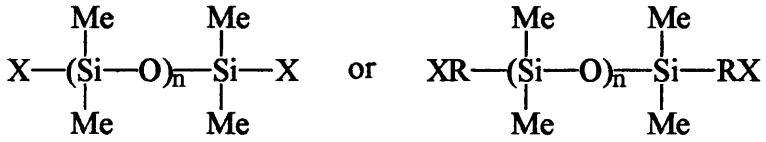

where X can be -Cl, -OH, $-NH_2$, $-NMe_2$, $-CH=CH_2$ and -OMe, among others, and R is an alkyl or aryl group.

Examples of the types of copolymers that have been synthesised by this method include, siloxane-urea, siloxane-imide, siloxane-ester, siloxane-carbonate and siloxane-urethane[41,51,52].

Hydrosilylation reactions are typically used for the synthesis of liquid crystalline polymers. Two different structures are possible using this method: incorporation of the siloxane into the polymer backbone, i.e. a block copolymer of the siloxane and mesogenic component, or a graft copolymer whereby the mesogenic group is grafted onto a siloxane main chain[41,53,54].

For the block copolymer structure (a main chain liquid crystalline polymer), hydrosilylation occurs between Si-H terminated siloxanes and vinyl terminated mesogenic compounds. For the graft copolymer (a side chain liquid crystalline polymer) a poly(hydrogen,methyl-dimethyl)siloxane is required, i.e. a siloxane with the general structure $[SiHMeO]_x[SiMe2O]_y$. The reaction occurring between the vinyl group of the mesogenic compound and the Si-H on the siloxane chain.

Hydrosilylation has also been employed to synthesise a siloxane-styrene copolymer using Si-H terminated PDMS and vinyl terminated polystyrene oligomers in the presence of chloroplatinic acid (H_2PtCl_6)[55].

Copolymers may also be produced using living polymerisation techniques. In principle, both D_3 and D_4 can be used, although D_3 is preferred because of its higher reactivity. Also, the kinetic polymerisation of D_3 allows good molecular weight control and equilibration is minimal. This technique has been widely used to produce siloxane-styrene copolymers[56,57]. The typical procedure involves the initial anionic polymerisation of styrene with butyl lithium to produce polystyrene with living polystyryl active centres. On addition of D_3, the polystyryl anion will initiate the ring-opening polymerisation of D_3 to produce the block copolymer. This technique is very useful, as fine control over the molecular weights of each block is possible allowing a range of copolymers to be produced. Cyclic trimers with phenyl groups can also be used allowing synthesis of phenyl siloxane-styrene copolymers[58].

Living polymerisation has also been used to produce 'macromonomers'. Macromonomers are polymers that contain a functional group through which further polymerisation can take place. The reaction of butyl lithium with D_3 will initiate

ring-opening polymerisation. This will afford a siloxane polymer with a living siloxanolate active centre at the chain-end. This can then be terminated with a functional group containing a vinyl component, such as [3-(methacryloxy)propyl]-dimethylchlorosilane. The resulting macromonomer is then a methacryloxy-terminated polysiloxane. The vinyl group on this macromonomer can then undergo a traditional free radical polymerisation with other vinyl monomers, such as methyl methacrylate[59], styrene[60] , and acrylonitrile[61] . Graft copolymers are produced consisting of the siloxane grafted onto the polymer backbone, i.e.,

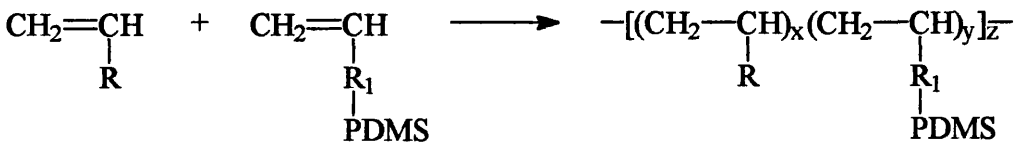

Free radical polymerisation can also be used to produce block copolymers as well as graft copolymers. This requires the use of a macroinitiator: PDMS oligomers with short segments containing a free radical initiator, such as an azo group.

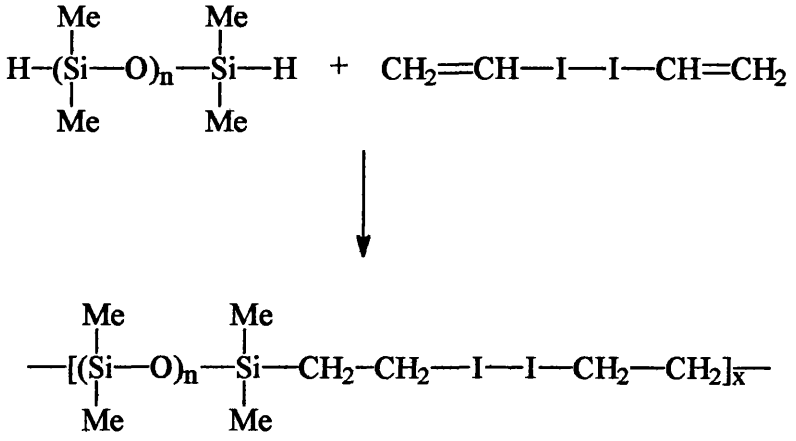

Macroinitiator

I-I is a free radical precursor

Thermal decomposition of the macroinitiator results in a formation of a macroradical. These macroradicals can initiate the polymerisation of a vinyl monomer, such as styrene[62] and methyl methacrylate[63], resulting in the formation of the block copolymer.

1.12 Ultrasound

1.12.1 What is Ultrasound?

Ultrasound is sound (vibrations travelling through a medium) which has a frequency higher than the limit of human hearing, i.e. sound with a frequency greater than 16 kHz. The upper limit of ultrasound frequency is not sharply defined, but is usually taken to be 500 MHz for liquids and 5 MHz for gases[64]. Ultrasound within this frequency range can be conveniently divided into two areas[65]:

Diagnostic Ultrasound (frequencies greater than 1 Mhz).

This area of ultrasound is of high frequency, but low power. It is used for non-destructive testing, diagnostics and imaging since the shorter wavelengths result in higher resolution.

Power Ultrasound (frequencies between 20 and 100 kHz).

This range of ultrasonic frequencies produces much higher power than high frequency ultrasound, and it is this area which is associated with chemical reactivity. Power ultrasound is used throughout this investigation.

1.12.2 The Propagation of Ultrasound

Sound waves propagate by causing the particles of the medium through which they are moving to vibrate. They are therefore transmitted through any substance that has elastic properties. They can propagate as longitudinal waves, in which the particles of the medium are made to vibrate in the same direction as the wave is travelling, or as transverse waves, where the particles vibrate perpendicular to the direction the wave is travelling[64] (figure 1.8).

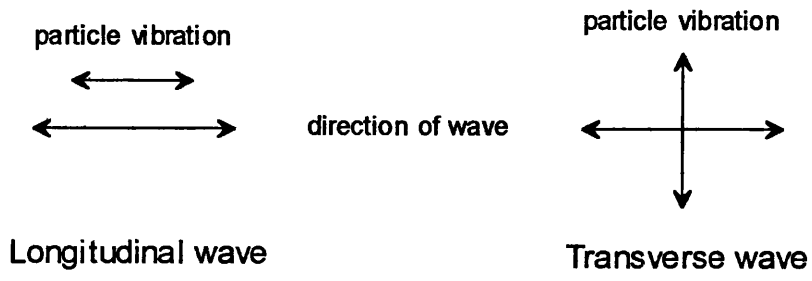

Figure 1.8 - The propagation of sound waves

Ultrasound can propagate through solids as both longitudinal and transverse waves, however, the attenuation of transverse waves is so high in liquids and gases that it is ignored in these two media[66]. Thus, an ultrasonic wave propagating through a liquid will be longitudinal, and will consist of an alternating cycle of compressions (where the liquid molecules are 'pushed together') and rarefactions (where the liquid molecules are 'pulled apart')[67]. The compression cycles will exert a positive pressure in the liquid (relative to the pressure in the absence of the acoustic field), while the rarefaction cycles will exert a negative pressure[68]. The alternating cycle of compressions and rarefactions can be represented as an acoustic pressure, P_A, which varies with time, t, as shown in figure 1.9.

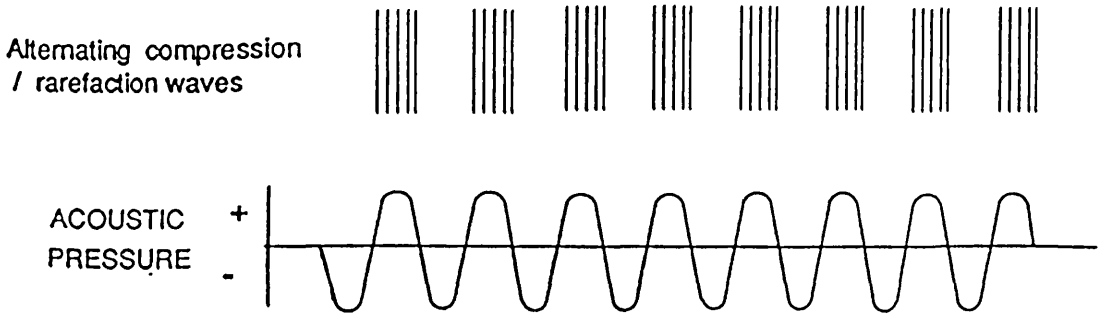

Figure 1.9 - Variation of acoustic pressure with time

It can be seen from this that the variation of acoustic pressure, and therefore the passage of the ultrasound, is sinusoidal. When the acoustic pressure is zero the molecules of the liquid are in their mean position, i.e. the position they occupy in the absence of an acoustic field.

The acoustic pressure is related to the frequency of ultrasound by:

$$P_A = P_m \sin(2\pi ft) \qquad (6)$$

where P_m is the maximum acoustic pressure generated and f is the frequency of the ultrasound.

The intensity of the ultrasound is defined as the energy transmitted through a unit area of the liquid in a unit time and is related to the maximum acoustic pressure by:

$$I = \frac{P_m^2}{2\rho c} \qquad (7)$$

where I is the intensity, ρ the density of the liquid and c the speed of sound in the liquid.

During the propagation of the sound wave through the liquid, the intensity of the wave (i.e. the maximum acoustic pressure generated) decreases as the distance from the source increases. This attenuation of the ultrasound occurs as energy is transferred to the surrounding liquid. As the molecules of the liquid vibrate, they experience viscous interactions which lowers the intensity. The energy is lost in the form of heat, which is seen by a small rise in the bulk temperature of the liquid during sonication[64].

1.13 Cavitation

In 1895, Barnaby and Thornycroft[69] reported that during speed trials the destroyer H.M.S. Daring suffered severe vibration and surface damage to the propellers. They suggested that these effects were due to large bubbles, or cavities, being formed by the propellers and subsequently imploded by the water pressure. This was the first identification of the phenomenon of cavitation.

Cavitation is the formation, growth and explosive collapse of microscopic bubbles on a microsecond timescale[70] and it is the principal effect of ultrasound on liquids. A cavitation bubble is a consequence of the pressure variation caused by the passage of an ultrasonic wave through the liquid. In the rarefaction period of the wave, there is a temporary negative pressure. If this is large enough, the intermolecular forces holding the molecules of the liquid together can be overcome and cavities will form in the liquid. These are cavitation bubbles.

Cavitation bubbles actually form at acoustic pressures considerably lower than those needed to overcome the tensile strength of the pure liquid. The acoustic pressure required to overcome the tensile strength of a pure, homogeneous liquid is of the order of hundreds of atmospheres, whereas cavitation occurs at considerable

lower values (<20 atm)[64]. This has lead to the conclusion that the cavitation bubbles form about small nucleation sites; weak spots in the liquid that effectively lower the liquids tensile strength. These are typically caused by the presence of dissolved gases and minute particulate matter, and evidence for this comes from the observation that the cavitation threshold (the value of the applied acoustic pressure (i.e. the ultrasound intensity) needed before cavitation will occur) is raised in rigorously degassed solutions[71,72] or in liquids where suspended particles have been removed by ultra-filtration[73].

Cavitation bubbles can either be empty, vapour-filled or gas-filled, and can be classified into two types; stable and transient.

1.13.1 Stable Cavitation

Stable cavitation involves bubbles that, once formed, oscillate about an equilibrium size for a relatively long period of time, i.e. a period of many acoustic cycles, and they are thought to contain mainly gas and some vapour[66]. Once formed the bubbles will oscillate in phase with the compression and rarefaction cycles, continually absorbing energy. During the rarefaction stage, gas will diffuse into the bubble, while during the compression stage, it will diffuse out. The amount of gas that diffuses in and out depends on the surface area of the bubble and since this is slightly greater during the rarefaction phase, more gas will diffuse into the bubble than will diffuse out. Thus, over many acoustic cycles, the bubble will grow. This is known as rectified diffusion. The growing bubble will eventually reach a critical size where it will most efficiently absorb energy from the acoustic field. This size is determined by the frequency and at 20 kHz the critical size is ~170 μm. At this point, the bubble will grow rapidly in the course of a single expansion cycle. However, once it has experienced this very rapid growth it can no longer absorb energy as efficiently from the sound waves and it will be unable to sustain itself. The compression forces will begin to dominate and the bubble will violently implode[70].

The oscillations of bubble size can cause disruption and movement of adjacent liquid molecules and these can be responsible for some of the mechanical effects associated with cavitation[65]. While if the bubbles grow until they are sufficiently buoyant they can float to the surface. This is the principle of ultrasonic degassing[64].

1.13.2 Transient Cavitation

In transient cavitation, the bubbles formed usually exist for no more than one acoustic cycle. During the rarefaction cycle of the sound wave the bubble grows rapidly, expanding to a radius of at least twice its original size (upto 200 μm), before collapsing violently[65]. The lifetime of these bubbles is too short (1 - 10 μs) to allow gas to diffuse into the bubbles, hence these are either voids or vapour-filled cavities[66]. When the bubbles collapse, they can disintegrate into smaller bubbles. These can be stable, transient or can act as nuclei for further bubbles.

1.13.3 Bubble Collapse

The implosion of a cavitation bubble generates very harsh conditions, with the collapse of a transient bubble being more violent than that of a stable bubble. This is due to the fact that a stable bubble contains gas, whereas a transient bubble will only contain some vapour at most. The gas will effectively 'cushion' the collapse of a stable bubble, hence it is not so violent.

Lord Rayleigh was the first to try and describe a collapsing bubble mathematically in response to Barnaby and Thornycroft's findings. Using his models, he predicted local pressures of 10 300 atm during their collapse[74].

Noltingk and Neppiras[75,76] and Flynn[77] assumed that the collapse was adiabatic (i.e. there is no energy exchange between the bubble and bulk liquid during the collapse). They showed that the maximum temperature (T_{max}) and pressure (P_{max}) generated within the bubble at the moment of collapse is given by,

$$T_{max} = T_0[P_l(\gamma-1)/P] \quad (8)$$

$$P_{max} = P[P_l(\gamma-1)/P]^{\gamma/(\gamma-1)} \quad (9)$$

where, T_0 is the temperature of the bulk liquid, P_l is the pressure in the liquid at the moment of transient collapse (equal to the acoustic pressure plus the ambient hydrostatic pressure of the liquid), P is the pressure in the bubble at its maximum size (usually assumed to correspond to the vapour pressure of the liquid) and γ is the ratio of the specific heats of the dissolved gases or vapour (i.e. the polytropic ratio).

Depending on the conditions used, solving the above equations leads to values of around 1000 atm and 5000 K[64] for the maximum pressure and temperature.

This theory of cavitation is often called the 'hot spot' theory due to the high temperatures and pressures generated on bubble collapse. It has received experimental evidence by Suslick and co-workers[78,79] who showed that sonoluminescence (the production of light when a liquid cavitates) induced in alkane solvents, is the same as that arising from their combustion at several thousand degrees Kelvin. They have also shown that chemical reactions such as the decomposition of metal carbonyls occurred under cavitation in the same manner as thermal processes at these high temperatures. However, Margulis and others have shown that there are some sonochemical phenomena not completely explained by the hot spot theory and they have proposed an 'electrical' theory. This theory considers the charge distribution, due to dipoles in the solvent, around a cavitation bubble. During bubble formation, very high electrical field gradients can be generated which are sufficient to cause bond breakage and chemical activity[80,81,82].

While there may be conflicting theories to explain the effects produced by cavitation, what is certain is that highly reactive species, such as free radicals, can be formed. For sonochemistry, it is convenient to define three regions around a cavitation bubble[65] (figure 1.10).

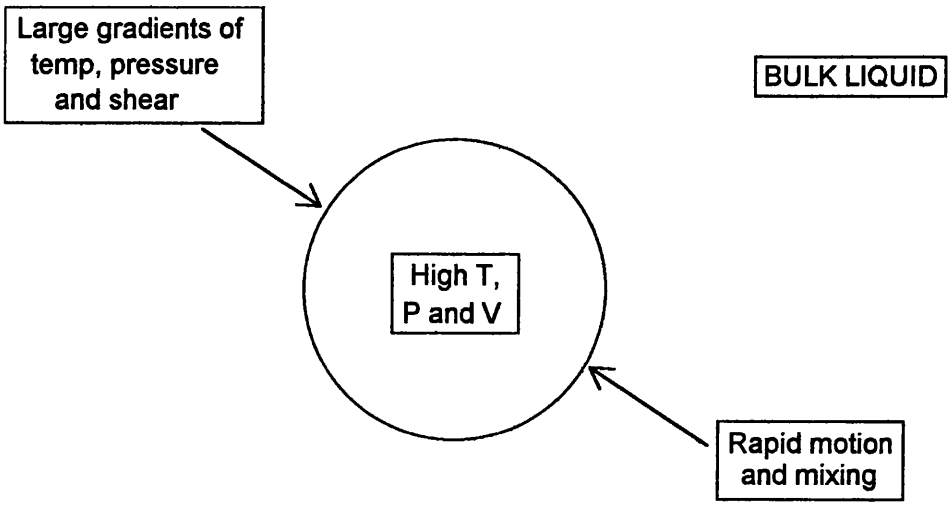

Figure 1.10 - Three regions around a cavitation bubble

The primary sonochemical activity, such as radical production, occurs inside the bubble where the extreme conditions are generated. In the bulk liquid there is little effect beyond a small heating (due to the attenuation of the ultrasound) and reaction of the intermediates produced. Around the interface of the bubble there are very large temperature, pressure and electrical field gradients. Rapid movements of the solvent molecules causes very large shear gradients to be set up, as well as causing mixing and stirring of the solution.

1.13.4 Parameters Affecting Cavitation

Cavitation has three distinct stages: nucleation, bubble growth and implosive collapse[83] . As has already been stated, the onset of cavitation can be affected by degassing and ultrafiltration of the solution. Removing the particulate matter and the dissolved gasses removes the weakspots in the liquid, resulting in an increase in the cavitational threshold. However, this is not the only way to affect cavitation. Changing the system conditions will also have an effect.

Effect of ultrasound intensity

There is generally a minimum intensity, below which cavitation does not occur. This is the cavitation threshold. Since $I \propto P_m^2$ (equation 7), once above this threshold, increasing the intensity increases the maximum temperatures and pressures generated on collapse, according to equations 8 and 9[64]. Increasing the intensity also results in an increased production of cavitation events. However, at very high intensities, the chemical effects associated with the bubble collapse may diminish due to an overproduction of bubbles. The bubbles effectively shroud the source of the ultrasound and disperse the acoustic wave[84] . Also, it is possible that the bubble will grow so large on rarefaction that it will not have sufficient time to collapse during compression[75,76].

Effect of ultrasound frequency

As the ultrasonic frequency is increased, the production of cavitation decreases[85] . Essentially, this is due to the fact that as frequency is increased, the time between the compression and rarefaction cycles decreases. The bubbles therefore have less time to grow and collapse, so lower final temperatures and pressures are reached.

Effect of solvent

To form bubbles, the negative pressure generated during rarefaction must overcome the cohesive forces within the liquid. Thus, cavitation is more difficult to produce (i.e. the cavitation threshold is increased) in more viscous liquids[66]. While solvents with lower surface tension should lead to a reduction in the cavitation threshold[86] . However, the vapour pressure of the solvent is the main factor. If the volatility of the solvent is high, the amount of vapour entering the bubble will also be high. The vapour in the bubble will 'cushion' the collapse, reducing the maximum temperatures and pressures generated. Thus, bubble collapse is more violent in solvents with lower vapour pressures and high enthalpies of vapourisation[65].

Effect of temperature

Increasing the temperature of the liquid will result in more vapour entering the bubble with the subsequent reduction in T_{max} and P_{max} (as described above). Bubble collapse is therefore more intense at lower temperatures[66].

Effect of dissolved gases

Gases with a high solubility in the solvent will reduce the cavitation threshold, but will also reduce the intensity of the bubble collapse. As described earlier, dissolved gases provide nucleation sites for cavitation. Thus, the more soluble the gas, the more nucleation sites there will be, resulting in a reduction of the cavitation threshold. However, dissolved gases can also enter the cavitation bubble, cushioning the collapse and reducing the maximum temperatures and pressures generated.

Effect of applied (hydrostatic) pressure

Increasing the hydrostatic pressure increases both the cavitational threshold and the intensity of the bubble collapse. By increasing the hydrostatic pressure, the inward pressure on the nucleating bubbles also increases. Thus, the negative pressures required to produce cavitation must also be increased[84]. But as P_l in equations 8 and 9 is equal to the sum of the hydrostatic pressure and the acoustic pressure, increasing the hydrostatic pressure results in an increase in T_{max} and P_{max} on bubble collapse.

1.14 Sonochemistry

The field of ultrasonics began in 1880 with the discovery of the piezoelectric effect by Pierre and Jacques Curie. They found that stress applied to a quartz crystal produced an electric charge, while an electric charge applied to the surface of the crystal produced a change in size. Application of an alternating current caused the crystal to oscillate in size and produce sound waves. In 1883 Galton developed the earliest form of an ultrasonic transducer which was developed in an attempt to investigate the threshold frequency of human hearing[64].

Langevin became the first person to transmit sound waves in water in 1917. His work arose out of a competition, set in 1912 in response to the Titanic disaster, to find a method of detecting icebergs. His echo-sounding technique enabled the estimation of the depths of water and the first commercial application was the detection of submarines (a result of the heavy loss of shipping during World War One). Developments and refinements of Langevin's system resulted in SONAR[64].

The first chemical effects of ultrasound were reported in 1927. Loomis and Wood published a paper entitled 'The Physical and Biological Effects of High Frequency Sound-Waves of Great Intensity'[87] in which they described some effects such as the heating of liquids, the formation of emulsions and the destruction of red blood cells. This was rapidly followed by a paper by Loomis and Richards[88], 'The Chemical Effects of High Frequency Sound Waves I. A Preliminary Study'. They described the degassing effect of ultrasound as well as the acceleration of some reactions, including the hydrolysis of dimethyl sulphate.

Since those initial studies, ultrasound has been found to affect a wide range of chemical processes and the use of ultrasound in chemistry has come to be termed 'Sonochemistry'.

1.14.1 Experimental Sonochemistry

Obviously, to conduct any sonochemistry, some method of transferring the ultrasound to the process is required and two types of apparatus are generally used for this: the ultrasonic bath, and the ultrasonic horn.

The ultrasonic bath can be found in many laboratories where it is usually used for routine cleaning of glassware (figure 1.11). However, it offers a simple and easy way of applying ultrasound to a reaction. The reaction vessel just needs to be

immersed in the bath and the bath switched on. The advantages of this system are its simplicity, low cost and wide availability. Also, standard glassware can be used so inert atmospheres can readily maintained[89].

There are a number of drawbacks, however. The ultrasonic intensity is generally low and is limited due to attenuation by the water and the walls of the reaction vessel. Temperature control is difficult and reproducibility of results can be poor if care is not taken to ensure that the vessel is placed in the same place for each reaction. Also, different baths operate at different frequencies and power outputs, so comparison of results with other laboratories can be difficult[65].

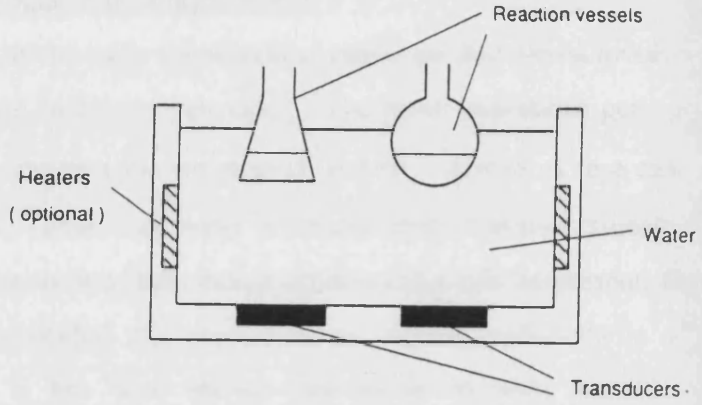

Figure 1.11 - Ultrasonic cleaning bath

The ultrasonic horn (figure 1.12) allows ultrasound to be introduced directly into the reaction medium, rather than rely on transfer through water and the reaction vessel.

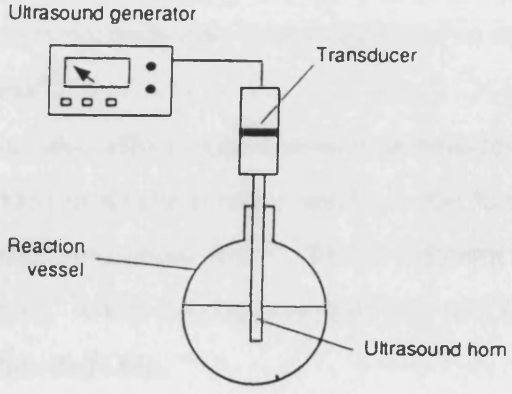

Figure 1.12 - Ultrasonic horn

Very high intensities are available, although adequate cooling may be necessary (usually through using a jacketed vessel) as large temperature rises can occur. However, unlike the bath, the intensity can be controlled, while the use of a jacketed vessel allows easier control over the temperature.

The main disadvantages of the horn system are its higher cost and the fact that more specialised glassware may be required if the horn is to be used in reactions involving reflux, inert atmospheres or elevated pressures[89]. Also, the tip of the horn is subject to cavitational erosion and particles from it (usually made of titanium alloy or stainless steel) may interfere with the chemical reaction.

1.14.2 Homogeneous Sonochemistry

One of the early sonochemical reactions discovered involved the sonication of water to form hydrogen peroxide[90]. The harsh conditions generated on cavitational collapse decomposes the water to $H^{\cdot}$ and $HO^{\cdot}$ radicals. These can recombine to form H_2O_2 and H_2. Given that water produces highly reactive radicals on sonication, it is not surprising to find that, should other compounds be present, further reactions can occur. In particular, the sonication of organic pollutants in water has attracted interest, as it has been shown that environmentally hazardous substances (for example, CFC's) can be converted into more benign substances when sonicated[91].

Organic liquids have also been shown to give rise to radical species when sonicated and, as with water, these can also promote further reaction. The sonication of *n*-alkanes generates H_2, methane, lower alkanes and alkenes and it has been shown that the degradation process is similar to high temperature pyrolysis[92]. However, it should be noted that organic solvents only decompose slowly on sonication and the solvent decomposition is normally only minor compared to any sonochemical reaction occurring in the solvent[89].

Ultrasound can also affect organometallic substances. The sonication of iron pentacarbonyl ($Fe(CO)_5$) in alkane solvents results in the formation of the compound $Fe_3(CO)_{12}$ together with amorphous iron[93]. This is different to the products that are obtained by thermolysis, which decomposes $Fe(CO)_5$ to CO and iron powder, and photolysis, which yields $Fe_2(CO)_9$.

1.14.3 Heterogeneous Sonochemistry

Heterogeneous sonochemistry can involve liquid-liquid systems and liquid-solid systems. In both cases, as well as cavitation in the bulk liquid, there will also be cavitation at, or near, any phase boundary and this can have a marked effect on the chemistry.

The collapse of cavitation bubbles at or near the interface of immiscible liquids will cause disruption of the boundary and mixing and emulsification will occur. Hence, any chemical process that requires the mixing of two immiscible liquids, or the formation of an emulsion, may benefit from being conducted under ultrasound.

In liquid-solid systems, the collapse of a cavitation bubble at or near a solid surface is asymmetrical. This generates a jet of liquid directed towards the surface that moves at speeds of roughly 400 km per hour[67]. This microjet can erode solid surfaces and remove non-reactive coatings (i.e. it cleans the surface), fragment brittle powders, break apart agglomerates and increase heat and mass transfer to the surface.

It is therefore not surprising to discover that ultrasound has been found to enhance those reactions that require the presence of a metal, either as a reagent, or as a catalyst[68]. The cleaning effect keeps the surface free from contaminants that can decrease reactivity, while enhanced mass transport will help increase the rate of reaction. If the process requires a powder, reductions in particle size will lead to an increase in surface area and therefore a faster rate of reaction. The Ullmann coupling reaction is an example of a heterogeneous reaction that can benefit from ultrasound. The reaction of 2-iodonitrobenzene to give a dinitrobiphenyl requires a tenfold excess of copper powder and heating for 48 hours. Using ultrasound gave a similar yield (80 %) but in only 1.5 hours using a fourfold excess of copper[89].

1.14.4 An Experimental Theory of Sonochemistry

There exists a large and diverse range of published work detailing the positive effects of ultrasound on many different chemical reactions. Luche has attempted to rationalise this disparate range of reactions and has proposed a system where sonochemical reactions can be classified into three types[94,95].

Luche Type 1

These are homogeneous reactions in solution in which a single electron transfer occurs in a rate-determining step, i.e. the mechanism involves radical intermediates. Homogeneous processes which have a purely ionic mechanism will be insensitive to sonication.

Luche Type 2

These are heterogeneous reactions which follow an ionic mechanism. The ionic mechanisms are not affected by sonication and so any effects seen will be due to the mechanical effects of ultrasound.

Luche Type 3

These are heterogeneous reactions which involve radical intermediates in the mechanism. These will be subject to both the mechanical and chemical effects of ultrasound.

In addition to these three classes of sonochemical reaction, there is also the effect of 'sonochemical switching'. If a reaction can follow either an ionic or a radical mechanism, sonication will favour the radical mechanism, resulting in an increased production of the product resulting from that mechanism.

1.15 Polymer Degradation

The first report on the effect of sound waves on polymers was in 1933. Flosdorf and Chambers[96] found that egg albumin was instantly coagulated and the hydrolysis of sucrose to glucose was accelerated when subjected to sound waves, although they used audible sound and not ultrasound. Also in 1933, Szalay found that subjecting ultrasound to the natural polymers starch, gum arabic and gelatin, caused a reduction in the viscosity of the solution[97].

In the late 1930's, Schmid and Rommel[98,99] found that there was a permanent reduction in the viscosity of solutions of polystyrene and poly(acrylates) when the solutions were subjected to ultrasound. It was found that the reduction in viscosity was initially quite fast, but it slowed with time and reached a limiting value. This suggested that the polymer chains were being broken, resulting in a lowering of the molecular weight, until a limiting molecular weight was reached. The term

'degradation' therefore refers to the reduction in molecular weight when a polymer is subjected to ultrasound. Many studies of the process have been published since then and the effect appears to be applicable to all types of polymer, whether synthetic or natural, organic, inorganic or biological[100].

1.15.1 General Features of Degradation

The basic effects of the ultrasonic degradation of polymers can be seen in figure 1.13. This shows how the number average and weight average molecular weights change for a 0.5 % solution of poly(dimethylsiloxane), PDMS, in toluene, sonicated at 30°C.

The rate of degradation is initially fast, when the molecular weight is high, but it decreases as the degradation progresses. Thus, the higher the molecular weight, the faster the degradation. The molecular weight does not fall indefinitely, but approaches a limiting value, M_{lim}, below which no further degradation will occur. M_n and M_w can be seen moving closer together as the sonication progresses, i.e. the molecular weight distribution is becoming narrower. The reduction in molecular weight is therefore also accompanied by a lowering of the polydispersity.

These features, the existence of a limiting molecular weight and a more rapid degradation at high molecular weights, have been noted by many workers and they are regarded as characteristic of ultrasonic degradation.

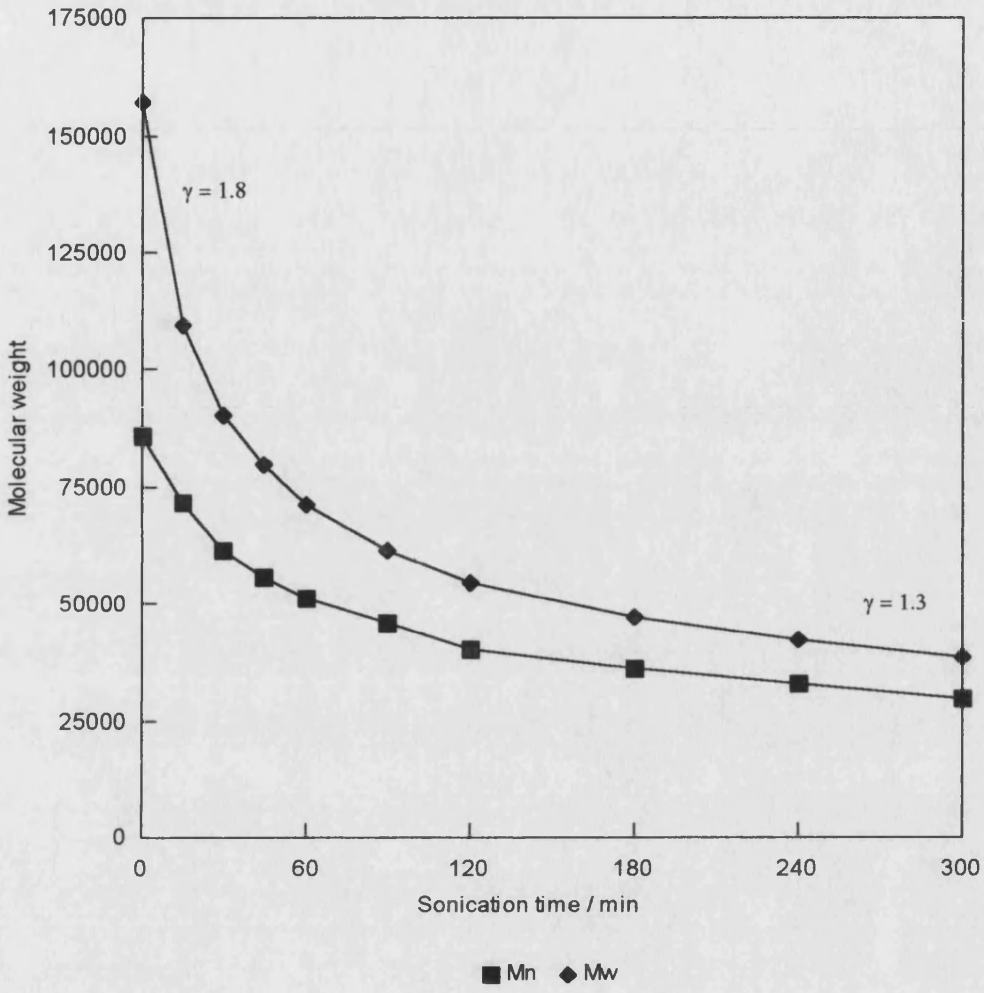

Figure 1.13 - Degradation of PDMS in toluene

1.15.2 The Kinetics of Degradation

A number of workers have attempted to derive kinetic schemes to describe the ultrasonic degradation of polymers. The first attempt was made by Schmid[101] who considered an initially monodisperse polymer and assumed that a chain will not be degraded if it is shorter than M_{lim}, while longer chains degrade at a rate proportional to the fraction of the total chain which exceeds M_{lim}. This can be represented as,

$$\frac{dx}{dt} = 0 \qquad \text{for } P_t < P_{lim}$$

$$\frac{dx}{dt} = k(P_t - P_{lim}) \qquad \text{for } P_t > P_{lim}$$

where, x is the number of chain breaks per unit volume, k is the rate constant, P_t is a molecule with degree of polymerisation, P, at time, t, and P_{lim} is a molecule with the limiting degree of polymerisation. From this he derived the following equation:

$$\frac{M_{lim}}{M_t} + \ln\left(1 - \frac{M_{lim}}{M_t}\right) = -\frac{k}{c}\left(\frac{M_{lim}}{m_0}\right)^2 t + \frac{M_{lim}}{M_i} + \ln\left(1 - \frac{M_{lim}}{M_i}\right) \qquad (10)$$

where, M_{lim} is the limiting molecular weight (number average),

M_t is the molecular weight at time, t,

M_i is the initial molecular weight,

m_o is the monomer molecular weight,

c is the concentration in base moles (moles of monomer) per unit volume, and

k is the rate constant.

Therefore, a plot of $M_{lim}/M_t + \ln(1-(M_{lim}/M_t))$ against t, should give a straight line with a gradient of $-(k/c)(M_{lim}/m_o)^2$. If the concentration of the solution is known, the rate constant for the degradation can subsequently be determined.

Schmid applied the treatment to results for the degradation of polystyrene in toluene and obtained linear plots, even though he used the weight average molecular weight (taken from viscosity measurements) and not the number average used in the derivation of the equation.

Ovenall and co-workers[102,103] proposed the following rate equation:

$$\frac{dx}{dt} = 0 \qquad \text{for } P_t < P_{lim}$$

$$\frac{dx}{dt} = kn_t(P_t - P_{lim}) \qquad \text{for } P_t > P_{lim}$$

where, n_t is the number of molecules having a degree of polymerisation, P_t. It was assumed that the rate constant, k, was independent of P_t and n_t, but was dependent on the polymer-solvent system and the experimental conditions. P_{lim} is the limiting degree of polymerisation, below which molecules will not degrade. Since polymers of length $P_{lim} + 1$ will degrade to lower values (i.e. less than P_{lim}), the measured value of P_{lim} after long sonication times will be less than the actual P_{lim}. Thus, they assumed that only fragments larger than $P_{lim}/2$ will break off from a polymer chain and that all bonds in the chain are equally likely to break, except those within $P_{lim}/2$ monomer units from the ends of the chain.

Therefore, if a molecule is large enough to be degraded the probability of a bond being broken in the degradable section of the chain, is proportional to the number of bonds in that section, whereas the particular bond broken in that section is random. Using this analysis, they derived the equation:

$$\ln\left(\frac{1}{M_{\lim}} - \frac{1}{M_t}\right) = \ln\left(\frac{1}{M_{\lim}} - \frac{1}{M_i}\right) - \frac{k}{c}\left(\frac{M_{\lim}}{m_0}\right)t \qquad (11)$$

where the units have the same meaning as in the Schmid equation. Hence a plot of $\ln(1/M_{lim} - 1/M_t)$ against t should give a straight line with a gradient of $-(k/c)(M_{lim}/m_o)$.

They applied this treatment to the degradation of polystyrene, poly(vinyl acetate) and poly(methyl methacrylate) in benzene and found the experimental results fitted the equation well.

Henglein[104] used DPPH (2,2-diphenyl-1-picrylhydrazyl) to measure the rate of degradation of poly(methyl methacrylate). He used Schmid's equation to analyse the results but found that good agreement was only obtained at low solution concentration (1.9 gdm^{-3}). Ovenall et al[103] fitted Henglein's results to their equation and found good agreement upto concentrations of 7.5 gdm^{-3}.

Brett and Jellinek[105] applied Schmid's equation to the degradation of polystyrene in benzene under various gases and found the equation gave good fits to their results.

More recently, Price et al have used Ovenall's equation to describe the degradation of polystyrene in toluene[106,107] and have also used both Schmid's and Ovenall's equations to analyse the degradation of PDMS in toluene[108]. For both polymers, the equations used were found to give good fits to the data.

Other kinetic schemes to describe ultrasonic degradation have been proposed, such as those of El'tsefon and Berlin[109] and Mostafa[110,111]. However, little work has been done to clarify which kinetic treatment most closely follows experimental results. Unfortunately, the nature of polymer molecules makes an exact definition of the rate equation difficult. When a polymer sample is sonicated there are a mixture of chain lengths all undergoing degradation at different rates, as (as described in section 1.15.1) the actual rate of chain breakage is dependent on the molecular weight. A strict analysis should therefore follow both the concentration of each molecular weight as well as the average molecular weight. An exact treatment would then require the solution of a large number of rate equations with an equally large number of rate constants[24,112].

The values of the rate constants determined using these models are therefore an average, although they do allow comparisons to be made between degradations. The changing molecular weight distribution during degradation makes a complete kinetic analysis very difficult.

1.15.3 The Mechanism of Degradation

It is quite clear that applying ultrasound to a polymer solution causes the molecular weight to fall. Therefore, sufficient energy must be available for the polymer chains to be broken.

The very first degradation studies were conducted on natural polymers such as starch and gelatin. In these studies, the reduction in viscosity after sonication was attributed to thixotropic effects. However, subsequent results showing the reduction in viscosity to be permanent proved that this was not the case[24].

Schmid and Rommel[98,99] suggested that the degradation was due to mechanical forces and proposed that frictional forces between the solvent molecules, set in motion by the ultrasound, and the polymer molecules were sufficient to cause degradation. The calculated forces were of the order to cause bond breakage if the polymer chains were held rigid. However, if the chains could move, the forces were

insufficient to cause degradation. Schmid therefore concluded that the degradation only occurred when the polymer chains were sufficiently entangled to prevent motion.

Another possibility was that degradation was thermal in origin. However, this was discounted by Melville and Murray[113] who compared the degradation of poly(methyl methacrylate) with two copolymers of poly(methyl methacrylate - acrylonitrile). The links between the methyl methacrylate and acrylonitrile were shown to be weak with regard to thermal degradation. Hence, if the mechanism of ultrasonic degradation was thermal in origin, it would be expected that the copolymers would degrade faster than the homopolymer. However, they found practically the same rate of degradation for all three polymers.

The fact that cavitation is necessary for degradation to occur was demonstrated by Weissler[114] . He showed that degradation did not occur when the polymer solution was rigorously degassed to prevent cavitation. It is therefore the presence of cavitation which is responsible for the ultrasonic degradation of polymers.

A collapsing cavitation bubble generates a high shear field. The generally accepted mechanism of polymer degradation is that the polymer chains are caught in this shear field and the chain segments of the polymer coil near the collapsing cavity will move at a higher velocity than those further away. Stresses are then set-up along the polymer chain due to the relative motion of the polymer segments and these are sufficient to cause bond cleavage[24,115] .

The stresses produced on the polymer chain will be greatest at the centre, therefore chain breakage would be expected to occur preferentially near the centre of the chain. This has been shown experimentally by Smith and Temple[116] who used GPC to study the degradation of narrow distribution polystyrene. The chromatograms they obtained showed secondary peaks at approximately half the molecular weight of the original polymer. Thus, ultrasonic degradation is similar to that seen for polymer solutions undergoing other shearing effects[117] .

This non-random cleavage can also explain the dependence of the rate of degradation on the molecular weight and the observed M_{lim}. The longer the polymer chain (i.e. the greater the molecular weight), the greater the stresses in the chain. It is therefore easier to degrade longer chains than shorter chains, so the rate of degradation is faster for longer chains. At M_{lim}, the stresses set-up in the chain are insufficient to cause bond cleavage and therefore no further degradation occurs.

1.16 Polymer Synthesis

The cleavage of a polymer chain as a result of cavitation gives rise to active sites at the chain ends. Homolytic cleavage of the bond will result in the formation of radicals at the chain ends, while heterolytic cleavage will produce ions.

$$P_{n+m} \longrightarrow P_n^{\bullet} + P_m^{\bullet} \qquad \text{homolytic cleavage}$$

$$P_{n+m} \longrightarrow P_n^{+} + P_m^{-} \qquad \text{heterolytic cleavage}$$

The most common polymers have a backbone of C-C bonds and these are homolytically cleaved. The first evidence for this came from Henglein[104] who used the stable free radical DPPH (2,2-diphenyl-1-picrylhydrazyl) to trap the macromolecular radicals produced during the degradation of poly(methyl methacrylate). Melville and Murray[113] demonstrated the existence of the radicals by sonicating polymers in the presence of vinyl monomers. The macromolecular radicals that were formed initiated the polymerisation of the monomers present to form copolymers. More direct evidence has come from Tabata et al[118] who used electron spin resonance spectroscopy (ESR) to show the existence of radicals. PDMS, however, has a backbone of Si-O bonds which are polar, unlike C-C bonds, and these do not cleave homolytically when sonicated. Thomas and de Vries[119] sonicated PDMS in the presence of ^{14}C-labelled methanol. They found that the lowering of the molecular weight was accompanied by the incorporation of the labelled isotope into the polymer. They postulated that the heterolytic cleavage of the PDMS produced an ion pair. As methanol is a strong nucleophile, it would react with the cation formed, resulting in the PDMS chains being capped with ^{14}C.

As described above, Melville and Murray[113] first produced block copolymers by sonicating a polymer in the presence of a monomer. The macromolecular radicals acting as intiators for the polymerisation of the monomer. This method has been used to produce a number of copolymers, such as polystyrene with methyl methacrylate[65], as well as water soluble copolymers, such as poly(acrylonitrile) with poly(ethylene oxide)[24]. A related reaction is to replace the monomer by another species susceptible to radical attack to produce an end-capped, or telechelic, polymer[120].

An alternative method of producing block copolymers is to sonicate a solution containing two homopolymers. The macromolecular radicals produced can recombine to form some of the 'cross-product' - a block copolymer. This was shown by Melville et al[121] and Henglein[122] both of whom sonicated polystyrene and poly(methyl methacrylate) to produce the block copolymer. The disadvantage of this method is that the amount of copolymer produced is small and recovery is difficult. However, the block copolymers formed can act as 'in-situ' generated compatabilisers, acting as a detergent to miscibilise two otherwise incompatible polymers[123].

Ultrasound has also been used to form homopolymers. The first report of an ultrasonically enhanced polymerisation reaction came in 1951 from Lindstrom and Lamm[124] who polymerised acrylonitrile in an aqueous solution. HO˙ radicals produced from the decompsition of the water were said to have initiated the polymerisation.

The early view was that an initiating species was necessary for polymerisation to occur under ultrasound, i.e. application of ultrasound to pure, dried monomers would not lead to polymerisation[125]. However, this view was proved wrong in 1983 when Kruus polymerised both styrene and methyl methacrylate under intense ultrasound[126,127]. Cavitation in the monomer gave rise to free radicals that initiated the polymerisation of the monomer. Using ultrasound in this way, there is no need for an added initiator. This method has also been used on other vinyl monomers such as vinyl acetate[100] and vinyl carbazole[120].

Price[123,128] has studied the ultrasonic polymerisation of methyl methacrylate and found that radical production under ultrasound at room temperature, was comparable to that for an added initiator, AIBN (azobis(isobutyronitrile)), at 70 - 80°C. Radical production was also faster at lower temperatures - a consequence of the more violent cavitational collapse at lower temperatures. However, conversions were quite low (<25 %) since the increased viscosity as the polymerisation progressed suppressed cavitation and prevented further formation of radicals. Conducting the polymerisation in solution gave higher conversions as the viscosity was lower.

A distinctive feature of the ultrasonic polymerisation is the effect on polymer molecular weight. High molecular weight material is formed early in the reaction, but it then falls at longer sonication times. This is a consequence of the polymer undergoing degradation. Once the growing chains are above a certain length they can be degraded as a result of cavitation. Thus, concurrent polymerisation and

degradation is occurring. This produces polymers with a narrower molecular weight distribution than those produced 'silently' and the possibility exists for the molecular weight to be controlled.

Ultrasound has also been found to affect other types of polymerisations. For example, PVC and polystyrene can both be produced by emulsion polymerisation, and ultrasound is very effective at producing emulsions. Using ultrasound in emulsion polymerisation has shown that the rate of polymerisation is increased and that more uniform emulsions and polymer particles can be produced[129].

The mechanical effects of ultrasound have also been used in the synthesis of poly(dimethylsiloxane) and polysilanes. Price et al[108] used sulphuric acid in the cationic ring-opening of D_4 and compared the silent polymerisation to that conducted on an ultrasonic bath at 30°C. The ultrasound was found to give a faster polymerisation, although the final yields were similar.

The Wurtz coupling of silanes to produce polysilanes requires the use of sodium in toluene at 110°C. The problem with the reaction is that it is irreproducible, the yields are low and the polymers have a wide distribution of molecular weight (usually bimodal). Using ultrasound has shown enhanced yields and reaction rates, at lower temperatures, and has also significantly narrowed the molecular weight distribution. Because the system is heterogeneous, cavitation near the sodium surface results in microjets. These will continually clean the surface and enhance mass transfer of the reactants to the surface. Thus, the reaction proceeds at a reasonable rate, at lower temperatures, while the degradation controls the molecular weight[123].

Polymerisation reactions employing other organometallic reagents have also been enhanced by ultrasound. Probably the most well known of these is the Ziegler-Natta polymerisation of polyethylene and polypropylene, which uses a mixed metal catalyst such as an alkyl aluminium with titanium tetrachloride. This reaction is employed industrially on a very large scale, the major advantage being that the polymers produced have a very stereospecific structure. However, molecular weight control is difficult due to the complexity of the reacting system. Using ultrasound has been found to speed up the reaction and the polymers produced had a narrow, well defined molecular weight distribution. More importantly, there was no loss of stereospecificity[65].

These examples serve to illustrate the positive effects ultrasound can have on polymerisation processes. In many cases the rates of polymerisation can be enhanced and lower temperatures can be used, while degradation offers the possibility of molecular weight control.

1.17 Aims of This Work

The fundamental aim of this research was to apply the sonochemical techniques described above to poly(dimethylsiloxane) and related materials - to see if ultrasound could be used to control the structure of the polymer through degradation, and to see if the polymerisation process could be enhanced. Thus, this thesis takes the following form:

Chapter two describes the experimental techniques used and the experiments conducted throughout the course of this research.

The ultrasonic degradation of PDMS is explored in chapter three. The effect of changing the experimental parameters are described for degradations conducted in toluene and D_4, and the results analysed using the Schmid and Ovenall kinetic models. An understanding of the degradation process offers the opportunity to alter the molecular weight in a controlled manner.

The cleavage of Si-O bonds during degradation will give rise active sites at the cleaved chain-ends and chapter four describes the experiments conducted to try and elucidate the nature of these active sites.

Chapter five is concerned with the ring-opening polymerisation of D_4. The cationic and anionic polymerisations conducted under ultrasound are described and compared to those conducted under 'silent' conditions to determine what enhancement, if any, ultrasound may offer.

Chapter six explores routes to copolymers of siloxanes with organic polymers, in particular, the technique of Atom Transfer Radical Polymerisation to obtain block copolymers.

Final conclusions are drawn in chapter seven and directions for future research are offered.

Chapter 2

Experimental

2 EXPERIMENTAL

2.1 Sonication Apparatus

2.1.1 Ultrasonic Horn

The apparatus used to conduct the experiments employing the ultrasonic horn is shown schematically in figure 2.1.

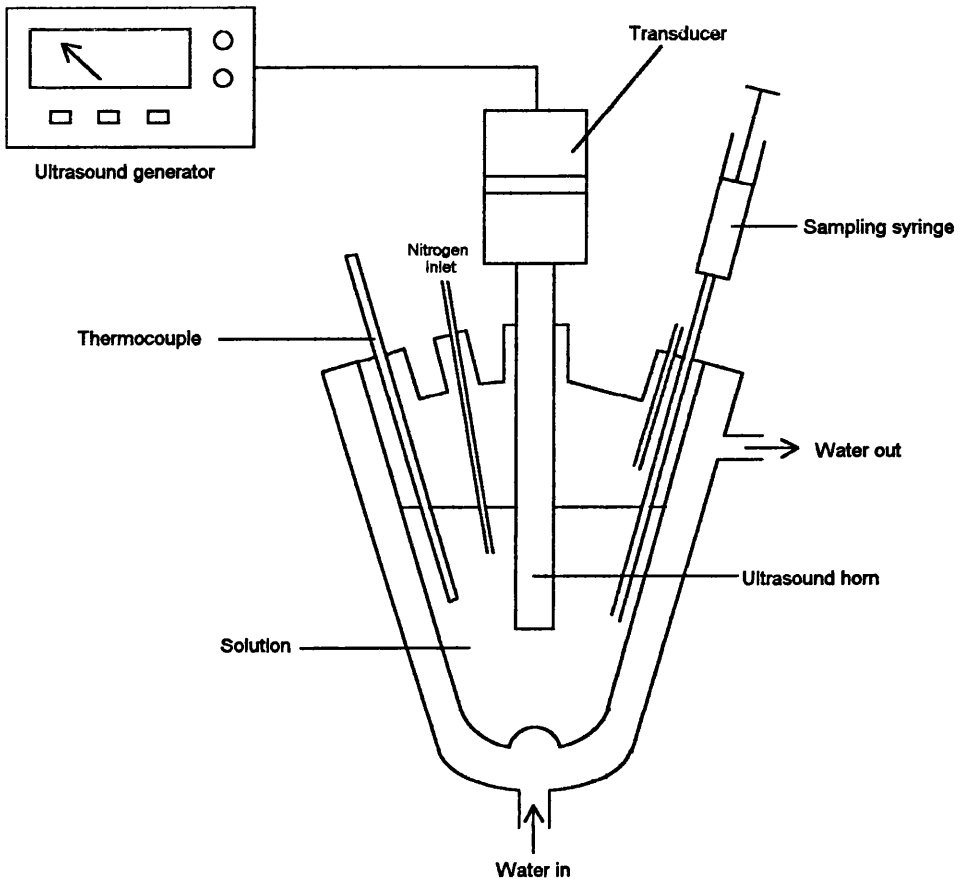

Figure 2.1 - The ultrasonic horn

The glass cell consisted of a pear shaped flask, modified by an indentation at the apex to assist the mixing caused by acoustic streaming. The flask was surrounded by a water jacket through which thermostatted water was circulated. This allowed sonications to be conducted at a controlled temperature (± 1°C).

The ultrasound generator was a Sonics and Materials VC600 sonicator, operating at a nominal frequency of 23 kHz.

2.1.2 Ultrasonic Bath

Where an ultrasonic bath was used, a Kerry Ultrasonics Pulsatron 325 cleaning bath was employed. A 'quick-fit' conical flask (with a capacity of a 100cm^3 or less) was used to contain the reaction material. Temperature control was difficult when using the bath, hence the water was generally at room temperature at the start of a sonication. However, an increase in temperature was inevitable with the magnitude of the rise being dependent on the length of sonication. It is also difficult to characterise the nature of the sound field in the bath, hence the actual acoustic power being transferred to a vessel in the bath is dependent on the position of the vessel, as well as the volume of water contained in the bath. This obviously affects the reproducibility of the results obtained from the bath.

2.2 Calibration of Ultrasound Intensity

The VC600 ultrasound generator is capable of operating over a range of intensities. However, the control is marked from 1 to 10 with no units and an analogue display shows the power being produced as a percentage of the maximum theoretical power output. This does not give any indication of the power that is being transferred from the horn to the solution, therefore the horn was calibrated to determine the ultrasonic intensity (i.e. the energy transmitted through a unit area in a unit time) at a number of different power settings. This was achieved using the following calorimetric approach.

100 cm^3 of distilled water was pipetted into the reaction vessel and the apparatus was set-up as for the sonication experiments. The water jacket of the reaction vessel was filled with water (non-circulating) and an electronic heater was placed in the solution. The system was allowed to equilibrate at 25°C and the heater was then switched on. The voltage and current through the heater were monitored using a Thander TS3021S multimeter and the temperature rise was monitored, using a Digitron thermocouple, every minute for five minutes. This was repeated three times to determine the average temperature rise.

The energy supplied by the heater to the system was calculated from

$$E = VIt \qquad (12)$$

where, V is the voltage, I is the current and t is the time (in seconds). The heat capacity, C, of the system could therefore be calculated from knowing the energy supplied and the average temperature rise.

The procedure was then repeated using the ultrasonic horn, instead of the heater, at one of the intensities. The ultrasonic power was calculated using

$$P = \frac{C\Delta T}{t} \qquad (13)$$

where, P is the ultrasonic power supplied at that intensity and ΔT is the temperature rise over five minutes. This value was then divided by the area of the horn tip (1.202 cm^2) to determine the power per unit area, i.e. the ultrasonic intensity. All the intensities used were calculated in this way.

In the synthesis study, only 50 cm^3 of liquid was used, hence the horn was recalibrated using only 50 cm^3 of water during the electrical and ultrasonic heating.

2.2.1 Calibration for Volumes of 100 cm^3

Electrical heating: Voltage = 22.2 V; Current = 0.218 A

Time (s)	Temp. (°C)
0	25.0
60	25.5
120	26.0
180	26.4
240	26.7
300	26.9

Temperature rise over 300 seconds = 1.9°C

Energy supplied = VIt = (22.2 x 0.218 x 300) = 1452 J

Hence, heat capacity, $C = E/\Delta T = 764\ JK^{-1}$

Uncertainties

The quantifiable errors arise from the stop clock and thermocouple readings.

Each stop clock reading is subject to ± 1 second.

Each thermocouple reading is subject to ± 0.1°C.

Then the uncertainty in the thermocouple is,

$$\text{uncertainty} = \sqrt{0.1^2 + 0.1^2} = 0.14°C$$

and the uncertainty in the heat capacity is,

$$\text{uncertainty} = 764\sqrt{\left(\frac{1}{300}\right)^2 + \left(\frac{0.14}{1.9}\right)^2} = 57\ JK^{-1}$$

Hence, the heat capacity, $C_{100} = 764 \pm 57\ JK^{-1}$.

Ultrasonic horn

The horn was calibrated for a range of ultrasonic powers. The calibrations were also repeated each time the tip of the horn was replaced as there was usually a small change in the calculated intensity when the tips were changed. Hence the following data is only a selection of the calibrations that were conducted.

	Power setting (as displayed by probe) of:				
	2	**6**	**10**	**14**	**18**
Temp. rise (°C)	4.45	11.25	15.75	22.8	27.6
Power (W)	11.3	28.7	40.1	58.1	70.3
Intensity (Wcm^{-2})	9.4	23.8	33.4	48.3	58.5

Uncertainties

Again, the quantifiable uncertainties are a result of the stop clock and the thermocouple. The uncertainty in the heat capacity also needs to be considered. So, for example, the uncertainty in the intensity for power = 10 is,

$$\text{uncertainty} = 33.4\sqrt{\left(\frac{1}{300}\right)^2 + \left(\frac{0.14}{15.75}\right)^2 + \left(\frac{57}{764}\right)^2} = 2.5\ Wcm^{-2}$$

The uncertainties for the other power settings can be calculated similarly, hence the final intensities are:

Power setting	Intensity (Wcm^{-2})
2	9.4 ± 0.8
6	23.8 ± 1.8
10	33.4 ± 2.5
14	48.3 ± 3.6
18	58.5 ± 4.4

2.2.2 Calibration for Volumes of 50 cm^3

The ultrasonic intensities, when only 50 cm^3 of liquid was used, were calculated in the same way as described above. However, in the electrical and ultrasonic heating only 50 cm^3 of water was used.

The heat capacity of the system containing 50 cm^3 of liquid was calculated as,

$$C_{50} = 485 \pm 10\ JK^{-1}.$$

and the following intensities were calculated,

Power setting	Intensity (Wcm^{-2})
4	17.1 ± 0.7
6	22.2 ± 1.3
10	30.8 ± 1.4

It can be seen that although a smaller volume of liquid was used, the calculated intensities of power settings of 6 and 10, are similar to those calculated for volumes of 100 cm^3.

2.3 Ultrasonic Degradations

The ultrasonic degradation of PDMS was conducted using two solvents: toluene and D_4. For each solvent, the effect of changing the ultrasonic intensity, the solution concentration and the solution temperature was investigated. Exact experiment conditions will be described with the relevant results.

In a typical degradation experiment, the glassware was thoroughly cleaned and dried at 120°C for 4 hours. 100 cm^3 of polymer solution was placed in the sonication vessel (figure 2.1) and the vessel fitted to the ultrasonic horn. Each sonication was run for 5 hours under a nitrogen atmosphere and samples of the solution (~1 cm^3) were extracted at regular intervals (0, 15, 30, 45, 60, 90, 120, 180, 240 and 300 minutes of sonication) for analysis by Gel Permeation Chromatography (GPC). The PDMS used was Dow Corning 'DC200' fluid with a viscosity of 100 000 cs, M_n = 85 000 and $\gamma = 1.8$.

Two further degradations were conducted. In the first a 1 % solution of PDMS in toluene was sonicated on the ultrasonic bath for 24 hours and samples extracted at regular intervals for molecular weight analysis. In the second, a 5 % solution of PDMS in D_4 was sonicated using the ultrasonic horn for 7 hours. Samples were extracted at regular intervals for analysis by HPLC to determine the proportions of PDMS and D_4.

In addition to these, bulk D_4 was sonicated using the horn for 5 hours, with a sample before and after sonication being analysed by GPC.

2.4 Determination of the Nature of the Chain-end During the Degradation of PDMS

Three sets of experiments were performed to determine the nature of the PDMS chain-end after it has been cleaved during sonochemical degradation.

2.4.1 A Radical Trap - DPPH

DPPH (2,2-diphenyl-1-picrylhydrazyl) is a stable radical which has a strong absorbance at 520 nm. The absorbance decreases as the radical reacts, thus the rate of consumption of DPPH can be followed by monitoring the absorbance.

100 cm^3 solutions of DPPH in THF, DPPH in a poly(isobutylene)/THF solution and DPPH in a PDMS/THF solution, were sonicated on the ultrasonic horn

at 31.6 Wcm^{-2} and 25°C. Nitrogen was bubbled through each of the solutions for 30 minutes prior to sonication and a nitrogen atmosphere was maintained throughout each sonication. This ensured that no oxygen was present that could react with any radicals produced. Small samples (~1 cm^3) were extracted from the solution every three minutes and their absorbance measured, using a Perkin-Elmer 330 UV/VIS spectrophotometer.

2.4.2 Use of an Ion Trap

Tetrabutylammonium fluoride (TBAF)

An attempt was made to use TBAF as an ion trap for silicon. It was reasoned that if a Si-O bond is broken to form Si^+ and O^-. F^- should react with the Si^+. This would therefore result in the siloxane chains being end-capped with fluorines. The presence of fluorine on the siloxane chains could then be confirmed using ^{19}F-NMR spectroscopy.

100 cm^3 of a 1 % w/v solution of PDMS in THF was placed in the sonication vessel. 1 cm^3 was removed for analysis by GPC and 1 cm^3 of TBAF (1 M solution in THF) was introduced to the PDMS/THF solution. This was then equilibrated at 25°C for 30 minutes, during which time nitrogen was bubbled through the solution. The solution was then sonicated for 3 hours at 31.6 Wcm^{-2} and 25°C. The flow of nitrogen was maintained throughout the sonication. The polymer was then precipitated into a tenfold excess of ice-cold methanol. The methanol and THF were removed at 50°C under vacuum.

Lithium fluoride

Attempts were also made to trap the chain-end species by using lithium fluoride. 2 g of PDMS and 0.5 g of LiF were charged to a 100 cm^3 volumetric flask. Anhydrous THF was added and the solution made up to the mark when the PDMS had dissolved. This was then placed in the sonication vessel and nitrogen bubbled through the solution for 15 minutes. The solution was then sonicated at an intensity of 33.4 Wcm^{-2} for 5 hours at 30°C. The flow of nitrogen was maintained throughout the sonication. After sonication, the THF was removed by heating to 55°C under vacuum and the product was then redissolved in $CHCl_3$ (in which LiF is insoluble). The solution was filtered under suction, to remove any particulate matter, and the $CHCl_3$

was then removed by again heating to 55°C under vacuum. The resulting product was analysed for fluorine by ^{19}F and ^{29}Si NMR.

For comparison, an analogous experiment was performed whereby poly(isobutylene), in place of PDMS, was sonicated in the presence of LiF using the same method as described above. As before the resulting product was analysed for fluorine by ^{19}F NMR.

A 'blank' experiment was also performed. In this experiment, the PDMS/LiF/THF solution was prepared as described above. However, it was then refluxed under a nitrogen atmosphere for 5 hours. The product was obtained as before and analysed using ^{19}F and ^{29}Si NMR.

2.4.3 Degradation of PDMS in the Presence of Water

Degradations of solutions of PDMS in THF were conducted with the recovered polymers being analysed for their silanol concentrations using FT-IR. The following degradations were conducted:

Degradation in anhydrous THF and toluene

100 cm^3 of a 5 % solution of PDMS in anhydrous THF was sonicated at an intensity of 33.4 Wcm^{-2} and 30°C for 5 hours. Nitrogen was bubbled through the solution for 15 minutes prior to the sonication and a 'blanket' of nitrogen was allowed to flow over the solution during sonication. The polymer was recovered by removing the THF at ~60°C under vacuum.

The experiment was repeated, but using toluene in place of the THF.

Degradation in THF with added water

2 cm^3 of distilled water was added to 100 cm^3 of a 5 % solution of PDMS in THF. This was sonicated as described above. As well as the FT-IR analysis, the recovered sample was also analysed by ^{29}Si NMR.

2.5 Synthesis of PDMS

The ring-opening polymerisation of D_4 was conducted under ultrasonic and 'silent' conditions, using both anionic and cationic initiators.

2.5.1 Cationic Polymerisation of D_4

The typical procedure for the cationic polymerisation was as follows. The glassware was cleaned, dried in an oven at 120°C for 4 hours and the equipment assembled as shown in figure 2.2. The flask was charged with 50 cm^3 of D_4 and 0.209 g of hexamethyldisiloxane and then flushed with nitrogen. Hexamethyl-disiloxane was used as an end-blocker to control the molecular weight, such that M_n would be approximately 35 000. A nitrogen atmosphere was maintained throughout the reaction. The stirrer and the hotplate were switched on and the temperature controller was set to the desired temperature. When the temperature was reached, a small sample (0.1 cm^3) was extracted for HPLC analysis. 0.2 cm^3 (0.4 % v/w) of 98 % sulphuric acid was then added by syringe and the polymerisation allowed to proceed. Samples (~0.1 cm^3) were extracted at regular intervals for HPLC analysis.

After 5 hours, the polymerisation was terminated by removing the heat and adding a tenfold excess (with respect to the acid) of sodium bicarbonate to neutralise the acid. The solution was cooled to room temperature, washed with water, to remove the acid and sodium bicarbonate, and the aqueous layer removed. The solution was then vacuum distilled to leave the methyl-terminated PDMS.

HPLC sample preparation:

An extracted sample (~0.1 cm^3) was syringed into a sample vial containing 0.9 cm^3 of toluene and a small amount of sodium bicarbonate (to neutralise any acid). The vial was agitated until the sample had dissolved in the toluene. It was then filtered through a 0.2 μm membrane filter to remove the particulate matter.

Each sample was analysed by HPLC twice. The data obtained was then used, along with the HPLC calibration data (section 2.7.2), to follow the conversion of D_4 to polymer during each polymerisation.

Polymerisations conducted:

Polymerisations were conducted at the following temperatures: 30, 40, 50, 60, 70, 80 and 90°C.

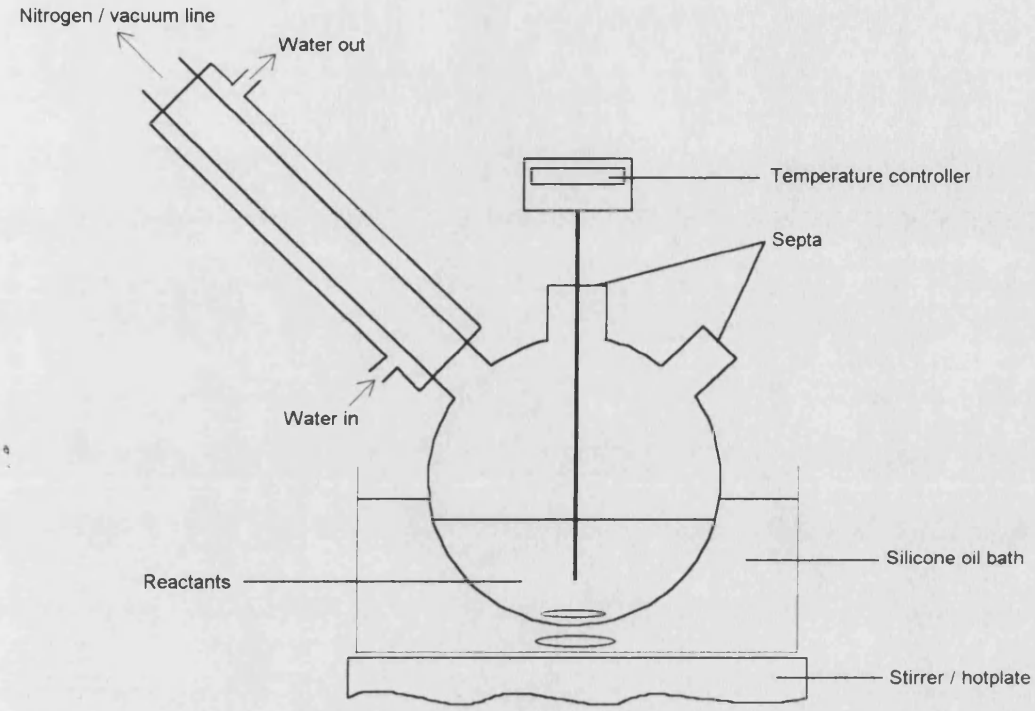

Figure 2.2 - Apparatus for conducting 'silent' polymerisations of D_4

2.5.2 Cationic Polymerisation Under Ultrasound

For the polymerisations conducted under ultrasound, the standard sonication vessel was used (figure 2.1). Again this was cleaned and dried at 120°C for 4 hours. 50 cm^3 of D_4 and 0.209 g of hexamethyldisiloxane were placed into the vessel, the sonication apparatus was assembled and thermostatted water circulated to raise the temperature of the solution to the required level. During this time, nitrogen was bubbled through to deoxygenate the solution. Once the required temperature had been reached, a sample was extracted. 0.2 cm^3 of 98 % sulphuric acid was added by syringe and the ultrasonic horn was switched on at the desired intensity. A nitrogen atmosphere was maintained throughout the sonication. Samples (~0.1 cm^3) were extracted at regular intervals for analysis by HPLC. Once the sonication had been stopped, the solution was allowed to cool to room temperature. As before, sodium

bicarbonate was added and the solution was washed with water. The aqueous layer was removed and the solution then vacuum distilled to leave the polymer.

The samples for HPLC were prepared in an identical manner to those for the 'silent' cationic polymerisations.

Polymerisations conducted:

An initial experiment used ultrasound at an intensity of 22.2 Wcm^{-2}, with the solution being heated to 50°C before sonication was begun. However, the temperature of the solution rose markedly during polymerisation and the thermostatted water was replaced with running tap water in an attempt to control the solution temperature. The sonication was stopped after two hours.

Because of the difficulty in temperature control, further experiments were conducted using an intensity of 17.1 Wcm^{-2}, pulsing the ultrasound so that it was on for 1 second, then off for 1 second. However, the temperature was still difficult to control. Hence the sonications were conducted over a temperature range, as opposed to a single defined temperature. The temperature ranges for the polymerisations were: 31 - 47, 39 - 57, 68 - 96 and 88 - 113°C.

A further experiment was conducted using the ultrasonic bath in place of the ultrasonic horn. The reagents being placed in a 100 cm^3 conical flask fitted with a septum and sealed under nitrogen. The bath was switched on for 5 hours and samples were extracted and analysed in the usual way.

2.5.3 Anionic Polymerisation of D_4

The procedure for the anionic polymerisation of D_4 was identical to that for the cationic polymerisation, except that the following reagents were used:

- 50 cm^3 of D_4
- 2.736 g of 20 cs DC200 fluid (a short chain PDMS). This was used as an end-blocker to control the molecular weight (M_n) to ~ 35 000.
- 0.0152 g (equivalent to 300 ppm) of potassium hydroxide

After 5 hours, the polymerisation was terminated by cooling to room temperature and adding 1 cm^3 of 2 M acetic acid to neutralise the base. The solution

was then washed with water and the aqueous layer removed, before being vacuum distilled to leave the polymer.

HPLC sample preparation:

An extracted sample (~0.1 cm^3) was syringed into a sample vial containing 0.9 cm^3 of toluene and a small amount of 2 M acetic acid. The vial was agitated until the sample had dissolved in the toluene. When the sample had separated into two layers, the upper organic layer was decanted off and then filtered through a 0.2 μm membrane filter to remove the particulate matter.

Polymerisations conducted:

Anionic polymerisations were conducted at the following temperatures:100, 110, 120, 130, 140 and 150°C.

2.5.4 Anionic Polymerisation Under Ultrasound

The procedure for the anionic polymerisation of D_4 conducted under ultrasound was identical to that described for the ultrasonic cationic polymerisations, except that the following reagents were used:

- 50 cm^3 of D_4
- 2.736 g of 20 cs DC200 fluid
- 0.0152 g (equivalent to 300 ppm) of potassium hydroxide

The termination of the polymerisation and the HPLC sample preparation, were identical to those described for the 'silent' anionic polymerisations.

Polymerisations conducted:

Polymerisations were conducted at an ultrasound intensity of 17.1 Wcm^{-2} and the following temperatures: 100, 110, 120, 135 and 152°C. However, temperature control during sonication proved to be difficult and fluctuations of upto ± 5°C about the desired temperature could occur.

2.6 Copolymer Synthesis

In an attempt to produce copolymers of PDMS with organic polymers, three strategies were attempted: sonication of the polymer in the presence of a monomer, anionic polymerisation of styrene and D_3, and ATRP using a siloxane-based initiator.

2.6.1 Sonication of Poly(isobutylene) with Methyl Methacrylate

10 cm^3 of methyl methacrylate and 90 cm^3 of a 2.5 % solution of poly(isobutylene) in toluene were charged to the sonication vessel, which was then wrapped in foil (to prevent photo-initiation of the methyl methacrylate). The vessel was then fitted to the ultrasonic horn and nitrogen was bubbled through the solution for 15 minutes. The solution was then sonicated for 3 hours at 25°C and an intensity of 31.6 Wcm^{-2}. A nitrogen atmosphere was maintained throughout sonication.

The polymer was recovered by precipitation into an excess of ice-cold methanol, before being dried at 60°C under vacuum and then analysed by IR spectroscopy.

2.6.2 Sonication of PDMS with Styrene and Methyl Methacrylate

The sonication of PDMS in the presence of styrene and methyl methacrylate was conducted using the ultrasonic bath, and the ultrasonic horn.

Ultrasonic bath

10 cm^3 of styrene and 90 cm^3 of a 1 % w/v PDMS in THF solution were charged to a conical flask fitted with a two-way tap connected to the vacuum line/nitrogen supply. A freeze-thaw cycle was conducted three time to remove any oxygen and the flask was sealed under a nitrogen atmosphere. The flask was then placed on the ultrasonic bath and sonicated for 90 minutes. The polymer was recovered by removing the solvent and unreacted styrene at 60°C under vacuum, and was analysed by IR spectroscopy

The experiment was then repeated with the sonication time being increased to 24 hours. As before, the recovered polymer was analysed by IR spectroscopy.

Ultrasonic horn

PDMS was dissolved in purified styrene to give a 5 % w/v solution. 50 cm^3 of the solution was placed in the sonication vessel which was then wrapped in foil to prevent photo-initiation of the styrene. Nitrogen was bubbled through the solution for 15 minutes and the solution was sonicated using the ultrasonic horn, at an intensity of 22.2 Wcm^{-2}, for 5 hours. The temperature of the solution was maintained at 30 ± 2°C by circulating running tap water through the water jacket of the vessel. A nitrogen atmosphere was maintained throughout the sonication.

After sonication, the solution was stirred into a tenfold excess of ice-cold methanol to precipitate the polymer. The methanol and unreacted styrene were removed by heating to 60°C under vacuum.

The recovered polymer was a very dark colour due to impurities of the degradation products of styrene, so the polymer was dissolved in THF and activated carbon added and left for three hours. The solution was then filtered under suction and the THF removed at 65°C under vacuum. The recovered polymer was then analysed by IR spectroscopy.

The experiment was repeated using methyl methacrylate in place of styrene. The same procedure was used and the recovered polymer was analysed by IR spectroscopy.

2.6.3 Anionic Polymerisation of Styrene

Anionic polymerisation of styrene with BuLi

Preliminary experiments were conducted to determine the effect that ultrasound has on the polymerisation of styrene initiated with *n*-butyl lithium. Tables 2.1 and 2.2 show the conditions used for the silent and ultrasonic experiments. The ultrasonic bath was used for the experiments conducted under ultrasound.

In a typical experiment, a thoroughly cleaned and dried two-necked round-bottomed flask was fitted with a rubber septum and a two-way tap connected to a vacuum line/nitrogen supply. The flask was subjected to a vacuum and then sealed under a nitrogen atmosphere. 90 cm^3 of dry THF and 10 cm^3 styrene (with the inhibitor removed) were then syringed into the flask and a freeze-thaw cycle conducted three times to remove any dissolved oxygen before being resealed under nitrogen. 0.1 cm^3 of *n*-BuLi (1.6 M in hexane) was then syringed into the flask and the

reaction allowed to proceed for the required time, either under ultrasound (on the ultrasonic bath) or with stirring (using a magnetic stirrer). The reaction was terminated by addition of 2 cm^3 of methanol. The polymer was recovered by precipitation into methanol and filtration, before being dried at 70°C under vacuum. The polymers produced were analysed by GPC.

Table 2.1 - Silent conditions

Expt. No.	Initiator?	Reaction time (hrs)	Temp / °C
1	Yes	1.5	25
2	Yes	2.5	25
3	No	2.5	25
4	Yes	1.5	-70

Table 2.2 - Ultrasonic conditions

Expt. No.	Initiator?	Reaction time (hrs)	Temp / °C
5	No	1.5	25
6	Yes	1.5	25

Styrene polymerisation with D_4

The anionic polymerisation of styrene was conducted under silent conditions, in the presence of D_4 to see if any siloxane was incorporated into the polystyrene. 10 cm^3 of styrene was polymerised in the presence of 14 cm^3 of D_4 (giving an approximate molar ratio of 2:1, styrene:D_4) with 0.1 cm^3 of *n*-BuLi (1.6 M in hexane) and 76 cm^3 of THF. Reaction time was 90 minutes at 25°C using the procedure described above.

The recovered polymer was analysed by IR spectroscopy.

2.6.4 BuLi Initiated Polymerisation of D_3

Reaction of D_3 and BuLi

A clean and dry two-necked round-bottomed flask was fitted with a rubber septum and a two-way tap connected to a vacuum line/nitrogen supply. 10 g of D_3 and 25 cm^3 of THF were charged to the flask and subjected to a freeze-thaw cycle three times to remove any oxygen. 0.1 cm^3 of *n*-BuLi (1.6 M in hexane) was then admitted to the flask by syringe and the reaction left for 90 minutes at 25°C. A nitrogen atmosphere was maintained throughout the reaction.

The reaction was terminated by the addition of 2 cm^3 of methanol to the flask. The contents of the flask were then stirred into a tenfold excess of ice-cold methanol to precipitate any polymer. The methanol and THF were removed by heating to 70°C under vacuum and the recovered polymer was analysed by HPLC.

BuLi initiated polymerisation of D_3 in the presence of styrene

A two-necked round-bottomed flask and magnetic stirrer were cleaned, dried and assembled, as described above. The 9.71g of D_3, 5 cm^3 of styrene (to give an approximate 1:1 molar ratio of styrene:D_3) and 25 cm^3 of THF were charged to the flask and subjected to a freeze-thaw cycle three times. 0.1 cm^3 of *n*-BuLi (1.6 M in hexane) was added to the flask by syringe, the stirrer was switched on and the reaction left for 90 minutes at 25°C. A nitrogen atmosphere was maintained throughout the reaction.

The reaction was terminated by the addition of 2 cm^3 of methanol. Again, the contents of the flask were stirred into an excess of ice-cold methanol and the unreacted styrene, THF and methanol removed at 70°C under vacuum. The recovered polymer was analysed by IR spectroscopy.

2.6.5 Atom Transfer Radical Polymerisation (ATRP)

Synthesis of the ATRP initiator (DB127) via hydrosilylation

A 0.24 wt% solution of chloroplatinic acid (H_2PtCl_6) in isopropyl alcohol (IPA) was prepared by dissolving 0.059 g of chloroplatinic acid in a small amount of IPA and making up to 25 cm^3 in a volumetric flask. 0.06 cm^3 of this solution and 0.9789 g of (chloromethyl)styrene (CMS - mixture of *m* and *p*-isomers) were then charged to a 50 cm^3 round-bottomed flask containing a magnetic stirrer. The flask

was fitted with a pressure equalising dropping funnel, containing 1.86 g of hydride-terminated PDMS (Mn ~ 580), which in turn was connected to a nitrogen line. The molar ratio of the CMS to the hydride-terminated PDMS was 2:1, while 5×10^{-5} equivalents (based on the CMS) of the catalyst were present.

The hydride-terminated PDMS was slowly metered into the round-bottomed flask over 2.5 hours, a positive pressure of nitrogen being maintained throughout. After 1 and 2 hours, the solution was heated gently with a hot air gun for a few minutes. The solution was stirred for a total of 3 hours after which time the solvent was removed by heating to 60°C under vacuum. The product was then filtered through a 0.2 μm membrane filter to remove any particulate matter and leave the end-functionalised PDMS (*DB127*).

ATRP of styrene using DB127 initiator

A 50 cm^3 round-bottomed flask was thoroughly cleaned and dried at 120°C overnight. 0.5 g DB127, 0.112 g copper (I) chloride, 0.353 g 2,2'-bipyridyl (bpy), 6.5 cm^3 styrene and 6.5 cm^3 *o*-xylene were charged to the flask, which contained a magnetic stirrer. The flask was cycled between nitrogen and a vacuum, before being sealed under a nitrogen atmosphere. The flask was then heated at 130°C. After 3 hours, the flask was cooled to room temperature and 20 cm^3 of toluene was added. The solution was filtered under suction and then added drop-wise to ice-cold methanol with vigorous agitation. The precipitate was collected by filtration before being redissolved in the minimum of toluene. This was again added drop-wise to ice-cold methanol with the precipitate being collected by filtration. The product was then dried in a vacuum oven at 60°C. After drying, the product was weighed and analysed by IR, ^1H NMR and DSC.

Further reactions were conducted using this method, however, one or more reagents were omitted from the procedure to determine the effect the absence of the component has on the polymerisation. The following additional reactions were conducted:

Expt	DB127-PDMS	CuCl	bpy	Styrene	*o*-Xylene
1	no	yes	yes	yes	yes
2	yes	no	no	yes	yes
3	no	no	no	yes	yes

ATRP under ultrasound

The ATRP of styrene was repeated using the method and amounts as described above, however, instead of heating to 130°C, the solution was sonicated using the ultrasonic bath at room temperature.

The ATRP was also conducted using the ultrasound horn, however because larger volumes are required, the amounts of DB127, bpy, CuCl and styrene were doubled, and the volume made up to 50 cm^3 with *o*-xylene. The solution was sonicated under nitrogen for 3 hours at 90°C and an intensity of 17.1 Wcm^{-2}.

The solution was then cooled, filtered and the product recovered by precipitation into ice-cold methanol.

ATRP of methyl methacrylate using DB127 initiator

The ATRP of methyl methacrylate was performed using exactly the same method as that described for styrene. The quantities of reagents were identical, except that 6.5 cm^3 of methyl methacrylate was used in place of styrene. The recovered polymer was analysed by IR, ^1H NMR and DSC.

Synthesis of the longer chain initiator (DB137)

0.03 cm^3 of the 0.24 % solution of chloroplatinic acid in IPA and 0.5290 g of CMS were charged to a 50 cm^3 round-bottomed flask containing a magnetic stirrer. The flask was fitted with a pressure equalising dropping funnel, containing 10 g of hydride-terminated PDMS (Mn ~ 5770). This gave a CMS to hydride-terminated PDMS molar ratio of 2:1, and 5 x 10^{-5} equivalents (based on the CMS) of the catalyst.

The hydride-terminated PDMS was slowly metered into the round-bottomed flask over 2.5 hours, a positive pressure of nitrogen being maintained throughout, and stirred for a further 1 hour. The IR spectrum showed that the reaction had not

occurred. The solution was then warmed with a hot air gun and stirred for another 1.5 hours, but again, the IR spectrum showed the reaction was not proceeding. The solution was finally heated at 50°C for a further 24 hours, with stirring, after which time the IR spectrum showed the reaction was complete. The siloxane layer was then separated from the IPA layer and placed in a vacuum oven at 70°C for 48 hours (*DB137*).

ATRP of DB137 with styrene and methyl methacrylate

The ATRP of the longer chain initiator, DB137, with styrene was identical to that described above for the ATRP with DB127, except that the solution was heated for 5 hours. The quantities of the CuCl, bpy, styrene and *o*-xylene used were the same as before, however, 3.4 g of DB137 was required.

Again, the ATRP of methyl methacrylate with DB137 was identical to that described for the ATRP with DB127, except that the solution was heated for 5 hours and 3.4 g of DB137 was required.

In both cases the recovered polymers were analysed by IR, ^{1}H NMR and DSC.

2.7 Analysis

2.7.1 The GPC

GPC was used to determine the molecular weights of the polymer samples. The chromatograph used was a Bruker LC41 fitted with a Polymer Laboratories Ltd, PLGel column. The chromatogram was controlled from an Epson QX16 data station. The eluent was toluene, pumped at a rate of 1 cm^3min^{-1} using a constant flow pump. All the samples analysed had a concentration of 1 % w/v, with 50 µl being injected into the GPC. The detector was a Bischoff 8110 measuring the refractive index of the species emerging from the column.

Because GPC is secondary method of analysis, it requires calibration with known samples. In this work, the GPC was calibrated using twelve polystyrene standards (Polymer Laboratories Ltd) of known molecular weight (ranging from 1050 to 2 650 000) and narrow polydispersity (γ<1.05). These were used to make three sample solutions, each solution containing four of the standards. Each of the three solutions were run through the GPC to determine the retention time of each molecular weight. From this data, a calibration curve was obtained which was used to determine

the molecular weight of the unknown samples. Figure 2.3 shows a chromatogram of one of the standard solutions, in which the four different standards in the solution can clearly be seen. Figure 2.4 shows a calibration curve obtained from the standards.

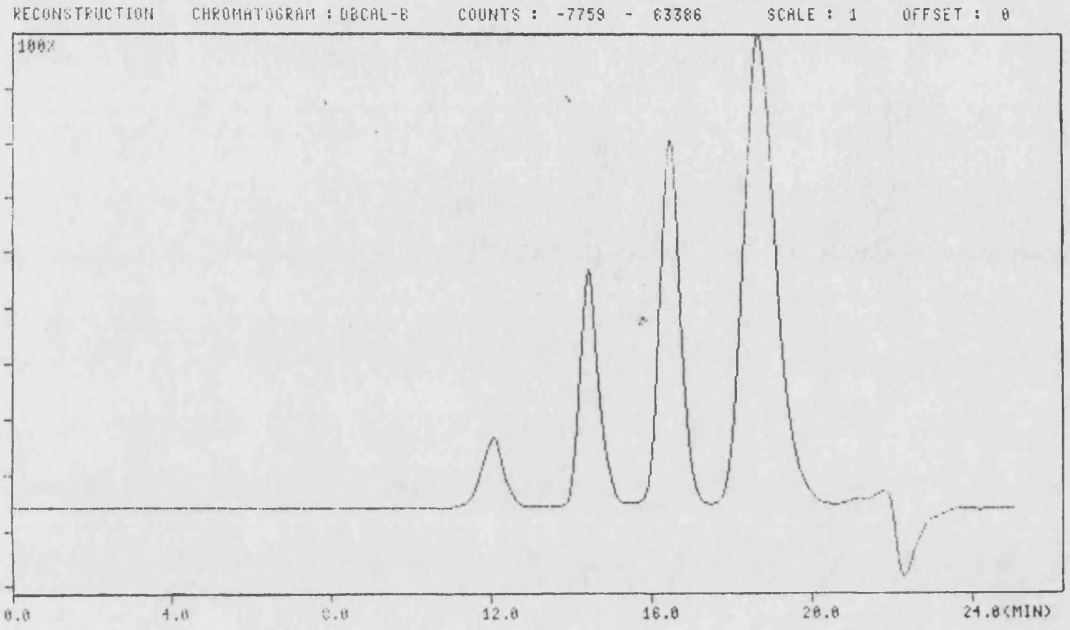

Figure 2.3 - GPC chromatogram of a polystyrene standard solution

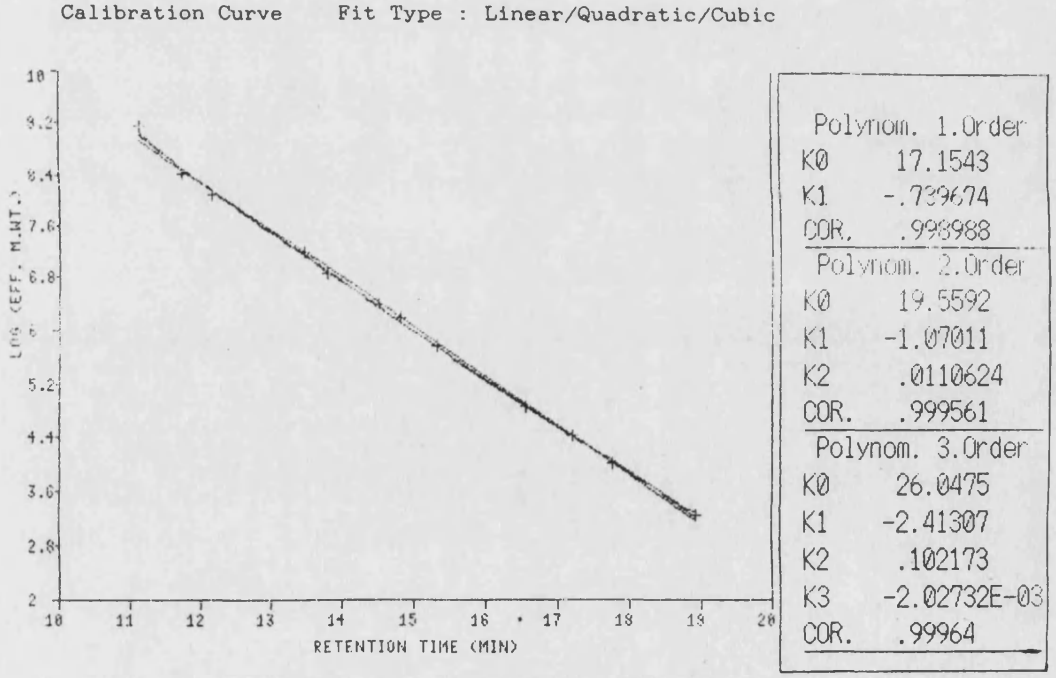

Figure 2.4 - GPC calibration curve

The GPC uses the absolute retention time (i.e. the time for the sample to reach the detector after being injected) when calculating the molecular weights. However, the same sample run at different times can give different results. This is likely to be due to changes in room temperature affecting the performance of the column. To account for this, an internal reference, 1,2-dichlorobenzene, was used. Two drops of 1,2-dichlorobenzene were added to each of the molecular weight standards and the retention time defined in the calibration file. Two drops are also added to the unknown samples and during the calculation, the GPC relates the retention time of the reference in the sample, to that defined in the calibration file. The relationship is then accounted for when the molecular weights are calculated for the unknown sample. By using this method, small changes in the performance of the column will not affect the final molecular weight determinations, giving more accurate and consistent results.

As polystyrene standards were used, not PDMS standards, all molecular weights quoted are 'polystyrene equivalent' molecular weights.

2.7.2 The HPLC

The HPLC was used to determine the relative amounts of D_4 and PDMS in an unknown sample. This allowed the conversion of D_4 to polymer to be monitored during the polymerisation experiments. The HPLC set-up consisted of an HPLC Technology solvent pump (RR/066) pumping toluene through a Polymer Laboratories Ltd, PLGel 5μ column at 0.85 cm^3min^{-1}. The detector was a Bischoff refractive index detector connected to a Hewlett Packard HP3394 integrator.

Calibration of the HPLC

As the detector detects refractive index (RI), the detector response depends on the difference between the reference solvent (toluene, $RI_{(20°C)} = 1.497$ [130]) and the sample (an unknown mixture of PDMS, $RI_{(20°C)} = 1.402$, and D_4, $RI_{(20°C)} = 1.3968$ [131], in toluene). As PDMS and D_4 have different refractive indices, the detectors response will depend on the ratio of PDMS to D_4 in the sample, i.e. a 50:50 ratio (by weight) of PDMS and D_4 will not give peaks with the same peak area. Hence, the HPLC system needs to be calibrated to determine how the % PDMS in D_4 (by weight) correlates to peak area %.

19 samples of PDMS in D_4 (each sample being ~1g in weight) ranging in concentration from 5 wt% PDMS in D_4 to 95 wt% PDMS were accurately prepared. 0.2 g of each sample was then dissolved in ~2 cm^3 of toluene and then filtered through a 0.2 μm membrane filter to give the sample for analysis. All samples were stored in a refrigerator until use. Each sample was run through the HPLC a minimum of four times, and the area of the PDMS and D_4 peaks were obtained from the integrator. Figure 2.5 shows a chromatogram obtained from the solution containing 15 % PDMS, while figure 2.6 shows that obtained from the solution containing 80 % PDMS.

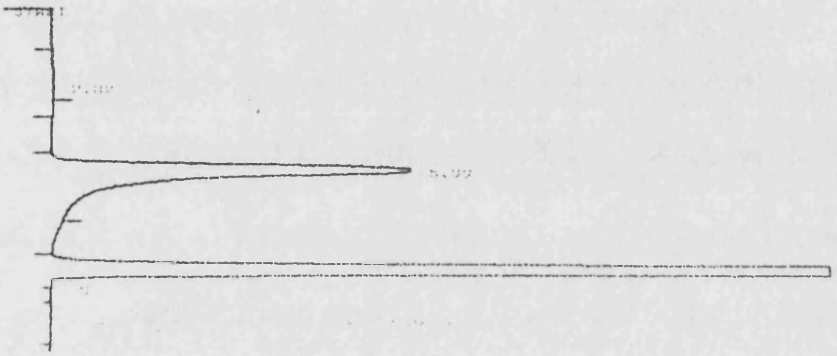

Figure 2.5 - HPLC chromatogram of 15 % PDMS in D_4

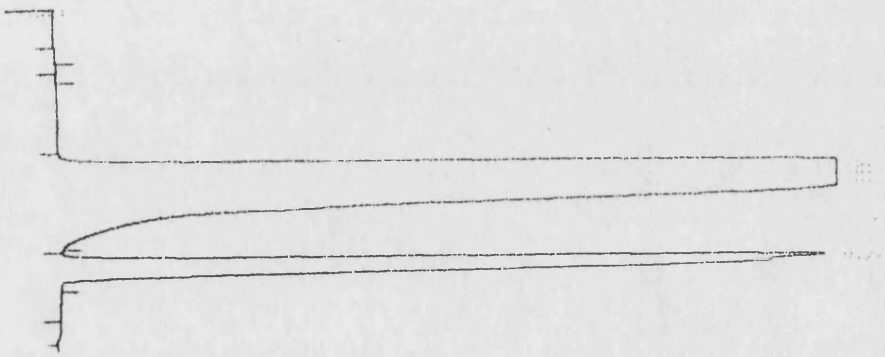

Figure 2.6 - HPLC chromatogram of 80 % PDMS in D_4

From these values, the area % for each peak was calculated and then the average area % of PDMS for each sample was determined. This allowed a calibration plot of area % PDMS against weight % PDMS to be constructed. Linear regression of the plot enabled an equation to be determined so that given the area % PDMS of an unknown sample run through the HPLC, the weight % PDMS (or D_4) could be determined. The calibration plot is shown in figure 2.7.

Calibration data

Sample	Weight %		Area %	
	PDMS	D_4	PDMS	D_4
0	0	100	0	100
1	5.276	94.724	6.023	93.977
2	9.966	90.034	10.977	89.023
3	15.07	84.93	13.96	86.04
4	19.95	80.05	20.407	79.593
5	24.954	75.046	23.393	76.607
6	30.067	69.933	29.049	70.951
7	35.094	64.906	33.88	66.12
8	39.887	60.113	38.48	61.52
9	44.728	55.272	43.146	56.854
10	49.799	50.201	47.066	52.934
11	54.851	45.149	52.876	47.124
12	60.101	39.899	58.218	41.782
13	65.317	34.683	63.123	36.877
14	69.436	30.564	66.398	33.602
15	74.904	25.096	71.65	28.35
16	80.004	19.996	77.735	22.265
17	84.22	15.78	81.665	18.335
18	90.487	9.513	89.09	10.91
19	95.119	4.881	94.623	5.377

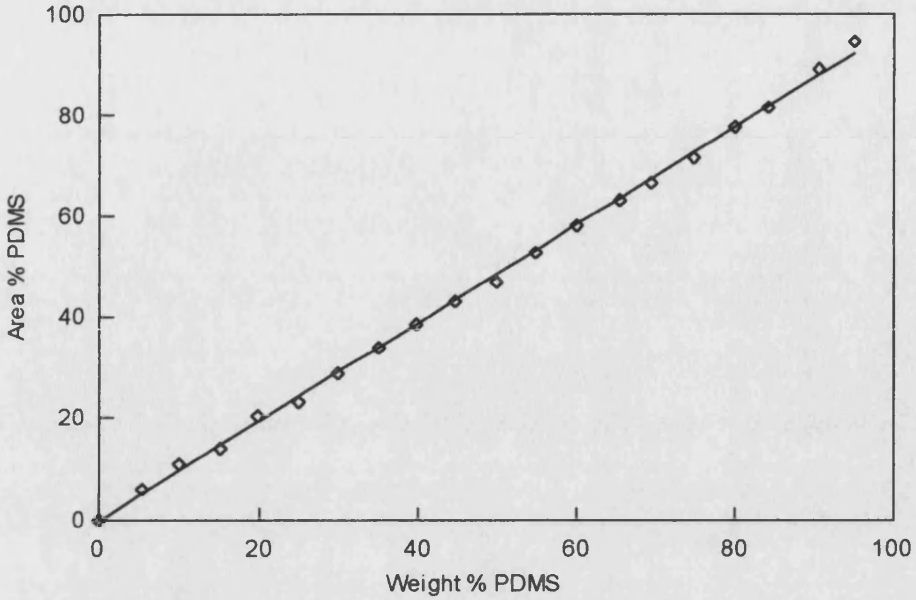

Figure 2.7 - HPLC calibration plot

As can be seen, the correlation between the weight% and the area% is linear. Linear regression of the data gives,

x coefficient = 0.972574, constant = -0.071894, $R^2 = 0.999$

Thus, knowing the area % of an unknown sample, the weight % PDMS (or D_4) of the sample can be determined from,

$$Wt\%\ PDMS = \frac{(Area\% + 0.071894)}{0.972574} \qquad (14)$$

and

$$Wt\%\ D_4 = 100 - Wt\%\ PDMS \qquad (15)$$

2.7.3 IR Spectroscopy

Infra-red spectroscopy was used, along with nuclear magnetic resonance, to determine the nature of the products in the copolymer experiments. A Perkin-Elmer 983 IR spectrophotometer was used to obtain all IR spectra. The polymer samples were analysed as films, the films being cast onto NaCl plates, from $CHCl_3$.

2.7.4 NMR Spectroscopy

Samples for NMR analysis were dissolved in $CDCl_3$ (~50 mg in 1.5 cm^3) and analysed using either a JEOL GX270 FT-NMR, or a JEOL GX400 FT-NMR. TMS was used as an internal standard except where the siloxane integrals were required, when an external TMS standard was used. ^1H, ^{19}F and ^{29}Si NMR were conducted.

2.7.5 UV/Vis Spectroscopy

UV/Vis spectroscopy was used in the experiments with DPPH, to find the absorbance of the solutions. The spectrophotometer used was a Perkin-Elmer 330. Quartz cells with a path length of 1 cm were used.

2.8 Materials

PDMS	100 000 cs DC200 fluid. Aldrich. Used as received.
D_4	Dow Corning Ltd. Distilled prior to use.
D_3	98 %. Aldrich. Used as received.
Hexamethyldisiloxane	Dow Corning Ltd. Used as received.
20 cs DC200 fluid	Dow Corning Ltd. Used as received.
Hydride-terminated PDMS	Mn ~ 580. Aldrich. Used as received.
	Mn ~ 5770. Dow Corning Ltd. Used as received.
Poly(isobutylene)	Mw ~ 400 000. Fisher. Used as received
Toluene	99.8 % HPLC grade. Aldrich. Used as received.
THF	99.9 + % HPLC grade. Aldrich. Used as received.
Anhydrous THF	99.9 %, inhibitor free. Aldrich. Used as received.
Potassium hydroxide	85 % ACS reagent. Aldrich. Used as received.
Sulphuric acid	95 - 98 % CP. Acros. Used as received.
Acetic acid	AnalaR. BDH. Diluted to 2 M solution.
Sodium bicarbonate	99 %. Aldrich. Used as received.

Styrene	99 %. Aldrich. Washed three times with 10 % w/v NaOH solution, then washed three times with distilled water. The aqueous layer was removed and the styrene was then vacuum distilled prior to use.
Methyl methacrylate	99 %. Aldrich. Vacuum distilled prior to use.
n-Butyl lithium	1.6 M solution in hexane, Aldrich. Used as received.
DPPH	98 %. Aldrich. Used as received.
TBAF	1.0 M solution in THF. Aldrich. Used as received.
Lithium fluoride	Anhydrous, 99.99 + %. Aldrich. Used as received.
Chloroplatinic acid	ACS reagent. Aldrich. Used as received.
2,2'-bipyridyl	99+ %. Aldrich. Used as received.
(Chloromethyl)styrene	99.8 %, mixture of *m* and *p*-isomers. Aldrich. Used as received.
Isopropyl alcohol	99.5 % HPLC grade. Aldrich. Used as received.
o-Xylene	99 %. Fisher. Used as received.
Methanol	99 %. BDH. Used as received.
Chloroform	99.9 % HPLC grade. Aldrich. Used as received.
d-Chloroform	99.8 atom% D. Aldrich. Used a received.
1,2-Dichlorobenzene	AnalaR. BDH. Used as received.
Polystyrene standards	12 narrow polydispersity standards. Polymer Laboratories. Used as received.

Chapter 3

Ultrasonic Degradation

3 ULTRASONIC DEGRADATION

The aim of this work was to investigate how changing the experimental parameters affects the ultrasonic degradation process for PDMS. An understanding of the process offers the opportunity to control the molecular weight of the polymer through manipulation of the experimental conditions. In addition, it will give an insight into how the degradation process may affect molecular weights during polymerisations conducted under ultrasound.

This chapter describes the effect that changing ultrasonic intensity, solution temperature and solution concentration have on the rate of degradation. Two solvents were used, toluene (a 'good' solvent for PDMS) and octamethylcyclotetrasiloxane (D_4). D_4 is the monomer from which PDMS is produced, so it is envisaged that by conducting the degradations in D_4, valuable information will be obtained as to how the polymerisation may be affected by degradation processes.

In all degradations the PDMS used was commercially available, high viscosity (100 000 cs) polymer, end-blocked with trimethylsilyl groups ($M_n \sim 85\ 000$, $\gamma \sim 1.8$). Unless stated, all degradations were conducted on the ultrasonic horn, and the results were analysed using the Schmid and Ovenall rate models (equations 10 and 11, section 1.15.2).

For the Schmid kinetic analysis, $(M_{lim}/M_t) + \ln(1-M_{lim}/M_t)$ was plotted against t, the slope of the plot then being, $-(k/c)(M_{lim}/m_o)^2$, where,

M_{lim} is the limiting molecular weight,

M_t, the molecular weight (M_n) at time, t, during the sonication,

m_o is the repeat unit molecular weight,

c is the concentration, and

k is the rate constant.

For the Ovenall kinetic analysis, $\ln(1/M_{lim} - 1/M_t)$ was plotted against t, the slope of the plot then being, $-(k/c)(M_{lim}/m_o)$. This allowed rate constants from both models to be determined.

3.1 Degradation of PDMS in Toluene

3.1.1 Effect of Changing Intensity

Figure 3.1 shows the change in molecular weight (M_n) for 1 % w/v solutions of PDMS in toluene, sonicated at 30°C and at intensities of 7.6, 15.9, 22.8 and 31.3 Wcm^{-2}. It can be seen that the reduction in M_n, for all the degradations, is initially fast (when M_n is high), but slows as the degradation progresses and the molecular weight is reduced. Increasing the ultrasonic intensity results in faster degradation and it can also be seen that increasing the intensity from 7.6 to 22.8 Wcm^{-2} results in a decrease in M_{lim} (the limiting molecular weight), although for 22.8 and 31.3 Wcm^{-2}, M_{lim} tends towards the same value.

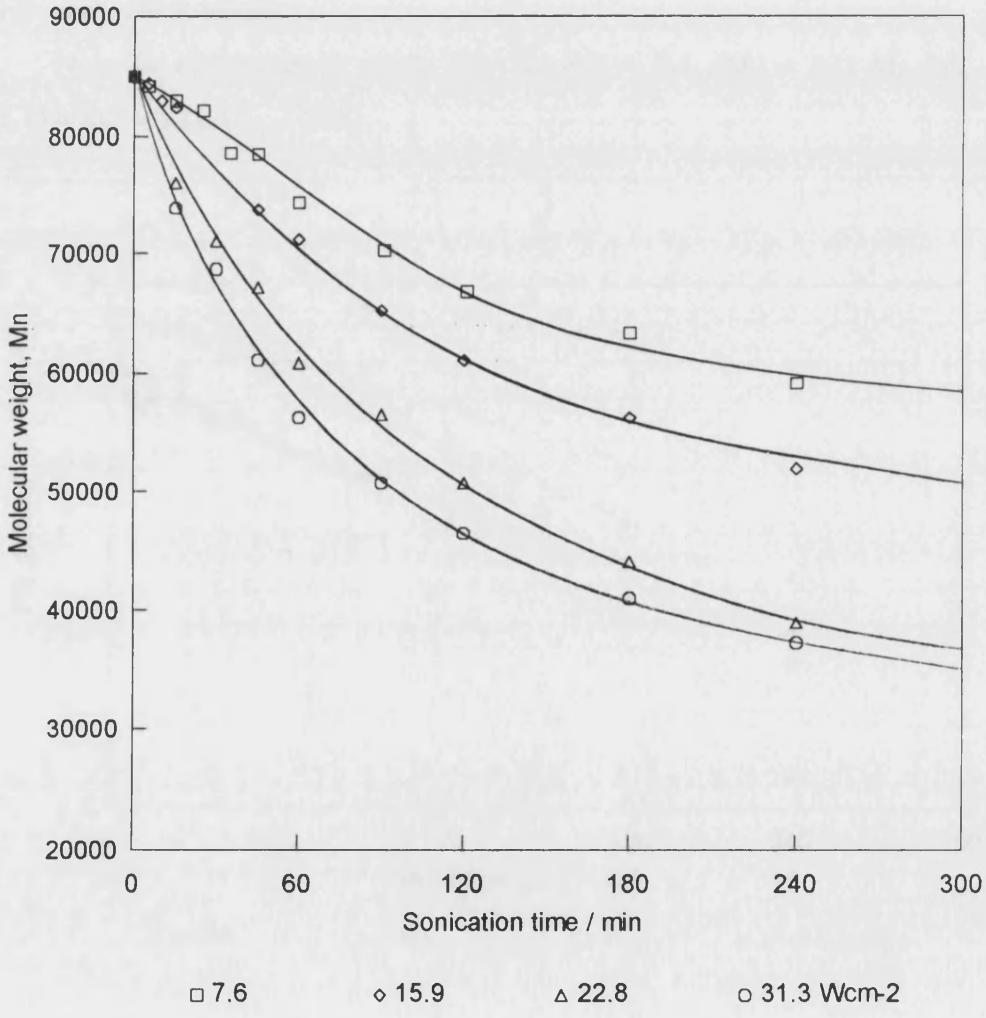

Figure 3.1 - Effect of ultrasound intensity on molecular weight during degradation of PDMS in toluene

These results can be explained by considering the effect that the ultrasound intensity has on cavitation. As the ultrasound intensity increases the temperatures and pressures generated on bubble collapse increase (section 1.13.4). Noltingk and Neppiras[75,76] also showed that the bubble radius is proportional to the square root of the intensity, so an increase in intensity leads to larger bubbles and therefore higher shear forces on bubble collapse. The forces acting on the polymer chain therefore increase as the intensity increases, and a lower M_{lim} results. The increase in intensity also increases the number of cavitation events per unit volume and this accounts for the faster rate of degradation.

Figures 3.2 and 3.3 show the Schmid and Ovenall kinetic plots for the data, while figures 3.4 and 3.5 show the relationship between the intensity and the Schmid and Ovenall rate constants.

Note, in all the kinetic plots, F(t), Schmid = $(M_{lim}/M_t) + \ln(1-M_{lim}/M_t)$, and F(t), Ovenall = $\ln(1/M_{lim} - 1/M_t)$.

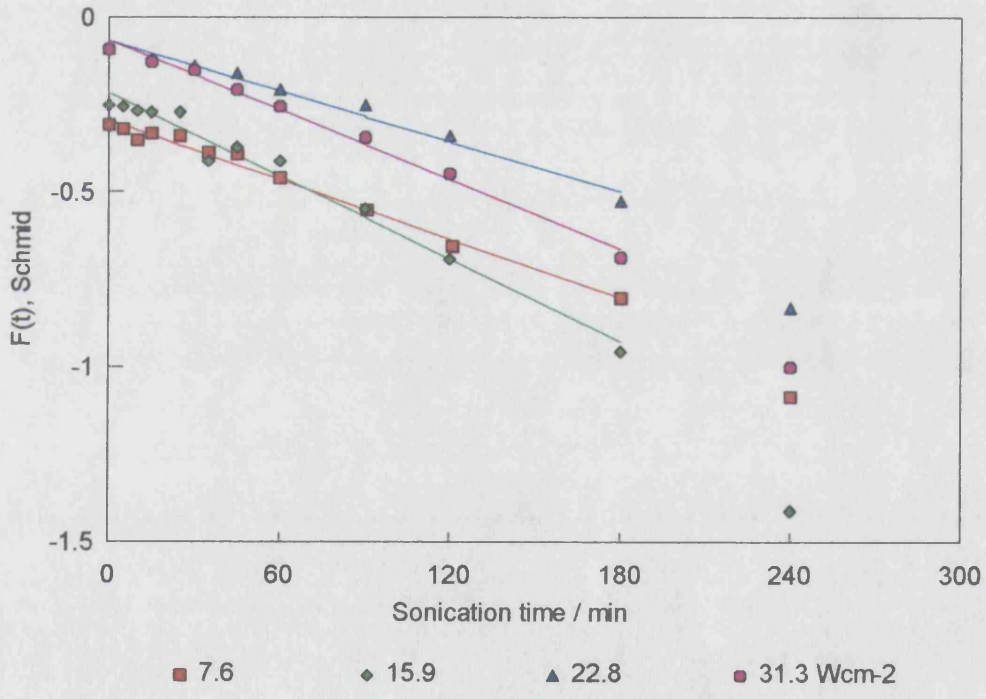

Figure 3.2 - Schmid kinetic plot for the degradation of PDMS in toluene at different ultrasonic intensities

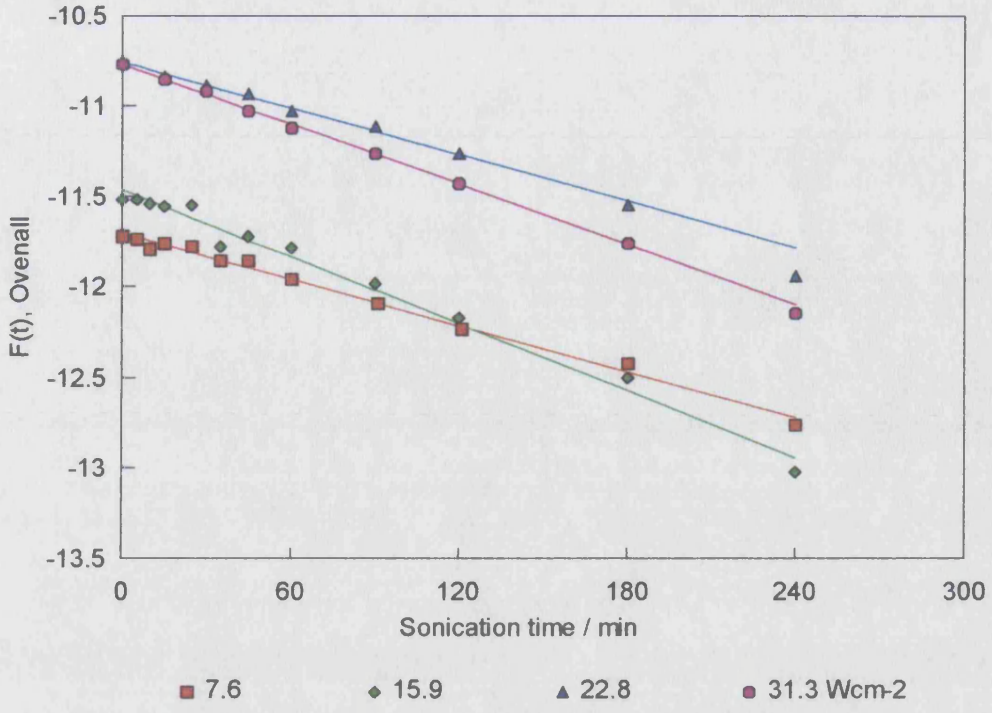

Figure 3.3 - Ovenall kinetic plot for the degradation of PDMS in toluene at different ultrasonic intensities

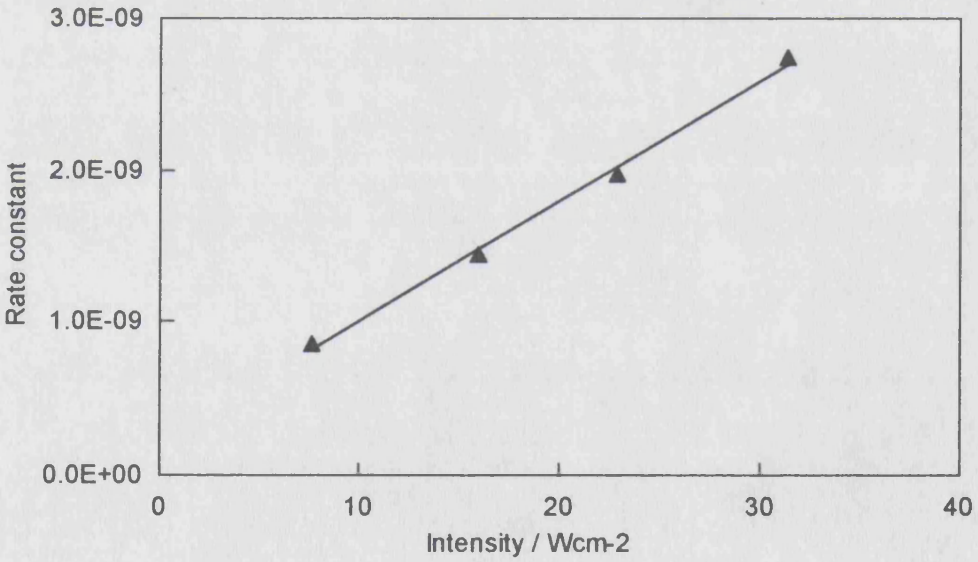

Figure 3.4 - Variation in Schmid rate constant with ultrasonic intensity for the degradation of PDMS in toluene

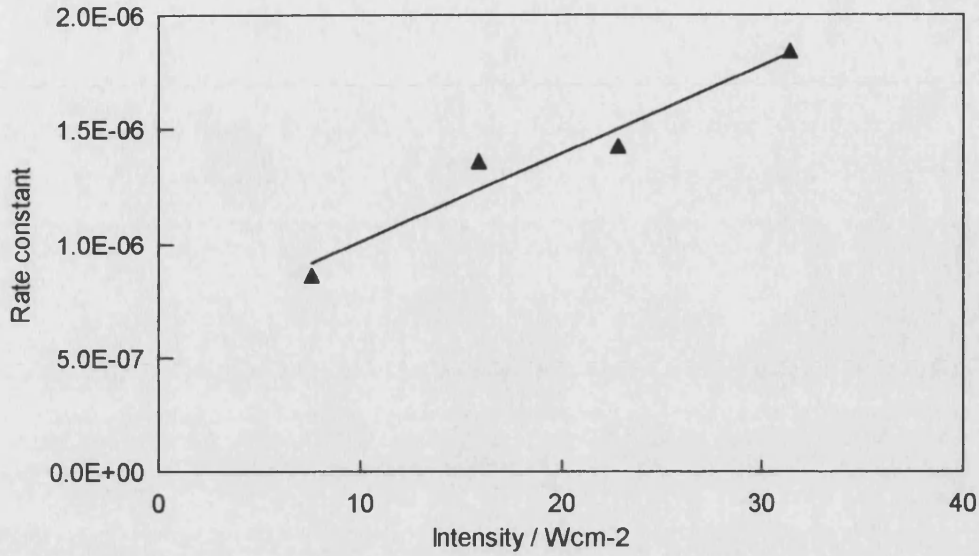

Figure 3.5 - Variation in Ovenall rate constant with ultrasonic intensity for the degradation of PDMS in toluene

The kinetic plots show good linear relationships up to 180 minutes of sonication for all intensities, although there is some scatter at the beginning for the two lower intensities. After approximately 180 minutes, the graphs tend to curve downwards, especially in the Schmid plots.

This effect is also apparent in the other degradation results, and arises for a number of reasons. Firstly, deficiencies in the models, such as the assumption of monodisperse samples and ignoring changes in polydispersity, are not accounted for. Also, as the molecular weight approaches M_{lim}, the experimental error in the values becomes increasingly large. Table 3.1 shows the rate constants determined for each degradation.

Table 3.1 - M_{lim} and Schmid and Ovenall rate constants for the degradation of PDMS in toluene at different intensities

Intensity (Wcm^{-2})	Schmid ($moldm^{-3}min^{-1}$)	Ovenall ($moldm^{-3}min^{-1}$)	M_{lim}
7.6	0.855×10^{-9}	0.860×10^{-6}	50 000
15.9	1.448×10^{-9}	1.363×10^{-6}	45 000
22.8	1.973×10^{-9}	1.427×10^{-6}	30 000
31.3	2.739×10^{-9}	1.845×10^{-6}	30 000

Both the Schmid and Ovenall rate constants show a linear increase with intensity, reflecting the fact that higher intensities produced faster rates of degradation. This is a similar result to that obtained by Mostafa[132] and Jellinek[133] who also obtained a linear result of rate constant with ultrasonic intensity for solutions of polystyrene in benzene. However, for solutions of polystyrene in toluene, Price and Smith[106] have shown that although the rate constant increases with intensity, the rise does not continue indefinitely but reaches a maximum value at an intensity of approximately 145 Wcm^{-2}. This effect was explained in terms of the number of cavitation bubbles produced during sonication. As the ultrasound intensity increases, the number of cavitation bubbles per unit volume increase, leading to a faster rate of degradation. However, above a certain intensity, the increased numbers of bubbles effectively shrouds the source of the ultrasound, dispersing the acoustic wave. The ultrasound does not pass through the solution as efficiently, reducing the cavitation and consequently, the rate of degradation. Another effect of the high intensity is that the cavitation bubbles will grow so large on rarefaction that there is insufficient time available for collapse during the compression cycle.

As degradation is a mechanical effect arising from cavitation, and not due to the chemical nature of the polymer, it is the nature of the solvent in which the cavitation is occurring that will affect the degradation process. As Price and Smith used the same solvent for their studies as that used here, it would be expected that the PDMS/toluene solutions would also show a maximum intensity. However, the intensities used for these were much lower than those used by Price and Smith and this would explain why the increase in rate with intensity does not show a maximum.

Price and Smith also found that the M_{lim} of the polystyrene gave a linear relationship with the intensity, with M_{lim} decreasing as the intensity increased. However, the results for the PDMS solutions only showed a decrease in M_{lim} as the intensity increased up to 22.8 Wcm^{-2}. Intensities of 22.8 and 31.3 Wcm^{-2} gave the same value of M_{lim}. It has been suggested by some workers that M_{lim} is independent of intensity[134,135], although it is obviously not the case here. Nevertheless, for this system, the results do suggest that there is a limiting molecular weight below which no further degradation can occur no matter how the intensity is increased. However, these results only a cover a small range of intensities and further work using a larger range of intensities is required to verify if this is the case.

3.1.2 Effect of Changing Temperature

Figure 3.6 shows the change in M_n for 1 % w/v PDMS solutions sonicated at 33.4 Wcm^{-2} at temperatures of 17, 31, 50 and 73°C. Note that the attenuation of the ultrasound in the solution causes a small bulk heating effect and although this is largely negated by the water jacket of the sonication vessel, there is an uncertainty in the temperature of ± 1°C.

Increasing the temperature at which the degradation occurs results in a decrease in the rate of degradation and an increase in M_{lim}. This result is qualitatively similar to that found by other workers for other polymer-solvents systems[24,106].

The Schmid and Ovenall kinetic plots (figures 3.7 and 3.8) give good linear fits although, as before, the linearity only extends to 180 minutes for the Schmid plot. The Ovenall plots are linear up to 240 minutes before they start to curve downwards. The rate constants obtained from the data are shown in table 3.2. All of the rate constants determined confirm the results seen in figure 3.6. Thus, an increase in temperature results in a decrease in the rate constant for the degradation.

The majority of chemical processes are accelerated by an increase in temperature, however, it can be seen that in the sonochemical case the opposite is true. Increasing the temperature at which the degradation occurs decreases the rate of degradation, with the subsequent decrease in the rate constant and increase in M_{lim}. The temperature effect on the rate of degradation can be understood by considering the cavitation process. At the higher temperatures the solvent (toluene) will have a higher vapour pressure and hence more vapour will enter the cavitation bubble. The

collapse of the bubble is then cushioned by the vapour, reducing the violence of the collapse and resulting in a lowering of the rate of degradation.

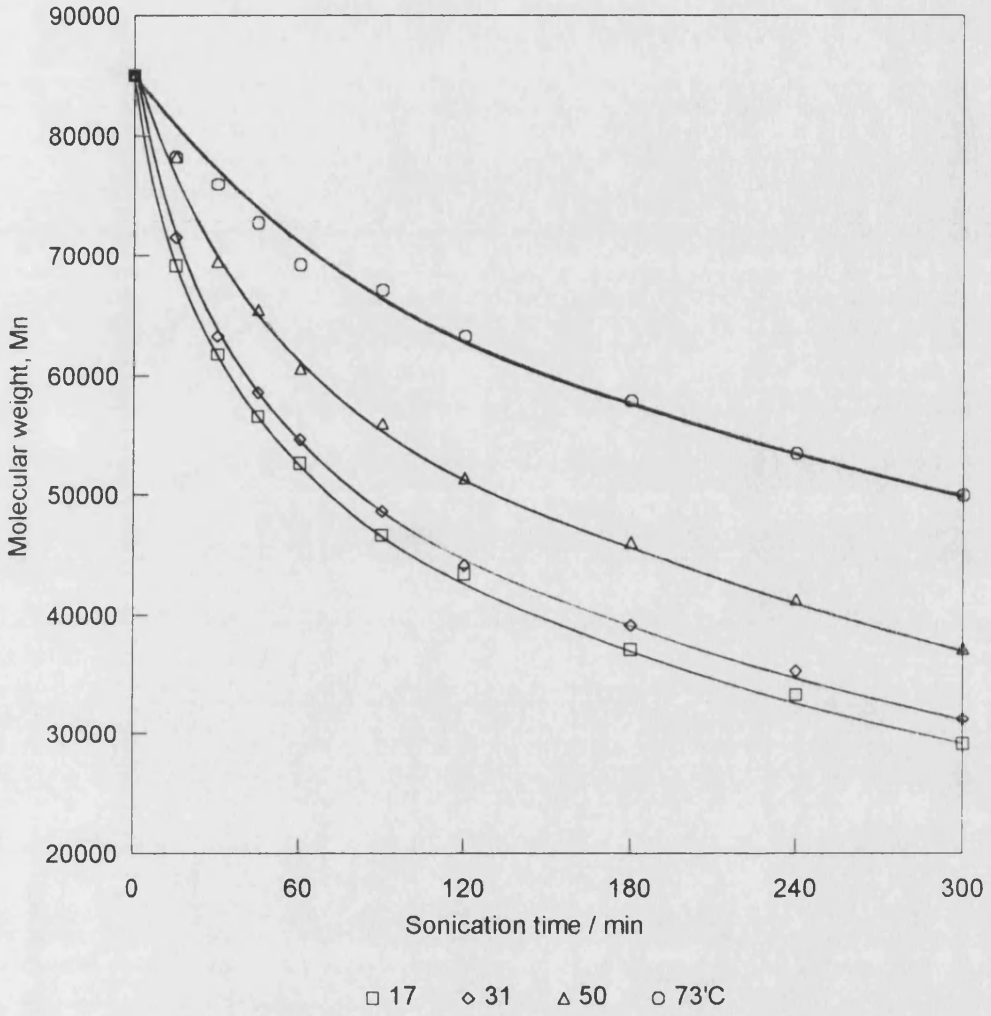

Figure 3.6 - Effect of solution temperature on molecular weight during degradation of PDMS in toluene

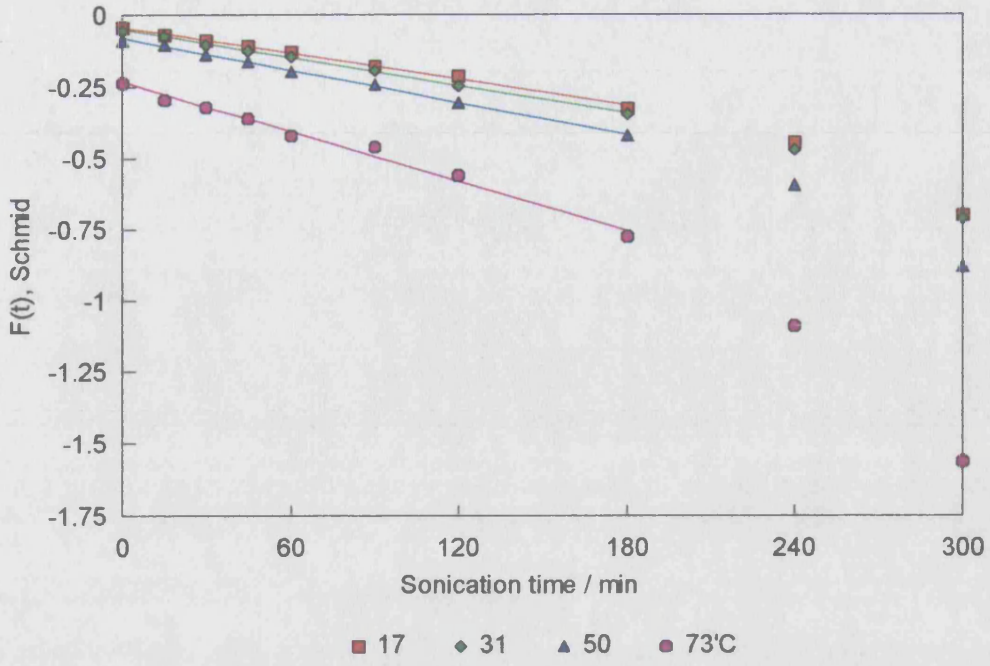

Figure 3.7 - Schmid kinetic plot for the degradation of PDMS in toluene at different solution temperatures

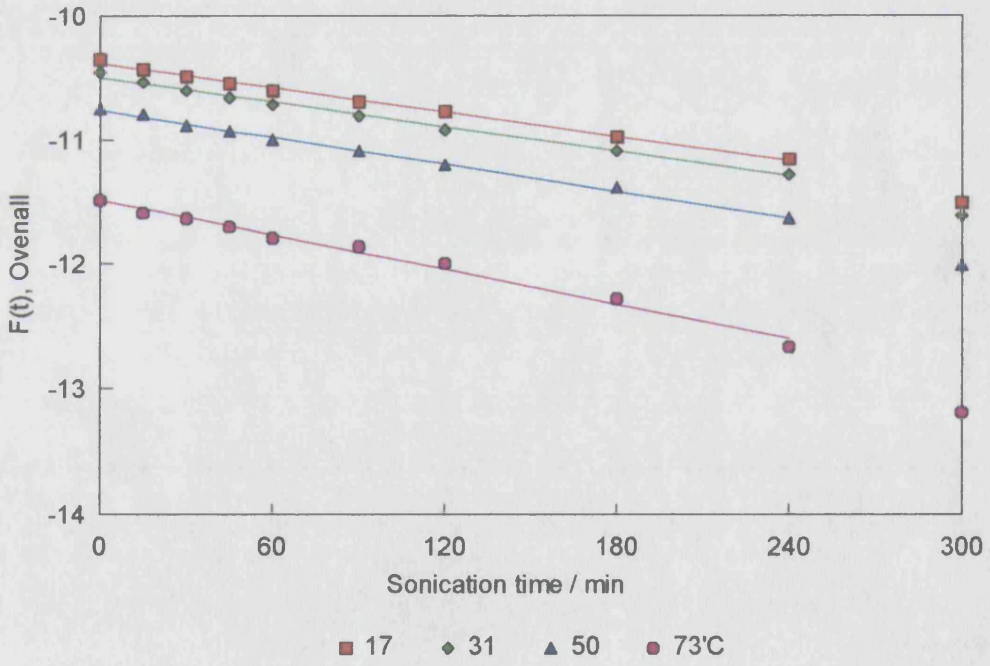

Figure 3.8 - Ovenall kinetic plot for the degradation of PDMS in toluene at different solution temperatures

Table 3.2 - M_{lim} and Schmid and Ovenall rate constants for the degradation of PDMS in toluene at different temperatures

Temp (°C)	Schmid ($moldm^{-3}min^{-1}$)	Ovenall ($moldm^{-3}min^{-1}$)	M_{lim}
17	2.179×10^{-9}	1.446×10^{-6}	23 000
31	2.023×10^{-9}	1.391×10^{-6}	25 000
50	1.568×10^{-9}	1.220×10^{-6}	30 000
73	1.073×10^{-9}	1.046×10^{-6}	45 000

Arrhenius Analysis

Applying the Arrhenius equation to the rate constants gives linear relations for both kinetic models (figure 3.9), although the apparent activation energies determined are, -10.8 ± 1.6 $kJmol^{-1}$ (Schmid) and -5.0 ± 0.6 $kJmol^{-1}$ (Ovenall). A negative apparent activation energy of -17.3 $kJmol^{-1}$ was also seen by Price and Smith for polystyrene in toluene[106]. These negative apparent activation energies obviously bear no relation to the chemical process of bond-breaking (the bond energy of the Si-O bond is 451 $kJmol^{-1}$, while the activation energy for the thermal depolymerisation of PDMS is 177 $kJmol^{-1}$ [137]), but can be qualitatively interpreted in terms of the effect of the solvent. As explained above, cavitational collapse becomes more violent at lower temperatures leading to faster rates of degradation, hence the apparent activation energy is negative.

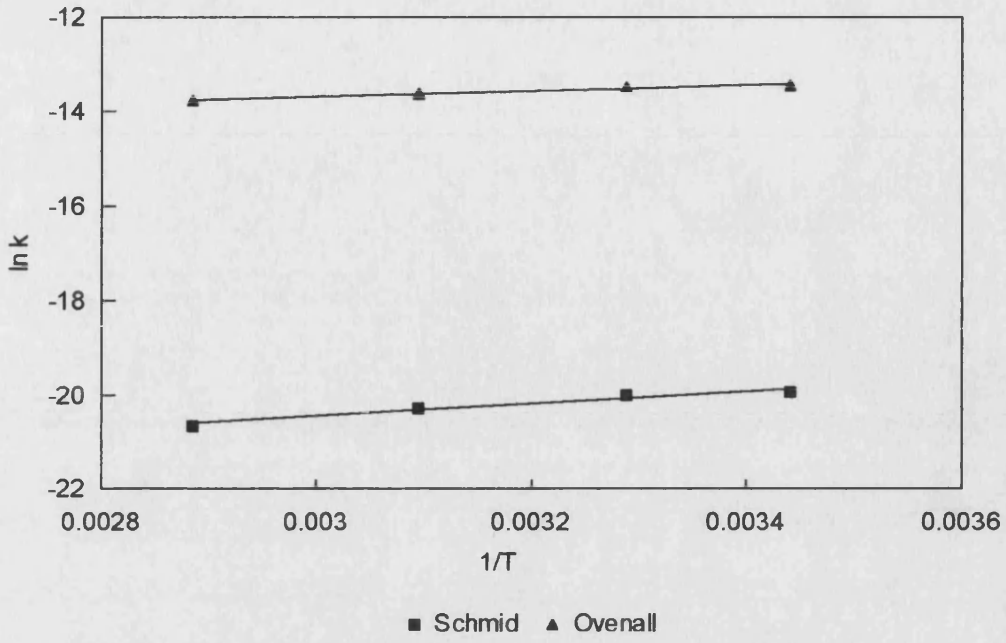

Figure 3.9 - Arrhenius analysis of the Schmid and Ovenall rate constants for the degradation of PDMS in toluene at different solution temperatures

3.1.3 Effect of Changing Concentration

Figure 3.10 shows the effect of changing the concentration of the PDMS solution, from 0.1 % w/v to 20 % w/v, when sonicated at 30°C and 33.4 Wcm^{-2}.

The general trend is that increasing the concentration results in a decrease in the rate of degradation and an increase in M_{lim}. This effect seems most pronounced between concentrations of 0.1 and 5 %. At the higher concentrations there is a lot of scatter at the beginning of the sonications. This is probably due to the fact that at high concentration, the solutions are very viscous. They will therefore not mix effectively and this results in a variation of the molecular weight throughout the solution.

The effect that changing the concentration has on the degradation can be explained by considering the viscosity of the solutions. As the concentration of a polymer solution increases, the viscosity will also increase. The higher the viscosity, the more difficult it is for cavitation to occur in the solution and subsequently the degradation effect is reduced.

Figures 3.11 and 3.12 show the Schmid and Ovenall kinetic plots determined from the data. All of the kinetic plots show good linear fit to the experimental data,

although at the higher concentrations there is a lot of scatter about the best fit line, reflecting that seen in the degradation plot. The rate constants determined are shown in table 3.3

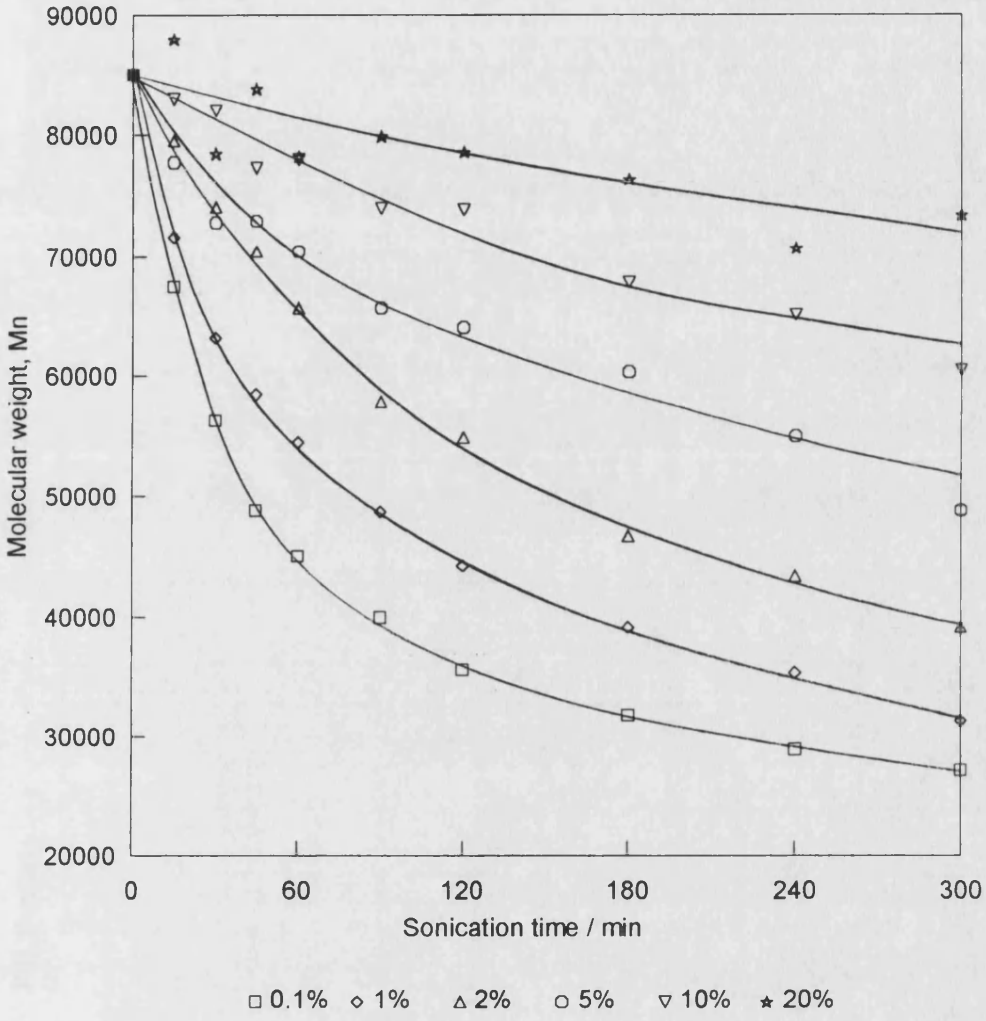

Figure 3.10 - Effect of solution concentration on molecular weight during degradation of PDMS in toluene

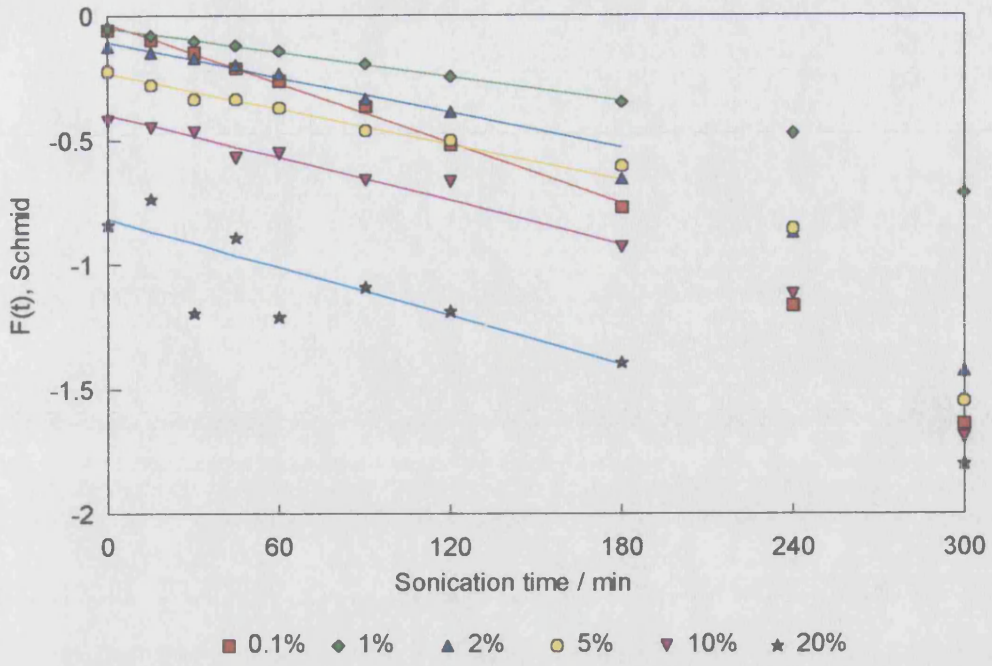

Figure 3.11 - Schmid kinetic plot for the degradation of PDMS in toluene at different solution concentrations

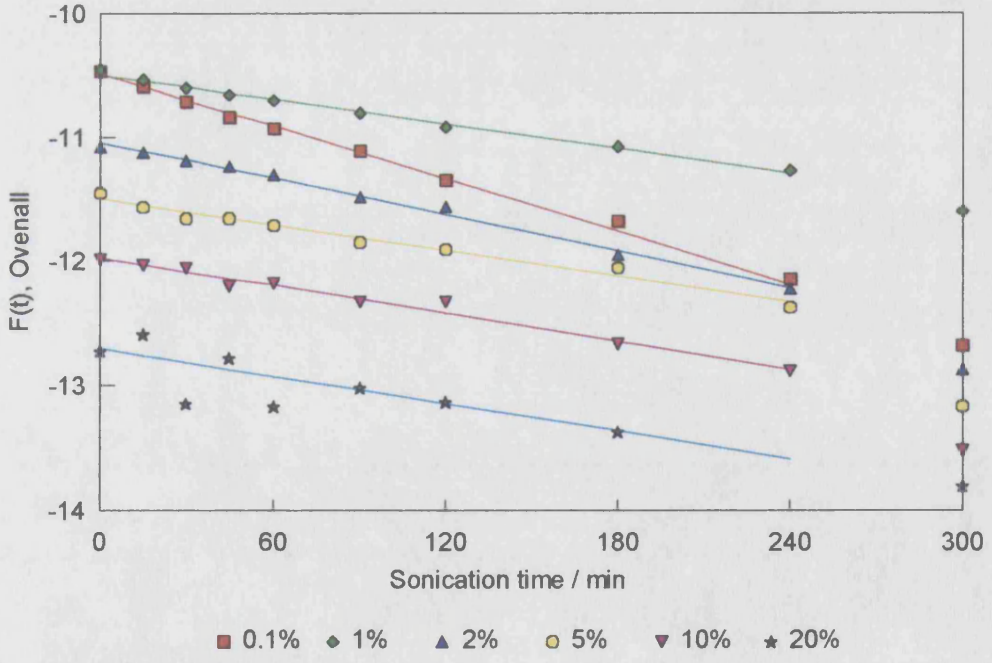

Figure 3.12 - Ovenall kinetic plot for the degradation of PDMS in toluene at different solution concentrations

Table 3.3 - M_{lim} and Schmid and Ovenall rate constants for the degradation of PDMS in toluene at different concentrations

Conc. (% w/v)	Schmid ($moldm^{-3}min^{-1}$)	Ovenall ($moldm^{-3}min^{-1}$)	M_{lim}
0.1	0.518×10^{-9}	0.308×10^{-6}	25 000
1	2.023×10^{-9}	1.391×10^{-6}	25 000
2	2.474×10^{-9}	2.653×10^{-6}	38 000
5	4.530×10^{-9}	3.972×10^{-6}	45 000
10	7.164×10^{-9}	6.862×10^{-6}	55 000
20	11.348×10^{-9}	11.249×10^{-6}	65 000

Both the Schmid and Ovenall rate constants increase as the concentration increases. This would appear to be at odds with the actual effect seen, which shows the rate of degradation decreasing as concentration increases. It is also opposite to the effect seen by Price and Smith[107] who obtained the expected decreasing rate constants with increasing concentration for the polystyrene/toluene solutions.

This effect is an unfortunate consequence of the concentration term in the Schmid and Ovenall equations. A better effect of the concentration on the rate can be seen if, rather than using the rate constant, k, the k/c term (with units of min^{-1}) is used instead. Figure 3.13 shows how the k/c term, for both Schmid and Ovenall, changes with concentration.

This representation follows closely the trend seen with the degradation curves with k/c decreasing as the concentration increases. It is also clear that, up to a concentration of 5 %, increasing the concentration has a marked effect on the rate of degradation. Once above 5 % there is little change in the degradation. Again, this reflects that seen in the degradation plot.

For polystyrene in toluene, Price and Smith[107] also found that the effect of changing the concentration on the degradation was most pronounced up to concentrations of 5 %. They determined the critical overlap concentration (the concentration at which the chains begin to entangle), c*, from,

$$c^* = 620\ M_w^{-0.78} \qquad (16)$$

This gave a value of 2.4 %, which coincided well with their observed result. Although this equation is for polystyrene in a good solvent, toluene is also a good solvent for PDMS and applying the equation to PDMS gives an interesting result.

In these experiments, M_w = 153 000 and this gives a critical overlap concentration of 0.056 gcm^{-3}, or 5.6 %. This coincides very well with the results seen in the degradation plot and the plot of k/c against c. Thus, increasing the concentration up to 5 % has a marked effect on the rate of degradation. Above 5 % the polymer chains begin to overlap and the effect on the degradation of increasing the concentration beyond this is much smaller.

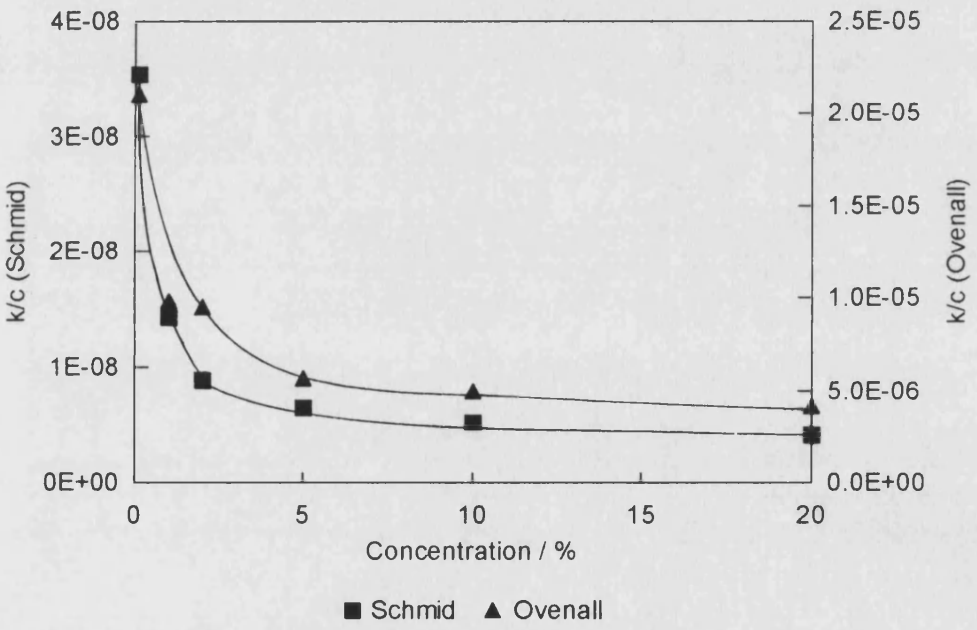

Figure 3.13 - Change in k/c with concentration for Schmid and Ovenall kinetic analyses

3.1.4 24 Hour Degradation

A 1% w/v solution of PDMS in toluene was sonicated on the ultrasonic bath for 24 hours at room temperature. The degradation curve can be seen in figure 3.14.

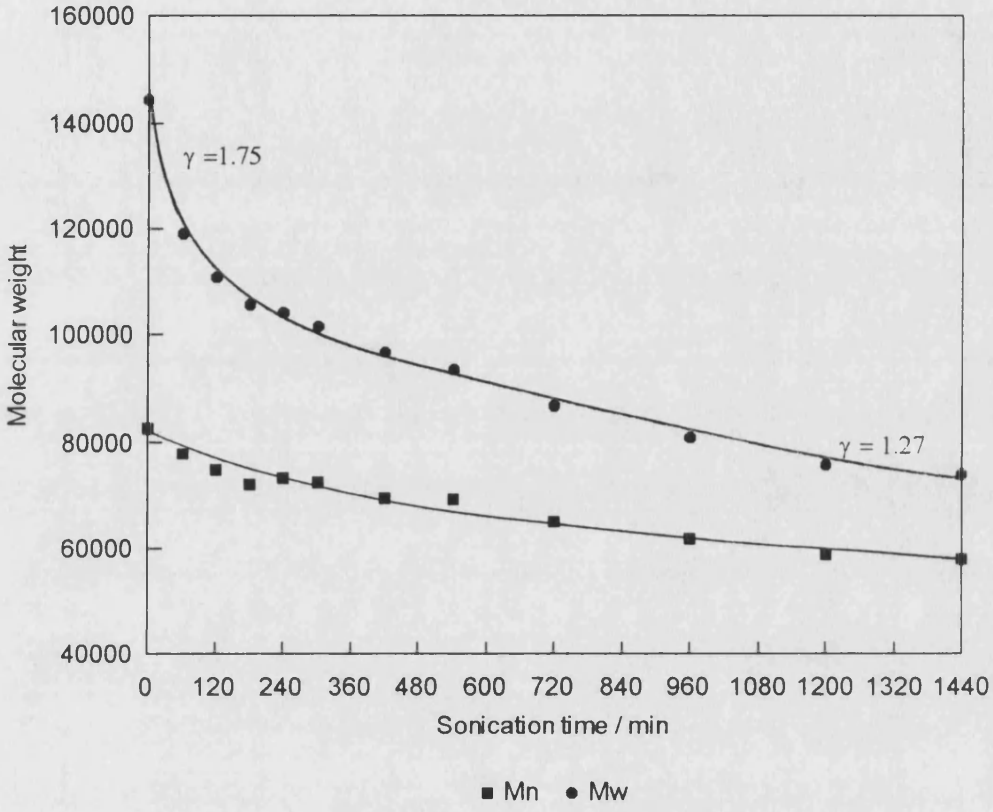

Figure 3.14 - Degradation of PDMS in toluene using the ultrasonic bath

The intensity of the ultrasonic bath is much lower than that of the ultrasonic horn, and temperature control is also much more difficult. Although the sonication was begun at room temperature (~ 22°C), after 24 hours the temperature of the bath was ~37°C. These effects result in the rate of degradation being much slower than those conducted with the horn and only the longer chains are degraded. It can be seen that even after 24 hours on the bath, the molecular weight (M_n) has only fallen to a value of 58 000, compared with an initial molecular weight of 82 000 (as a comparison, using the ultrasonic horn at 33.4 Wcm^{-2} this drop in molecular weight can be accomplished in approximately 45 minutes). However, the weight average molecular weight (M_w), which is influenced by high molecular weight material, falls quite substantially. The net

effect of this is that while the average molecular weight does not change by much, the distribution of molecular weights becomes narrower as the longer chains are preferentially degraded. This is evident in the polydispersity value, which falls from 1.75 to 1.27.

3.2 Degradation of PDMS in D_4

The ring-opening polymerisation of D_4 is one method of producing PDMS. Hence, to understand how ultrasound may affect the polymer formed during a polymerisation, solutions of PDMS in D_4 were degraded and the effect of changing intensity, temperature and concentration were examined.

3.2.1 Effect of Changing Intensity

Figure 3.15 shows the effect changing the intensity has on the degradation of 1 % w/v solutions of PDMS in D_4, sonicated at 40°C. The Schmid and Ovenall plots are shown in figures 3.16 and 3.17 and the rate constants are shown in table 3.4.

As with the degradation in toluene, faster rates of degradation are obtained as the intensity increases, with very little degradation occurring at 9.4 Wcm^{-2}. Figures 3.18 and 3.19 show the relationship between the intensity and the Schmid and Ovenall rate constants.

This series of degradations was conducted over a wider range of intensities than the degradations in toluene but, as with the degradations in toluene, both the Schmid and Ovenall rate constants show a linear increase with ultrasonic intensity. There is no evidence from these results of a maximum as seen by Price and Smith[106]. However, although the intensity range was wider, the highest intensity used here (58.5 Wcm^{-2}) was still some way below their measured maximum of 145 Wcm^{-2}.

Again, the M_{lim} values decrease with increasing intensity but, as for the degradations in toluene, the M_{lim} does not appear as though it will decrease indefinitely, but is tending towards a lower limit. This can be seen clearly in figure 3.20. These results verify those found with the degradation in toluene and suggests that there is a lower limit for M_{lim} which, once reached, will not get any lower even if the intensity is increased.

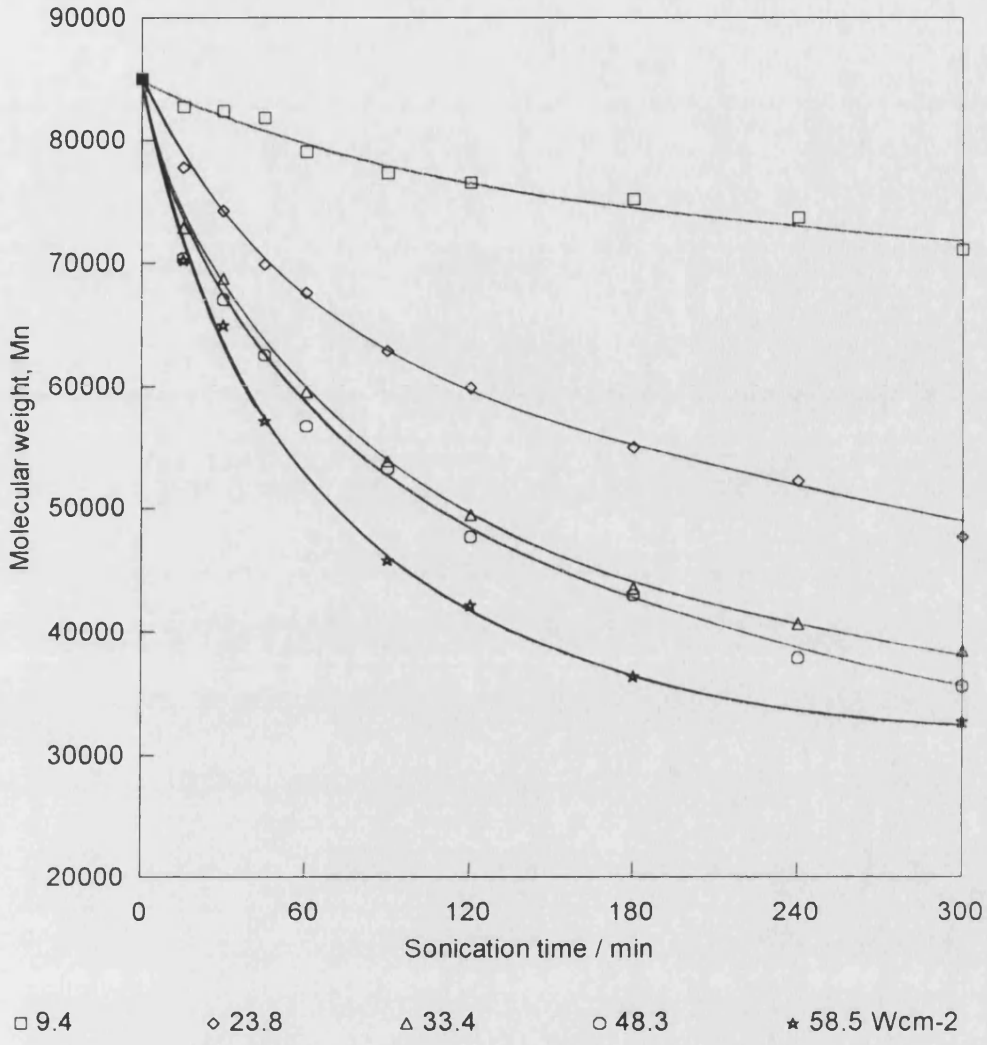

Figure 3.15 - Effect of ultrasound intensity on molecular weight during degradation of PDMS in D_4

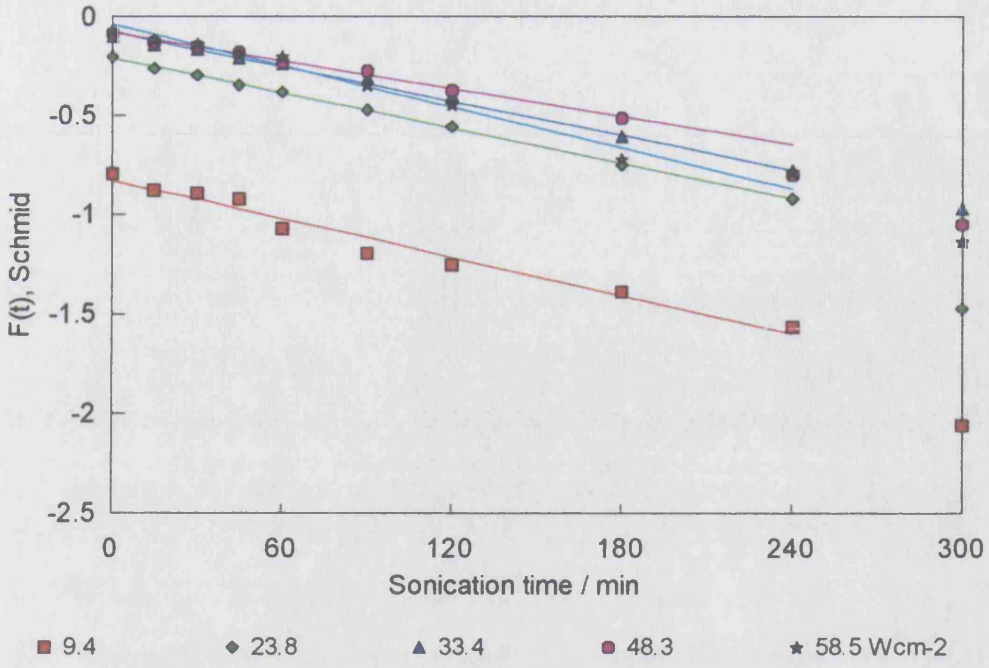

Figure 3.16 - Schmid kinetic plot for the degradation of PDMS in D_4 at different ultrasonic intensities

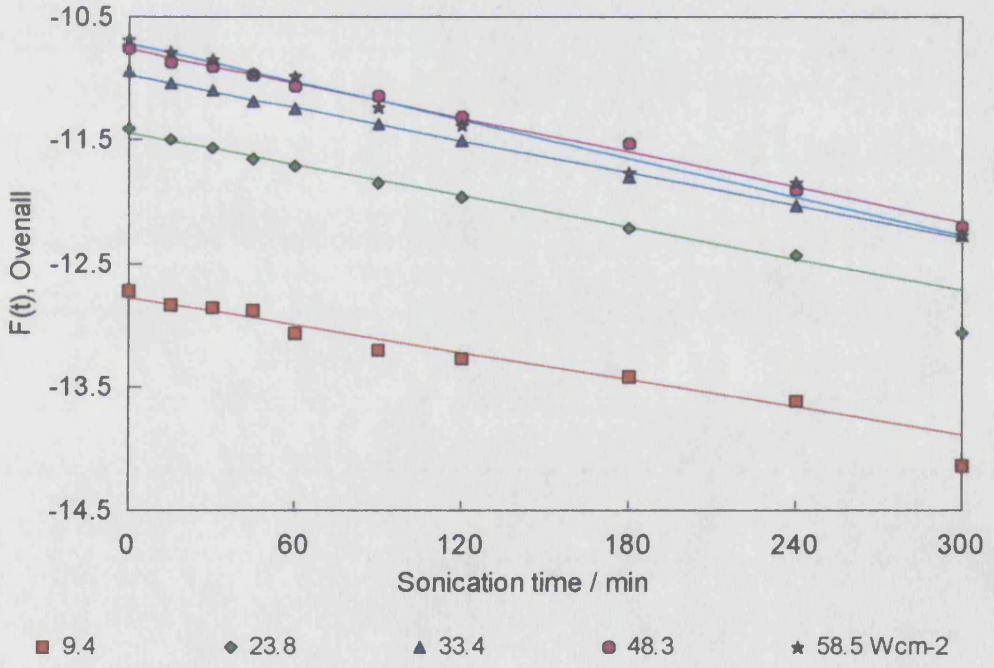

Figure 3.17 - Ovenall kinetic plot for the degradation of PDMS in D_4 at different ultrasonic intensities

Table 3.4 - M_{lim} and Schmid and Ovenall rate constants for the degradation of PDMS in D_4 at different intensities

Intensity (Wcm^{-2})	Schmid ($moldm^{-3}min^{-1}$)	Ovenall ($moldm^{-3}min^{-1}$)	M_{lim}
9.4	0.528×10^{-9}	0.567×10^{-6}	69 000
23.8	1.203×10^{-9}	1.022×10^{-6}	44 000
33.4	1.873×10^{-9}	1.335×10^{-6}	35 000
48.3	2.055×10^{-9}	1.653×10^{-6}	30 000
58.5	3.202×10^{-9}	1.878×10^{-6}	29 000

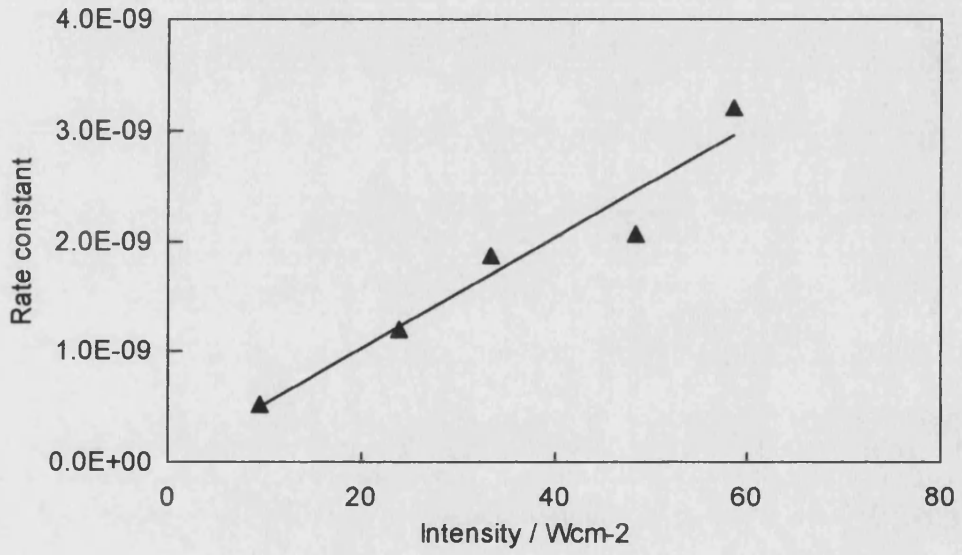

Figure 3.18 - Variation in Schmid rate constant with ultrasonic intensity for the degradation of PDMS in D_4

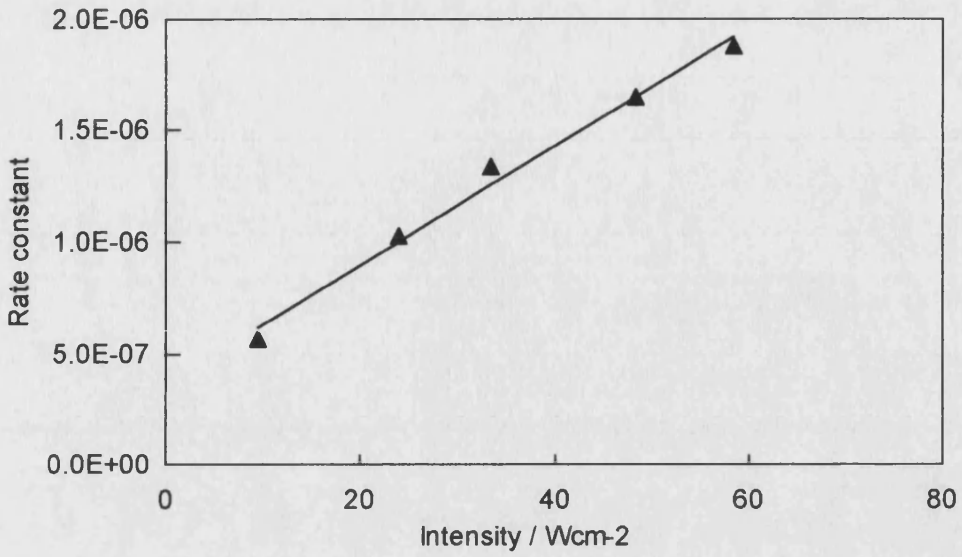

Figure 3.19 - Variation in Ovenall rate constant with ultrasonic intensity for the degradation of PDMS in D_4

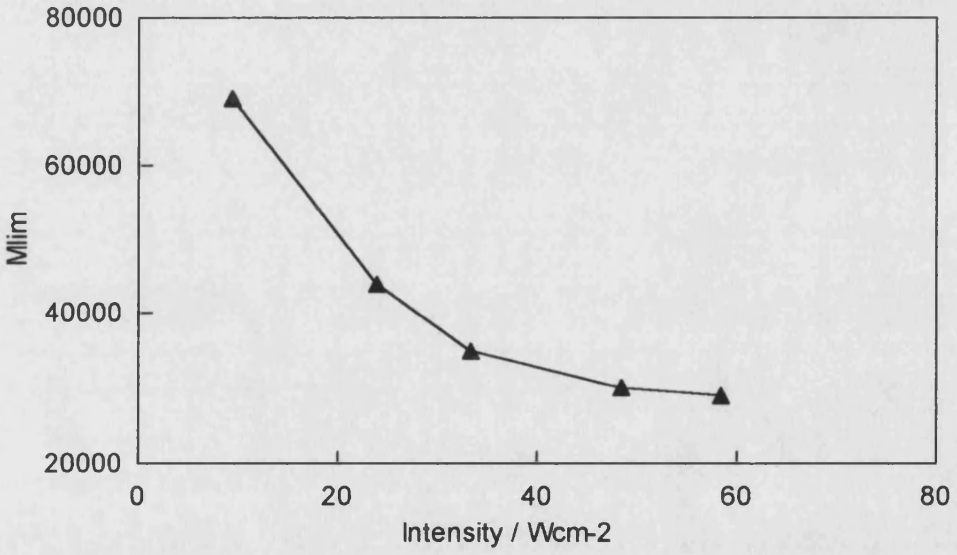

Figure 3.20 - Variation in M_{lim} with ultrasonic intensity for the degradation of PDMS in D_4

3.2.2 Effect of Changing Temperature

Figure 3.21 shows the change in M_n for 1 % w/v solutions of PDMS in D_4 sonicated at 33.4 Wcm^{-2} and at temperatures of 40, 60 , 80 and 100°C.

As with the PDMS/toluene solutions, increasing the temperature at which the sonication is conducted, results in a decrease in the rate of degradation and an increase in the value of M_{lim}.

Figures 3.22 and 3.23 show the Schmid and Ovenall kinetic plots obtained from the degradation data.. Table 3.5 gives the rate constants determined from the Schmid and Ovenall plots.

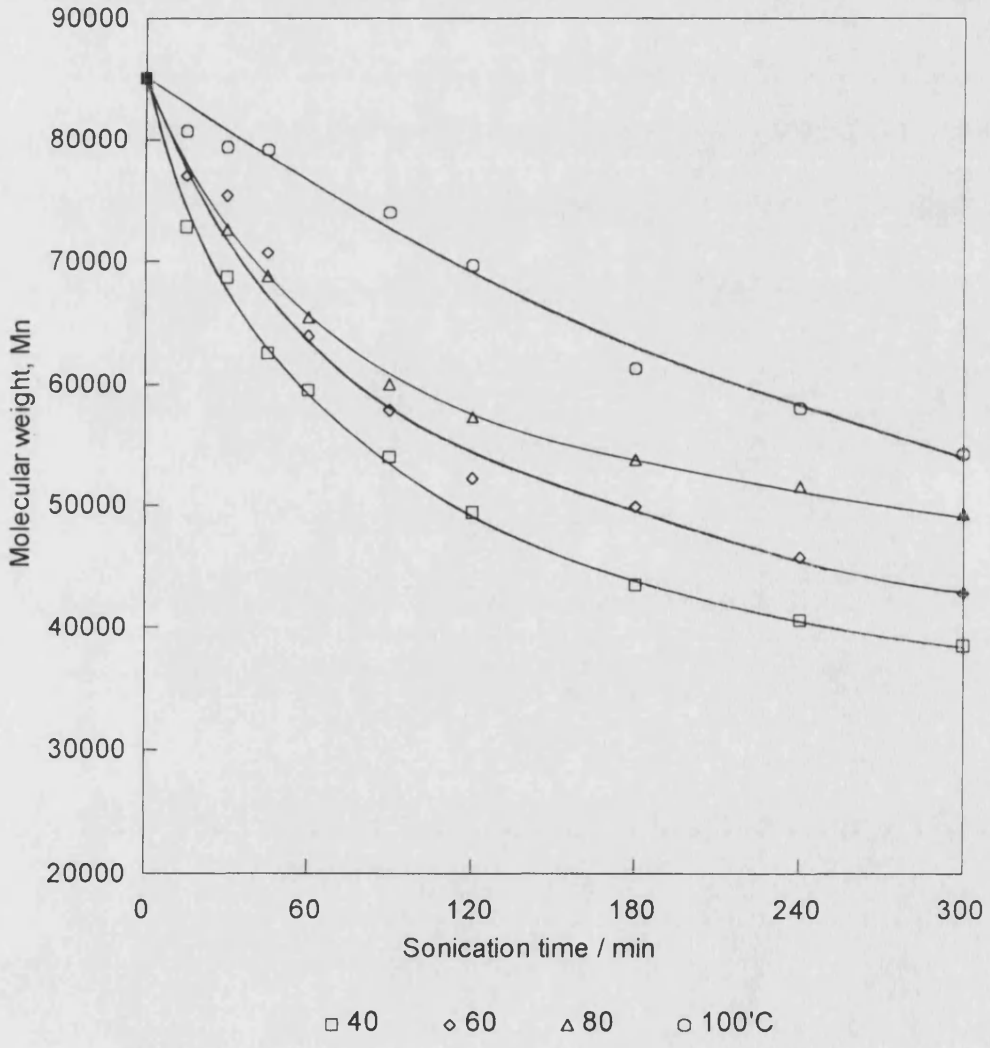

Figure 3.21 - Effect of solution temperature on molecular weight during degradation of PDMS in D_4

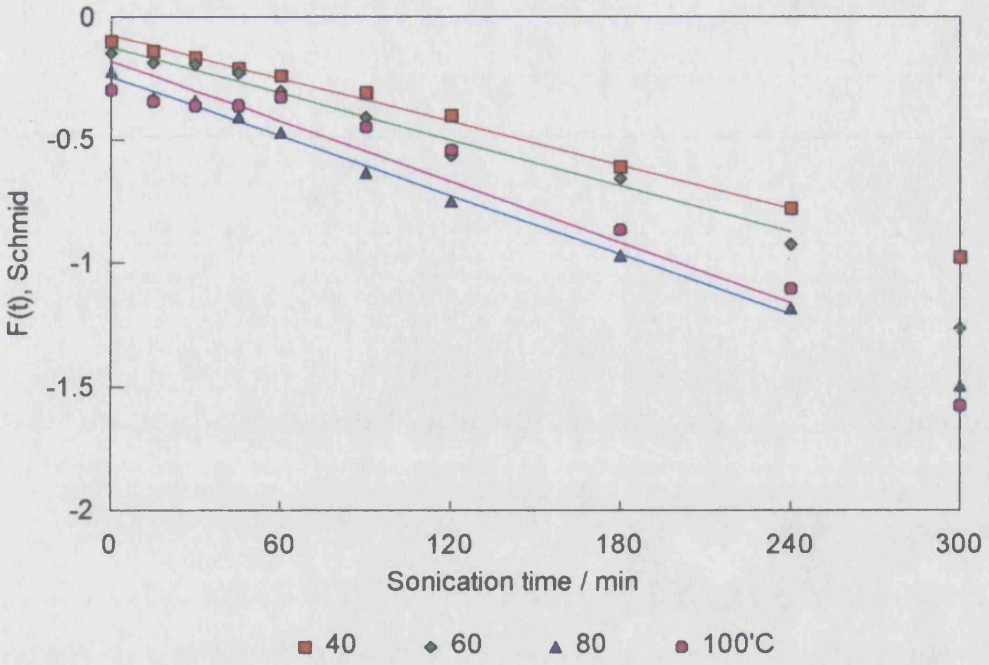

Figure 3.22 - Schmid kinetic plot for the degradation of PDMS in D_4 at different solution temperatures

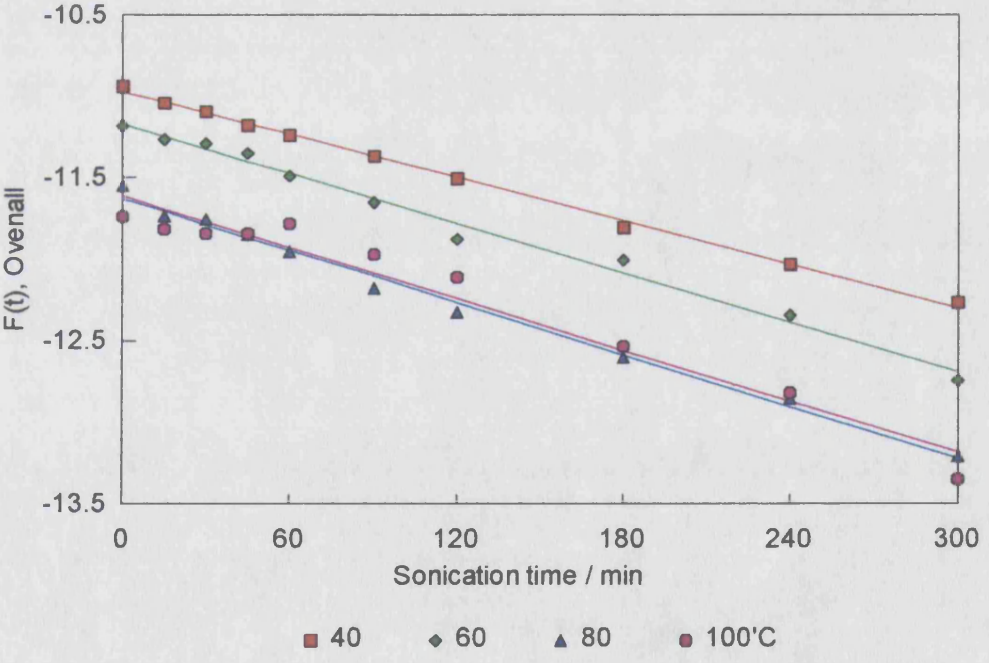

Figure 3.23 - Ovenall kinetic plot for the degradation of PDMS in D_4 at different solution temperatures

Table 3.5 - M_{lim} and Schmid and Ovenall rate constants for the degradation of PDMS in D4 at different temperatures

Temp. (°C)	Schmid ($moldm^{-3}min^{-1}$)	Ovenall ($moldm^{-3}min^{-1}$)	M_{lim}
40	1.873×10^{-9}	1.335×10^{-6}	35 000
60	1.480×10^{-9}	1.301×10^{-6}	40 000
80	1.348×10^{-9}	1.179×10^{-6}	49 000
100	1.164×10^{-9}	1.046×10^{-6}	52 000

As the temperature of the solution increases M_{lim} increases and both the Schmid and Ovenall rate constants decrease, reflecting the trend seen in the degradation curves, and the results for the degradation in toluene. As stated previously, this effect is a result of the increase in vapour pressure at higher temperatures, reducing the severity of the bubble collapse, and therefore the extent of degradation.

Arrhenius Analysis

Arrhenius analysis of the rate constants (figure 3.24) again shows a linear relation with apparent activation energies of -7.4 ± 0.8 $kJmol^{-1}$ (Schmid) and -4.0 ± 0.9 $kJmol^{-1}$ (Ovenall). These apparent activation energies are close to those determined for PDMS in toluene, indeed, those calculated using the Ovenall rate constants are the same within uncertainty.

As the effect of temperature can be related to the vapour present in the cavitation bubble, it is informative to consider the enthalpies of vapourisation (ΔH_{vap}) of D_4 and toluene. Clearly, the lower the enthalpy of vapourisation of a solvent, the higher the volatility. More vapour will then enter the bubble and the rate of degradation will be reduced for solvents with a high volatility. ΔH_{vap} for toulene[136] is 38.3 $kJmol^{-1}$, while for D_4[31] it is 36.8 $kJmol^{-1}$. These values are remarkably similar, so the effect on cavitation, and therefore degradation, can also be expected to be similar and this is manifested in the apparent activation energies.

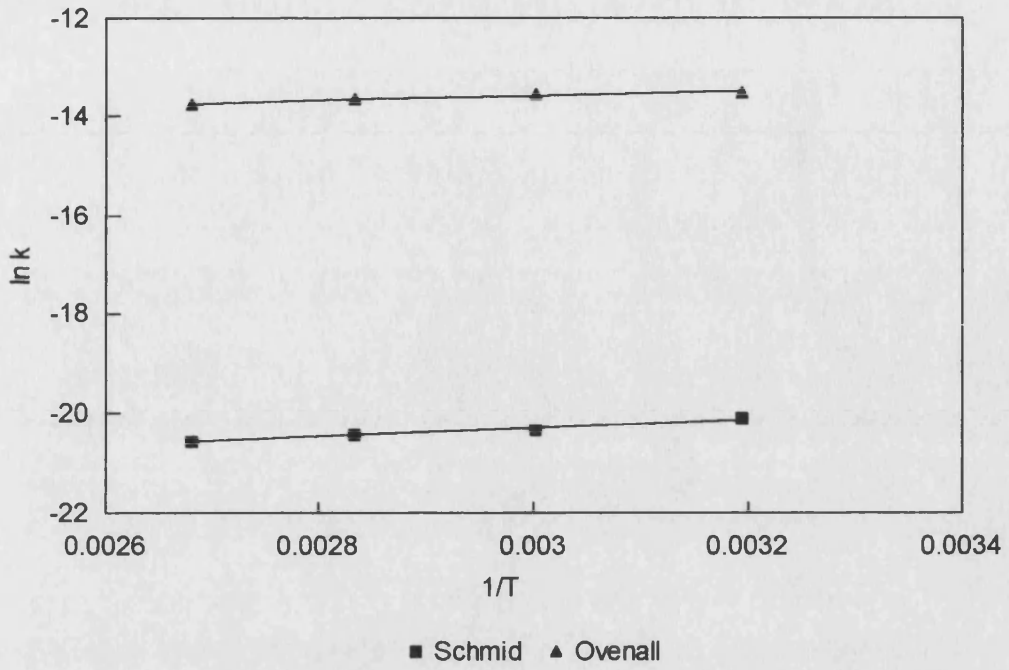

Figure 3.24 - Arrhenius analysis of the Schmid and Ovenall rate constants for the degradation of PDMS in D_4 at different solution temperatures

3.2.3 Effect of Changing Concentration

Figure 3.25 shows the effect of changing the concentration of the solutions of PDMS in D_4, from 1 % w/v to 20 % w/v, when sonicated at 40°C and 33.4 Wcm^{-2}.

As with the PDMS in toluene solutions, increasing the concentration of the solution results in an increase in viscosity, with a subsequent decrease in the rate of degradation and an increase in M_{lim}. Again, increasing the concentration from 1 to 5 % has the most pronounced effect on the rate of degradation. There is little difference between the degradations at 10 and 20 %. As seen before, some scatter is apparent at the higher concentrations due to inefficient mixing.

The Schmid and Ovenall plots obtained from the data are shown in figures 3.26 and 3.27, while the rate constants determined for each degradation are shown in table 3.6.

As before, increasing the concentration has resulted in an increase in the Schmid and Ovenall rate constants, even though the rate of degradation is clearly decreasing. Again, for this situation, because of the dominant effect the concentration

term in the equations, it is more informative to see how the term, k/c, changes with concentration, as opposed to k. Figure 3.28 shows the plot of k/c against concentration.

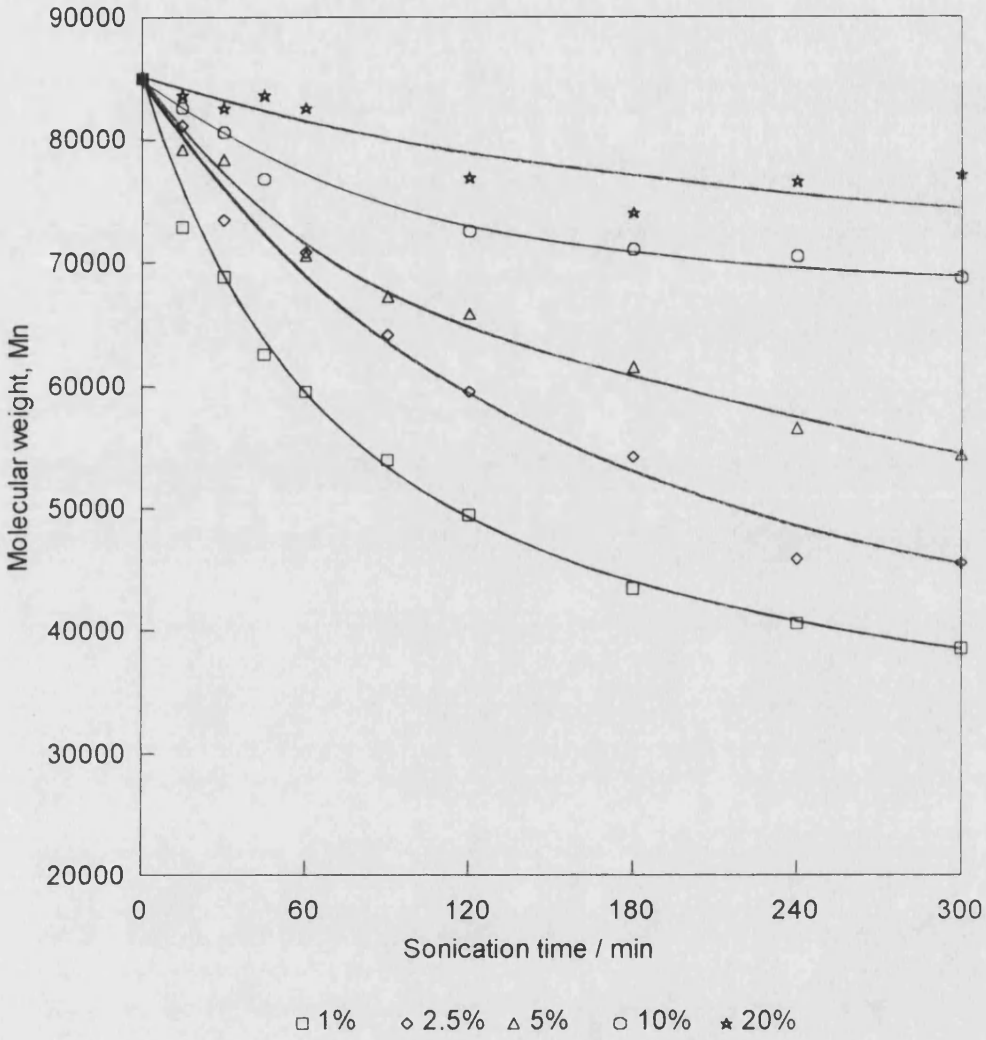

Figure 3.25 - Effect of solution concentration on molecular weight during degradation of PDMS in D_4

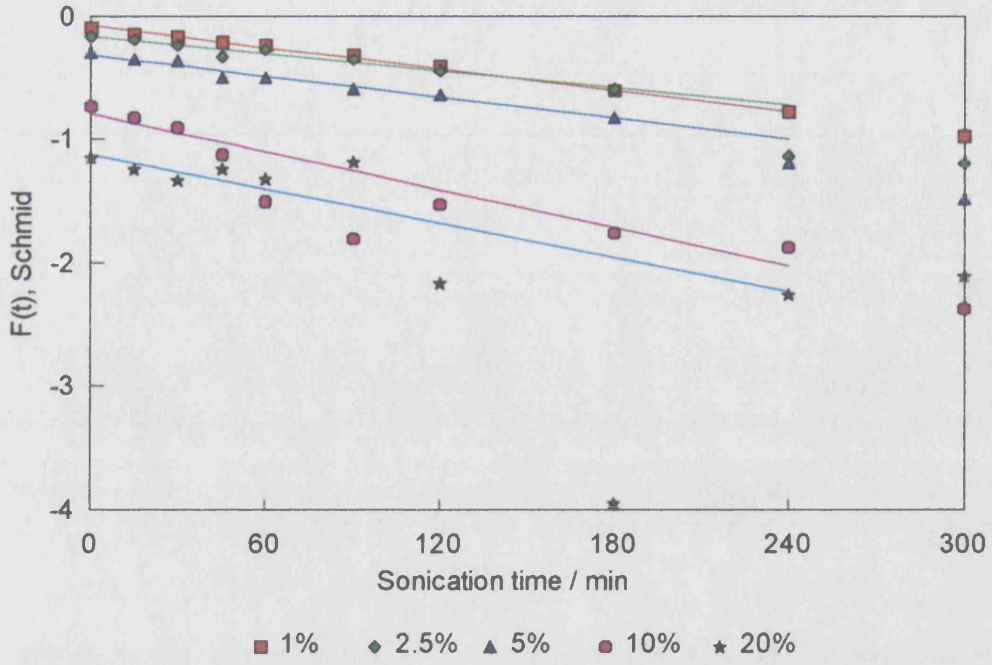

Figure 3.26 - Schmid kinetic plot for the degradation of PDMS in D_4 at different solution concentrations

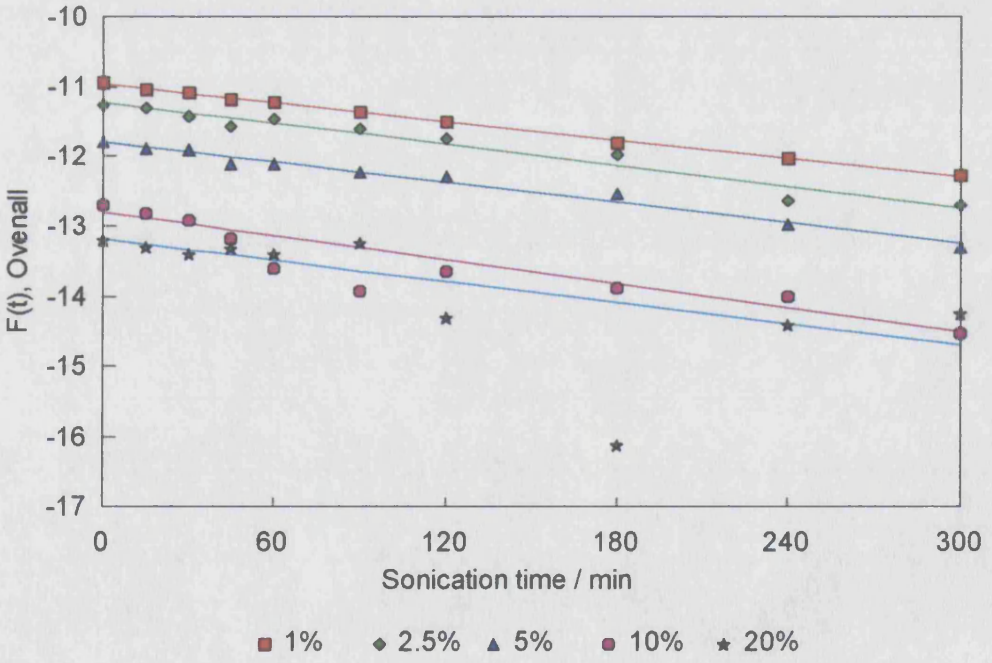

Figure 3.27 - Ovenall kinetic plot for the degradation of PDMS in D_4 at different solution concentrations

Table 3.6 - M_{lim} and Schmid and Ovenall rate constants for the degradation of PDMS in D_4 at different concentrations

Conc. (% w/v)	Schmid ($moldm^{-3}min^{-1}$)	Ovenall ($moldm^{-3}min^{-1}$)	M_{lim}
1	1.873×10^{-9}	1.335×10^{-6}	35 000
2.5	2.449×10^{-9}	2.998×10^{-6}	42 000
5	3.527×10^{-9}	4.399×10^{-6}	55 000
10	7.167×10^{-9}	7.858×10^{-6}	73 000
20	12.972×10^{-9}	13.794×10^{-6}	73 000

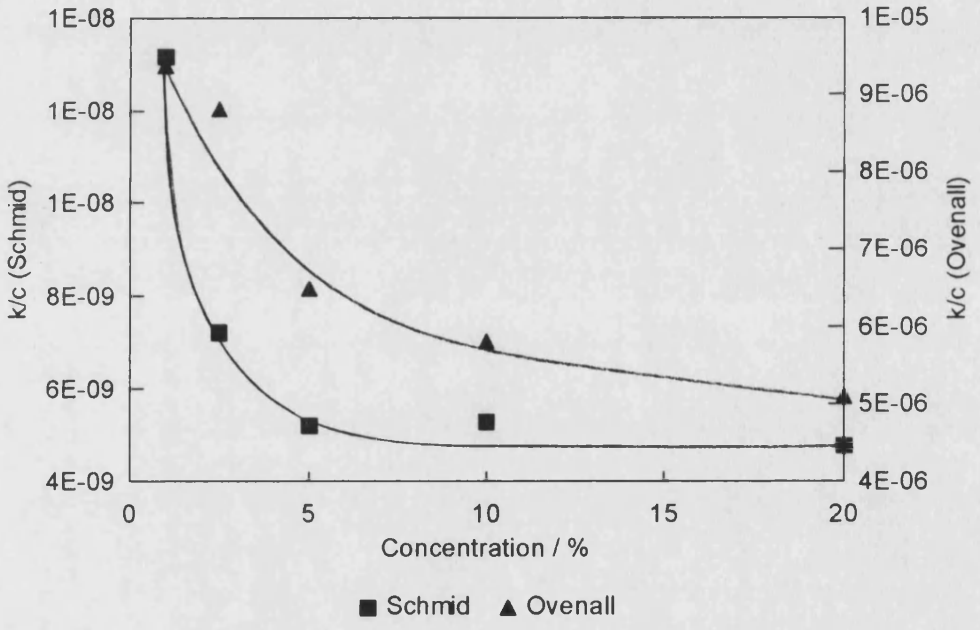

Figure 3.28 - Change in k/c with concentration for Schmid and Ovenall kinetic analysis

The plot of k/c clearly reflects the trends seen in the degradation plot, i.e. increasing the concentration results in a slower degradation, with the largest effects occurring on increasing the concentration up to 5 %. Increasing the concentration beyond this does not have such a marked effect and, as before, this can be attributed to the polymer chains overlapping above concentrations of 5 %.

3.2.4 Variation in the PDMS/D_4 Equilibrium During Sonication

When using D_4 as a solvent, it was assumed that it was not affected by the ultrasound, other than being the medium in which cavitation is occurring. The results for the degradations in D_4 are qualitatively similar to those obtained in toluene and would seem to support this assumption. However, in order to determine whether there was any change in the equilibrium between D_4 and PDMS during degradation, a 5 % solution of PDMS in D_4 was sonicated for 7 hours at a temperature of 45°C and an intensity of 33.4 Wcm^{-2}. Samples were extracted at regular intervals and analysed using the HPLC to determine the relative proportions of D_4 and PDMS. Figure 3.29 shows the proportions of D_4 and PDMS during the sonication.

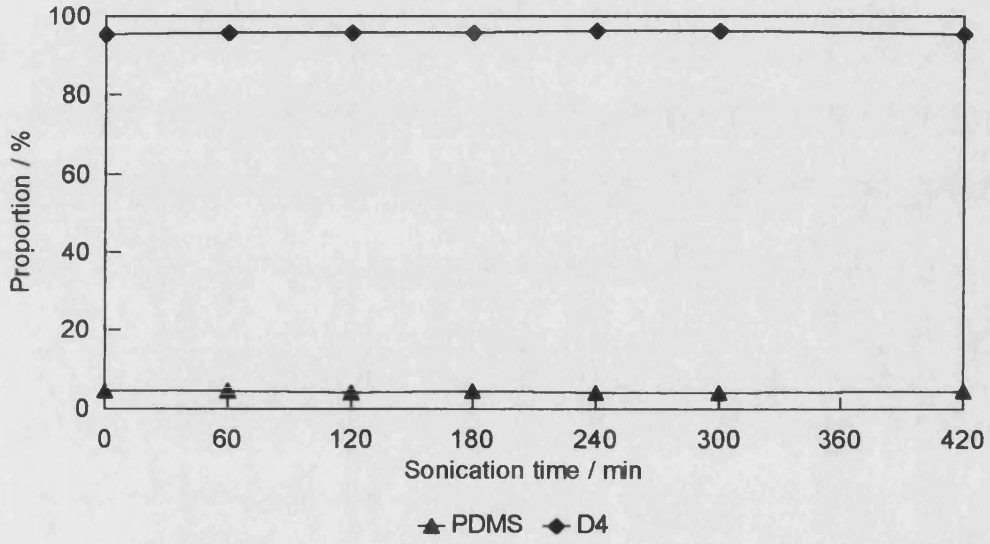

Figure 3.29 - Proportion of PDMS and D4 during sonication of a 5 % solution

It is clear from this that there was no change in the ratio of PDMS to D_4 during the sonication.

To further check this assumption, 100 cm^3 of D_4 was sonicated at an intensity of 33.4 Wcm^{-2}, at 40°C for 5 hours. Gel permeation chromatograms of samples before (figure 3.30) and after (figure 3.31) sonication were identical and showed no signs of the ultrasound having caused any change to the D_4 during the sonication.

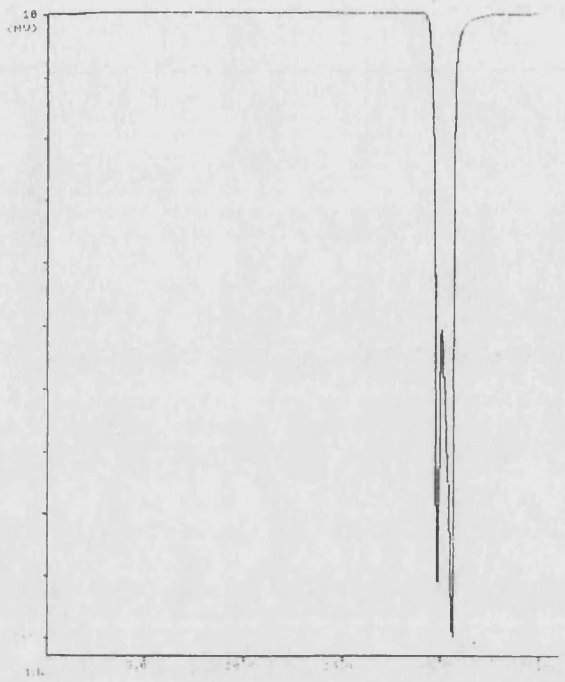

Figure 3.30 - GPC chromatogram of D_4 before sonication

Figure 3.31 - GPC chromatogram of D_4 after sonication

3.3 Conclusions

The collapse of cavitation bubbles, formed when an ultrasonic wave propagates through a polymer solution, causes the polymer molecules to be cleaved resulting in a lowering of the molecular weight and a narrowing of the polydispersity. The rate of degradation, and the extent to which the polymer molecules are degraded, can be controlled by consideration of the experimental conditions. The Schmid and Ovenall kinetic models provide a useful tool to quantify the degradation rate and allow comparisons between degradations to be made.

Increasing the ultrasonic intensity results in an increase in the rate of degradation. For both toluene and D_4, a linear relationship between rate constant and intensity was found. Some workers[106] have found that there is a maximum intensity, above which increasing the intensity still further will cause the rate of degradation to begin to decrease. However, this effect was not observed under these conditions, although this is probably due to the range of intensities used in this study being lower.

With regard to M_{lim}, some workers[134] have proposed that it should be independent of intensity, while others[106] have found that it decreases linearly as intensity increases. The results from this study lie between these two extremes. M_{lim} was found to decrease as intensity increased, but it tended towards a limiting value, suggesting that there is a lower limit for M_{lim}, below which increasing the intensity further will have no effect.

Increasing the temperature of the solution decreases the rate of degradation as a result of increased vapour in the cavitation bubbles cushioning the collapse. Apparent activation energies were negative for both toluene and D_4, a result that has also been shown to occur for the degradation of polystyrene in toluene[106]. This reflects the fact that degradation is a mechanical effect as a result of cavitation.

Increasing the concentration of the solutions results in a decrease in the rate of degradation and an increase in M_{lim}. The greatest effects were observed for concentrations up to 5 %. Above this, the polymer chains begin to overlap, and increasing the concentration further does not have such a marked effect on the degradation. Using the Schmid and Ovenall rate models, it has been found that it is more appropriate to use the term k/c as opposed to just the rate constant, k, when comparing degradations at different concentrations.

The degradation of PDMS occurs just as well in D_4 as in toluene, This can attributed to the fact the enthalpies of vapourisation of both liquids are very similar, so their effect on cavitation, and therefore degradation, will also be similar.

Although three parameters, using two solvents, have been studied in this work, a number of other experimental parameters remain to be investigated. As only two solvents were used, the effect of changing the solvent needs to be investigated more thoroughly. In particular, using solvents with a higher and lower ΔH_{vap} than either toluene or D_4 to determine if there is a relationship between ΔH_{vap} and the rate of degradation.

Other parameters that have not been studied here but require investigation are the effect of dissolved gases on the degradation, and the effect of changing the frequency of the ultrasound.

These results show that the manipulation of the experimental conditions allows the degradation, and therefore the molecular weight, of PDMS to be closely controlled. The fact that the degradation occurs equally as well in D_4 as in toluene has implications for the polymerisations conducted under ultrasound. If the conditions are favourable (e.g. low concentration, low temperature) degradation processes may well occur concurrently with the polymerisation. The change in molecular weight during polymerisation may then be different for the ultrasonic polymerisations compared with the silent polymerisations.

Chapter 4

Determination of the Nature of the Chain-End During the Degradation of PDMS

4 DETERMINATION OF THE NATURE OF THE CHAIN-END DURING THE DEGRADATION OF PDMS

When a polymer undergoes ultrasonic degradation, bonds are cleaved. The bond cleavage can either be homolytic, resulting in the formation of free radicals, or heterolytic, giving rise to ions. Polymers with a C-C backbone have been shown to cleave homolytically, and the free radicals produced have been detected and used in further reactions (section 1.16).

The Si-O bond of PDMS is polar, and it has been suggested that the bond cleaves heterolytically to give ions. Thomas and de Vries[119] provided evidence for this view when they sonicated PDMS in the presence of ^{14}C-labelled methanol and found that it was incorporated into the polymer. Methanol is a strong nucleophile and they suggested that it reacted the ions formed when PDMS was ultrasonically degraded.

This work was therefore directed at trying determine if the PDMS chains do indeed cleave heterolytically during ultrasonic degradation. PDMS was initially sonicated in the presence of a radical trap to determine if radicals are produced on sonication. An attempt was then made to try and positively identify heterolytic cleavage by using ion traps.

4.1 A Radical Trap - DPPH

The radical trap 2,2-diphenylpicrylhydrazyl (DPPH) was used to determine the rate of production of radicals during sonication of the following solutions: THF, poly(isobutylene) (PIB) in THF, and PDMS in THF. DPPH is a stable free radical with a strong absorbance at 520 nm. This absorbance will decrease as the DPPH molecules react with any radicals present in the solution. Thus, the rate of radical production can be followed by UV/Vis spectroscopy.

4.1.1 The Beer-Lambert law

The absorbance of a solution is related to the concentration of the absorbing species by the Beer-Lambert law:

$$A = \varepsilon c l \qquad (17)$$

where A is the absorbance of the solution, ε is the molar absorption coefficient (equal to 970 $m^2 mol^{-1}$ for DPPH in THF [138]), c is the concentration of the species (i.e. DPPH)

in solution, and l is the path length of the cell used in the spectrophotometer (1 cm). As the absorbance of the solution, the path length and the molar absorption coefficient are known, the concentration can be determined.

Plotting concentration against sonication time therefore allows the rate of consumption of DPPH to be determined. As DPPH only reacts with radicals, this will therefore be equal to the rate of production of radicals in the solution.

4.1.2 Rate of Radical Production

The three solutions sonicated were:

i. 10^{-4} M solution of DPPH in THF
ii. 10^{-4} M solution of DPPH in a 0.5 % w/v solution of PIB in THF.
iii. 10^{-4} M solution of DPPH in a 0.5 % w/v solution of PDMS in THF.

The solutions were sonicated for fifteen minutes at an intensity of 31.6 Wcm^{-2} and a temperature of 25°C. The absorbance of the solution was measured every three minutes. The concentration was then determined and a graph of concentration against time plotted to determine the rate of radical production.

Figure 4.1 shows the plot of concentration against time for each of the three different solutions. It is clear from this plot that the decrease in absorbance for the PIB solution is much faster than for the THF 'blank' and the PDMS solution. Linear regression of each set of data allows the rate of radical production to be determined. These results are listed in table 4.1.

Table 4.1- The rate of radical production for each solution

Solution	THF	PIB/THF	PDMS/THF
Slope	-4.07×10^{-7}	-3.52×10^{-6}	-3.60×10^{-7}
Rate of radical production (mol dm^{-3} min^{-1})	$4.07 \pm 0.57 \times 10^{-7}$	$3.52 \pm 0.40 \times 10^{-6}$	$3.60 \pm 0.56 \times 10^{-7}$

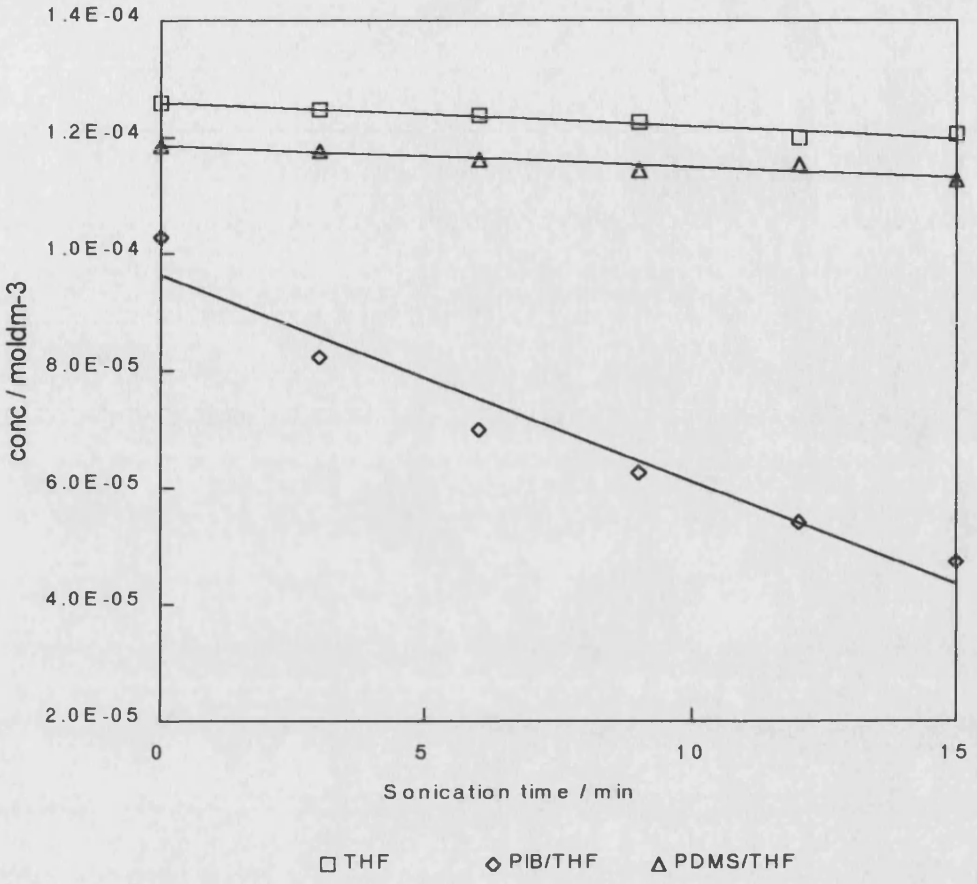

Figure 4.1 - Concentration of DPPH during sonication of three solutions

As can be seen, the rate of radical production in the PDMS/THF solution is identical (within experimental error) to the rate of radical production in THF alone. This would imply that in the PDMS/THF solution, only THF is contributing to the radical production during sonication, i.e. the cleavage of the PDMS molecules does not result in radicals being formed at the chain-ends. This is feasible considering the nature of the Si-O bond: the Si-O bond is polar, with a δ- on the more electronegative oxygen, and a δ+ on the silicon. Hence when the bond is broken, there is a tendency for the electrons to associate with the oxygen resulting in heterolytic cleavage.

In the PIB/THF solution, however, the rate of radical production is an order of magnitude greater than in THF. Therefore, radicals must be being produced from the cleavage of the PIB molecules to account for this increase in rate. The cleavage of the PIB molecules must therefore be homolytic, i.e. radicals will be produced at the

chain-ends when the molecules are cleaved. This would be expected as the C-C bonds in polymers are not polar, and therefore the two carbon atoms will each take one electron from the bond when the bond breaks, forming the chain-end radicals.

These results indicate that while PIB will cleave homolytically to produce radicals, PDMS does not. The radical nature of the chain-end of C-C polymers undergoing degradation has been proven by other workers and is regarded as one of the characteristic features of the ultrasonic degradation of C-C polymers[24]. However, this experiment has shown that PDMS does not produce radicals when degraded. This confirms the result of Thomas and De Vries[119] who also found that no reaction with DPPH occurred on sonicating with PDMS.

Unfortunately, although this experiment demonstrates that radicals are not produced, it does not give any indication as to whether the chain-ends are ionic in nature. Hence, further experiments attempted to trap the ionic chain-ends, in an analogous way to DPPH trapping the radical chain-ends.

4.2 Use of Ion Traps

In an attempt to trap the ionic chain-ends, should they form when PDMS undergoes ultrasonic degradation, two species were used; tetrabutylammonium fluoride (TBAF) and lithium fluoride. Both these compounds contain the fluoride anion, hence assuming that the Si-O bond breaks to form Si^+ and O^- at the chain-ends, the F^- would combine with the Si^+ ended chain and the resulting fluorine-terminated chain could then be detected by ^{19}F NMR.

4.2.1 TBAF

TBAF is THF soluble and was used as a 1 M solution in THF. 1 cm^3 of the TBAF solution was added to 99 cm^3 of a 1 % w/v solution of PDMS in THF and sonicated for 3 hours at 31.6 Wcm^{-2} and 25°C under nitrogen. After sonication an attempt was made to recover the polymer by precipitation into ice-cold methanol, and then removing the solvent by heating under vacuum.

As 1.0 g of polymer was originally used (in 100 cm^3 of solution), a substantial proportion should have been recovered. However, no polymer was recovered. Evaporation left behind a virtually empty vessel. The experiment was repeated, this

time using a larger amount of PDMS (2.5 g), however, the same result was obtained. No polymer was recovered after PDMS had been sonicated with TBAF.

This result can be explained by considering what happens to the chains once they have been cleaved in the presence of TBAF. If Si^+ and O^- ions are produced when sonicated, they will react very quickly. If TBAF is present, the Si^+ will become associated with the fluoride ion to form a Si-F bond. The O^- formed will actually be a silanolate anion, with the tetrabutylammonium cation being its counter-ion. The reactivity of a silanolate is dependent on its counter-ion (section 1.9.3, ref. 43) and quaternary ammonium silanolates are very reactive. They are usually used in the polymerisation of D_4, however there is no D_4 present, only polymer. Thus, once formed the silanolate will begin to 'back-bite' (section 1.9.5) causing the 'unzipping' of the polymer chain, i.e. the chain is broken up by a series of reactions into cyclic species (mostly D_4, although other cyclics will be present but in a smaller proportion) and hence no polymer is recovered.

4.2.2 Lithium Fluoride

Further attempts to trap the chain-end species were made using lithium fluoride. 0.5 g of LiF was dissolved in 100 cm^3 of a 2 % solution of PDMS in THF (the solubility of LiF in THF is 0.6 gcm^{-3} [139]). This was sonicated for 5 hours at 33.4 Wcm^{-2} and 30°C. The THF was removed at 55°C under vacuum, and the resulting material redissolved in chloroform. The solution was filtered to remove any particulate matter, before the chloroform was removed at 55°C under vacuum. In addition, a solution of PDMS/LiF in THF (as above) was refluxed for 5 hours and the resulting polymer recovered. Also, an analogous experiment was conducted whereby a 2 % PIB in THF solution was sonicated in the presence of LiF, in the same manner as described above. All three polymer samples were recovered and then analysed by ^{19}F NMR. In addition, the two PDMS samples were also analysed by ^{29}Si NMR.

The spectrum obtained from the ^{19}F NMR analysis for the sonicated PDMS solution is shown in figure 4.2.

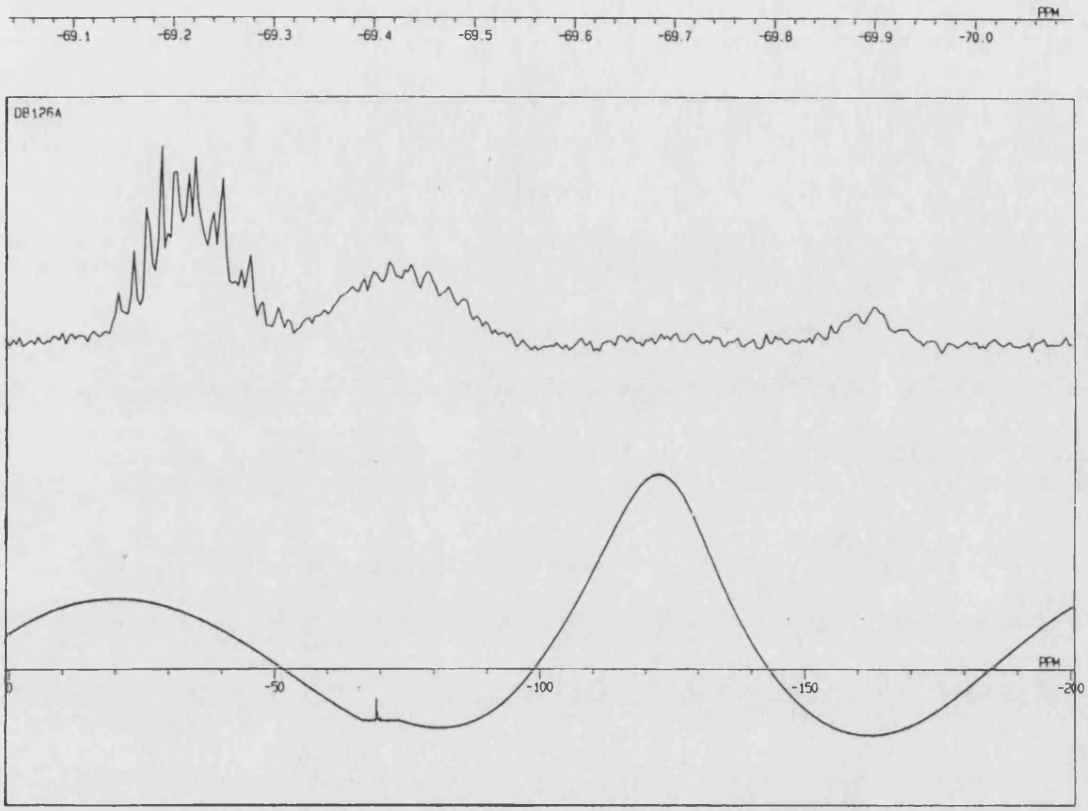

Figure 4.2 - ^{19}F NMR spectrum of PDMS sonicated with LiF

The baseline from 0 to -200 ppm is very curved, although a multiplet is visible at approximately -69 ppm. This is extremely small however, and it was not possible to perform any data reduction. ^{19}F NMR analysis on the PDMS that had been refluxed, and the PIB that had been sonicated, failed to detect the presence of any fluorine in the samples.

It is clear that there is fluorine present in the PDMS sample that had been sonicated. It is possible that this is due to the presence of residual LiF, or fluorine containing species not removed before analysis. However, if this were the case it would be expected that the two other solutions, which were handled in an identical manner, would also contain the same species and would have given rise to similar spectra. The fact that they did not implies that there is a good possibility that the Si^+ chain-ends have indeed been trapped by the F^-. Unfortunately, there are scant literature references detailing ^{19}F NMR chemical shifts for the fluorine atom in $-OSiMe_2F$ containing molecules, although a number of workers have determined the shift for

-$SiMe_2F$ containing molecules. Damrauer et al[152] found the chemical shift for the fluorine in $(C_6H_5)CH_2SiMe_2F$ to be −160.12, while for $(Me_3Si)_2C(SiEt_2Cl)(SiMe_2F)$, Eaborn et al[153] obtained a chemical shift of −144.7 ppm. The value obtained for the sonicated sample is therefore ~ 80 ppm down field of these values.

^{19}F NMR has substantially larger chemical shifts than proton NMR (~ 40 times), with the range of recorded ^{19}F shifts spanning 1300 ppm[140]. The chemical shift of the fluorine atom is also very sensitive to changes in molecular structure, as evidenced above by the 15 ppm difference in shift, even though the immediate fluorine environments (-$SiMe_2F$) are the same. It would not therefore be surprising if the chemical shift altered by 80 ppm, by changing the environment from -$SiMe_2F$, to -$OSiMe_2F$. However, this is not definitive proof that the multiplet seen in the spectrum is due to Si-F formed after ultrasonic cleavage. The ^{19}F NMR data does not, therefore, give conclusive evidence for the generation of Si-F from the heterolytic cleavage of the siloxane bond. Substantially more convincing evidence for heterolytic cleavage is obtained from the ^{29}Si NMR of the samples.

The ^{29}Si NMR spectra of the two PDMS samples are shown in figures 4.3 (sonicated PDMS) and 4.4 (refluxed PDMS).

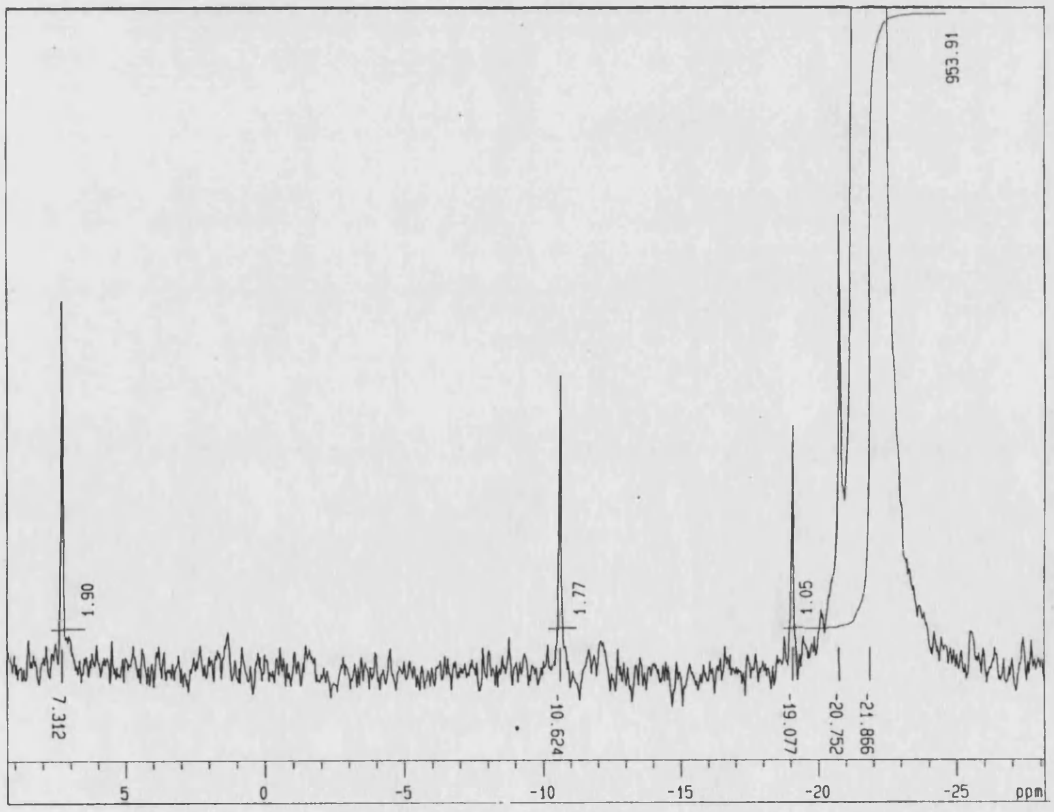

Figure 4.3 - ^{29}Si NMR spectrum of PDMS sonicated with LiF

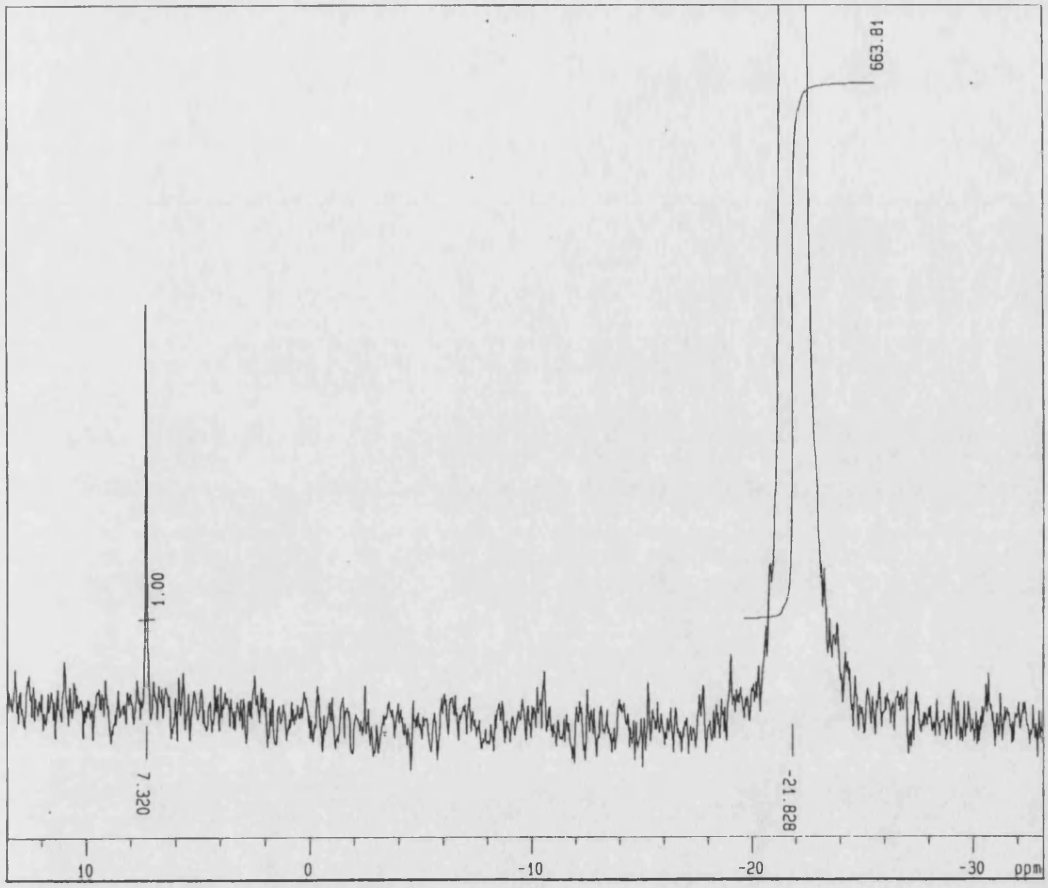

Figure 4.4 - ^{29}Si NMR spectrum of PDMS refluxed with LiF

The 'D' units of the polymer chain are obvious at -21.9 ppm. The singlet at +7.3 ppm is due to the trimethyl-end group ('M') on the chains. Both spectra therefore show the repeat unit and the end groups of the polymer. In addition, however, there are two singlets present in the spectrum of the sonicated PDMS that are absent in the spectrum of the refluxed PDMS. The singlet at -10.6 ppm can be attributed to silanol (SiOH) end groups. These could have formed as a result of the presence of water in the THF, the cleaved PDMS chains reacting with the water to generate the silanol group. This is further evidence supporting heterolytic cleavage and the formation of ions at the chain-ends.

The singlet at -19.1 ppm is characteristic of D_4. For D_4 to have formed during the sonication of the PDMS/LiF solution, the silanolate is required. If the PDMS chains are being degraded to give Si^+ and O^- chain-ends, the F^- will react with the Si^+ formed, while the Li^+ becomes the counter-ion to the silanolate anion. Once formed, the silanolate can back-bite to form D_4, however, as stated before, the activity of the silanolate is dependent on its counter-ion, and lithium silanolate is not very reactive

(section 1.9.3, ref. 43). Hence, the back-biting only happens slowly and only a small amount of D_4 (as seen) is formed.

Missing from the ^{29}Si NMR spectrum of the sonicated PDMS, however, is any peak associated with Si-F. If the ^{19}F NMR detected any fluorine and if it was as Si-F, then we would expect to see a corresponding peak in the ^{29}Si NMR. It is possible that the peak seen in the ^{19}F NMR spectrum is a result of residual HF formed, given that there is some water present (as seen by the formation of the silanol groups). However, the chemical shift of HF in ^{19}F NMR is usually in the approximate range of -150 to -210 ppm, not at -69 ppm[140]. A more likely explanation is that the actual amount of SiF that formed is just too small to be visible above the baseline. ^{19}F has a natural abundance of 100 % yet gave an extremely small multiplet in the spectrum. As ^{29}Si has a natural abundance of only 4.7 % [31] the size of the signal in the ^{29}Si spectrum would be so small that it would be swamped by the background noise. This can be illustrated by considering the number of chain breaks that would occur during the sonication.

From the degradation experiments, the molecular weight of PDMS, sonicated as a 2 % solution at 33.4 Wcm^{-2} and 30°C for 5 hours, would be expected to fall from ~ 85 000 to ~ 40 000. The number of chain breaks per chain can therefore be determined from,

$$\text{number of chain breaks} = \frac{M_{n\,(t=0)}}{M_{n\,(t=t)}} - 1 \qquad (18)$$

This gives an average of 1.1 chain breaks per chain during the degradation. As each chain break will only give rise to one Si^+, assuming every Si^+ reacts with an F^-, there will be an average of one F atom per PDMS chain (M_n ~ 40 000). This is already a very small amount, but ^{29}Si is only 4.7 % abundant, thus only 4.7 % of these will give rise to a signal in the ^{29}Si NMR. Hence, the signal will be too weak to be seen above the background noise.

Polymers with a C-C backbone cleave homolytically to give radicals when subjected to an ultrasonic field. The experiment with DPPH proved that this is not the case for PDMS, which has the Si-O backbone. It has been postulated that the chains cleave heterolytically, giving rise to ionic species at the chain-ends which could then undergo further reaction[119]. The evidence collected from the experiments with TBAF

and lithium fluoride would suggest that this is correct and that PDMS does indeed cleave heterolytically.

4.3 Degradation of PDMS in the Presence of Water

In the experiment with lithium fluoride described above, it was noticed that the degradation of the PDMS in THF resulted in the formation of silanol end groups on the polymer chains. This has arisen as a result of the reaction between the cleaved chains and the water present in the THF. To further study this effect a number of further sonications were conducted. Three solutions were prepared: 5 % PDMS in anhydrous THF, PDMS in THF containing 2 % added water, and PDMS in toluene (a much drier solvent than THF). Each solution was sonicated under nitrogen for 5 hours, at 30°C and an intensity of 33.4 Wcm^{-2}. The polymers were recovered and then analysed by FT-IR to determine the silanol concentration. A sample of the starting material was analysed by FT-IR and ^{29}Si NMR (figure 4.5). The polymer recovered from the 'wet' THF was also analysed by ^{29}Si NMR (figure 4.6).

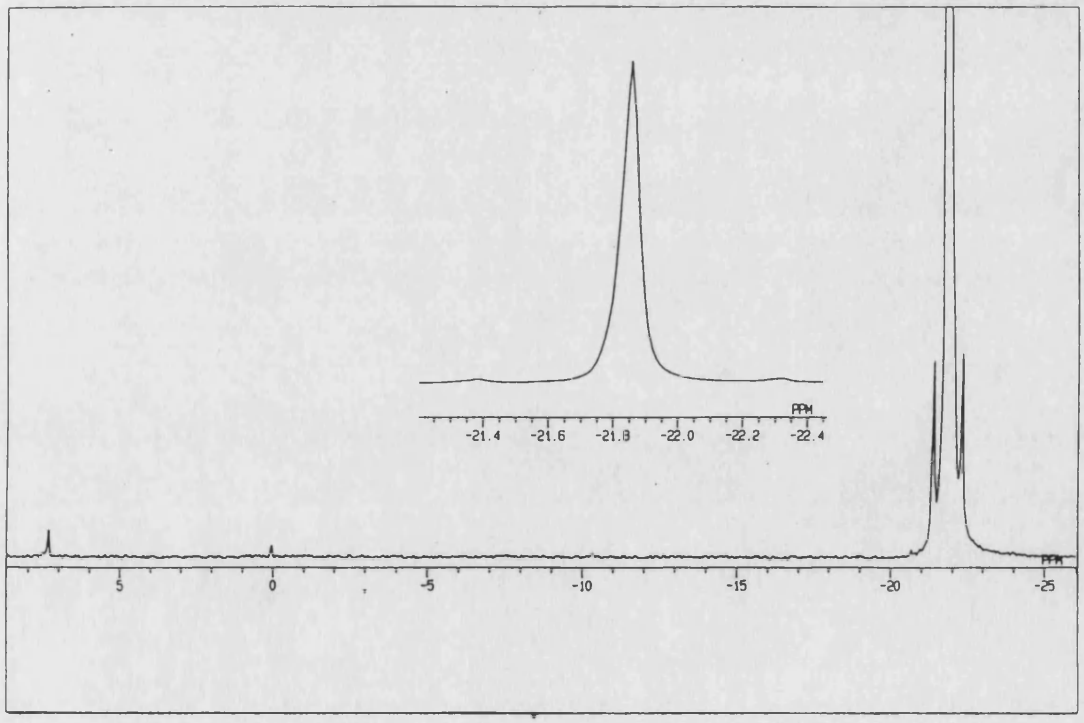

Figure 4.5 - ^{29}Si NMR spectrum of the PDMS before sonication

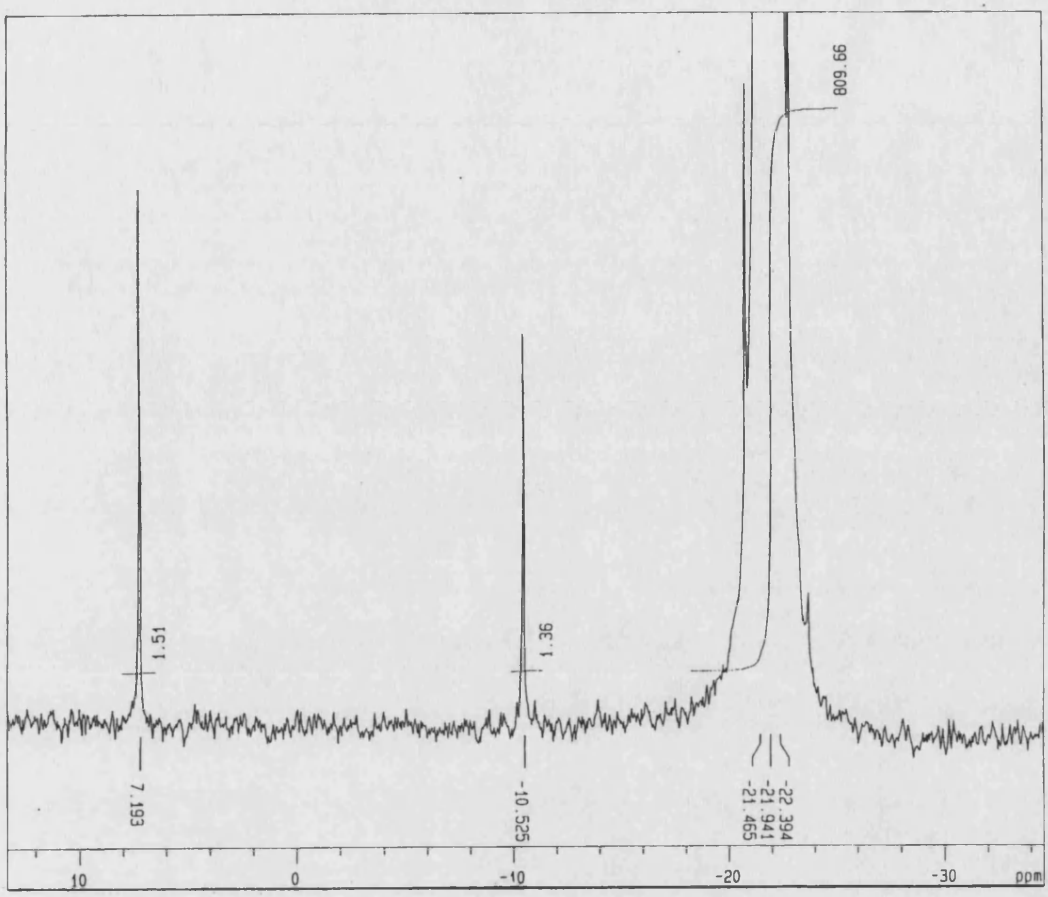

Figure 4.6 - ^{29}Si NMR spectrum of the PDMS after sonication in 'wet' THF

The D repeat unit and the M terminating groups are visible in both spectra at shifts of -21.9 and +7.2 ppm respectively. The subsequent appearance of the silanol at -10.5 ppm after sonication is obvious.

Table 4.2 lists the silanol concentrations of the samples.

Table 4.2 - Concentration of silanol groups in PDMS samples

PDMS sonicated in:	**Silanol conc. (ppm)**
Anhydrous THF	81
THF + water	330
Toluene	95
Starting material	69

These results correlate with the NMR findings. The PDMS sonicated in anhydrous THF and toluene show low silanol concentrations similar to that of the starting material. However, the silanol concentration increases markedly when the PDMS is sonicated in the presence of water.

This is a potentially useful way of preparing silanol groups. Their appearance has only arisen as a result of the PDMS undergoing ultrasonic degradation, with the cleaved polymer chains reacting with the water in the solvent to create the silanol end group. Given the knowledge of the degradation kinetics previously obtained (chapter 3), it is theoretically possible to set the conditions such that each polymer chain will, statistically, only undergo one chain break, before reaching M_{lim}. If the chain can then react with any water present, given that only one end of the chain is able to react, only one end of the chain will be functionalised with a silanol group. The other end will still be trimethyl-terminated. It may also be possible to conduct the sonication with an alcohol, under anhydrous conditions. Thus, when the chain is cleaved, two smaller chains will result with an alkoxy group incorporated onto the end of one chain, and a silanol group on the end of the other.

4.4 Conclusions

The experiment with DPPH has shown that PDMS does not produce radicals when degraded by ultrasound. This confirms the result of Thomas and de Vries[119]. As radicals are not produced the cleavage of the Si-O bond could result in the formation of ions and the results of the sonications with TBAF and LiF support this view. In the case of TBAF, the fact that little polymer was recovered after sonication can be explained by the Si-O bond undergoing heterolytic cleavage. The O^- formed is a very reactive silanolate when the tetrabutylammonium cation is the counter-ion, and this silanolate quickly 'unzips' the polymer via back-biting to leave cyclic oligomers. In the sonication with LiF, the silanolate formed as a result of the cleaved Si-O bond will have a lithium counter-ion. Lithium silanolate is much less reactive than the tetrabutyl-ammonium silanolate, hence back-biting only happens slowly. Thus, after sonication, the polymer contained only a small amount of D_4.

An unexpected result of the LiF sonications was the incorporation of a silanol functionality into the chain. Experiments with 'wet' and anhydrous THF confirm that the silanol arises as a result of the reaction between the cleaved chain-end and the

water present in the solvent. By controlling the degradation, this method offers a technique whereby the polymer chains can be monofunctionally-terminated with silanol, a process that would be very difficult to achieve via traditional synthetic methods.

There is much scope for further work with this technique; to confirm if monofunctional termination is possible by controlling the degradation, and also to see if the method could be used to produce monofunctional polymers with groups other than silanol.

Chapter 5

Synthesis of PDMS

5 SYNTHESIS OF PDMS

After studying the degradation of PDMS under ultrasound, the polymerisation of D_4 was investigated. Both anionic (KOH) and cationic (H_2SO_4) catalysts were used and for both systems, the polymerisations under ultrasound were compared with those under 'silent' (i.e. stirring) conditions.

5.1 Cationic Polymerisations

5.1.1 Silent

The cationic polymerisation of D_4 under silent conditions, using H_2SO_4 as a catalyst, was conducted at 30, 40, 50, 60, 70, 80 and 90°C. Hexamethyldisiloxane ($Me_3SiOSiMe_3$) was employed as an end-blocker to control the molecular weight (M_n) to approximately 35 000. All polymerisations were followed by HPLC allowing the conversion of D_4 to polymer to be monitored. The plot of conversion against time is shown in figure 5.1.

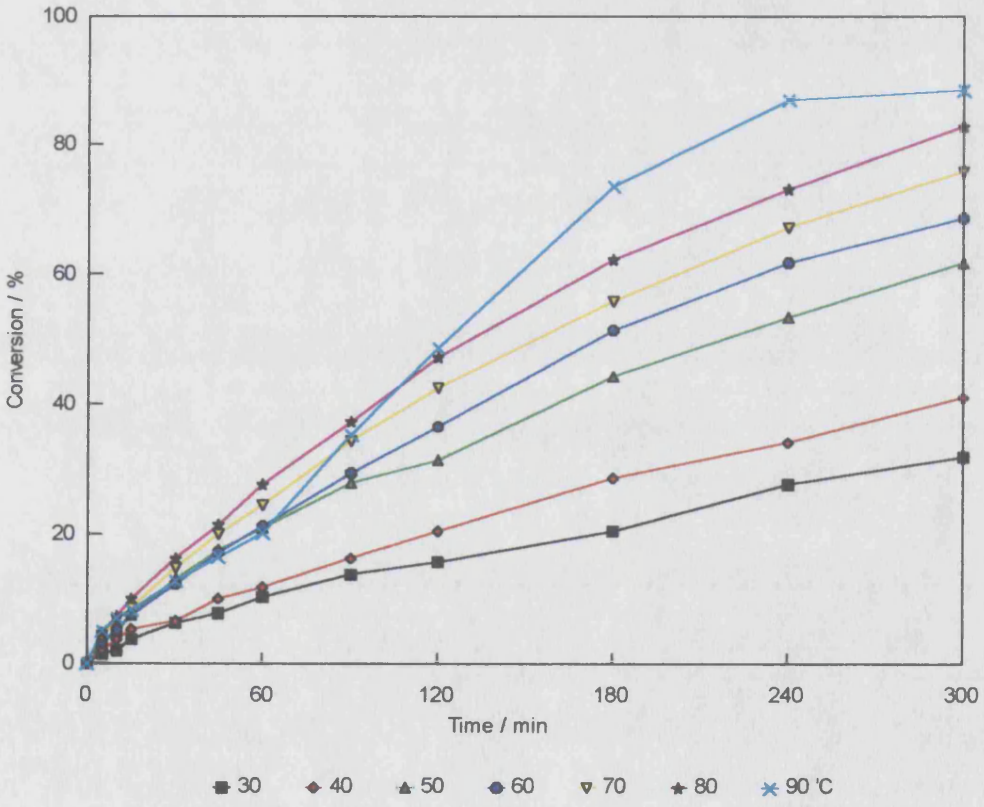

Figure 5.1 - Conversion during silent, cationic polymerisations

As expected, the higher the temperature the faster the polymerisation, although the polymerisation at 90°C is initially slower than expected. The first order rate plots are shown in figure 5.2. A good linear fit is obtained at all temperatures, although at 90°C, the fit is not so good.

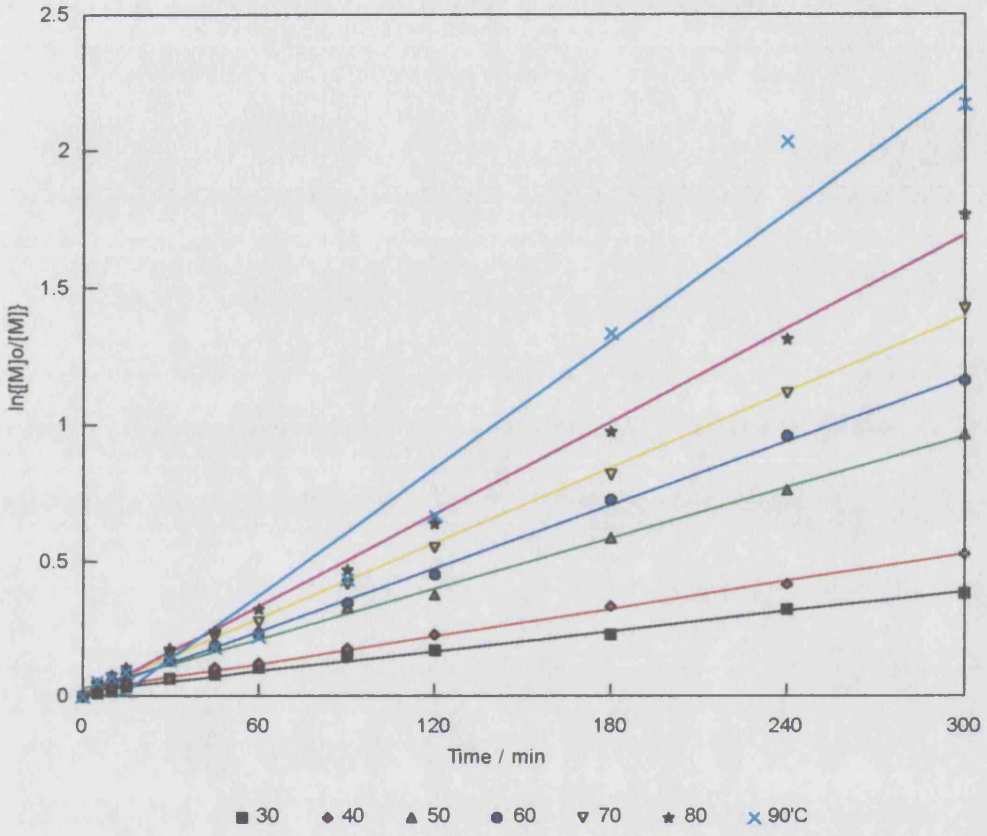

Figure 5.2 - First order rate plots for silent, cationic polymerisations

The data for 90°C is unusual and is not as 'well behaved' as the polymerisations at the lower temperatures. The fact that the rate is initially slower than expected suggests that the polymerisation is being retarded in some way. The most likely explanation being that the presence of an impurity has hindered the initial polymerisation.

The results suggest that under cationic conditions, the rate of consumption of D_4 is first order. The polymerisation of D_4 using triflic acid (CF_3SO_3H) has been studied by many workers and the polymerisation is initially approximately first order in monomer[49,141]. However, the kinetics of cationic polymerisation are much more

complex than this[43,49]. The polymerisation of D_4 initiated by strong acids follows a complex rate law in which it is necessary to consider both the mechanisms described in section 1.9.4 (addition polymerisation and acidolysis/condensation). In particular, small quantities of additives, especially water, are found to have a profound effect on the rate[42].

An Arrhenius treatment of the rate constants determined for each polymerisation, was used to calculate an activation energy for the cationic ring-opening polymerisation. The Arrhenius plot (of ln k against 1/T) is shown in figure 5.3. From the slope of the line the activation energy is determined as being 27 ± 2 kJmol^{-1}. This compares well to the values reported by Chojnowski et al who, in the polymerisation of D_4 in dichloromethane with triflic acid, obtained values of 24 and 27 kJmol^{-1}, for two different acid concentrations[49].

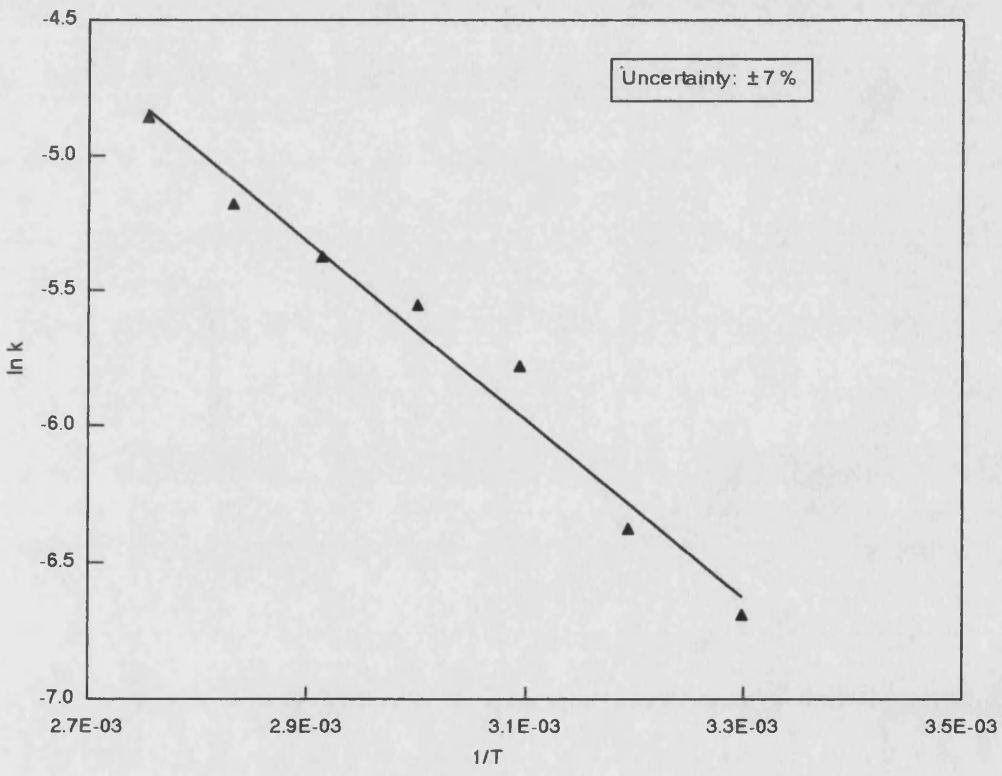

Figure 5.3 - Arrhenius plot for silent, cationic polymerisations

5.1.2 Ultrasonic

For the cationic polymerisations under ultrasound, an initial experiment was conducted employing the ultrasonic horn at an intensity of 22.2 Wcm^{-2}, with the solution being heated to 50°C before sonication was begun. During sonication, the temperature of the solution rose rapidly and the thermostatted water was replaced with running tap water in an attempt to control the temperature. The conversion during the sonication is shown in figure 5.4, along with the solution temperature. As can be seen, the polymerisation proceeds rapidly, however, the temperature is not constant but increases as the polymerisation proceeds. The temperature only becomes constant when the polymerisation is effectively over. The maximum temperature reached was ~80°C, yet the reaction was much faster than the silent polymerisation conducted at 80°C.

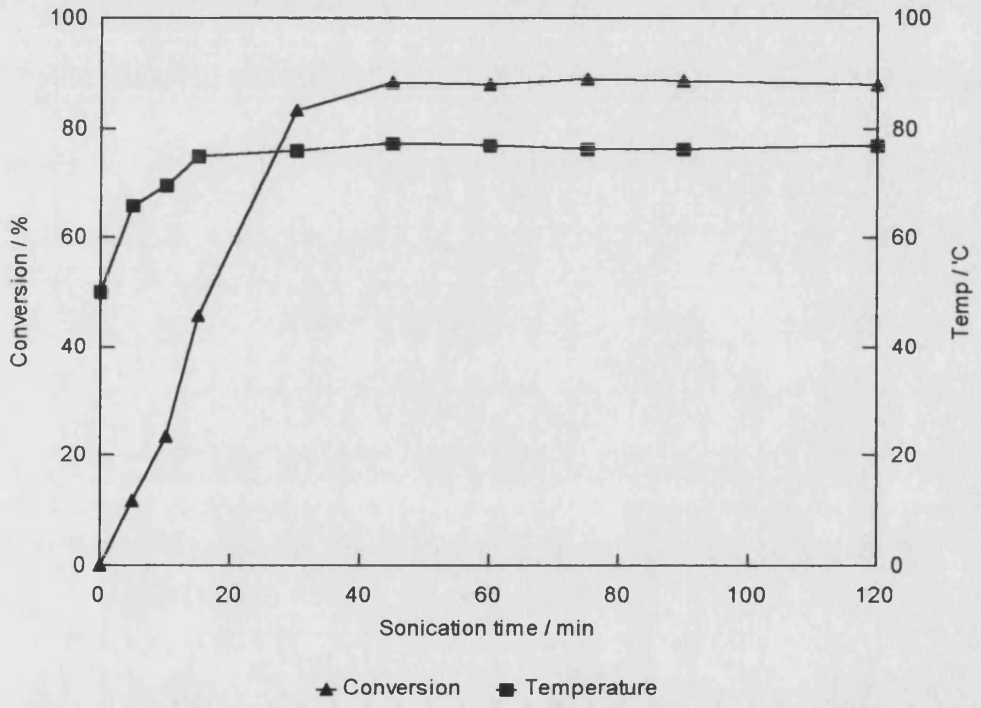

Figure 5.4 - Cationic polymerisation under ultrasound (22.2 Wcm^{-2})

In an attempt to control the temperature, further experiments were conducted using a lower ultrasonic intensity of 17.1 Wcm^{-2}, pulsing the ultrasound so that it was on for 1 second, then off for 1 second. However, the temperature was still difficult to control and in each case followed a similar pattern to that described above, i.e. the

temperature increased as the polymerisation progressed, only reaching a constant value when the polymerisation was over. Hence, the sonications were conducted over a temperature range, as opposed to a single defined temperature. Figure 5.5 shows the conversion during each sonication.

It is clear that the polymerisations conducted under ultrasound proceed much faster compared with the silent reactions. For example, even at the lowest temperature range used under ultrasonic conditions, 31 - 47°C, the polymerisation is effectively over after 120 minutes. Yet at 50°C the silent polymerisation has only reached 31 % conversion after this time, while at 90°C it takes 4 hours before the polymerisation nears completion. It can also be seen that the rate of polymerisation increases as the temperature increases.

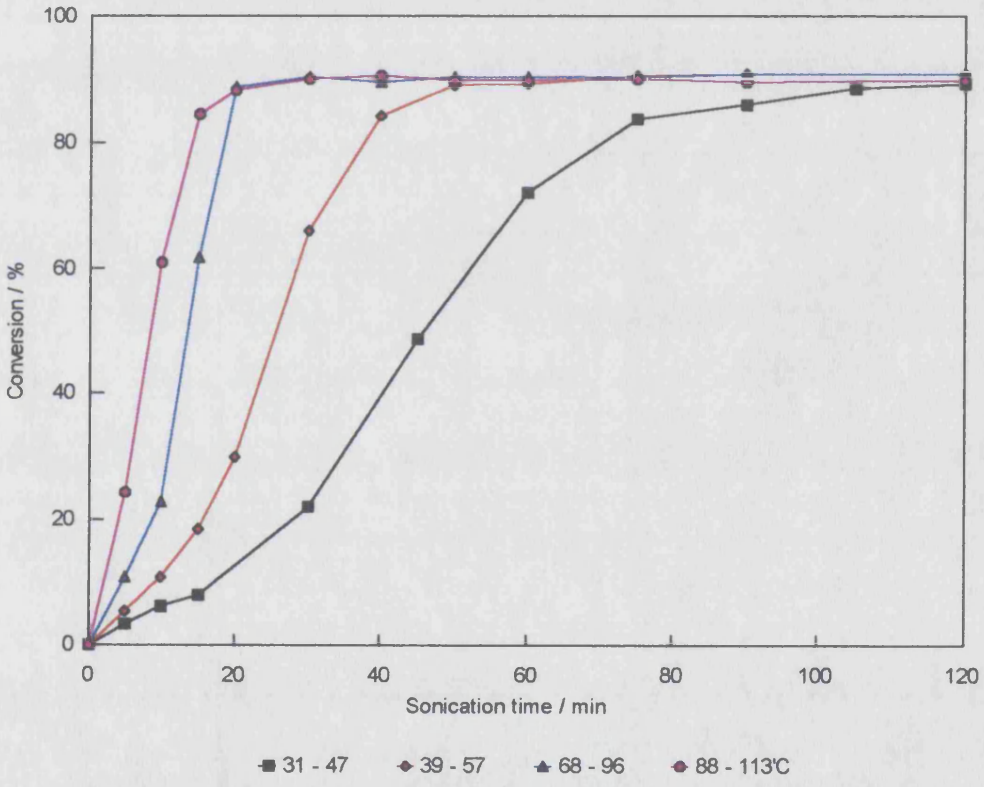

Figure 5.5 - Conversion during cationic polymerisations under ultrasound

The acceleration of the polymerisations conducted under ultrasound can be attributed to the dispersion and mixing effects of ultrasound. As the acid and D_4 are

immiscible, the acid needs to be dispersed throughout the D_4 for the reaction to proceed. The ultrasound obviously leads to a much better dispersion of the acid catalyst throughout the reaction, compared with a simple stirring. The initial ring-opening is therefore much more rapid, resulting in faster polymerisation. There is also likely to be enhanced mass transport throughout the system and this will also help to increase the rate of polymerisation.

The first order rate plots for the ultrasonic polymerisations are shown in figure 5.6.

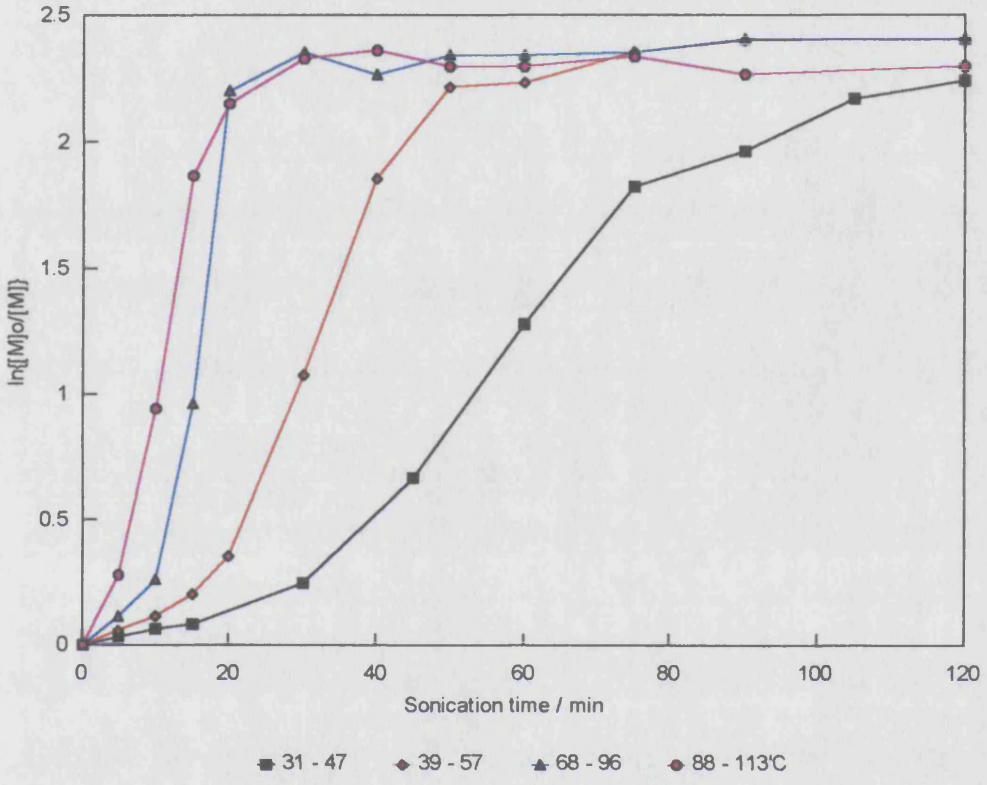

Figure 5.6 - First order rate plots for cationic polymerisations under ultrasound

These plots are markedly different from the first order plots obtained with the silent reactions, although they do appear to be linear during polymerisation before levelling to a constant value when polymerisation is complete. However, as the temperature was not constant during the ultrasonic polymerisations, caution must be used in interpreting this data. Because of the changing temperature during sonication, it is not possible to say if the polymerisation is truly first order in D_4.

A further experiment was conducted to determine whether any sonochemical enhancement is present when the ultrasonic bath is used in place of the ultrasonic horn. The conversion during the sonication is shown in figure 5.7.

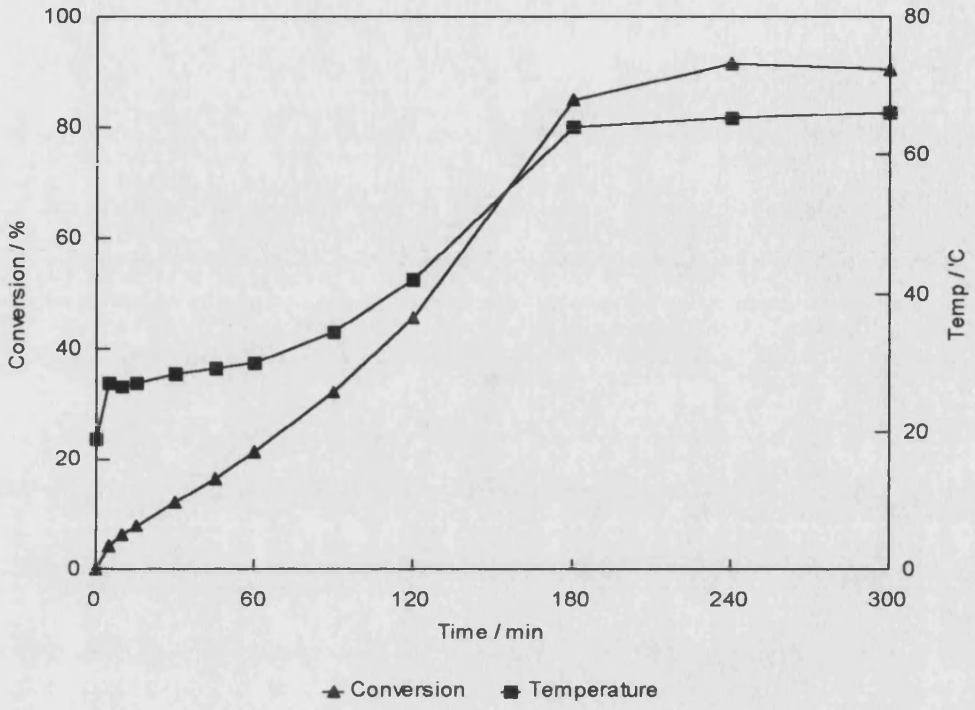

Figure 5.7 - Cationic polymerisation using the ultrasonic bath

As with the ultrasonic horn, the sonochemical polymerisation is clearly faster than that under silent conditions. The polymerisation is complete before 4 hours of sonication, the temperature reaching a maximum of 66°C. In comparison, at 70°C the silent polymerisation only reached a conversion of 67 % after this time. However, due to the much lower intensity of the bath, the rate of reaction is comparatively slower than when using the ultrasonic horn. Temperature control is again difficult, so although the temperature was 20°C at the start of the sonication, this had increased to 66°C after 5 hours.

This is a qualitatively similar result to that obtained by Price et al[108] who sonicated D_4 with H_2SO_4 using an ultrasonic bath, although their polymerisation was conducted in diethyl ether. They found the rate of polymerisation under ultrasound to be faster than the silent polymerisation conducted at 30°C.

The problem of temperature control is a consequence of conducting the reaction in bulk D_4. As the polymerisation proceeds, the viscosity of the solution increases. This results in an increase in the attenuation of the ultrasound, which subsequently causes heating of the solution. The greater the viscosity, the greater the attenuation and therefore, the greater the heating.

Unfortunately, no molecular weight data is available for either the ultrasonic or the silent polymerisations. Hence, the change in molecular weight during the polymerisation, and whether it is affected by the ultrasound is unknown at this stage. Similarly, it has not been possible to determine how the equilibrium is affected, as only the relative amounts of D_4 and polymer were measured. There is no data on the distribution of the individual cyclic species. The ultrasonic polymerisation is clearly occurring much faster than the silent polymerisation, so it may be possible that, under ultrasound, there is insufficient time for redistribution and back-biting reactions to occur. This would result in the cationic ring-opening initially producing just linear polymers, which could then equilibrate if given enough time, i.e. under ultrasound, will kinetically controlled polymerisation occur?

5.2 Anionic Polymerisation

5.2.1 Silent

The anionic polymerisation of D_4 under silent conditions, using KOH as a catalyst, was conducted at 100, 110, 120, 130, 140 and 150°C. An end-blocker (a short chain PDMS (Dow Corning, 20 cs DC200 fluid)) was again used to control molecular weight to approximately 35 000. The conversion during the polymerisations is shown in figure 5.8.

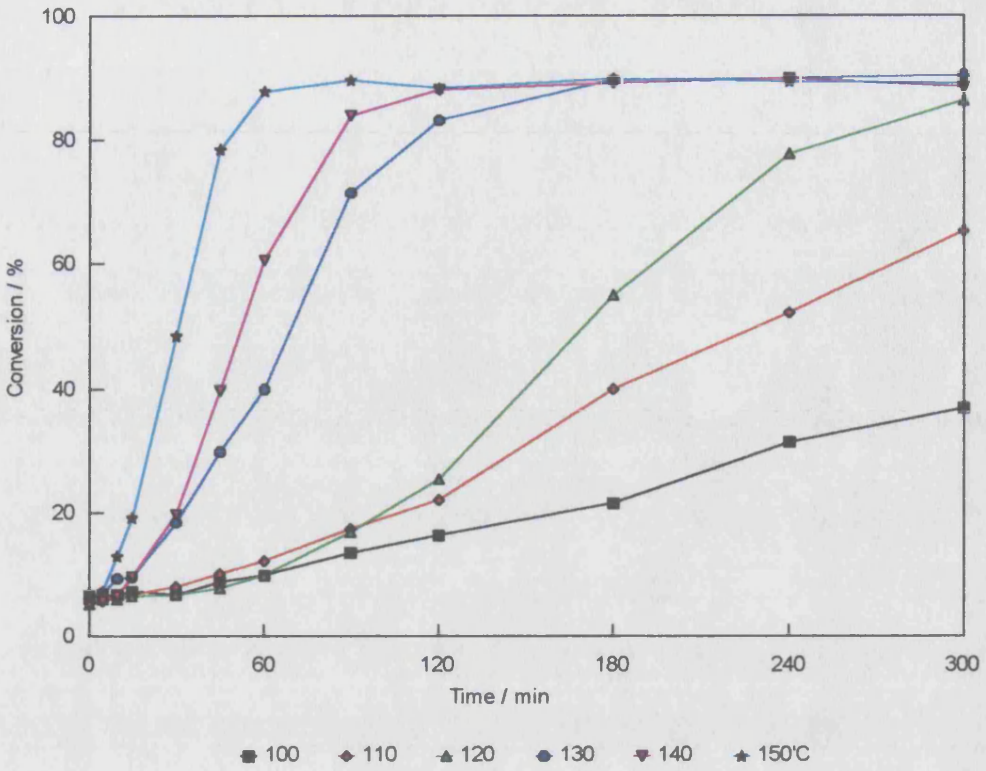

Figure 5.8 - Conversion during silent, anionic polymerisations

The first order rate plots for these polymerisations are shown in figure 5.9.

There is general agreement on a number of features of the anionic polymerisation of D_4 [43]:

- The polymerisation exhibits an induction period which is more pronounced at lower temperatures.
- The rate of consumption of monomer obeys first order kinetics
- The order in catalyst is fractional and often 0.5

From figure 5.9 the induction period at the start of the reaction is clear. This induction period becomes shorter as the temperature of the polymerisation is increased. Thus, at 100, 110 and 120°C, the induction period lasts approximately 60 minutes, whereas at 130°C it is approximately 30 minutes, at 140°C it is approximately 15 minutes and at 150°C it is under 10 minutes.

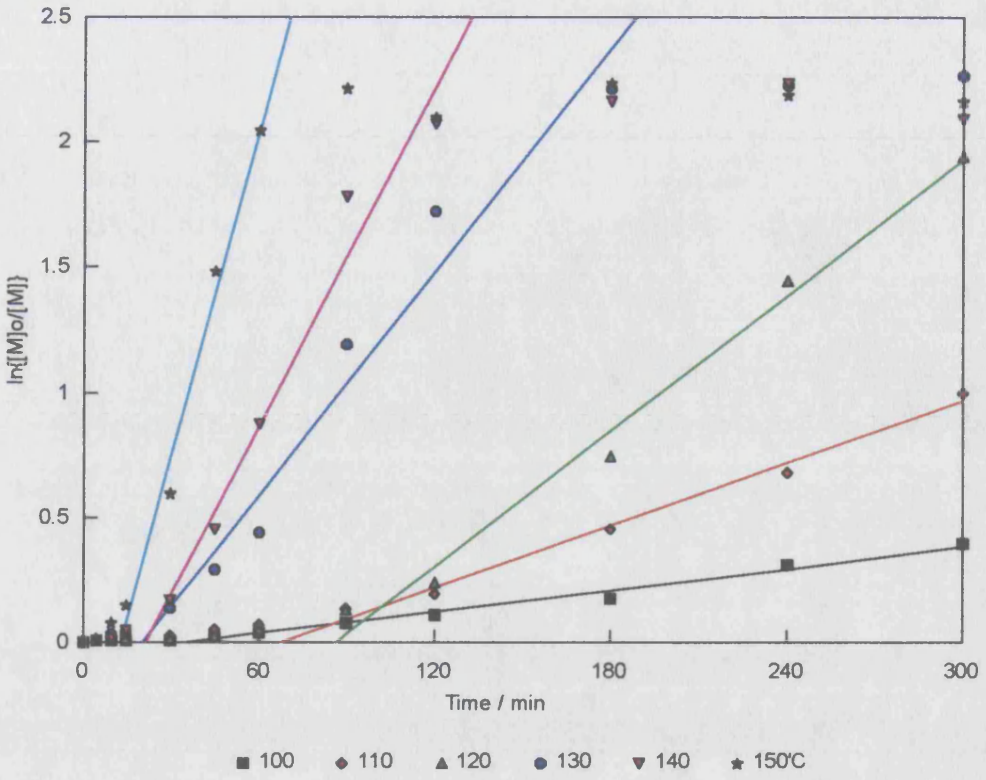

Figure 5.9 - First order rate plots for silent, anionic polymerisations

Once the polymerisation has begun, the consumption of D_4 follows first order kinetics and the first order plot is then linear until, for the polymerisations at 130, 140 and 150°C, the conversion reaches a constant value of 90 %. These results therefore confirm the first two points. As a constant concentration of base was used for all the polymerisations, it is not possible from these results to determine the order in the catalyst.

Arrhenius analysis of the first order rate constants is shown in figure 5.10. The plot is linear and the activation energy is calculated as being 85 ± 6 $kJmol^{-1}$. This compares very well to the reported value for the anionic polymerisation of approximately 19.5 $kcalmol^{-1}$ (~82 $kJmol^{-1}$)[39].

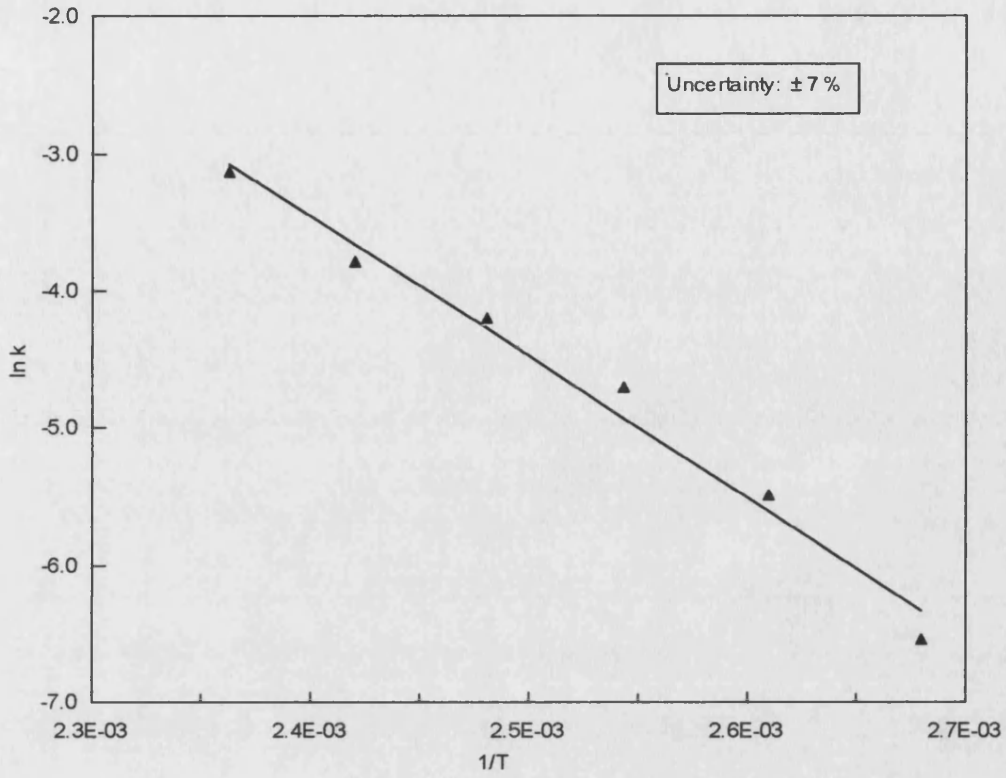

Figure 5.10 - Arrhenius plot for silent, anionic polymerisations

5.2.2 Ultrasonic

For the polymerisations conducted under ultrasound, an intensity of 17.1 Wcm^{-2} was used. Although this is the same intensity as that used for the cationic polymerisations, for the anionic polymerisations the intensity was not pulsed but was continuous. It was possible to use continuous ultrasound as the temperature control was not as difficult as with the cationic polymerisations, due to the fact that much higher temperatures were used. However, fluctuations of upto ± 5°C about the desired temperature could occur and it was therefore not possible to conduct the ultrasonic polymerisations at exactly the same temperature as the silent polymerisations. Temperatures of 100, 110, 120, 135 and 152°C were used and again, an end-blocker was used to keep the M_n to 35 000. The conversion during each sonication is shown in figure 5.11.

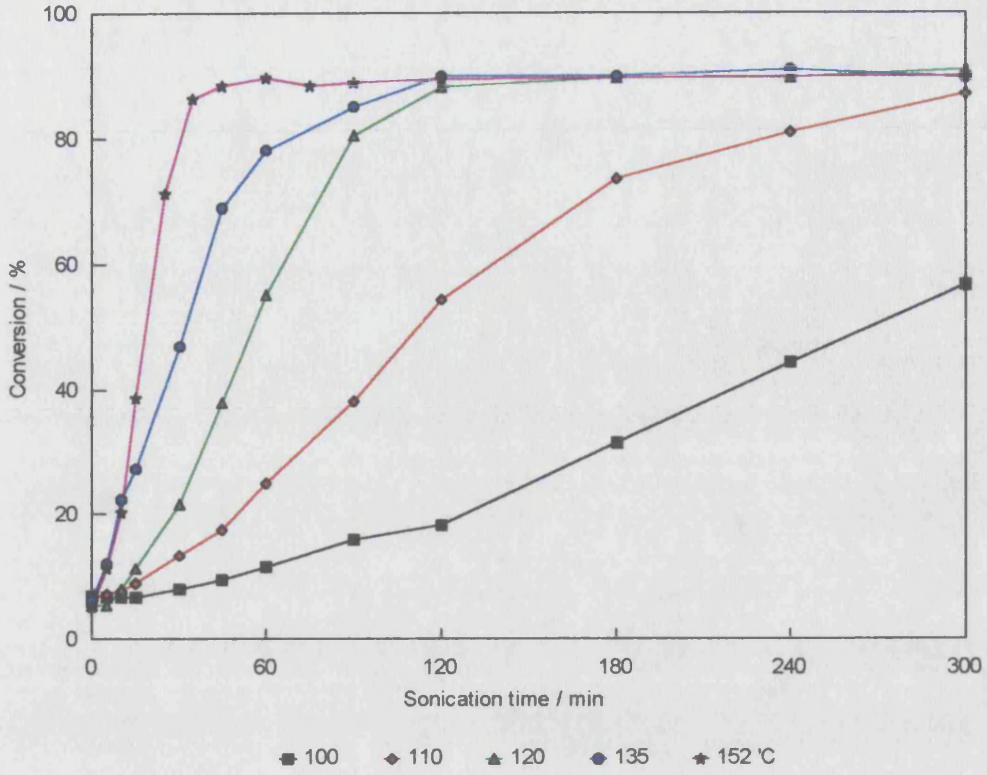

Figure 5.11 - Conversion during anionic polymerisations under ultrasound

This plot shows the same general features as that for the silent polymerisations in that the higher the temperature of the solution, the faster the polymerisation. However, if there is an ultrasonic enhancement, it is not as clear as that shown by the cationic polymerisation.

The first order rate plots are shown in figure 5.12. Again, there is an induction period before the polymerisation begins which decreases as the temperature increases. The induction period is shorter for the ultrasonic polymerisations than for the silent. For example, at 120°C, the induction period for the silent polymerisation was approximately 60 minutes, whereas under ultrasound it was approximately 15 minutes. As with the silent polymerisations, once polymerisation has begun, the consumption of D_4 appears to follow first order kinetics and the first order plot is linear until, for 120, 135 and 152°C, the conversion reaches a constant value.

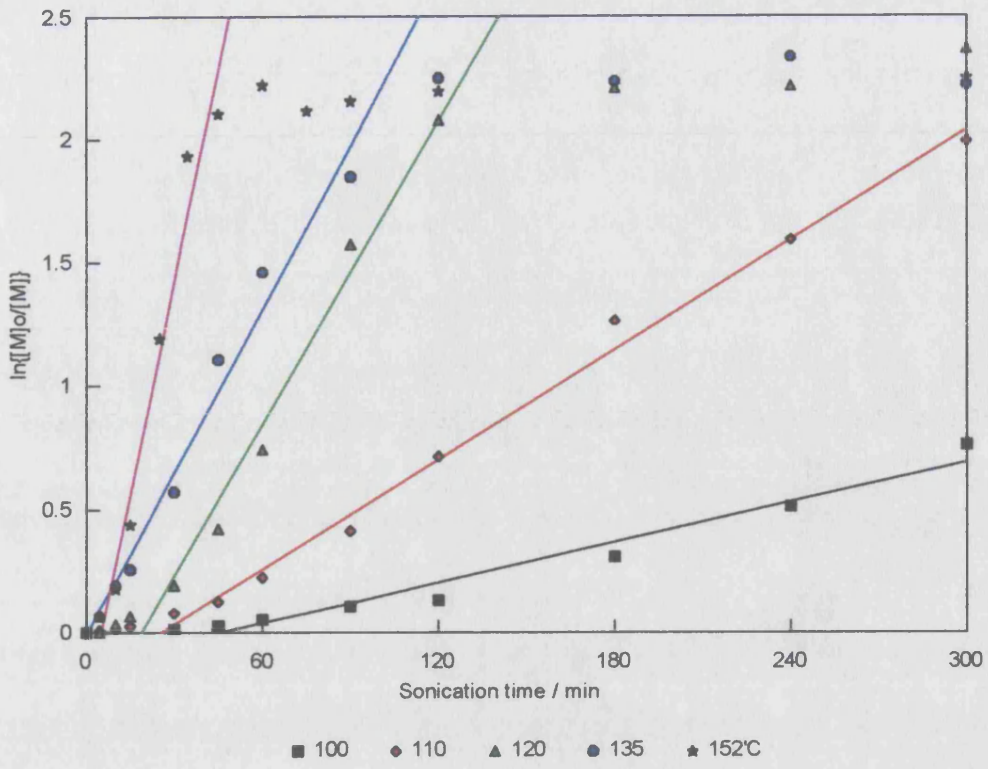

Figure 5.12 - First order rate plots for anionic polymerisations under ultrasound

Arrhenius analysis of the first order rate constants is shown in figure 5.13. The plot is linear, although the correlation is not as good as with the silent polymerisations. This will be due in part to the uncertainty of the temperature during the ultrasonic polymerisations. The activation energy was determined as being 72 ± 12 $kJmol^{-1}$, which is marginally lower than that determined under silent conditions, although there is a large uncertainty as a consequence of the uncertainty in the temperature.

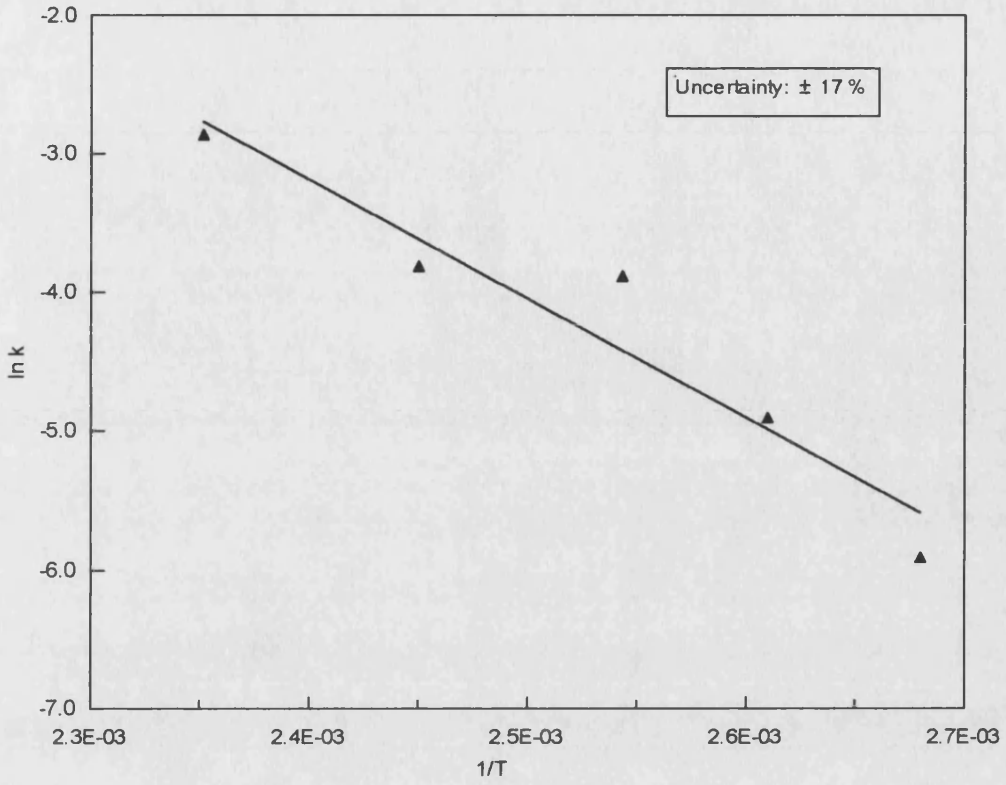

Figure 5.13 - Arrhenius plot for ultrasonic, anionic polymerisations

As it is not immediately obvious from figures 5.8 and 5.11 whether there has been any enhancement due to ultrasound, Figure 5.14 shows the silent and ultrasonic polymerisations at 100°C, with the corresponding rate plots shown in figure 5.15. While figure 5.16 compares the silent polymerisation at 140°C with the ultrasonic polymerisation at 135°C, with the corresponding rate plots shown in figure 5.17.

In both cases, the reduction in induction time with ultrasound is obvious. At 100°C it can be seen that the polymerisation under ultrasound is proceeding faster than that under silent conditions. However, comparing ultrasound at 135°C with the silent polymerisation at 140°C, it would appear that once polymerisation has begun, the rate of polymerisation is approximately the same, i.e. the polymerisation under ultrasound at 135°C is as fast as that at 140°C under silent conditions.

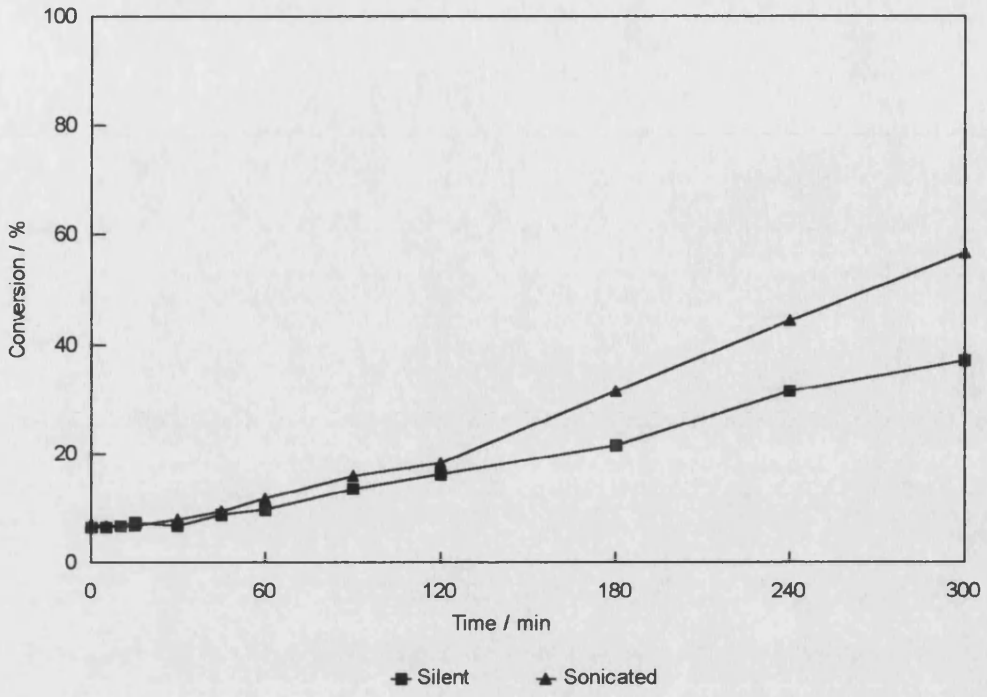

Figure 5.14 - Comparison of silent and ultrasonic, anionic polymerisations at 100°C

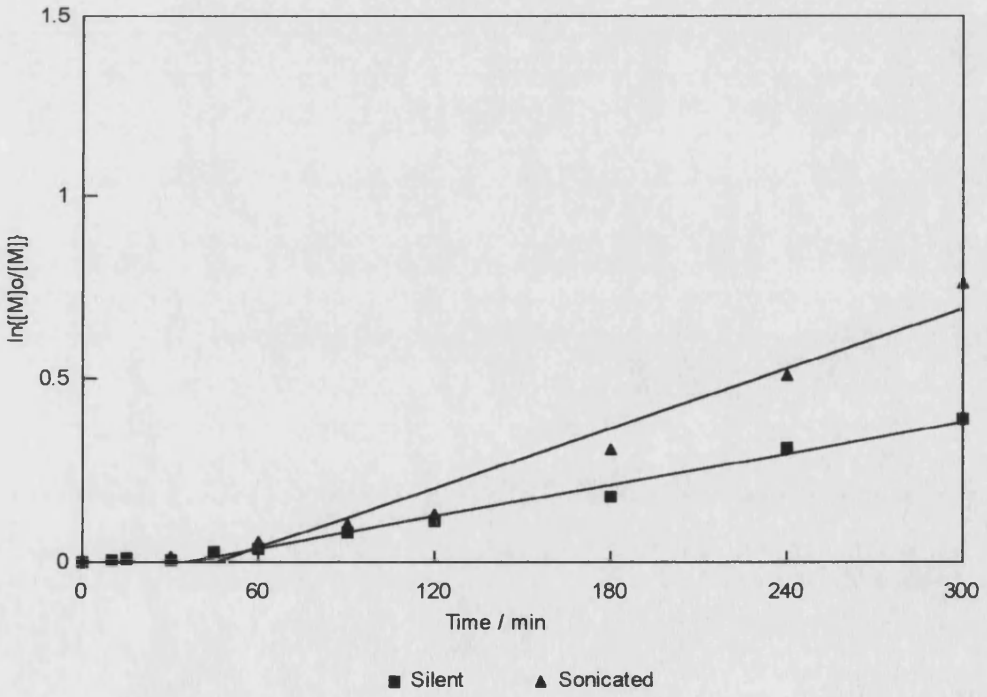

Figure 5.15 - First order rate plots from figure 5.14

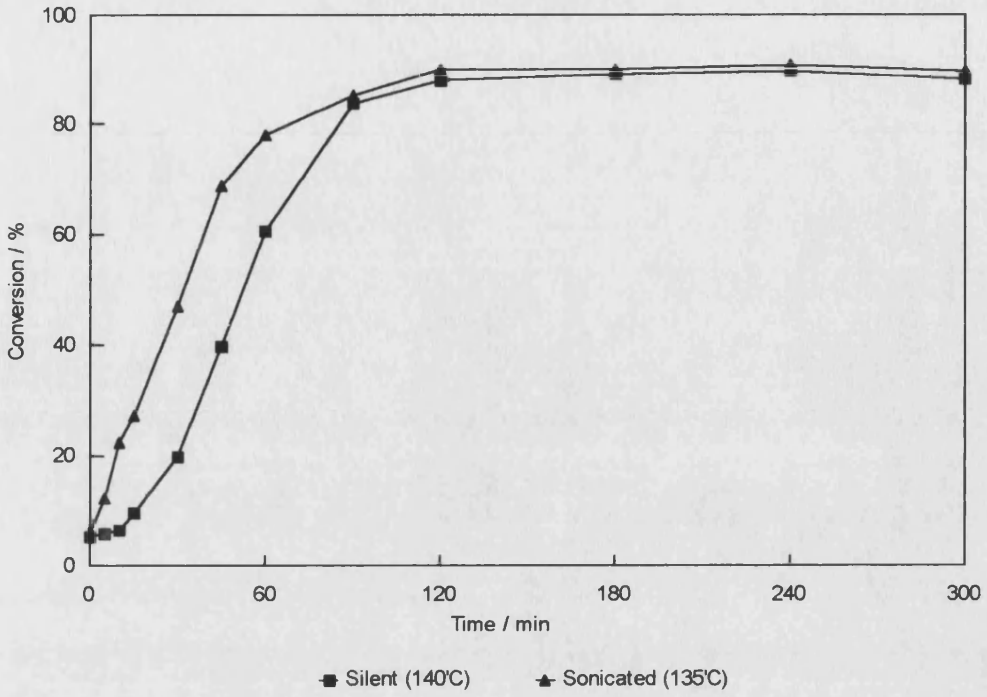

Figure 5.16 - Comparison of silent (140°C) and ultrasonic (135°C) anionic polymerisations

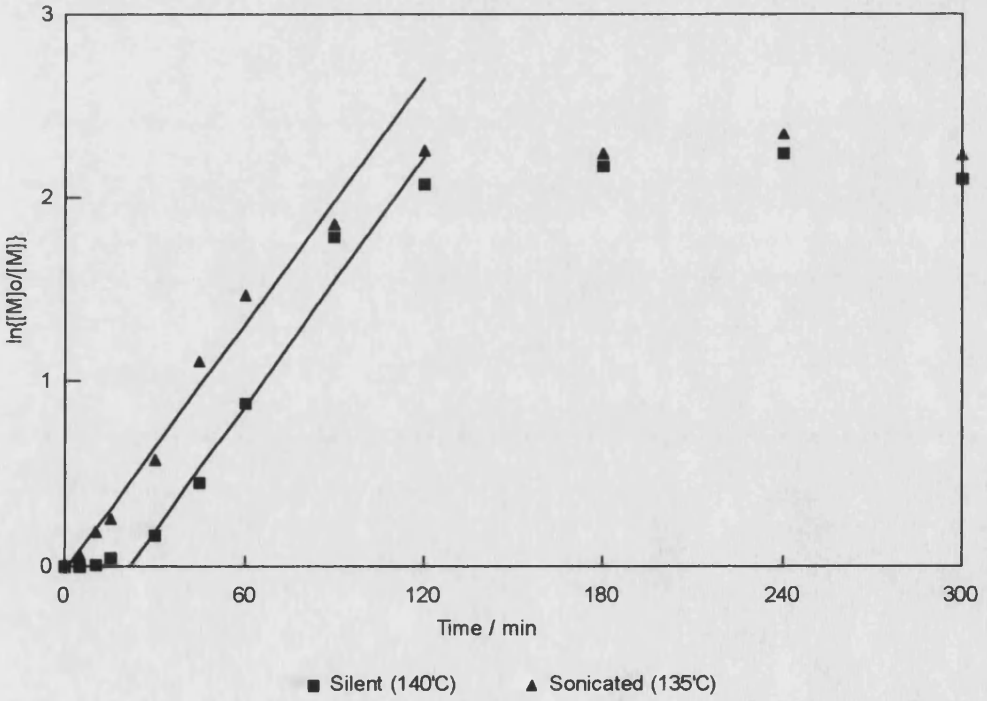

Figure 5.17 - First order rate plots from figure 5.16

It is clear that by conducting the anionic polymerisation under ultrasound, the reaction proceeds faster than the silent polymerisation at the same temperature, although this enhancement is not as great as that seen for the cationic polymerisations. The actual mechanism of the ultrasonic enhancement is due to the collapse of the cavitation bubbles. Microjet and shockwave impacts at the surface of the KOH particles will have two effects: any water present on the surface will be removed and it will also cause erosion and particle size reduction, leading to an increase in the surface area of the KOH. The net effect of these two processes is that initiation of the polymerisation will be faster under ultrasound, i.e. the induction period that is seen will be reduced, so that the polymerisation can then begin. Once polymerisation has begun, the rapid movement in the solution generated by cavitational collapse will enhance mass transport, resulting in the increase in rate of the ultrasonic polymerisations.

As with the cationic polymerisations, no molecular weight data has been obtained for either the ultrasonic or the silent reactions. Hence, it is not known how the molecular weight changes during the polymerisations, or how this is affected by the ultrasound. Similarly, it has again not been possible to determine how the equilibrium is affected, as only the relative amounts of D_4 and polymer were measured and there is no data regarding the distribution of the individual cyclic species that may be present.

5.3 Conclusions

Both the cationic and anionic polymerisations have shown enhancement when conducted under ultrasound, although the effect was greater for the cationic polymerisation. The mechanism of this enhancement can be attributed to the physical effects of the ultrasound on the systems. In both cases, the ultrasound has lead to an effective dispersal of the catalyst throughout the system. The initial ring-opening is therefore more rapid under ultrasound than under silent conditions, resulting in a faster polymerisation.

At this stage it is not clear whether ultrasound has any affect on the actual mechanism of the polymerisation, or if the ring-chain equilibrium is affected in any way. Empirical research has shown that ultrasound will only affect the mechanism of a reaction if the mechanism involves radical intermediates. While in heterogeneous

systems, such as the polymerisations studied here, ionic reactions can be stimulated by mechanical effects, although the products will be the same as in the silent reaction (section 1.14.4, refs. 94 and 95). As both the anionic and cationic polymerisation proceed via an ionic mechanism, it is unlikely that using ultrasound will affect the mechanism of the polymerisation. This would seem to be borne out by the results of the anionic polymerisations, which under ultrasound showed qualitatively similar behaviour, such as an induction period and first order dependence of monomer consumption, and resulted in similar results being obtained for the activation energy in the silent and ultrasonic cases.

For the cationic polymerisation, the difficulty in controlling the temperature has made quantitative comparison of the silent and ultrasonic cases more difficult. However, what is clear is that by using ultrasound the polymerisation is much faster and is over much more quickly. Because of the rapidness of the conversion of D_4 to polymer, it may be possible that, under ultrasonic conditions, there is not as much time for redistribution and back-biting reactions to occur. This would imply that kinetically controlled polymerisation is occurring, i.e. that the polymerisation initially forms high molecular weight polymer which will then undergo equilibration if given enough time. Unfortunately, as there is no data regarding molecular weight or the distribution of cyclic species formed during the polymerisation, this hypothesis cannot be investigated. However, it does merit further investigation.

In all the polymerisations conducted, an end-blocker was used to control the molecular weight (M_n) to ~ 35 000. From the results obtained from the degradation studies (chapter 3), at this molecular weight and at the temperatures used, no degradation should occur. Again, however, as no molecular weight data is available this assumption cannot be verified. An interesting extension to this work would be to conduct the polymerisation without end-blocker and follow the molecular weight, to see if ultrasonic degradation affects the molecular weight, and if this in turn affects the equilibrium distribution.

Chapter 6

Copolymer Synthesis

6 COPOLYMER SYNTHESIS

Polymers have proven to be useful for a myriad of applications, however, some applications require properties that cannot be met by using just one homopolymer. The development and use of copolymers has therefore become widespread, as they can exhibit the physical properties of both components. Polysiloxanes have some very desirable properties (section 1.7.4), such as low Tg, transparency to visible and UV light, high permeability to various gases, and chemical and physiological inertness. However, to develop useful mechanical properties, PDMS rubbers generally require cross-linking and then filling with a finely divided, high surface area, silica filler[41].

Copolymerisation offers an alternative method of improving the mechanical properties, without cross-linking and filling. The synthesis of block copolymers of the weak and rubbery polysiloxane with a glassy or crystalline polymer, such as poly(methyl methacrylate), allows many copolymers to be produced whose properties depend on the nature of the blocks, the block lengths and the relative composition of the components in the copolymer.

The possibilities exist for a wide range of copolymers, each with different properties depending on the exact nature of the blocks, and the synthesis of these copolymers is of much interest.

This work attempted to produce copolymers of PDMS with polystyrene and poly(methyl methacrylate). Three strategies were used. In the first, the PDMS was sonicated in the presence of styrene or methyl methacrylate to see if the ions formed when the Si-O bond is ultrasonically cleaved could initiate ionic polymerisation of the monomer. The second strategy attempted to use the anionic polymerisation of styrene and D_3, initiated with butyl lithium. While the third investigated the new method of Atom Transfer Radical Polymerisation (ATRP), using siloxane-based initiators.

6.1 Sonication of PDMS with a Monomer

When polymers with a C-C backbone, such as polystyrene, are ultrasonically degraded, free radicals are generated at the cleaved chain-ends. These free radicals can be used to initiate the polymerisation of a second monomer, present in the solution, to form a block copolymer. This technique has been used by many workers to produce block copolymers, such as poly(styrene-methyl methacrylate) and

poly(vinyl chloride-styrene)[24]. PDMS, however, does not produce free radicals when ultrasonically degraded. The evidence suggests that the Si-O bonds are cleaved heterolytically to give ions. As the radical end of a cleaved polymer chain can initiate the polymerisation of another monomer, an analogous experiment was attempted to see if the ions produced when PDMS is cleaved, could be used to initiate the ionic polymerisation of styrene or methyl methacrylate.

Prior to this, an initial experiment was conducted to show that the free radical technique can be used to produce a copolymer of poly(isobutylene) (PIB), with methyl methacrylate.

6.1.1 Sonication of PIB with Methyl Methacrylate

A 2.5 % solution of PIB in toluene was sonicated in the presence of methyl methacrylate using the ultrasonic horn (intensity of 31.6 Wcm^{-2}) for 3 hours at 25°C. After sonication the polymer was recovered and analysed by IR spectroscopy. Figure 6.1 shows the IR spectrum of the recovered polymer, while figures 6.2 and 6.3 show the spectra of the PIB and poly(methyl methacrylate) (PMMA) homopolymers.

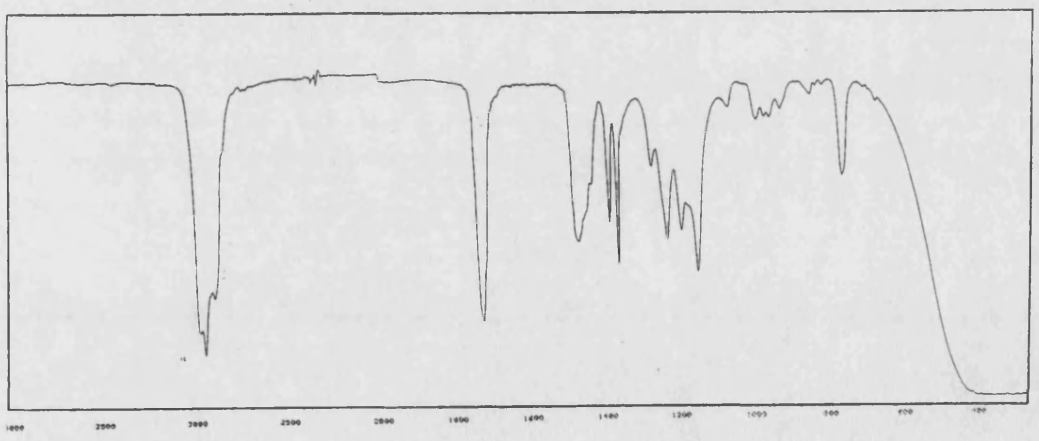

Figure 6.1 - IR spectrum of the recovered polymer

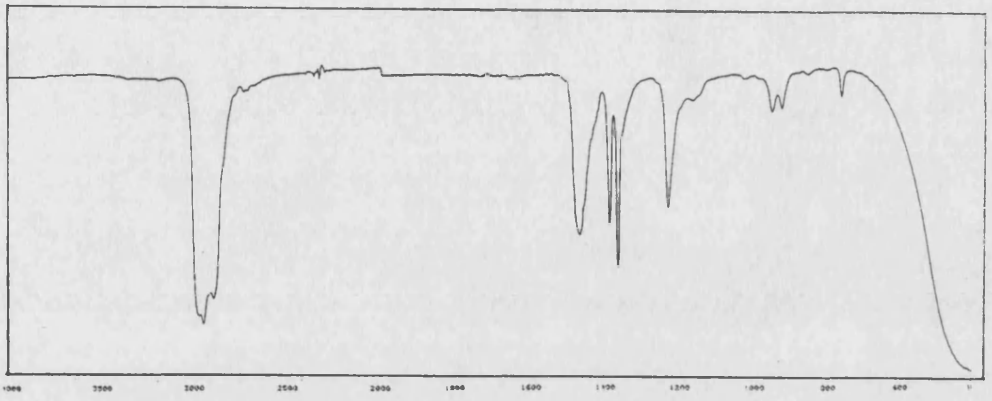

Figure 6.2 - IR spectrum of PIB

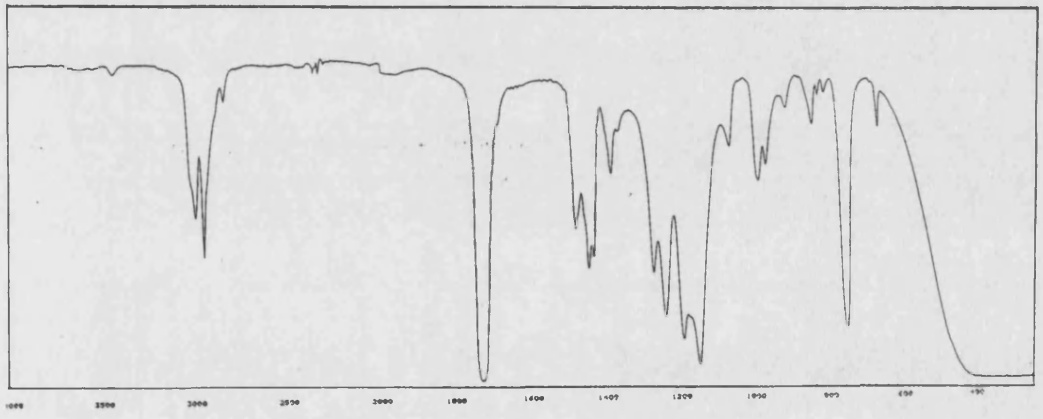

Figure 6.3 - IR spectrum of PMMA

Comparison of the product spectrum with the spectra of the homopolymers shows that the recovered polymer does indeed contain both PMMA and PIB. The peaks at 3000, 1500 and 1400 cm^{1} can be assigned to the PIB blocks, while the peaks at 1700, 1200 and 750 cm^{-1} are due to PMMA. Hence, it is quite clear that the radicals formed when the PIB chains are cleaved are capable of initiating the polymerisation of the methyl methacrylate, resulting in the formation of the copolymer.

6.1.2 Sonication of PDMS with Styrene and Methyl Methacrylate

The work described in chapter 4 demonstrated that PDMS does not produce radicals when ultrasonically degraded, but the evidence suggests that ions are formed instead. These experiments attempted to use these ions to initiate ionic polymerisation of a monomer present during sonication.

Styrene was initially chosen as it can undergo both anionic and cationic polymerisation and therefore, if polymerisation were to occur, it could occur with either 'half' of a cleaved PDMS chain, i.e. with either the Si^+ or the O^-.

In an initial experiment, 10 cm^3 of styrene was added to 90 cm^3 of a 1 % PDMS/THF solution and sonicated on the ultrasonic bath for 90 minutes. This was then repeated but sonicating for 24 hours. The IR spectra of the recovered polymers are shown in figures 6.4 and 6.5, while figures 6.6 and 6.7 show the IR spectra of PDMS and polystyrene

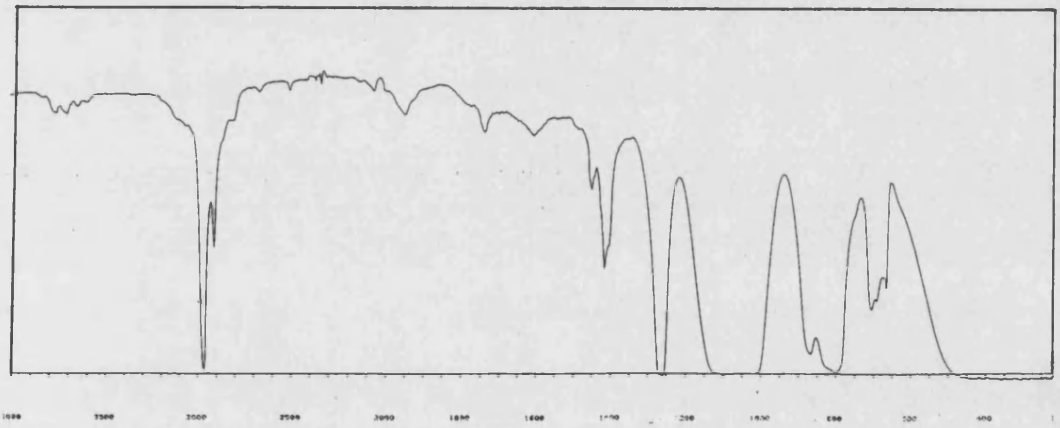

Figure 6.4 - IR spectrum of recovered polymer after 90 minutes sonication

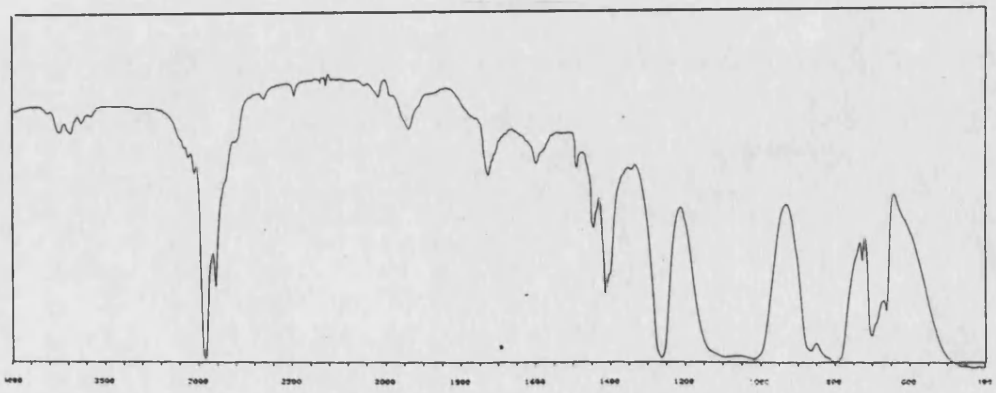

Figure 6.5 - IR spectrum of recovered polymer after 24 hours sonication

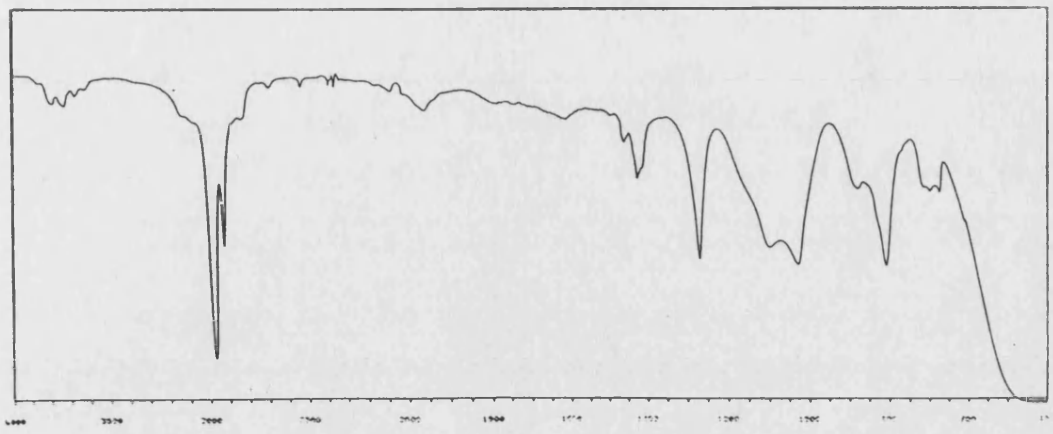

Figure 6.6 - IR spectrum of PDMS

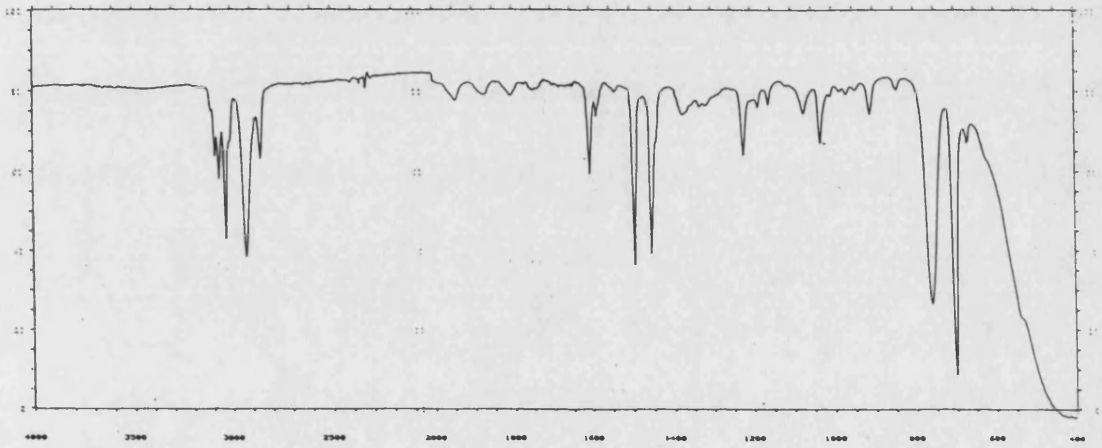

Figure 6.7 - IR spectrum of polystyrene

The spectra of the recovered polymers is clearly that of PDMS - there is no styrene component present in either of the polymers. GPC of the PDMS after the 90 minute sonication shows the molecular weight (M_n) to be 83 000. Since the initial value of M_n is ~85 000, little degradation has occurred and hence the chances of a cleaved chain initiating styrene polymerisation are very small. Much greater degradation occurs when the PDMS is sonicated for 24 hours using the bath, with the molecular weight falling to ~ 58 000. However, even this more extensive degradation has not resulted in the formation of any of the copolymer.

It is possible that because the PDMS and the styrene were both present in small concentrations, the likelihood of a cleaved PDMS chain being near a styrene

molecule before the ion reacts with other species present, was very small. Also, due to the low intensity of the ultrasonic bath, the extent of degradation was not great, i.e. the number of chains degraded, and therefore the number of ions formed, was very small.

Further experiments were conducted using the ultrasonic horn. As much higher ultrasonic intensities are available when using the horn, the extent of degradation will be greater. Also, a higher concentration of PDMS was used (5 %) using the monomer as the solvent, so that the chances of a cleaved PDMS chain reacting with a monomer molecule are maximised.

Two monomers were used: styrene and methyl methacrylate. Both solutions were sonicated at an intensity of 22.2 Wcm^{-2} for 5 hours, at a temperature of 30°C. Figure 6.8 shows the IR spectrum of the recovered polymer after sonication in styrene, while figure 6.9 shows the IR spectrum of the recovered polymer after sonication in methyl methacrylate.

Both spectra show only PDMS, there is no evidence of either styrene or methyl methacrylate being incorporated into the polymer. Thus, the sonication of PDMS in styrene, and in methyl methacrylate, did not result in the polymerisation of either monomer and therefore no copolymer was produced.

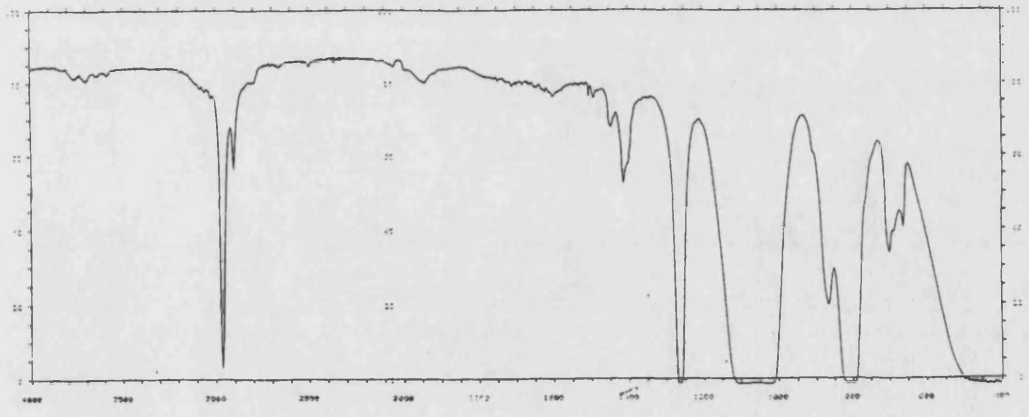

Figure 6.8 - IR spectrum after sonication in styrene

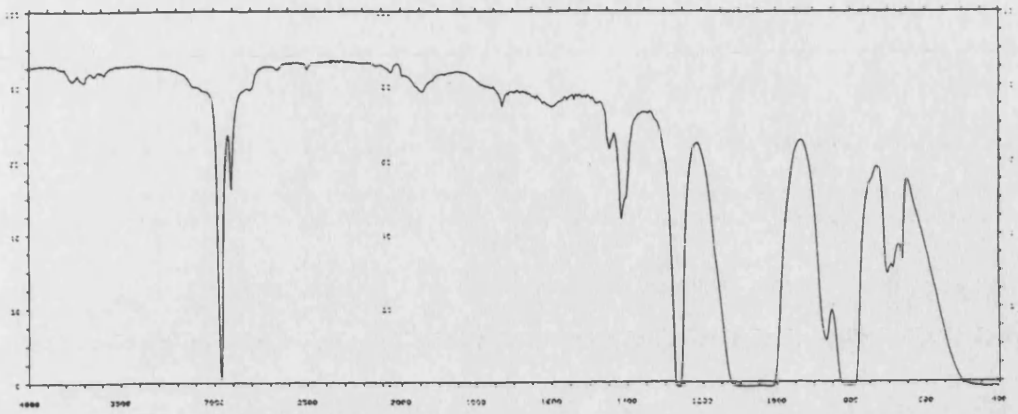

Figure 6.9 - IR spectrum after sonication in methyl methacrylate

Attempts to initiate the ionic polymerisation of vinyl monomers using the active centre at the ends of ultrasonically cleaved PDMS chains, have not been successful. The species formed when the Si-O bond is broken has been shown not to be a radical, and the evidence suggests formation of Si^+ and O^- at the chain-ends. However, although both styrene and methyl methacrylate are susceptible to ionic polymerisation, both failed to be initiated by the species formed from the cleavage of the Si-O bond. It is possible that the ions have reacted with impurities that may have been present, although a more probable explanation is that the ionic species formed do not exist for long enough as free, discrete ions, to be able to initiate polymerisation.

6.2 Anionic Polymerisation of Styrene

The anionic polymerisation of styrene was studied as a possible way of preparing poly(styrene-dimethylsiloxane) block copolymers. Two sets of experiments were conducted; to determine how ultrasound affects anionic polymerisation and to see if the presence of D_4 during polymerisation will result in any siloxane being incorporated into the polystyrene.

6.2.1 Polymerisation of Styrene with BuLi

The anionic polymerisation of styrene was conducted under ultrasonic (using the ultrasonic bath) and silent conditions, using *n*-butyl lithium (*n*-BuLi) as the initiator.

A number of silent polymerisations were conducted to determine the effect of changing the reaction time and the temperature, while the ultrasonic polymerisations were conducted with and without initiator. The recovered polymers were analysed by GPC to determine their molecular weight and polydispersity. Table 6.1 lists the results for the silent polymerisations, while table 6.2 lists those for the ultrasonic polymerisations.

Table 6.1 - silent polymerisations

Expt. No.	Initiator?	Time (hrs)	Temp (°C)	Yield (%)	Mn	Mw	γ
1	Yes	1.5	25	56	21 800	39 600	1.82
2	Yes	2.5	25	22	18 500	32 700	1.76
3	No	2.5	25	0	-	-	-
4	Yes	1.5	-70	28	15 900	32 300	2.05

These results show that styrene will polymerise with *n*-BuLi as an initiator. However, the yields and the molecular weights are quite low, and the molecular weight distributions are broad for polymers produced by anionic polymerisation. It is obvious that although polymerisation is occurring, living polymerisation conditions are not being achieved. This suggests that there are impurities in the reaction vessel (residual H_2O and/or O_2) that are prematurely terminating the reaction.

Table 6.2 - ultrasonic polymerisations

Expt. No.	Initiator?	Time (hrs)	Temp (°C)	Yield (%)	Mn	Mw	γ
5	No	1.5	25	0	-	-	-
6	Yes	1.5	25	23	11 000	22 500	2.05

The results from the ultrasonic polymerisations show that the use of ultrasound does not affect the polymerisation. A similar yield to the silent polymerisations was obtained, molecular weight was low and the polydispersity was broader than expected for living polymerisation. As before, it is clear that not all of the impurities were completely removed from the reaction system.

Ultrasound would not be expected to affect this polymerisation as *n*-BuLi is an anionic initiator and ultrasound only affects those homogeneous reactions in solution if the reaction mechanism involves radical processes[94,95]. This confirms the result found by Schultz et al[142], who found that ultrasound had no effect on the BuLi initiated polymerisation of styrene.

6.2.2 Polymerisation of Styrene in the Presence of D_4

10 cm^3 styrene was anionically polymerised, using *n*-BuLi, in the presence of 14 cm^3 D_4 (giving a styrene:D_4 molar ratio of 2:1). Reaction time was 90 minutes at 25°C. Figure 6.10 shows the infrared spectrum produced by the recovered polymer,

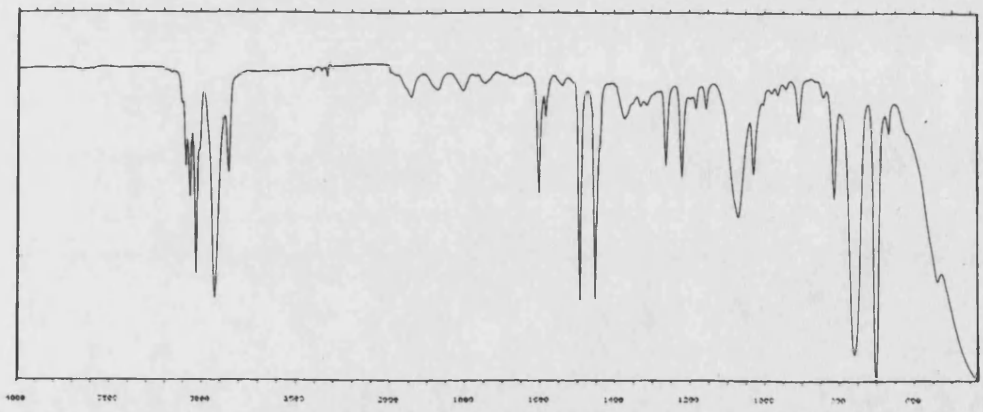

Figure 6.10 - IR spectrum of recovered polymer

The spectrum of the product clearly indicates that it is polystyrene. There are no peaks in this spectrum that could attributed to a siloxane component. Hence, this experiment has been unsuccessful. Neither the butyl anion or the polystyryl anion have

initiated the ring-opening of D_4 and no siloxane has been incorporated into the polystyrene.

Given that D_4 is an unstrained ring, strong initiators are required for ring-opening to occur, hence the use of strong acids/bases as initiators for polymerisation. The use of D_3 would be a more suitable as it is a strained ring and is therefore more susceptible to ring-opening. Hence further experiments using D_3 and *n*-BuLi were conducted.

6.3 BuLi Initiated Polymerisation of D_3

6.3.1 Reaction of D_3 and BuLi

The aim of this experiment was to see if *n*-BuLi could initiate the ring-opening of D_3. 0.1 cm^3 of BuLi was added to a 40 % w/v solution of D_3 in THF and stirred for 90 minutes at 25°C.

The product of the reaction was a viscous liquid indicating a polymeric product, i.e. PDMS. The formation of a polymer can be seen on the chromatogram from the HPLC (figure 6.11): the large peak at 7.53 minutes being due to the polymer product. The smaller peak at 9.31 minutes is due to the presence of unreacted D_3, while the other peaks registered on the chromatogram will be due to the presence of low molecular weight cyclic products that are formed during the polymerisation.

Yield of polymer produced = 76%

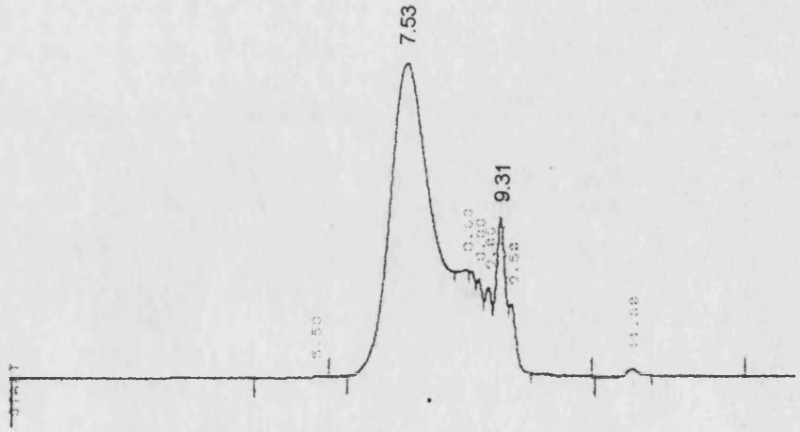

Figure 6.11 - HPLC chromatogram from D_3 polymerisation with BuLi

6.3.2 BuLi Initiated Polymerisation in the Presence of Styrene

As BuLi can initiate the polymerisation of both D_3 and styrene, this experiment attempted to produce a poly(styrene-dimethylsiloxane) copolymer by adding *n*-BuLi to a mixture of D_3 and styrene in THF. The amounts of D_3, styrene and *n*-BuLi were chosen so that there was a 1:1 molar ratio of D_3:styrene, and ~1:500 molar ratio of *n*-BuLi to monomer (i.e. D_3 + styrene). Reaction time was 90 minutes at 25°C.

The IR spectrum of the recovered polymer is shown in figure 6.12. As can be seen, there are no peaks that can be attributed to styrene - the spectrum is that of PDMS. Thus, while a polymer has been formed no styrene has been incorporated into the polymer and only PDMS has been produced.

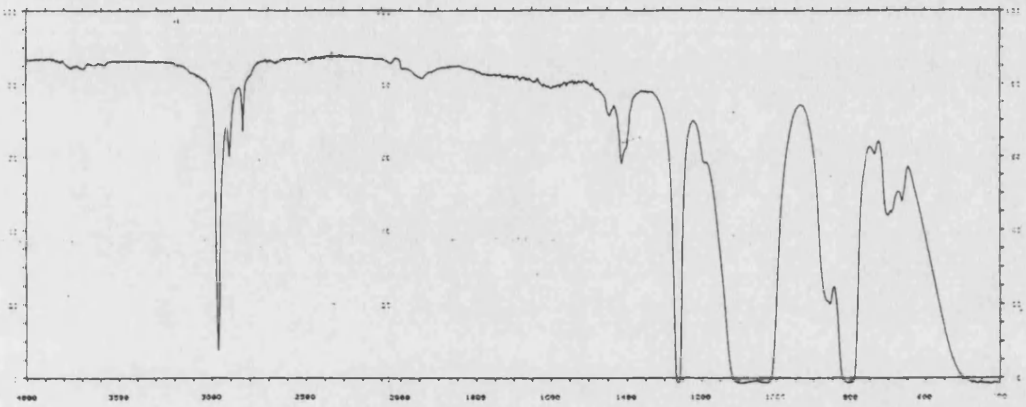

Figure 6.12 - IR spectrum of recovered polymer

The *n*-BuLi has obviously favoured the initiation of the D_3 polymerisation as opposed to the styrene polymerisation. This could be due to the fact that the anionic polymerisation of styrene is very susceptible to impurities, whereas the D_3 polymerisation is far more robust and will be largely unaffected by impurities. The polymerisation of D_3 will also be driven by the fact that D_3 is a strained ring.

BuLi has previously been used to produce copolymers from styrene and D_3 [56,57], however, these methods have added the monomers sequentially. The BuLi being used to initiate styrene polymerisation before the D_3 was added. Performing the polymerisation this way avoids the problem of the BuLi just initiating the D_3 polymerisation. However, it obviously relies on the use of very clean and pure,

glassware and reagents, if the styrene polymerisation is not to be prematurely terminated before the polystyryl anion can initiate the ring-opening of D_3.

No further work on preparing the poly(styrene-dimethylsiloxane) copolymers using variations of this method were attempted. Instead, efforts were focused on the use of Atom Transfer Radical Polymerisation (ATRP) as a possible mechanism for producing these copolymers.

6.4 Atom Transfer Radical Polymerisation

6.4.1 Mechanism of Polymerisation

As described in section 1.5, ATRP is a relatively new technique that attempts to produce polymers by a radical process, but under "living" conditions. The obvious benefits of this method, apart from the molecular weight/structural control of the polymer properties, is the fact that low temperatures are not required and the reaction is not as affected by impurities compared with classical ionic living polymerisations.

A general reaction mechanism for ATRP is:

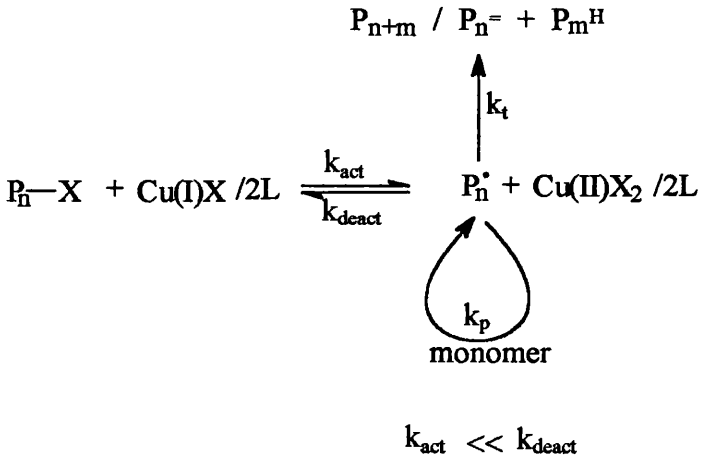

The required reagents for ATRP include an initiator, monomer, catalyst and complexing ligand. The catalyst used in many ATRP's is copper (I) chloride, which complexes with the complexing ligand. The first complexing ligand used was 2,2'-bipyridyl (bpy), initially in a molar ratio of 1:3, catalyst:ligand, although it was later found that a ratio of 1:2 gave identical results[16]. The initiator is required to have a halide functionality so that a halogen atom transfer reaction can occur between the

initiator and the complex. This forms the radical species which can then start the polymerisation of a suitable monomer. However, as the halogen atom abstraction is actually an equilibrium, only a small number of molecules are active at any one time and it is this dynamic equilibrium which is responsible for the controlled behaviour of the polymerisation.

6.4.2 Synthesis of a Short Chain Initiator

The aim of this series of experiments was to produce a poly(styrene-dimethlysiloxane) copolymer by ATRP. It was therefore envisaged that the initiator would contain a PDMS component, modified at the chain-ends with a functional group containing a halide. The ATRP of styrene would then occur at the chain-ends of the siloxane resulting in the formation of an ABA-type, triblock copolymer.

To form the initiator, hydride-terminated PDMS (H-PDMS), M_n = 580, was subjected to a hydrosilylation reaction with (chloromethyl)styrene (CMS - mixture of *m* and *p*-isomers), using chloroplatinic acid as catalyst.

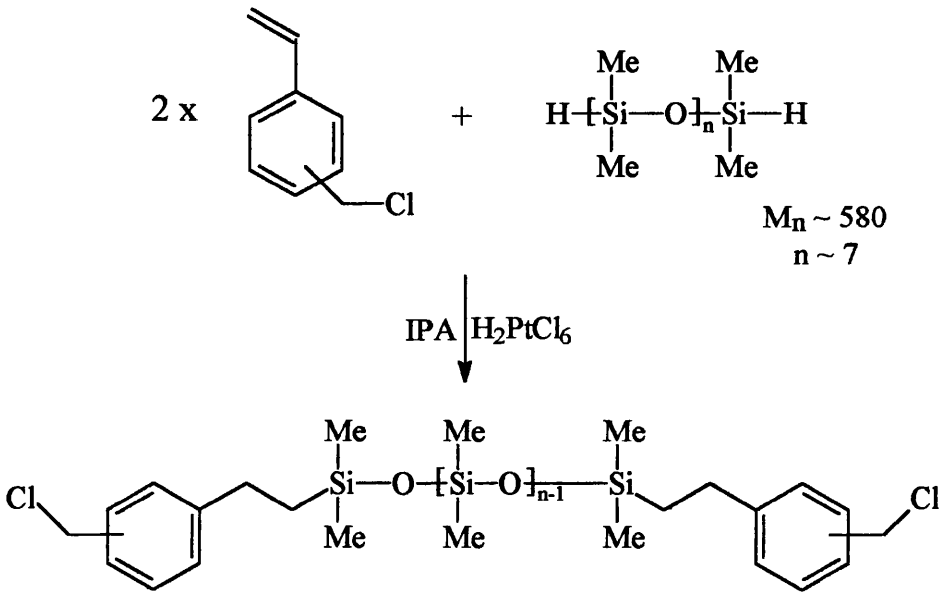

DB127 M_n ~ 885

The CMS and H-PDMS were present in a molar ratio of 2:1 to ensure that both ends of the H-PDMS were functionalised. 5 x 10^{-5} equivalents (based on the CMS) of the catalyst were present.

An M_n = 580 for the H-PDMS means that there are ~ 7 siloxane ('D') repeat units in the H-PDMS and also, therefore, the functionalised initiator (DB127). The resulting M_n of DB127 being ~ 885. The yield of the final product ranged from 60 to 80 %.

IR spectroscopy was used to ensure that the reaction had occurred. Figures 6.13 and 6.14 show the IR spectra of H-PDMS and CMS respectively. Immediately noticeable in the spectrum of H-PDMS is the peak at ~ 2125 cm^{-1} due to Si-H.

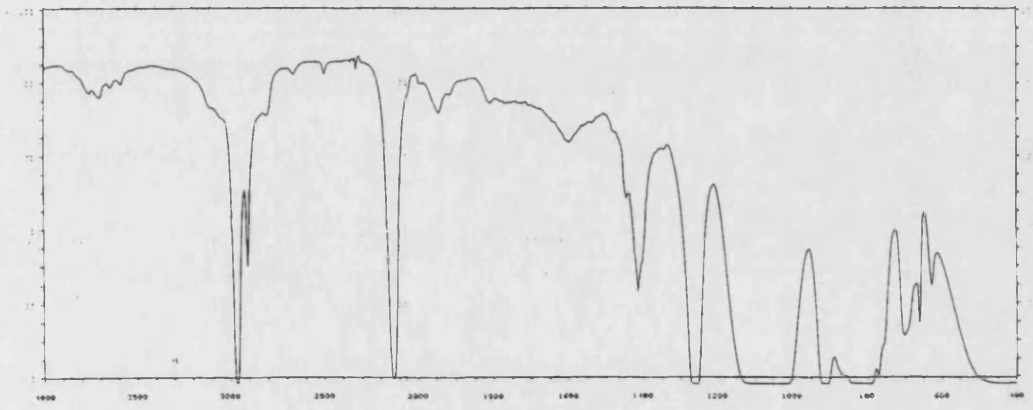

Figure 6.13 - IR spectrum of H-PDMS

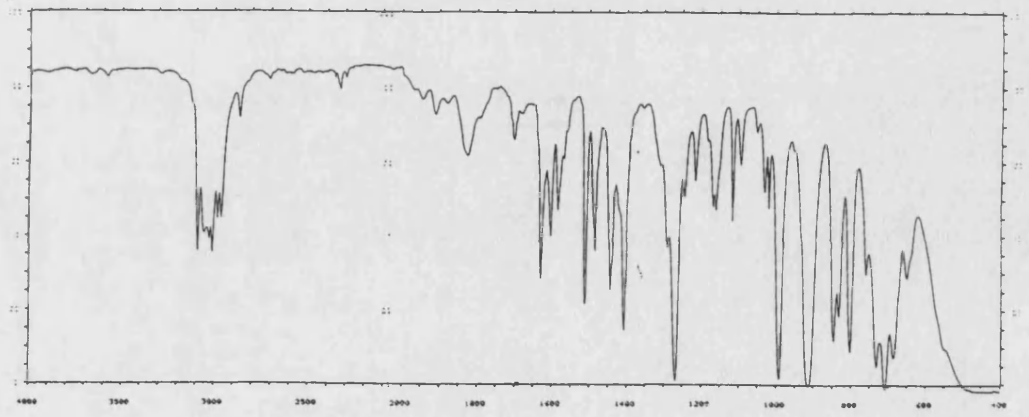

Figure 6.14 - IR spectrum of CMS

The spectrum of the product DB127 is shown in figure 6.15. It can be seen that the spectrum shows peaks due to both the H-PDMS and CMS. However, the very strong SiH peak at ~ 2125 cm^{-1} has disappeared. This confirms that the hydrosilylation has occurred and that DB127 has been produced.

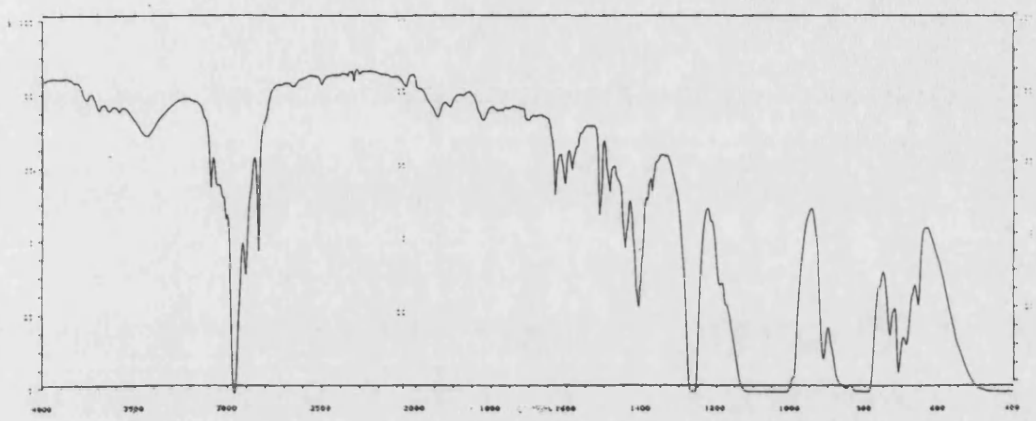

Figure 6.15 - IR spectrum of DB127

Figure 6.16 shows the ^1H NMR of DB127. From this it can be seen that the hydrosilylation occurred in two ways, i.e.

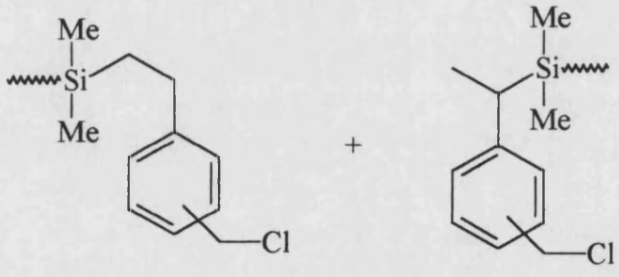

Note: only one end of the polysiloxane chain is shown for clarity.

^1H NMR (ppm, $CDCl_3$): 7.3 complex multiplet (aromatic ring), 4.7 singlet (CH_2Cl), 2.8 multiplet ($PhCH_2$), 2.3 quartet (PhCH), 1.5 multiplet (CH_3), 1.0 multiplet ($SiCH_2$), 0.2 multiplet ($SiCH_3$).

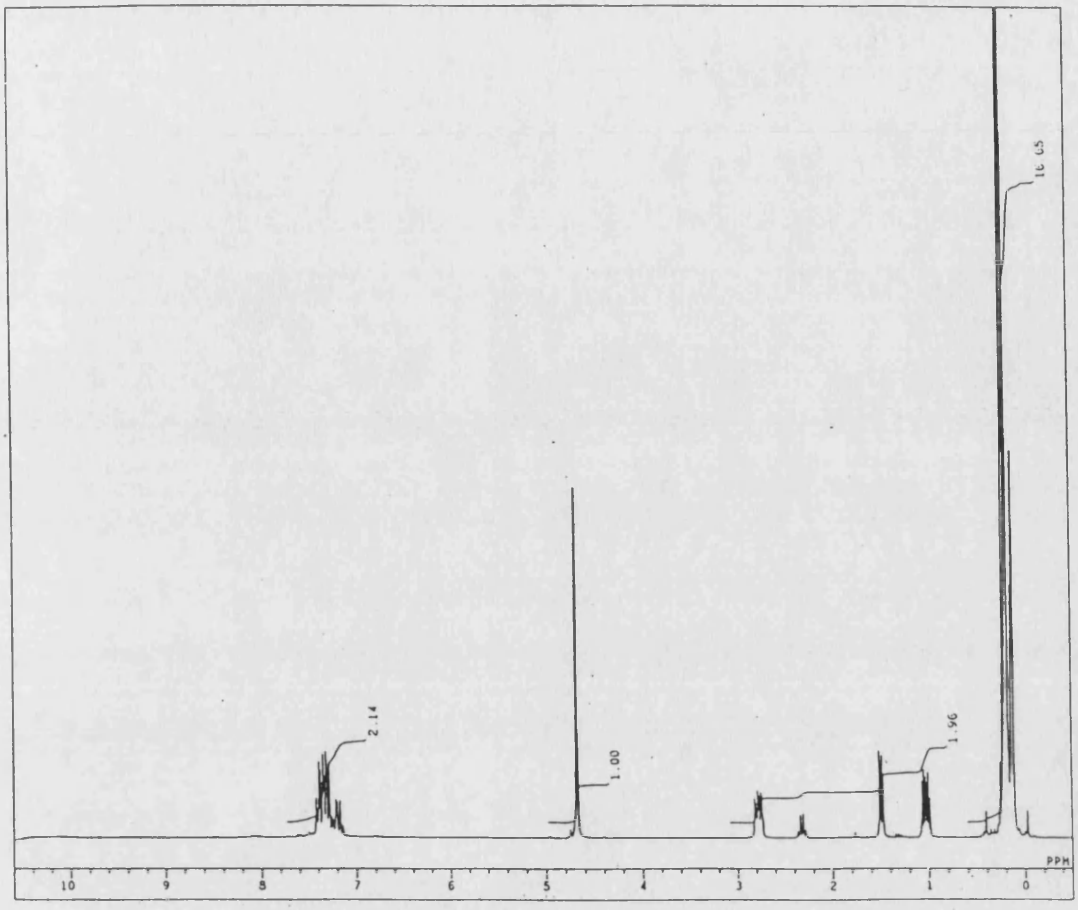

Figure 6.16 - ^{1}H NMR of DB127

6.4.3 ATRP with DB127 and Styrene

DB127 was used as the initiator for the ATRP of styrene. Copper (I) chloride was used as the catalyst with 2,2'-bipyridyl (bpy) as the complexing ligand. The molar ratio of DB127:CuCl:bpy used was 1:2:4. The ratio of DB127:styrene was 1:100. Assuming all the initiator is used and all monomer is converted to polymer, this should result in polystyrene chains being polymerised on both ends of the DB127, with each polystyrene block having approximately 50 repeat units, i.e. a triblock copolymer should be produced with the PDMS component being the centre block.

The reaction was conducted in *o*-xylene, under an atmosphere of nitrogen, at 130°C for 3 hours. The recovered polymer was obtained in a 20 % yield and was analysed by IR, ^{1}H NMR and DSC.

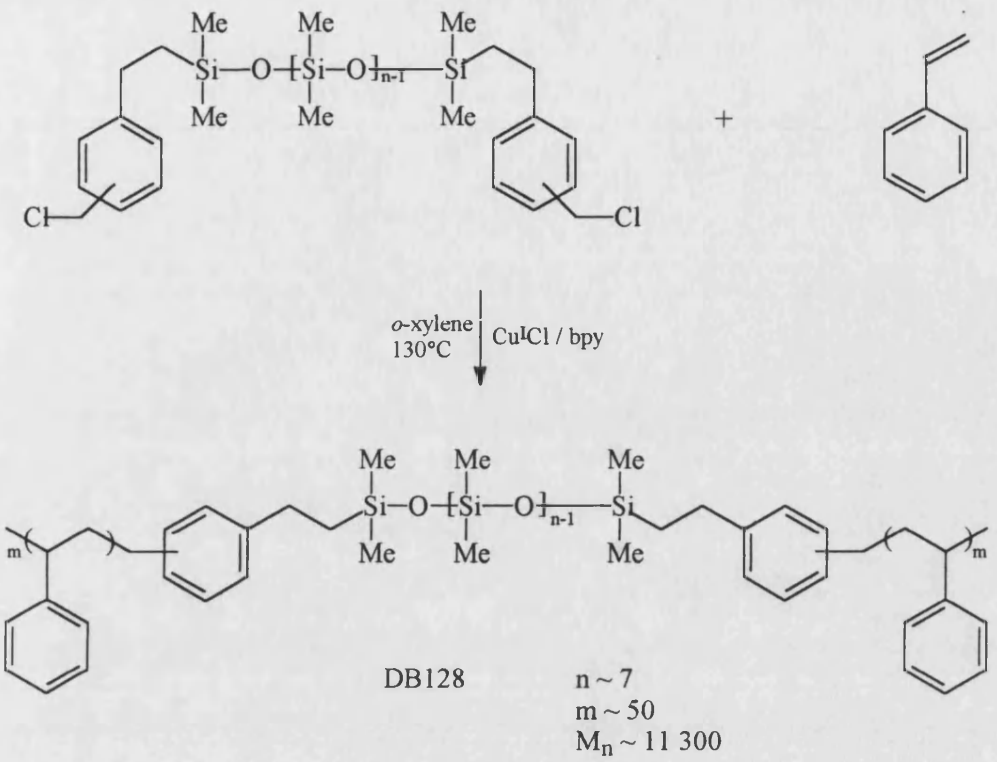

Figure 6.17 shows the IR of the recovered polymer. The characteristic spectrum of polystyrene can be clearly seen, although it is difficult to discern any contribution from the PDMS component. However, this is unsurprising given that each copolymer chain will contain a centre PDMS block of only 7 siloxane repeat units, with polystyrene terminal blocks of ~ 50 repeat units. With such a low level of PDMS, the spectrum will be dominated by the polystyrene.

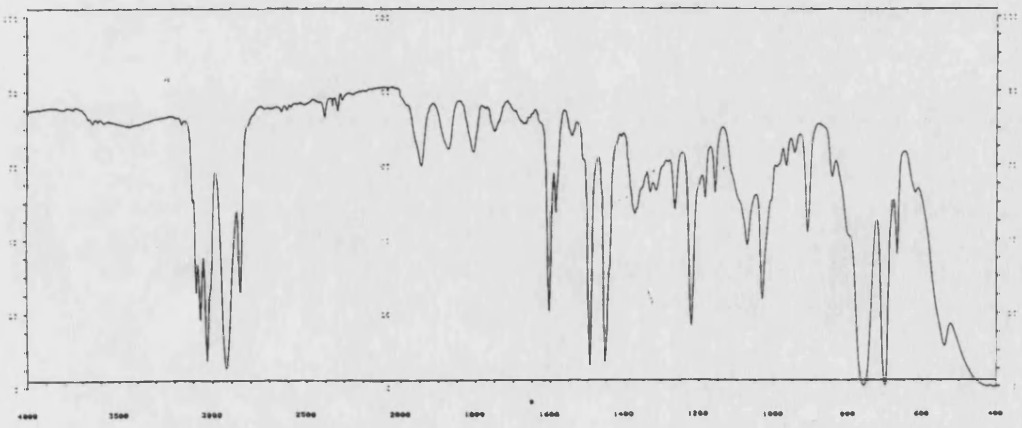

Figure 6.17 - IR spectrum of the DB127-styrene copolymer product

Figure 6.18 shows the ^1H NMR of the recovered polymer. $CDCl_3$ was used containing no added TMS. Hence the singlet seen at ~ 0.1 ppm is due solely to the PDMS block. The characteristic ^1H NMR of polystyrene is obvious. The singlet at 2.4 ppm is due to the presence of residual toluene (as a result of the recovery procedure). The IR and NMR spectra therefore confirm that the ATRP of styrene has indeed occurred and a block copolymer containing polystyrene and PDMS blocks has been produced. However, it can be seen that the integrals of the NMR spectrum indicate that the polystyrene blocks are larger than 50 repeat units long. If the expected structure had been obtained (i.e. 100 polystyrene units and 7 siloxane units in each molecule) the ratio of the polystyrene and siloxane integrals should have been 16.7:1, however, the NMR actually shows a ratio of 62:1. There are therefore 3.7 times as many protons in the polystyrene blocks as expected, so instead of each block containing 50 repeat units, there are actually ~ 185 units in each block. Given that only a 20 % yield was obtained, it is likely that not all of the initiator was used, so each block on the initiator that did react grew longer than theoretically expected.

The initiator efficiency will play a large part in determining whether or not the final molecular weight is close to the theoretical value. In ATRP a low stationary concentration of growing radicals is required and the reversible exchange between growing radicals and dormant species needs to be fast. If these conditions are met, the molecular weight will be determined by the ratio of monomer to initiator[20]. However, if the observed rate constant for the initiation step (abstraction of the halide atom from the initiator to form a radical, followed by addition of the first monomer unit to the radical) is slower than the rate constant for propagation, the result will be inefficient initiation and high molecular weight polymer will be formed throughout the polymerisation (in much the same way as in a conventional radical polymerisation). In a study of methyl methacrylate ATRP using various initiation systems, Matyjaszewski et al[21] found that the efficiency of an initiator markedly affected the observed molecular weight. For one inefficient initiator, the M_n was 3.5 times larger than expected from the initiator:monomer ratio (an actual M_n of 76 000, compared to the theoretical M_n of 22 000).

The larger than expected number of repeat units in the polystyrene blocks, shown in the NMR, can therefore be attributed to DB127 being an inefficient initiator,

with the rate of initiation being lower than the rate of propagation, and higher molecular weights than expected being obtained as a result.

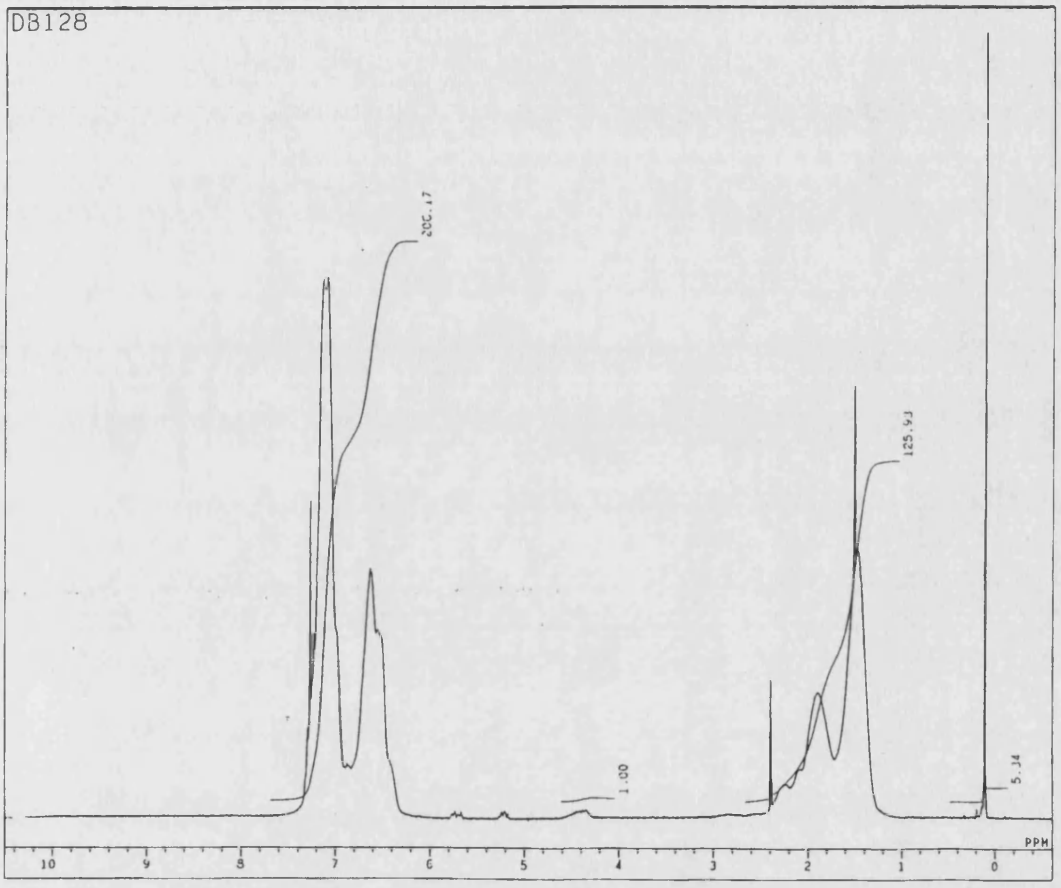

Figure 6.18 - ^{1}H NMR of the DB127-styrene copolymer product

Figures 6.19, 6.20 and 6.21 show the DSC traces obtained from the product, polystyrene and 1000 cs PDMS, respectively.

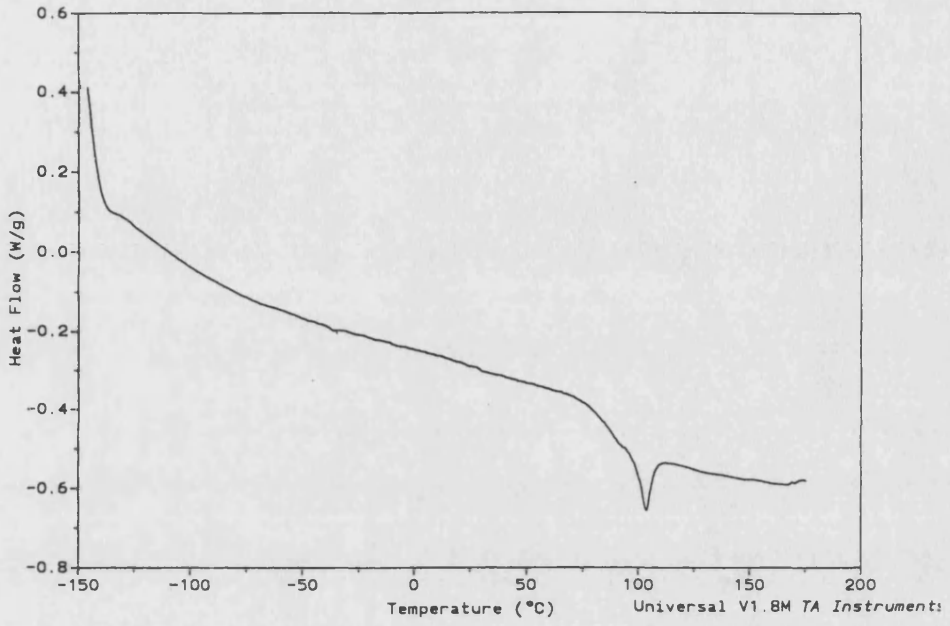

Figure 6.19 - DSC trace for the DB127-styrene copolymer product

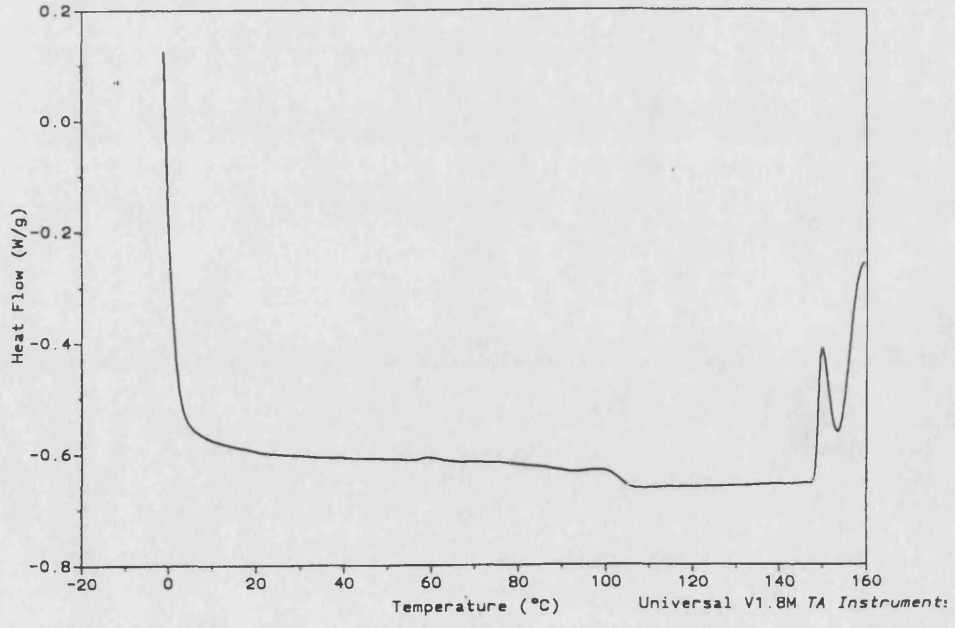

Figure 6.20 - DSC trace for polystyrene

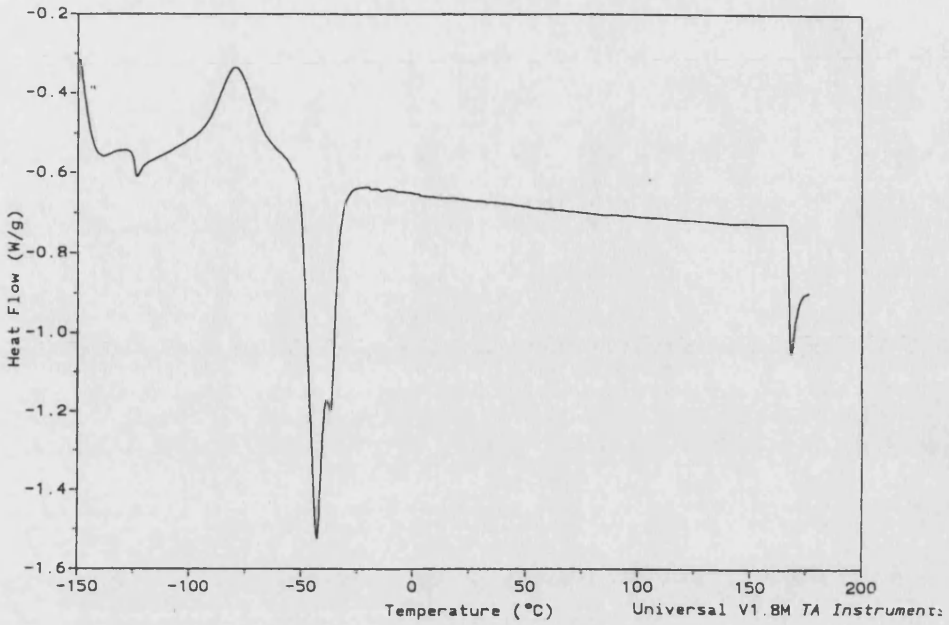

Figure 6.21 - DSC trace for PDMS

In the trace obtained with polystyrene (figure 6.20), the glass transition temperature (Tg) can be seen at 105°C. In the DSC trace for the PDMS, the Tg can be observed at approximately -125°C, while there is a prominent crystallisation exotherm at approximately -80°C followed by melting at -40°C. The much lower Tg of PDMS, compared to polystyrene, arises as a result of the much greater flexibility of the PDMS chains.

In the DSC trace from the product, there is a change of slope beginning at 75°C and ending at about 95°C, before a sudden peak centred around 100°C. The first change in slope will be due to the Tg of the polystyrene component of the copolymer. Thus, the presence of the flexible PDMS block in the copolymer has had a marked effect on the thermal behaviour of the polystyrene, even though there are only 7 siloxane repeat units in each copolymer chain, and the Tg has fallen from 105°C to ~ 85°C. It is possible that the peak at 100°C could be due to the melting transition of the copolymer, however a far more likely explanation is that it is due to the presence of water either in the sample, or on the sample container.

None of the characteristic PDMS features can be seen in the DSC trace of the product, however, this is unsurprising given that it contains such a small amount of PDMS, with the polystyrene component being much larger than expected.

These results show that ATRP using a siloxane-based initiator can be used to produce a PDMS-polystyrene copolymer. However, given that the polymerisation was conducted at 130°C, it is possible that the free radical polymerisation of the styrene could have been thermally initiated and there could therefore be homopolymer present with the product. In order to determine whether any homopolymer will form under ATRP conditions, a further three experiments were performed. The ATRP conditions were kept the same, however, one or more of the reagents was omitted (table 6.3).

Table 6.3 - Reaction conditions

Experiment	Initiator (DB127)	Catalyst/ Ligand	Styrene	Product	Yield (%)
1	No	Yes	Yes	Yes	0.1
2	Yes	No	Yes	Yes	25
3	No	No	Yes	Yes	25

When DB127 is removed from the system negligible polymerisation occurs. Removing the CuCl/bpy complex from the reaction, however, results in the thermal polymerisation of the styrene occurring, with a 25 % yield of polystyrene being obtained whether the initiator (DB127) is present or not. The presence of the CuCl/bpy complex appears to completely inhibit the thermal polymerisation of styrene. Thus, polymerisation only occurs if the initiator is present (giving rise to ATRP and the block copolymer) or the CuCl/bpy complex is removed (resulting in the thermal polymerisation of the styrene). Therefore, under the ATRP conditions used, a negligible amount of polystyrene homopolymer will be thermally produced, and the product will be the copolymer produced by ATRP.

6.4.4 ATRP Under Ultrasound

Two experiments were conducted in an attempt to perform ATRP under ultrasound. In the first, the heating (at 130°C) was replaced by sonication using the ultrasonic bath, at room temperature, for 3 hours. The same quantity of reagents as described in section 6.4.3 were used. In the second experiment, the reaction was conducted using the ultrasonic horn at a temperature of 90°C and an intensity of 17.1 Wcm^{-2}.

Because of the much bigger volume of the sonication vessel, the amount of reagents used had to be increased. Hence, twice as much DB127, CuCl, bpy and styrene were used, with the *o*-xylene added to bring the total volume to 50 cm^3.

When using the ultrasonic bath, no polymer was recovered. This result can be attributed to the low temperature at which the sonication was conducted. The water in the bath was at room temperature (~ 22°C) at the start of the sonication. After 3 hours of continuous operation the temperature had increased to 30°C (the attenuation of the ultrasound resulting in a bulk heating of the water). Given that the 'silent' ATRP was conducted at 130°C, room temperature is obviously too low for ATRP to occur with this particular system of initiator/catalyst.

In the second experiment some product was recovered, but only in a yield of less than 1 %. Again it would seem that the temperature was too low for the ATRP to proceed at a reasonable rate. The sonication was conducted at 90°C as this was the highest temperature that could be obtained using a water bath to heat the reaction. Thus, in order to see if ultrasound does have an effect on ATRP, the sonications need to be conducted at 130°C so that the results can be compared to the 'silent' ATRP.

These two experiments with ultrasound have therefore proved inconclusive, as the temperatures at which they were conducted were too low for ATRP to proceed at a reasonable rate. Further experiments obviously need to use temperatures comparable to that used in the 'silent' ATRP, if any ultrasonic enhancement is to be seen.

6.4.5 ATRP with Methyl Methacrylate

The ATRP of DB127 was attempted using methyl methacrylate (MMA) in place of styrene. The amounts of the reactants were identical to those used with styrene. This means that the molar ratio of MMA:DB127 was slightly different

compared to the ATRP with styrene; 106:1 as opposed to 100:1. Assuming complete conversion, this should produce an ABA-type triblock copolymer with each PMMA block having ~ 53 repeat units.

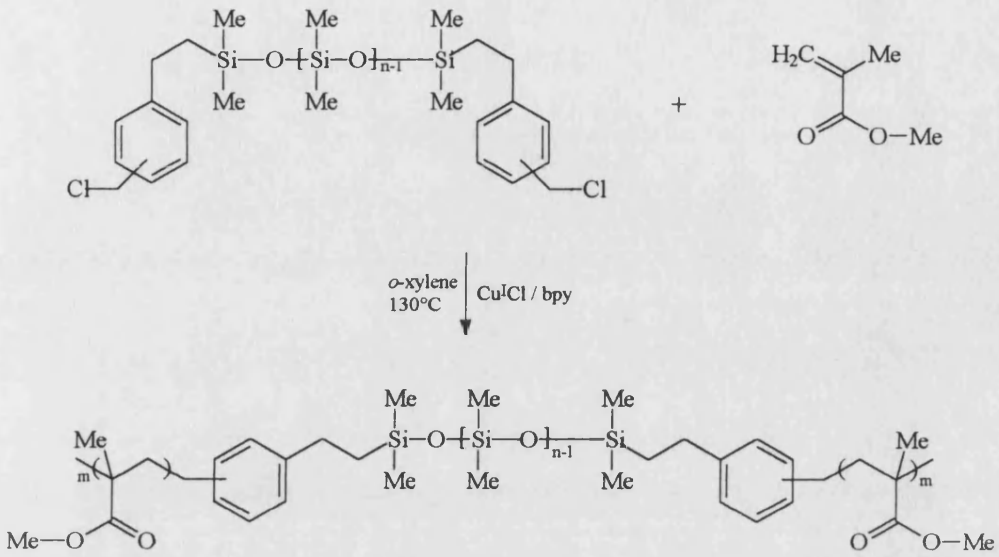

DB130 $n \sim 7$, $m \sim 53$, $M_n \sim 11\,500$

The method was identical to that used for styrene. The resulting polymer was produced in a 17 % yield and was analysed by IR, DSC and NMR.

Figure 6.22 shows the IR spectrum of the product.

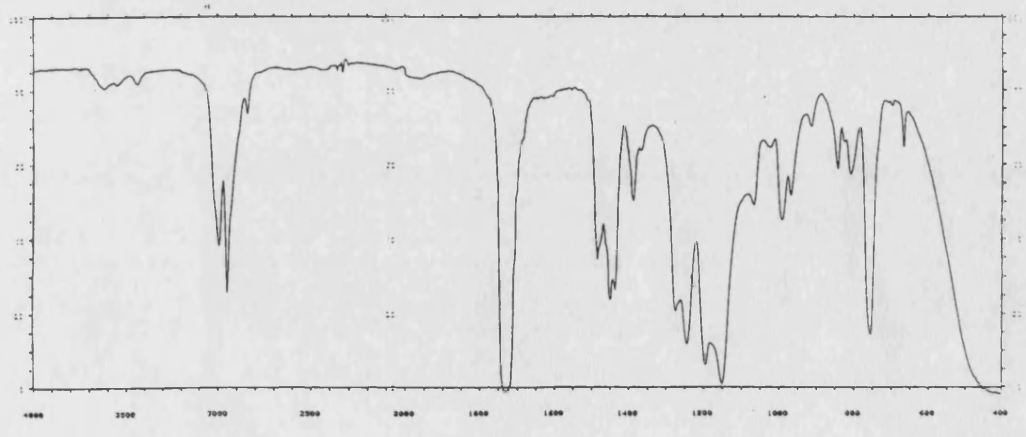

Figure 6.22 - IR spectrum of the DB127-MMA copolymer product

The spectrum is clearly that of PMMA, however, as with the ATRP with styrene, it is not possible to discern any PDMS component as a result of the PDMS blocks being so small. The ^1H NMR of the product (figure 6.23) shows the characteristic PMMA resonances at 1, 2 and 3.6 ppm. The spectrum was run in $CDCl_3$ with no TMS, hence the singlet at 0.1 ppm is due to the PDMS component in the copolymer. The aromatic resonances at 7.3 ppm are unusual and it could be that this is due to unreacted initiator that was not removed from the copolymer product. However, comparison of the aromatic integral with the siloxane integral at 0.1 ppm discounts this. The ratio of aromatic:siloxane protons in the initiator is 1:6 and therefore, if unreacted initiator is present, the integrals of the NMR should show this ratio (or greater - because of the siloxane component of the copolymer). However, the observed ratio is ~ 1:1, so the resonance at 7.3 ppm cannot, therefore, be due to unreacted initiator. The resonance at 2.4 ppm can be assigned to the methyl protons of residual toluene from the recovery procedure. The ratio of aromatic:methyl protons in toluene is 5:3, and this is also the ratio seen for the integrals of the 7.3 and 2.4 ppm resonances, suggesting that residual toluene is responsible for the observed aromatic resonances.

As with the ATRP with styrene, the integrals of the PMMA and siloxane resonances suggest a larger molecular weight than theoretically expected for the product. If the theoretical product was obtained, the PMMA:siloxane integrals should be in the ratio of 17.7:1. However, the NMR actually shows a ratio of 32:1, i.e. there are 1.8 times as many PMMA protons as expected. Therefore, each block contains ~ 95 repeat units as opposed to the theoretical 53 repeat units. As explained previously, the larger than expected molecular weight can be attributed to a low initiator efficiency; the rate of propagation being faster than the rate of initiation, resulting in high molecular weight polymer being formed during the polymerisation.

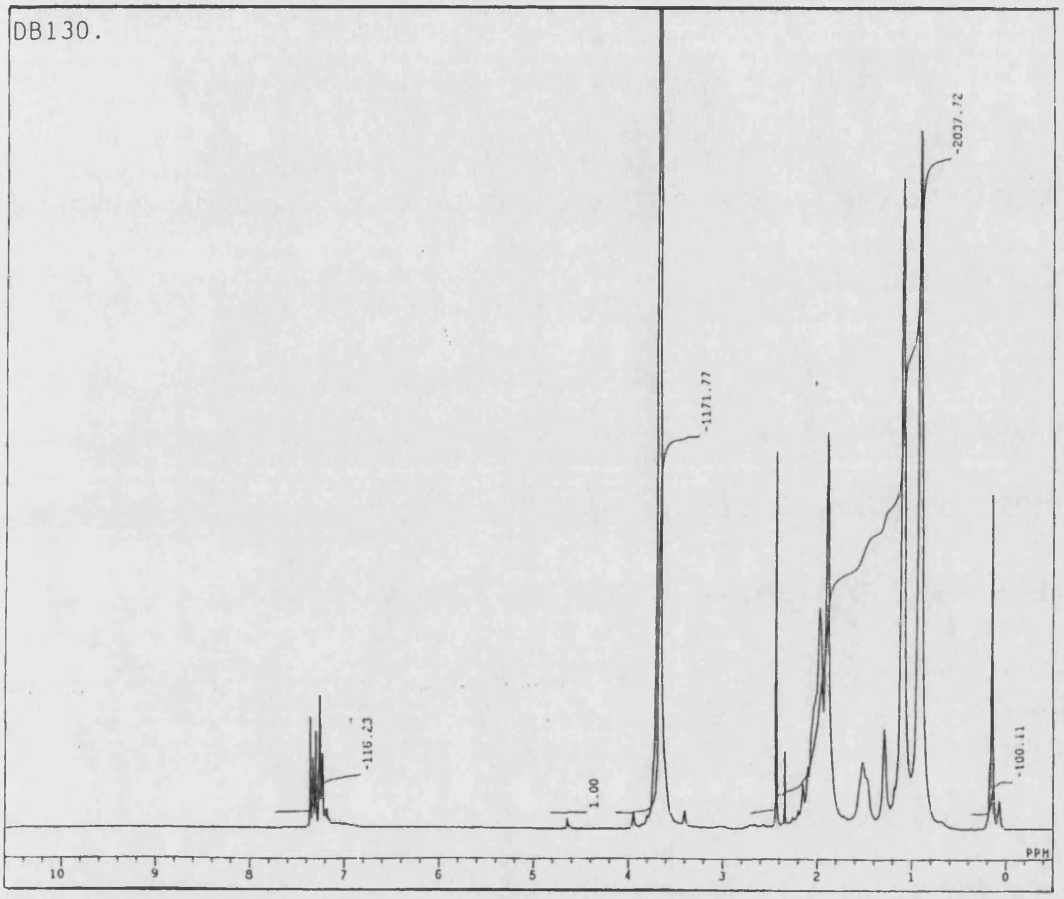

Figure 6.23 - ^{1}H NMR of the DB127-MMA copolymer product

The DSC of the product is shown in figure 6.24, while that for PMMA is shown in figure 6.25. In figure 6.25, the Tg of the PMMA is visible at ~ 110°C, however, in the copolymer the Tg has dropped to ~ 25°C. The inclusion of the PDMS block appears to have drastically changed the thermal behaviour of the PMMA. Much more so than it did with the polystyrene. The lowering of the Tg being a consequence of the PDMS block in the copolymer chains giving increased flexibility to the chains, compared with the PMMA homopolymer.

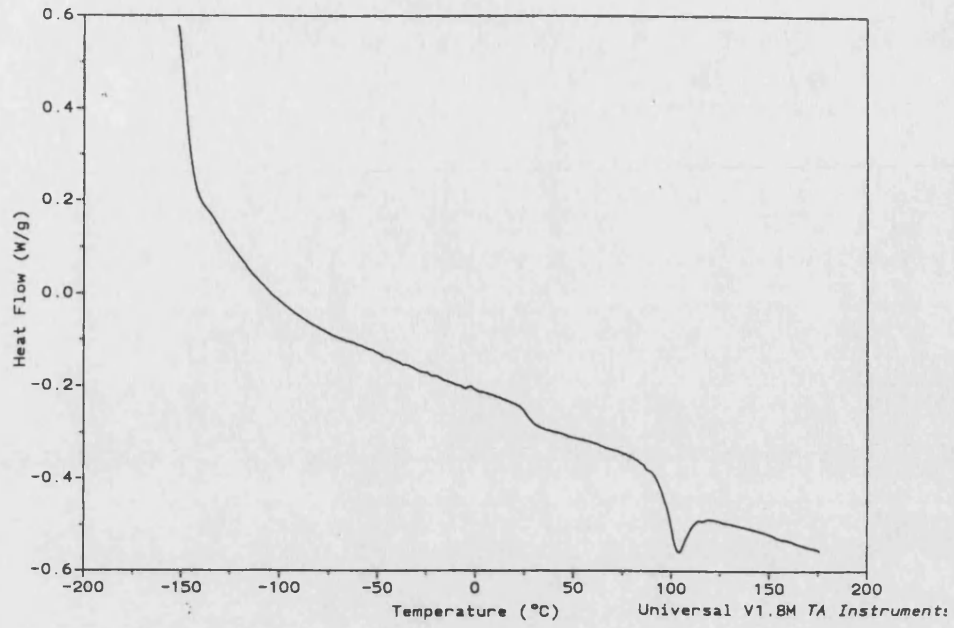

Figure 6.24 - DSC trace of the DB127-MMA copolymer product

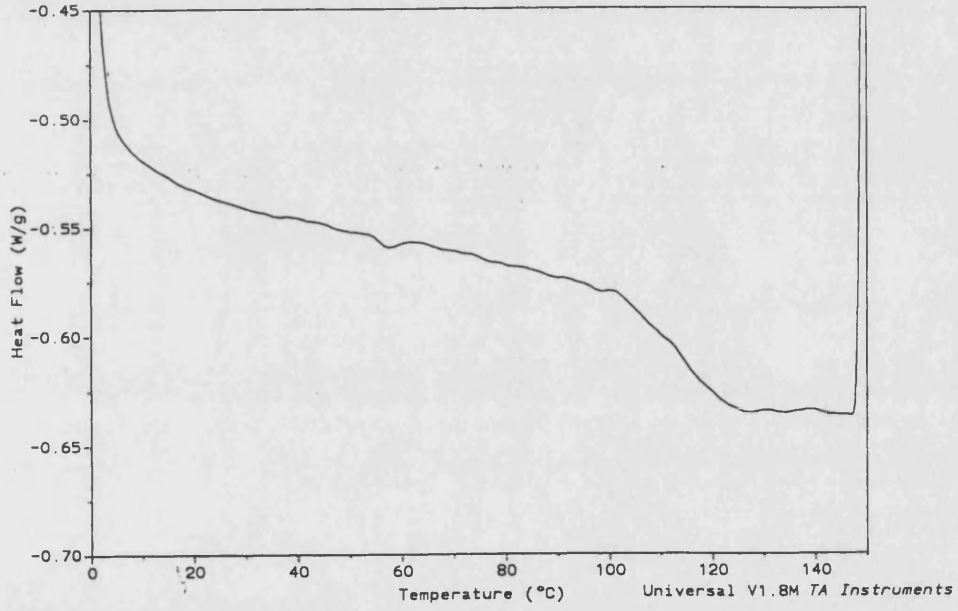

Figure 6.25 - DSC trace of PMMA

The DSC trace of the product also appears to show a melting peak centred around 100°C, however, as for the PDMS-polystyrene copolymer, this could actually be due to the presence of water. Again, none of the characteristic features of the PDMS component are seen in this DSC trace, but this is not unexpected given that the proportion of PDMS in the copolymer is so low and the PMMA blocks are much larger than expected.

The ATRP method has therefore been shown to work with methyl methacrylate as well as styrene. The incorporation of the small, flexible, PDMS blocks has a marked effect on the observed Tg for both polystyrene and PMMA.

6.4.6 Synthesis of a Longer Chain Initiator

Because the first initiator contained only 7 siloxane repeat units, an attempt was made to synthesise a possible ATRP initiator with a greater number of siloxane units in the chain. Again, a hydride-terminated PDMS was reacted with CMS via a hydrosilylation reaction. The PDMS used had an M_n = 5770, giving approximately 77 repeat units in each chain. As before, chloroplatinic acid was used as the catalyst and the CMS and H-PDMS were present in a molar ratio of 2:1 to ensure that both ends of the PDMS were functionalised. 5 x 10^{-5} equivalents (based on the CMS) of the catalyst were present.

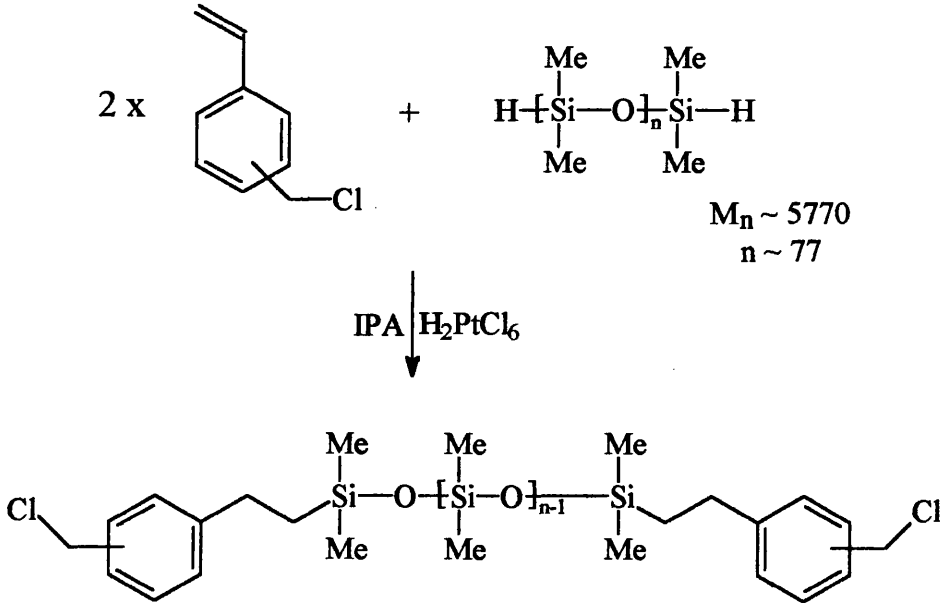

DB137 M_n ~ 6075

The H-PDMS was initially added to the CMS/H_2PtCl_6 over a period of 2.5 hours at room temperature, and then stirred for a further 1 hour. However, the IR spectrum of the reaction mixture clearly showed the Si-H peak at 2150 cm^{-1}, indicating that no reaction had occurred. The solution was warmed with a hot air gun and stirred for a further 1.5 hours, but again the IR spectrum showed that the reaction

had still not occurred. The reactants were finally heated to 50°C, with stirring, for a further 24 hours and the IR spectrum after this time showed no Si-H present.

The product layer was separated from the IPA layer and placed in a vacuum oven at 70°C for 48 hours. The final yield of the product, DB137, obtained was 90 %.

Figure 6.26 shows the IR spectrum of the H-PDMS, while figure 6.27 shows that of the product.

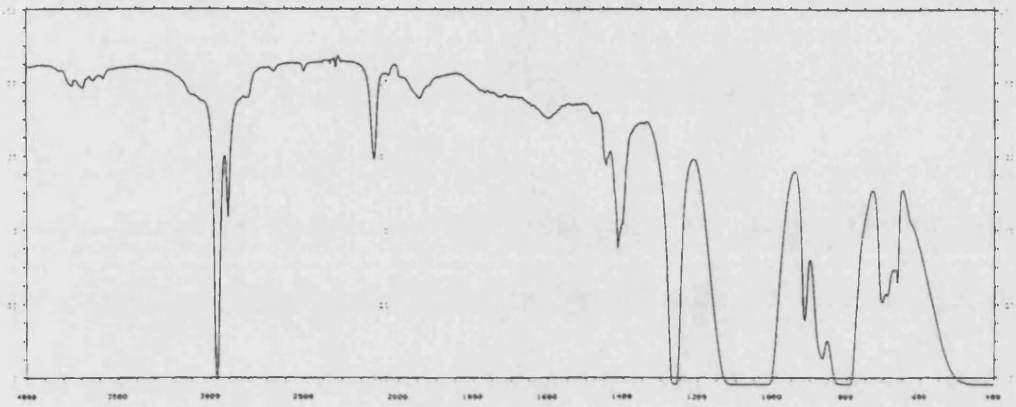

Figure 6.26 - IR spectrum of H-PDMS, DP ~ 77

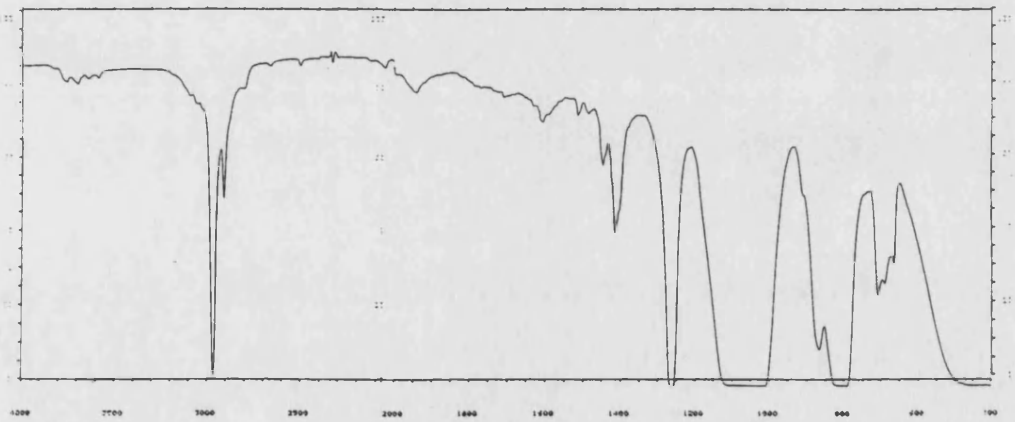

Figure 6.27 - IR spectrum of product DB137

From the spectra, the disappearance of the Si-H from the hydride-terminated PDMS is obvious. It would appear that the spectrum of the product is virtually

identical to that for the H-PDMS, with only the Si-H peak at 2150 cm^{-1} missing. There do not seem to be any peaks that could be attributed to the CMS, as there are in the spectrum of DB127 - the initial initiator synthesised. However, it has to be remembered that DB127 contained only 7 siloxane repeat units in each chain, while DB137 contains an average of 77 repeat units per chain. Hence, there is a much smaller proportion of CMS in DB137 and the spectrum is then dominated by the PDMS component of the molecule.

6.4.7 ATRP with DB137 and Styrene

DB137 was used as the initiator for the ATRP of styrene. As with the previous ATRP's conducted, CuCl was used as the catalyst with bpy as the complexing ligand. The only difference in method being that the solution was heated for 5 hours instead of 3 hours. The molar ratios of DB137:CuCl:bpy and DB137:styrene were identical to those used before. Assuming complete conversion, this should result in each polystyrene block, at either end of the chain, having ~ 50 repeat units, giving an M_n of approximately 16 500 for the copolymer product.

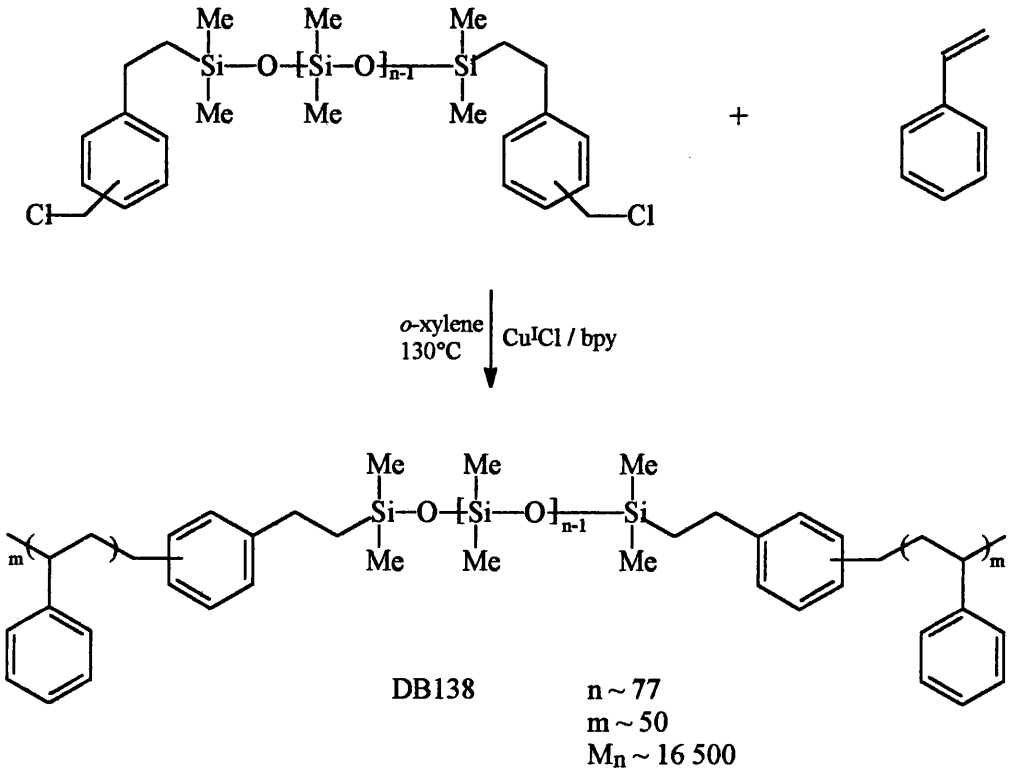

DB138 n ~ 77
m ~ 50
M_n ~ 16 500

The reaction conditions were identical to those for the ATRP of DB127 with styrene and the recovered polymer was obtained in a 50 % yield. The product was analysed by IR, ^{1}H NMR and DSC.

Figure 6.28 shows the IR of the recovered polymer. The presence of both the PDMS and the polystyrene components is immediately obvious in the spectrum.

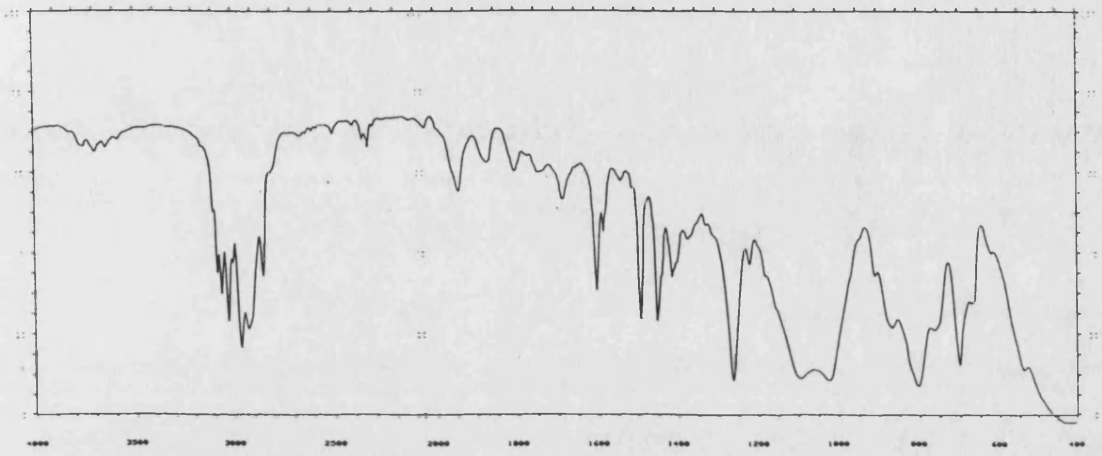

Figure 6.28 - IR spectrum of the DB137-styrene copolymer product

Figure 6.29 shows the ^{1}H NMR of the recovered polymer. The characteristic resonances of polystyrene are evident, however, the much larger PDMS block has given rise to a large singlet visible at 0.1 ppm (note, there was no TMS present).

As with the previous ATRP's using the short chain initiator, analysis of the NMR integrals show that the expected degree of polymerisation for the polystyrene blocks has not been obtained. With the expected structure of 50 polystyrene repeat units in each block, the NMR should show polystyrene and PDMS integrals with a ratio of 1.7:1 (polystyrene:PDMS), however, the actual ratio is only 0.94:1, indicating that each block only contains ~ 27 repeat units, not 50. This result, and the fact that when using the longer chain initiator (DB137) the polymerisations were conducted for 5 hours (as opposed to the 3 hours with DB127), implies that the rate of polymerisation with DB137 is slower than with DB127. Obviously, because complete conversion of monomer to polymer had not been achieved, it is not possible to say whether or not the final molecular weight would be close to the theoretical value, i.e. from this result it is not clear whether or not DB137 is a more efficient ATRP initiator than DB127.

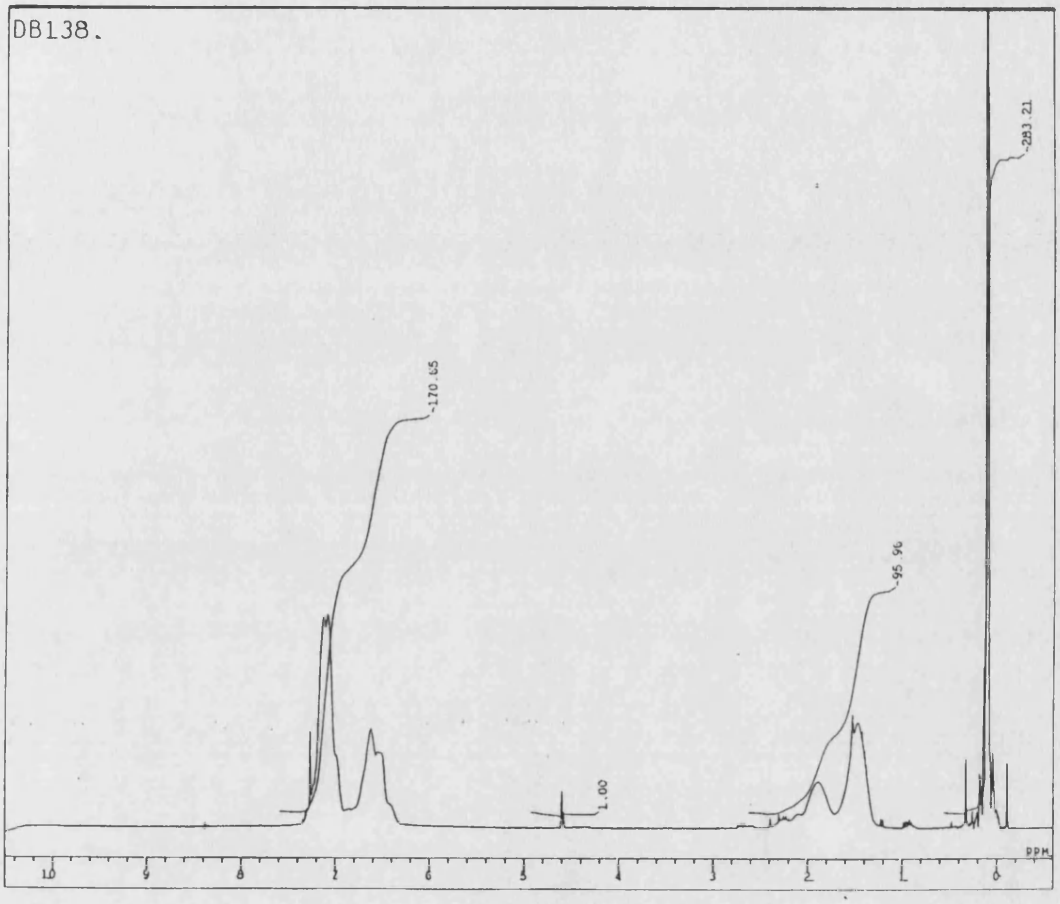

Figure 6.29 - ^{1}H NMR of the DB137-styrene copolymer product

Figure 6.30 shows the DSC trace obtained from the product. The melting temperature of the PDMS block at approximately - 50°C is very clear and is a consequence of the copolymer product containing a much longer PDMS block, than the previous copolymers (with DB127). The Tg of the polystyrene is just visible at ~ 80°C, and this is a similar value to that for the DB127-styrene copolymer obtained previously, although it has become much less defined as a result of the increased proportion of PDMS, and the significantly lower amount of polystyrene, in the product. The lowering of the Tg (relative to polystyrene homopolymer) can be attributed to the PDMS giving increased flexibility to the polymer chains, so that they become mobile at a lower temperature. However, the Tg of the polystyrene blocks is

less noticeable, and the temperature not as sharply defined, as the chains are already very flexible near that temperature, because of the longer PDMS blocks.

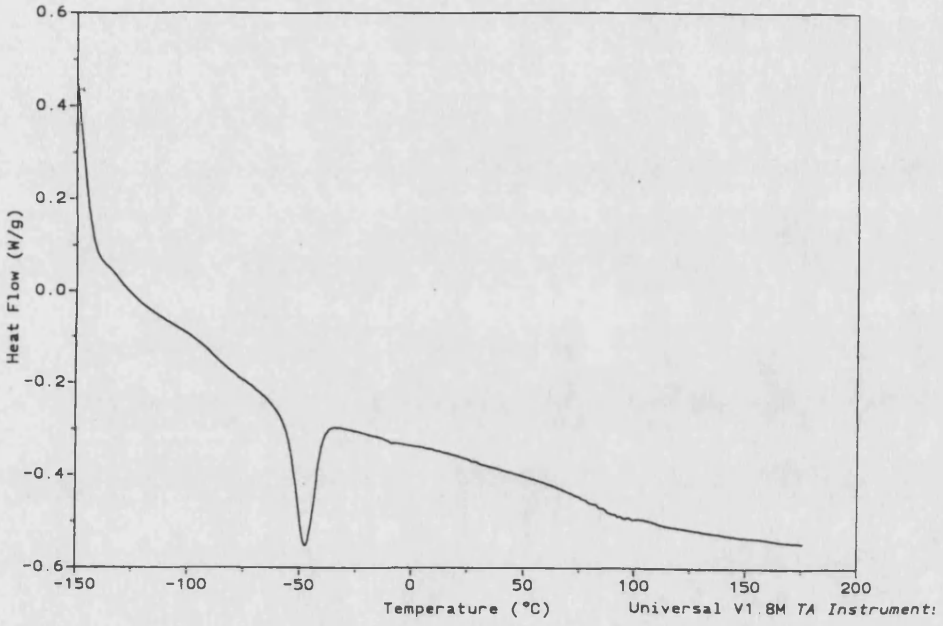

Figure 6.30 - DSC trace of the DB137-styrene copolymer product

6.4.8 ATRP with DB137 and MMA

The ATRP of DB137 with MMA was conducted in exactly the same way as with DB127 and MMA, except the reaction was heated for 5 hours instead of 3 hours. The ratios of DB137:CuCl:bpy and DB137:MMA were identical to those used previously, hence, assuming complete conversion, each block of PMMA should be approximately 53 repeat units long, and the resulting polymer should have an M_n of approximately 16 700.

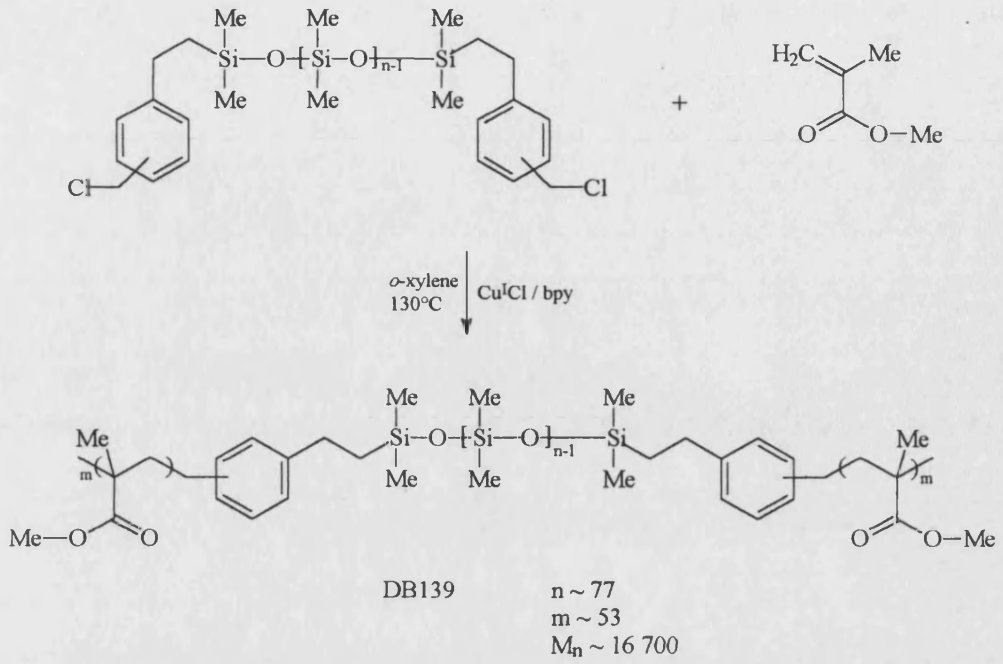

The recovered polymer was obtained in a 58 % yield. Figure 6.31 shows the IR spectrum of the polymer.

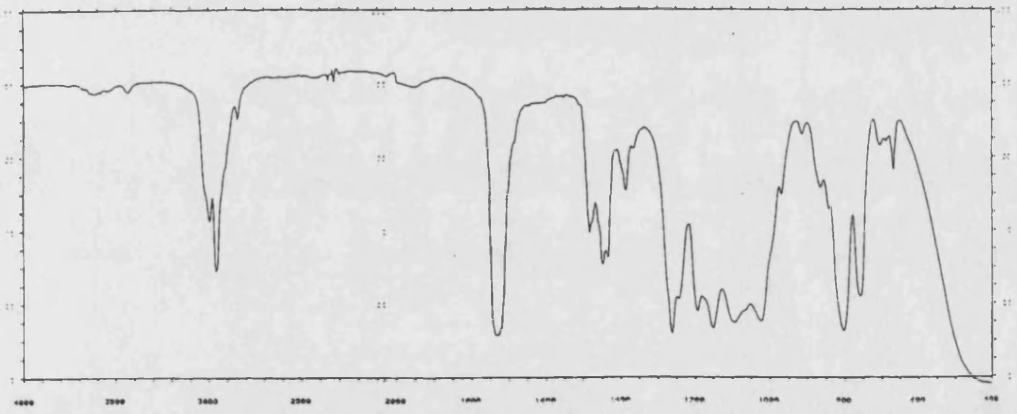

Figure 6.31 - IR spectrum of the DB137-MMA copolymer product

The IR spectrum clearly shows the presence of both the PDMS and PMMA components in the product.

Figure 6.32 shows the ^1H NMR of the product, the characteristic resonances of PMMA appearing at 1, 2 and 3.6 ppm, while the PDMS gives rise to the singlet at

0.1 ppm. The integrals for the PMMA and PDMS resonances should be in the ratio of 1.8:1 (PMMA:PDMS), if each PMMA block contains 53 repeat units. However, the observed ratio is 2.28:1 and the PMMA blocks are therefore 1.26 times larger than expected, i.e each block contains ~ 67 repeat units, and not 53. Thus, as with the ATRP's with the short chain initiator (DB127), and unlike the ATRP with styrene, the actual block lengths are longer than theoretically expected, although they are not as long as the PMMA blocks from the ATRP of DB127 with MMA (section 6.4.5). As with DB127, the higher than expected molecular weight suggests that the rate of initiation is not as fast as the rate of propagation, resulting in inefficient initiation. However, it is clear from both ATRP's that the rate of polymerisation is clearly slower with the longer chain initiator (DB137) than with the short chain initiator (DB127). The initiation will therefore be more efficient with DB137, than with DB127, and the molecular weight will be closer to the theoretical value.

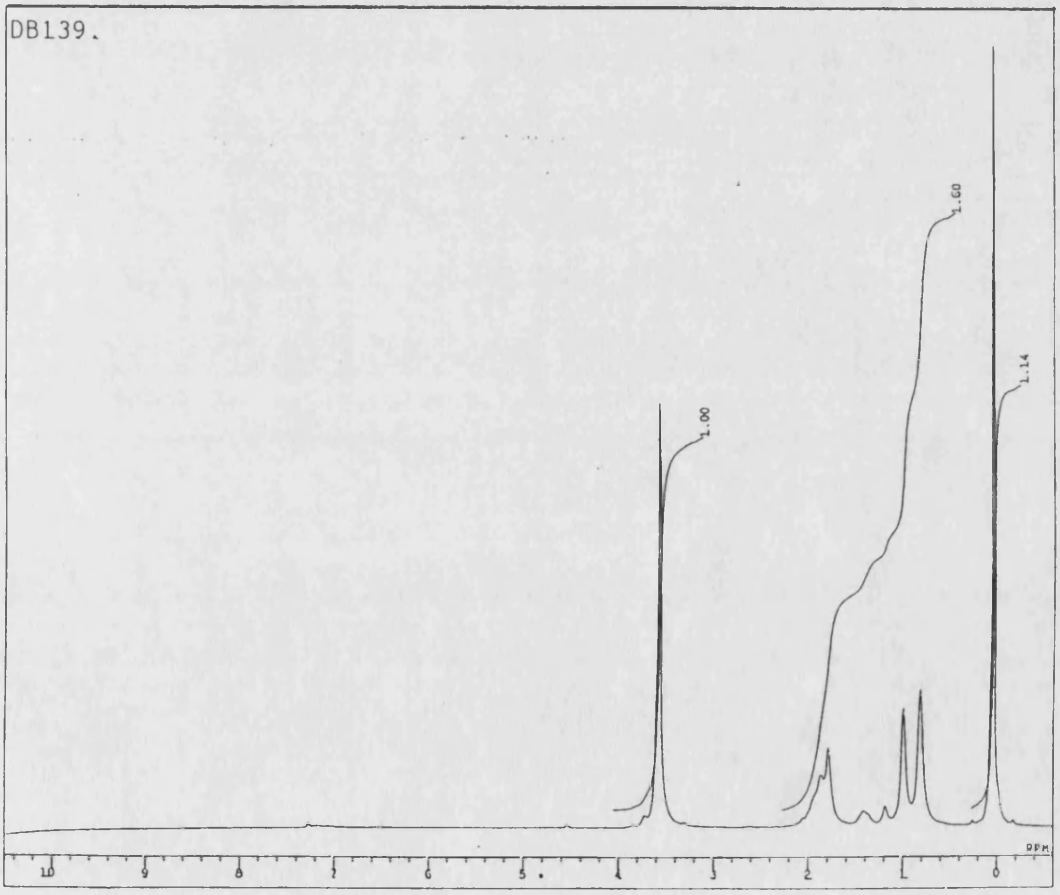

Figure 6.32 - ^{1}H NMR of the DB137-MMA copolymer product

Figure 6.33 shows the DSC trace obtained for the product. The Tg of the siloxane can be seen at approximately -125°C, while the melting endotherm is visible at about -40°C. The Tg of the PMMA appears to be at ~ 125°C. This is similar to the Tg of PMMA homopolymer. However, the product obtained with DB127 appeared to have a much lower PMMA Tg as a consequence of the PDMS blocks imparting flexibility to the chains as a whole. Also, the changes in heat flow do not appear to be as large. The smaller changes in heat flow can be attributed to the fact that there is a much smaller amount of PMMA in this product, compared to the previous product, as the PDMS blocks are so much larger. However, the fact that the DSC trace appears to show both the PDMS and PMMA features at the temperatures expected of the homopolymers, could imply that the PDMS-PMMA copolymer exists as a phase-separated material, i.e. phases of the PDMS blocks dispersed in a phase of the PMMA blocks (or vice versa). In this way, although the product is a copolymer, each different phase will behave like its parent homopolymer.

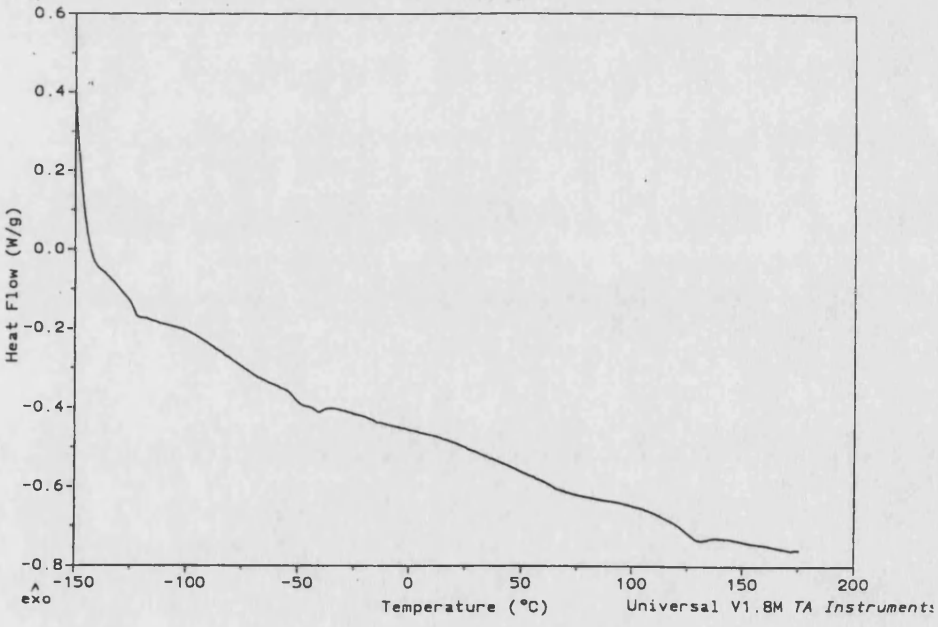

Figure 6.33 - DSC trace of the DB137-MMA copolymer product

6.5 Conclusions

Copolymers of polysiloxanes with organic polymers are important materials as they can display the desirable properties of the polysiloxane, but show improved mechanical properties. Therefore, possible routes to their synthesis are of much interest.

Sonication of PIB with MMA resulted in the degradation of the PIB. The free radicals generated at the cleaved chain-ends initiated the polymerisation of the MMA to form the copolymer. In an analogous experiment, PDMS was sonicated with either styrene or MMA to see if the ions formed when the PDMS chains are cleaved could be used to initiate the ionic polymerisation of the monomer. Attempts conducted using the ultrasonic bath and the ultrasonic horn proved unsuccessful. The probable reason for this being that the active species generated on chain cleavage are poor initiators for the ionic polymerisation of the vinyl monomers.

Using BuLi as an initiator was also unsuccessful in producing copolymers. When added to a solution of styrene and D_4, BuLi selectively polymerised the styrene. No siloxane was incorporated into the polymer. When added to a solution of styrene and D_3, the D_3 was selectively polymerised. No styrene was incorporated into the polymer. This is a result of the higher reactivity of D_3 due to the fact that it is a strained ring. A method that has been shown to be successful by other workers is to use the BuLi to initiate the polymerisation of styrene, and then add the D_3. The polystyryl anion will then initiate the D_3 ring-opening to produce the copolymer[56].

ATRP was employed successfully to produce copolymers of PDMS with polystyrene and PMMA. Two siloxane-based initiators, of differing chain lengths, were used to initiate the ATRP of styrene and methyl methacrylate, resulting in the formation of ABA-type triblock copolymers with the PDMS component being the centre block. This technique has also been used by Matyjaszewski et al[143] who used siloxane-based initiators to produce copolymers of PDMS with polystyrene. Although in addition to the triblock copolymers, they also produced graft copolymers of polystyrene from a PDMS backbone.

Apart from the ATRP of DB137 with styrene, all the other ATRP's resulted in the polymer blocks (polystyrene or PMMA) being larger than theoretically expected. This effect was more pronounced for the short chain initiator which, along with the shorter polymerisation time (compared to the longer chain initiator), implies that the

rate of polymerisation is faster with the short chain initiator. For efficient ATRP, the rate of initiation needs to be faster than the rate of propagation so that all of the chains grow at the same rate. However, both initiators used resulted in larger than expected degrees of polymerisation and this can be attributed to inefficient initiation - the rate of initiation being slower than the rate of propagation. These initiation systems, although producing the required copolymers, are therefore not very efficient and do not produce copolymers with molecular weights close to the theoretical value. Further work in this area should therefore investigate improving the efficiency of these initiators.

The copolymers produced using ATRP displayed interesting thermal behaviour, and these require further investigation. The short chain PDMS has the effect of lowering the Tg in both the polystyrene and PMMA blocks (compared to the respective homopolymers), and this can be attributed to PDMS being very flexible. The copolymer of polystyrene with the longer chain PDMS also displayed a lowering of the polystyrene Tg, although the Tg was not well defined and the DSC trace was dominated by the PDMS melting endotherm - a result of the long PDMS block and the shorter than expected polystyrene blocks. The DSC trace from the copolymer of the longer chain PDMS with PMMA suggests that this copolymer exists as a phase-separated material, as it displayed the characteristic behaviour of the respective homopolymers.

ATRP was only conducted under ultrasound twice in this work and no effect was observed. However, this is probably a consequence of the temperature not being sufficiently high for the polymerisation to proceed at a reasonable rate, as opposed to there being no effect whatsoever from the ultrasound. The results from the ultrasonic experiments are therefore inconclusive.

ATRP has been proposed to proceed via a radical mechanism, and ultrasound is known to affect those reactions that involve radicals[94,95]. Hence, ultrasound may well affect ATRP and this area of research remains to be explored.

Chapter 7

Conclusions

7 CONCLUSIONS

The aim of this work was to apply sonochemical techniques to the synthesis and modification of poly(dimethylsiloxane). To enhance polymerisation and to control the structure of the polymer.

Subjecting a polymer solution to an ultrasonic field results in the polymer chains being cleaved - a consequence of cavitation. In this work the ultrasonic degradation of PDMS, in toluene and D_4, was studied. The effect on degradation of changing the ultrasonic intensity, solution temperature and solution concentration was investigated. For both solvents, the fastest rates of degradation were obtained with higher intensities, lower temperatures and lower concentrations, leading to lower molecular weights and narrower polydispersities. These effects can be explained in terms of the cavitation process and how this is affected by changes in the experimental conditions. The degradation in D_4 was found to occur similarly to that in toluene. This was attributed to the fact that the enthalpies of vapourisation for the two liquids are very similar. Thus, their effect on cavitation, and therefore degradation, will also be similar. The Schmid and Ovenall kinetic models were used to quantify the rate of degradation. Both models were found to give good fits to the experimental data and they allowed comparisons between the degradations to be made. Thus, by manipulation of the experimental conditions the degradation and consequently, the molecular weight, of PDMS can be closely controlled.

It is well known that polymers with a C-C backbone cleave homolytically during degradation to generate radicals at the cleaved chain-ends. The experiment with the radical trap DPPH, however, demonstrated that PDMS does not produce radicals when ultrasonically degraded. The evidence from the sonications with lithium fluoride and TBAF, suggests that the Si-O bond cleaves heterolytically, forming ionic species at the chain-ends. If the silanolate anion generated this way is stabilised by a suitable counter-ion, back-biting can occur resulting in the formation of oligomeric, cyclic species. The presence of water in the system can give rise to silanol functionalisation of the chains. This arises through reaction of the water with the ionic chain-ends.

The ring-opening polymerisation of D_4, under both cationic and anionic conditions, was conducted under ultrasound and compared to the 'silent' polymerisation. Both the cationic and anionic polymerisations were accelerated when

conducted under ultrasound, although the effect was more pronounced for the cationic polymerisation than for the anionic. As both polymerisation processes are hetereogeneous, the enhancement can be explained in terms of the mechanical effects of ultrasound. In the cationic polymerisation, the cavitation process will lead to an effective dispersal of the catalyst throughout the system, resulting in faster rates of polymerisation. While in the anionic polymerisation, cavitation will effectively remove any water on the surface of the KOH particles, as well as causing particle size reduction (leading to an increase in surface area) - both factors which will affect the rate of polymerisation. The rapid movement of the solution as a result of cavitation, will also enhance mass transport in both types of polymerisation and this may also act to increase the rate of polymerisation. Unfortunately, no molecular weight data was available, so it is unknown at this stage if ultrasound affects the molecular weight during the polymerisation.

Attempts to produce copolymers of PDMS with polystyrene and poly(methyl methacrylate) by degrading PDMS in the presence of the monomers were unsuccessful. The species produced at the cleaved PDMS chain-ends did not initiate polymerisation of the vinyl monomers used. The use of butyl lithium as an anionic initiator, was also unsuccessful. When added to a mixture of styrene and D_4, only the styrene was polymerised, but when added to a mixture of styrene and D_3, only the D_3 was polymerised. No copolymer product was formed. Other workers have shown that butyl lithium can be used to form the copolymer, however, it is first necessary to initiate the polymerisation of the styrene only, before adding D_3.

Atom transfer radical polymerisation (ATRP) is a technique that offers the opportunity to produce polymers via a free radical mechanism, under "living" conditions. In this work, the method was employed successfully to produce copolymers of PDMS with polystyrene and poly(methyl methacrylate). Two initiators, of differing siloxane chain length, were used and both were capable of initiating the ATRP of styrene and methyl methacrylate, although larger than expected degrees of polymerisation were obtained for the final copolymer. This can be attributed to inefficient initiation, i.e. the rate of propagation being faster than the rate of initiation.

The copolymers produced in this way displayed interesting thermal properties. The most noticeable effect being that the flexible PDMS block results in the Tg of the

product becoming noticeable smaller than the parent (polystyrene or PMMA) homopolymer. This was not the case for the copolymer of PMMA with the longer PDMS chain, however. DSC analysis showed the characteristic behaviour of the respective homopolymers, suggesting that this copolymer exists as a phase-seperated material.

Areas for Future Research

The ultrasonic degradation of PDMS in solvents other than toluene and D_4 should be investigated, as should the effect of dissolved gases in the solution, and the effect of changing the ultrasonic frequency.

Degradation of PDMS gives rise to ionic species at the cleaved chain-ends which can react with any water present to give a silanol. Further work in this area could attempt to functionalise the chain-ends with groups other than silanol and to see if monofunctional termination is possible by controlling the degradation.

Although ultrasound has been shown to increase the rate of polymerisation of D_4, it is not clear whether the ultrasound effects the mechanism of the polymerisation, or if the ring-chain equilibrium is affected. Also, no molecular weight data during polymerisation was available. Hence, at this stage it is not known if degradation processes occur concurrently with the polymerisation. All of these areas merit further investigation.

Atom Transfer Radical Polymerisation is believed to proceed via a free radical mechanism and ultrasound has been shown to affect reactions that involve radical intermediates. The study of ATRP under ultrasonic conditions therefore warrants further investigation. The initiators used in this work were found to be inefficient and, in most cases, resulted in the molecular weights of the final copolymers being larger than expected. Further work should therefore attempt to increase the efficiency of these siloxane-based initiators.

The theme running through this thesis has been the application of sonochemical methodology to enhance polymerisation and to give control over the structure of the final polymer. Ultrasound has been shown to have a positive effect in both areas, although many questions remain and the area offers plentiful research opportunities.

References

REFERENCES

[1] J. M. G. Cowie, *Polymers: Chemistry and Physics of Modern Materials*, 2nd ed., Blackie, London, 1991

[2] F. W. Billmeyer, *Textbook of Polymer Science*, 3rd ed., Wiley-Interscience, New York, 1984

[3] J. W. Nicholson, *The Chemistry of Polymers*, The Royal Society of Chemistry, Cambridge, 1991

[4] K. Ziegler, E. Holzkamp, H. Breil and H. Martin, *Angew. Chem.* (1955) **67** 426

[5] G. Natta, P. Pino, P. Corradini, F. Danusso, E. Mantica, G. Mazzanti and G. Moranglio, *J. Am. Chem. Soc.* (1955) 77 1708

[6] M. Szwarc, M. Levy and R. Milkovich, *J. Am. Chem. Soc.* (1956) **78** 2656

[7] O. W. Webster, *Science* (1991) **251** 887

[8] D. Greszta, D. Mardare and K. Matyjaszewski, *Macromolecules* (1994) **27** 638

[9] T. Otsu, T. Matsunaga, A. Kuriyama and M. Yoshida, *Eur. Polym. J.* (1989) **25** 643

[10] S. R. Turner and R. W. Blevins, *Macromolecules* (1990) **23** 1856

[11] M. K. Georges, R. P. N. Veregin, P. M. Kazmaier and G. K. Hamer, *Macromolecules* (1993) **26** 2987

[12] C. J. Hawker, G. G. Barclay, A. Orellana, J. Dao and W. Devonport, *Macromolecules* (1996) **29** 5245

[13] D. M. Haddleton, D. J. Duncalf, D. Kukulj, A. M. Heming, A. J. Shooter and A. J. Clark, *J. Mater. Chem.* (1998) **8** 1517

[14] M. Kato, M. Kamigaito, M. Sawamoto and T. Higashimura, *Macromolecules* (1995) **28** 1721

[15] J. S. Wang and K. Matyjaszewski, *J. Am. Chem. Soc.* (1995) **117** 5614

[16] K. Matyjaszewski, T. E. Patten and J. Xia, *J. Am. Chem. Soc.* (1997) **119** 674

[17] T. E. Patten, J. Xia, T. Abernathy and K. Matyjaszewski, *Science* (1996) **272** 866

[18] D. M. Haddleton, D. Kukulj, D. J. Duncalf, A. M. Heming and A. J. Shooter, *Macromolecules* (1998) **31** 5201

[19] K. Matyjaszewski, *Macromolecules* (1998) **31** 4710

[20] J. S. Wang and K. Matyjaszewski, *Macromolecules* (1995) **28** 7901

[21] K. Matyjaszewski, J. L. Wang, T. Grimaud and D. A. Shipp, *Macromolecules* (1998) **31** 1527

[22] J. Xia and K. Matyjaszewski, *Macromolecules* (1997) **30** 7697

[23] A. Kajiwara and K. Matyjaszewski, *Macromolecules* (1998) **31** 3489

[24] G. J. Price, *Adv. Sonochem.* (1990) **1** 231

[25] Z. Grubisic, P. Rempp and H. Benoit, *J. Polym. Sci.* (1967) **B5** 753

[26] C. Friedel and J. M. Crafts, *Ann.* (1865) **136** 203

[27] P. R. Dvornic and R. W. Lenz, *High Temperature Siloxane Elastomers*, Hüthig and Wepf, Basel, 1990

[28] F. S. Kipping, *J. Chem. Soc.* (1912) **101** 2108

[29] E. G. Rochow, *J. Am. Chem. Soc.* (1945) **67** 963

[30] R. West and T. J. Barton, *J. Chem. Ed.* (1980) **57** 165

[31] A. L. Smith (Ed.), *The Analytical Chemistry of Silicones*, Wiley-Interscience, New York, 1991

[32] H. H. Moretto, M. Schulze and G. Wagner in *Ullmann's Encyclopedia of Industrial Chemistry*, Vol. A24, B. Elvers, S. Hawkins, W. Russey and G. Schulz (Eds.), VCH Publishers, Weinheim, 1993

[33] H. F. Mark, N. M. Bikales, C. G. Overberger, G. Manges and J. I. Kroschwitz (Eds.), *Encyclopedia of Polymer Science and Engineering*, 2nd Ed., Vol. 15, Wiley-Interscience, New York, 1989

[34] J. E. Mark, H. R. Allcock and R. West, *Inorganic Polymers*, Prentice Hall, New Jersey, 1992

[35] P. J. Flory, *Statistical Mechanics of Chain Molecules*, Wiley-Interscience, New York, 1969

[36] R. N. Meals and F. M. Lewis, *Silicones*, Reinhold Publishing Corporation, New York, 1961

[37] B. Arkles, *Chemtech*, (1983) **13** 542

[38] S. Fordham (Ed.), *Silicones*, George Newnes Limited, London, 1960

[39] P. Hagen, J. Hand and J. Oxley in *Encyclopedia of Chemical Processing and Design*, Vol. 50, J. J. McKetta (Ed.), Marcel Dekker Inc., New York, 1995

[40] J. Chojnowski in *Siloxane Polymers*, S. J. Clarson and J. A. Semlyen (Eds.), Prentice Hall, New Jersey, 1993

[41] I. Yilgör and J. E. McGrath, *Adv. Polym. Sci.* (1988) **86** 1

[42] T. C. Kendrick, B. Parbhoo and J. W. White in *The Chemistry of Organic Silicon Compunds*, S. Patai and Z. Rappoport (Eds.), John Wiley and Sons Ltd, Chichester, 1989

[43] T. C. Kendrick, B. M. Parbhoo and J. W. White in *Comprehensive Polymer Science*, Vol. 4, G. Allen, J. C. Bevington, G. C. Eastmond, A. Ledwith, S. Russo and P. Sigwalt (Eds.), Pergamon Press, Oxford, 1989

[44] H. Jacobson and W. H. Stockmayer, *J. Phys. Chem.* (1950) **18** 1600

[45] W. T. Grubb and R. C. Osthoff, *J. Am. Chem. Soc.* (1955) 77 1405

[46] D. W. Scott, *J. Am. Chem. Soc.* (1946) **68** 2294

[47] J. F. Brown and G. M. J. Slusarczuk, *J. Am. Chem. Soc.* (1965) **87** 931

[48] A. K. Gilbert and S. W. Kantor, *J. Polym. Sci.* (1959) **40** 35

[49] L. Wilczek, S. Rubinsztajn and J. Chojnowski, *Makromol. Chem.* (1986) **187** 39

[50] J. J. Lebrun and H. Porte in *Comprehensive Polymer Science*, Vol. 5, G. Allen, J. C. Bevington, G. C. Eastmond, A. Ledwith, S. Russo and P. Sigwalt (Eds.), Pergamon Press, Oxford, 1989

[51] I. Yilgör, J. S. Riffle, G. L. Wilkes and J. E. McGrath, *Polym. Bull.* (1982) **8** 535

[52] P. J. A. Brandt, C. L. S. Elsbernd, N. Patel, G. York and J. E. McGrath, *Polymer* (1990) **31** 181

[53] C. Aguilera, J. Bartulin, B. Hisgen and H. Ringsdorf, *Makromol. Chem.* (1983) **184** 253

[54] R. C. Allen, G. L. Wilkes, I. Yilgör, D. Wu and J. E. McGrath, *Makromol. Chem.* (1986) **187** 2909

[55] P. Chaumont, G. Beinert, J. Herz and P. Rempp, *Polymer* (1981) **22** 663

[56] J. G. Zilliox, J. E. L. Roovers and S. Bywater, *Macromolecules* (1975) **8** 573

[57] S. Petitjean, G. Ghitti, R. Jérôme, Ph. Teyssié, J. Marien, J. Riga and J. Verbist, *Macromolecules* (1994) **27** 4127

[58] B. Gerharz, Th. Wagner, M. Ballauff and E. W. Fischer, *Polymer* (1992) **33** 3531

[59] S. D. Smith, J. M. DeSimone, H. Huang, G. York, D. W. Dwight, G. L. Wilkes and J. E. McGrath, *Macromolecules* (1992) **25** 2575

[60] G. G. Cameron and M. S. Chisholm, *Polymer* (1985) **26** 437

[61] G. G. Cameron and M. S. Chisholm, *Polymer* (1986) **27** 1420

[62] E. E. Hamurcu, B. Hazer, Z. Misirli and B. M. Baysal, *J. Appl. Polym. Sci.* (1996) **62** 1415

[63] J. V. Crivello, J. L. Lee and D. A. Conlon, *J. Polym. Sci., Polym. Chem. Ed.* (1986) **24** 1251

[64] T. J. Mason and J. P. Lorimer, *Sonochemsitry: Theory, Applications and Uses of Ultrasound in Chemistry*, Ellis Horwood, Chichester, 1988

[65] G. J. Price in *Current Trends in Sonochemistry*, G. J. Price (Ed.), The Royal Society of Chemistry, Cambridge, 1992

[66] J. P. Lorimer and T. J. Mason, *Chem. Soc. Rev.* (1987) **16** 239

[67] K. Suslick, *Sci. Amer.* (1989) **260** 62

[68] P. D. Lickiss and V. E. McGrath, *Chemistry in Britain* (1996) **March** 47

[69] J. Thornycroft and S. W. Barnaby, *Proc. Inst. Civ. Eng.* (1895) **122** 67

[70] K. Suslick, *Science* (1990) **247** 1439

[71] W. J. Galloway, *J. Acoust. Soc. Am.* (1954) **26** 849

[72] G. W. Willard, *J. Acoust. Soc. Am.* (1953) **25** 669

[73] M. Greenspan and C. E. Tschiegg, *J. Res. Natl. Bur. Std.* (1967) **C71** 229

[74] Lord Rayleigh, *Philos. Mag.* (1917) **34** 94

[75] B. E. Noltingk and E. A. Neppiras, *Proc. Phys. Soc.* (1950) **B63** 674

[76] E. A. Neppiras and B. E. Noltingk, *Proc. Phys. Soc.* (1951) **B64** 1032

[77] H. G. Flynn, *Physical Acoustics*, Vol. 1B, Academic Press, New York, 1964

[78] K. E. Suslick, D. A. Hammerton and R. E. Cline, *J. Am. Chem. Soc.* (1986) **108** 5641

[79] E. B. Flint and K. E. Suslick, *Science* (1991) **253** 1397

[80] M. A. Margulis, *Ultrasonics* (1992) **30** 152

[81] M. A. Margulis, *Ultrasonics Sonochem.* (1994) **1** S87

[82] T. LePoint and F. Mullie, *Ultrasonics Sonochem.* (1994) **1** S13

[83] K. S. Suslick, S. J. Doktycz and E. B. Flint, *Ultrasonics* (1990) **28** 280

[84] N. Serpone and P. Colarusso, *Res. Chem. Intermed.* (1994) **20** 635

[85] W. Gaertner, *J. Acoust. Soc. Am.* (1954) **26** 977

[86] H. H. G. Jellinek, *J. Polym. Sci.* (1956) **22** 149

[87] R. W. Wood and A. L. Loomis, *Phil. Mag.* (1927) **4** 414

[88] W. T. Richards and A. L. Loomis, *J. Am. Chem. Soc.* (1927) **49** 3086

[89] T. J. Mason, *Chem. Soc. Rev.* (1997) **26** 443

[90] F. O. Schmitt, C. H. Johnson and R. A. Olson, *J. Am. Chem. Soc.* (1929) **51** 370

[91] D. Peters, *J. Mater. Chem.* (1996) **6** 1605

[92] K. S. Suslick in *Ultrasound: Its Chemical, Physical and Biological Effects*, K. S. Suslick (Ed.), VCH Publishers Inc., New York, 1988

[93] K. S. Suslick, *Adv. Organomet. Chem.* (1986) **25** 73

[94] J. L. Luche, C. Einhorn and J. Einhorn, *Tetrahedron Lett.* (1990) **31** 4125

[95] J. L. Luche, *Ultrasonics* (1992) **30** 156

[96] E. W. Folsdorf and L. A. Chambers, *J. Am. Chem. Soc.* (1933) **55** 3051

[97] A. Szalay, *Z. Phys. Chem.* (1933) **A164** 234

[98] G. Schmid and O. Rommel, *Z. Elektrochem.* (1939) **45** 659

[99] G. Schmid, *Phys. Z.* (1940) **41** 326

[100] G. J. Price, *Chemistry and Industry* (1993) **February** 75

[101] G. Schmid, *Z. Phys. Chem.* (1940) **186** 113

[102] D. W. Ovenall, G. W. Hastings and P. E. M. Allen, *J. Polym. Sci.* (1958) **33** 207

[103] P. E. M. Allen, G. M. Burnett, G. W. Hastings, H. W. Melville and D. W. Ovenall, *J. Polym. Sci.* (1958) **33** 213

[104] A. Henglein, *Makromol. Chem.* (1955) **15** 188

[105] H. W. W. Brett and H. H. G. Jellinek, *J. Polym. Sci.* (1954) **13** 441

[106] G. J. Price and P. F. Smith, *Polymer* (1993) **34** 4111

[107] G. J. Price and P. F. Smith, *Eur. Polym. J.* (1993) **29** 419

[108] G. J. Price, M. P. Hearn, E. N. K. Wallace and A. M. Patel, *Polymer* (1996) **37** 2303

[109] B. S. El'tsefon and A. A. Berlin, *Polym. Sci. USSR* (1964) **5** 668

[110] M. A. Mostafa, *J. Polym. Sci.* (1956) **22** 535

[111] M. A. Mostafa, *J. Polym. Sci.* (1958) **27** 473

[112] A. M. Basedow and K. H. Ebert, *Adv. Polym. Sci.* (1977) **22** 83

[113] H. W. Melville and A. J. R. Murray, *Trans. Faraday Soc.* (1950) **46** 996

[114] A. Weissler, *J. Appl. Phys.* (1950) **21** 171

[115] G. J. Price, P. J. West and P. F. Smith, *Ultrasonics Sonochem.* (1994) **1** S51

[116] W. B. Smith and H. W. Temple, *J. Phys. Chem.* (1968) **72** 4613

[117] T. Q. Nguyen, Q. Z. Liang and H. H. Kausch, *Polymer* (1997) **38** 3783

[118] M. Tabata, T. Miyazawa, J. Sohma and O. Kobayashi, *Chem. Phys. Lett.* (1980) **73** 178

[119] J. R. Thomas and L. de Vries, *J. Phys. Chem.* (1959) **63** 254

[120] G. J. Price, *TRIP* (1994) **2** 174

[121] P. E. M. Allen, J. M. Downer, G. W. Hastings, H. W. Melville, P. Molyneux and J. R. Unwin, *Nature* (1956) **177** 910

[122] A. Henglein, *Makromol. Chem.* (1956) **18** 37

[123] G. J. Price, *Ultrasonics Sonochem.* (1996) **3** S229

[124] O. Lindstrom and O. Lamm, *J. Phys. Colloid Chem.* (1951) **55** 1139

[125] I. E. El'Piner, *Ultrasound: Physical, Chemical and Biological Effects*, Consultants Bureau, New York, 1964

[126] P. Kruss, *Ultrasonics* (1983) **21** 193

[127] P. Kruss, L. A. Dupont and T. J. Patraboy, *Ultrason. Int.* (1983) 502

[128] G. J. Price, D. J. Norris and P. J. West, *Macromolecules* (1992) **25** 6447

[129] S. Biggs and F. Greiser, *Macromolecules* (1995) **28** 4877

[130] J. Fabri, U. Graeser and T. A. Simo in *Ullmann's Encyclopedia of Industrial Chemistry*, Vol. A27, B. Elvers and S. Hawkins (Eds.), VCH Publishers, Weinheim, 1996

[131] J. Rich, J. Cella, L. Lewis, J. Stein, N. Singh, S. Rubinsztajn and J. Wengrovius in *Encyclopedia of Chemical Technology*, Vol. 22, 4th Ed., J. Kroschwitz and M. Howe-Grant (Eds.), Wiley-Interscience, New York, 1997

[132] M. A. Mostafa, *J. Polym. Sci.* (1958) **28** 519

[133] H. H. G. Jellinek, *J. Polym. Sci.* (1959) **37** 485

[134] B. B. Thomas and W. J. Alexander, *J. Polym. Sci.* (1957) **25** 285

[135] M. Okuyama, *Z. Elektrochem.* (1955) **59** 565

[136] E. D. Ozokwelu in *Encyclopedia of Chemical Technology*, Vol. 24, 4th Ed., J. Kroschwitz and M. Howe-Grant (Eds.), Wiley-Interscience, New York, 1997

[137] S. J. Clarson in *Siloxane Polymers*, S. J. Clarson and J. A. Semlyen (Eds.), Prentice Hall, New Jersey, 1993

[138] P. J. West, PhD Thesis, University of Bath, 1993

[139] J. R. Elliott, W. L. Roth, G. F. Roedel and E. M. Boldebuck, *J. Am. Chem. Soc.* (1952) **74** 5211

[140] C. J. Jameson in *Multinuclear NMR*, J. Mason (Ed.), Plenum Press, New York, 1987

[141] R. Bischoff and P. Sigwalt, *Polymer Int.* (1996) **40** 99

[142] D. N. Schultz, J. A. Sissano and C. A. Costello, *Polym. Prepr. ACS* (1994) **35** 514

[143] Y. Nakagawa, P. J. Miller and K. Matyjaszewski, *Polymer* (1998) **39** 5163

[144] A. E. Reed and P. von Ragué Schleyer, *J. Am. Chem. Soc.* (1990) **112** 1434

[145] S. Shambayati, J. F. Blake, S. C. Wierschke, W. L. Jorgensen and S. L. Schreiber, *J. Am. Chem. Soc.* (1990) **112** 697

[146] Q. Wang, H. Zhang, G. K. Surya Prakash, T. E. Hogen-Esch and G. A. Olah, *Macromolecules* (1996) **29** 6691

[147] J. B. Lambert, L. Kania and S. Zhang, *Chem. Rev.* (1995) **95** 1191

[148] Z. Xie, D. J. Liston, T. Jelinek, V. Mitro, R. Bau and C. A. Reed, *J. Chem. Soc., Chem. Commun.* (1993) 384

[149] G. A. Olah, H. Doggweiler, J. D. Felberg and S. Frohlich, *J. Org. Chem.* (1985) **50** 4847

[150] M. Kira, T. Hino and H. Sakurai, *J. Am. Chem. Soc.* (1992) **114** 6697

[151] Z. Xie, R. Bau and C. A. Reed, *J. Chem. Soc., Chem. Commun.* (1994) 2519

[152] R. Damrauer, R. A. Simon and B. Kanner, *Organometallics* (1988) **7** 1161

[153] C. Eaborn, P. D. Lickiss and S. T. Najim, *J. Chem. Soc., Perkin Trans. 2* (1993) **3** 391